SEPTEMBER 2018 Ph.D. in Civil Engineering MOHAMMED MUKHLIF KHALAF

UNIVERSITY OF GAZİANTEP

GRADUATE SCHOOL OF

NATURAL & APPLIED SCIENCES

EFFECTS OF SIZE AND SHAPE OF SAND GRAINS ON SOME ENGINEERING PROPERTIES OF A CLAYEY SOIL

Ph.D. THESIS

IN

CIVIL ENGINEERING

BY

MOHAMMED MUKHLIF KHALAF

SEPTEMBER 2018

Effects of Size and Shape of Sand Grains on Some Engineering Properties of a Clayey Soil

Ph.D. Thesis

in

Civil Engineering

University of Gaziantep

Supervisor

Prof. Dr. Ali Firat Çabalar

By

Mohammed Mukhlif Khalaf

September 2018

REPUBLIC OF TURKEY
UNIVERSITY OF GAZİANTEP
GRADUATE SCHOOL OF NATURAL & APPLIED SCIENCES
CIVIL ENGINEERING DEPARTMENT

Name of the thesis: Effects of Size and Shape of Sand Grains on Some Engineering Properties of a Clayey Soil

Name of the student: Mohammed Mukhlif KHALAF

Exam date: 11.9.2018

Approval of the Graduate School of Natural and Applied Sciences

Prof. Dr. Ahmet Necmeddin YAZICI
Director

I certify that this thesis satisfies all the requirements as a thesis for the degree of Doctor of Philosophy.

Prof. Dr. Hanifi ÇANAKCI
Head of Department

This is to certify that we have read this thesis and that in our opinion it is fully adequate, in scope and quality, as a thesis for the degree of Doctor of Philosophy.

Prof. Dr. Ali Fırat ÇABALAR
Supervisor

Examining Committee Members:	Signature
Assoc. Prof. Dr. Murat ÖRNEK	………………….
Assoc. Prof. Dr. Esra METE GÜNEYİSİ	………………….
Assoc. Prof. Dr. Talha EKMEKYAPAR	………………….
Assist. Prof. Dr. Volkan IŞBUĞA	………………….
Prof. Dr. Ali Fırat ÇABALAR	………………….

I hereby declare that all information in this document has been obtained and presented in accordance with academic rules and ethical conduct. I also declare that, as required by these rules and conduct, I have fully cited and referenced all material and results that are not original to this work.

Mohammed Mukhlif KHALAF

ABSTRACT

EFFECTS OF SIZE AND SHAPE OF SAND GRAINS ON SOME ENGINEERING PROPERTIES OF A CLAYEY SOIL

KHALAF, Mohammed Mukhlif
Ph.D. in Civil Engineering
Supervisor: Prof. Dr. Ali Fırat ÇABALAR
September 2018
156 pages

This thesis presents an experimental research studying in the effect of shape and size of sand grains on some geotechnical properties of a clayey soil using unconfined compression and triaxial compression machines equipped with a pair of bender elements. The materials used in this study were low plasticity clay, Narli Sand and Crushed Stone Sand. Three different gradations of the sands (0.6-0.3, 1.0-0.6, and 2.0-1.0) mm were chosen. Five contents of clay-sand (90-10, 80-20, 70-30, 60-40 and 50-50) by dry weight were investigated. Series of bender elements (BE) tests were carried out on clay-sand mixtures to measure small strain shear modulus (G_{max}). Unconfined compression (UC) tests were conducted on these mixtures to have a correlation between G_{max} and unconfined compressive strength (q_u). G_{max} and q_u increased with increasing roundness and sphericity of sand grains. The q_u values decreased, and the G_{max} values increased when sand content in the mixture increased. As size of sand grains increased, G_{max} and q_u values increased. For the results that obtained from triaxial compression machine equipped with bender elements tests, the deviatoric stress increased with increasing content, size, roundness and sphericity of sand grains. The pore water pressure decreased as sand content increased and it is increased as size, roundness and sphericity decreased. The effective cohesion (c') decreased and effective angle of friction (ϕ') increased as sand content increased. A correlation between G_{max}, voids ratio and effective stress was developed for rounded and angular sand of clay-sand mixtures.

Keywords: Sand, clay, shear modulus, bender element test, triaxial test

ÖZET

KUM DANELERİNİN ŞEKİL VE BÜYÜKLÜĞÜNÜN BİR KİLİN BAZI GEOTEKNİK ÖZELLİKLERİNE ETKİSİ

KHALAF, Mohammed Mukhlif
Doktora tezi, İnşaat Mühendisliği bölümü
Tez Danışmanı: Prof. Dr. Ali Fırat ÇABALAR
Eylül 2018
156 sayfa

Bu tez çalışmasında, bir çift bender eleman ile donatılmış üç eksenli basınç cihazı ve serbest basınç cihazı kullanılarak kum tanelerinin şekil ve tane çapı özelliklerinin killi bir zeminin mühendislik parametrelerine etkisi sunulmaktadır. Bu çalışmada düşük plastisiteli kil, Narlı kumu ve Kırmataş kumu örnekleri kullanılmıştır. Üç farklı kum gradasyonu (0.6-0.3 mm, 1.0-0.6 mm, and 2.0-1.0 mm) deneysel çalışmalarda kullanılmak üzere seçilmiştir. Kuru ağırlık itibari ile hazırlanan beş farklı kil-kum oranının (90-10, 80-20, 70-30, 60-40 ve 50-50) özellikleri incelenmiştir. En büyük kayma modülü (G_{max}) değerlerini bulmak için kum-kil karışımları üzerinde bender eleman (BE) testleri gerçekleştirilmiştir. Buna ilaveten, G_{max} değerleri ile serbest basınç mukavemeti (q_u) değerleri arasında ilişki kurabilmek için bir dizi serbest basınç testi de yapılmıştır. Bender elemanlar ile donatılmış üç eksenli basınç deney aletinden elde edilen sonuçlar deviatorik gerilme değerlerinin kum danelerinin yüzdesi, dane büyüklüğü, yuvarlaklık ve küresellik özellikleri arttıkça arttığını göstermiştir. Karışımlardaki kum yüzdesi arttıkça boşluk suyu basıncı değerleri azalırken, kum danelerinin büyüklük, yuvarlaklık ve küresellik özelliklerinin azalmasıyla boşluk suyu basıncı değerleri artmıştır. Kum içeriği arttıkça efektif kohezyon (c') değeri azalmış ve efektif içsel sürtünme açısı (ϕ') artmıştır. G_{max}, boşluk oranı, ve çevre basıncı arasında, yuvarlak ve köşeli kum danelerinin bulunduğu kum-kil karışımları için bir ilişki geliştirilmiştir.

Anahtar kelimeler: Kum, kil, kayma modulü, bender eleman testi, üç eksenli basınç testi.

To my parents

ACKNOWLEDGEMENTS

I would like to express my deepest gratitude to my supervisor, Prof. Dr. Ali Fırat Çabalar, for his unlimited guidance, patience and support during this research. Without his supervision and advice, this thesis would not have been possible.

I gratefully acknowledge Mosul University and the Ministry of Higher Education and Scientific Research in Iraq for the PhD scholarship provided by them.

I would like to sincerely and gratefully thank my parents, father and mother, brother and sisters for their endless support and encouragement during my study period.

Finally, I would like to thank my wife for her endless support and sacrifice, and my wonderful kids for their endless energy, without their encouragement, I would not have finished this thesis.

TABLE OF CONTENTS

Page

LIST OF TABLES

Page

LIST OF FIGURES

Page

CHAPTER 1

INTRODUCTION

1.1 General

Most of the engineering design methods of structures on soil have been developed for natural soils such as pure clays or pure sands. However, these soils are rarely found in nature. In general, soils are composed of a mixture of clay and sand in different proportions, shapes, and sizes. Furthermore, when the soils in the field do not meet the requirements of a particular geotechnical application, the cohesive soil is mixed with sand or gravel and made suitable for the intended purpose as cores of embankment dams (Jafari and Shafiee, 2004; Shafiee et al., 2008), and impervious blankets (Chapuis, 1990; Pandian et. al., 1995). It is difficult to identify the properties of the clay-sand mixture since it has both the properties of clay and sand.

The dynamic and static behaviour of clay can be significantly affected by the presence of sand in the mixture. Actually, it is of great importance to identify the dynamic behavior of such soils in order to make an accurate stability analysis of any systems subjected to cyclic loads, for example those resulting from earthquakes, machine foundation, blasts, sea waves, wind, and traffic loads (Lehane et al., 1993; Fakharian and Evgin, 1997; Castelli et al., 2016; Ghayoomi et al, 2017). Many problems with such loadings are dominated by wave propagation effects where only low levels of strain are induced in the soil. Shear modulus and damping ratio are the most significant soil characteristics influencing such small strain behaviour. Very small strains, typically shear strains less than 0.001%, do not cause a significant nonlinear stress-strain response in the soil (Kramer, 1996). Hence, a linear model can be adopted. The most considerable stiffness parameter at this level is the small strain shear modulus (G_{max}). The G_{max} is a parameter required for advanced soil modelling as well as solving dynamic soil problems. A common method of evaluating G_{max} is to measure the shear wave velocity (Vs) as presented in the following relationship (Fabbrocino et al., 2015):

$$G_{max} = \rho \, Vs^2 \qquad (1.1)$$

where ρ: soil mass density.

For determination of G_{max} of soils, one of the commonly used laboratory tests is Bender Element (BE), which consists of two thin plates of piezoelectric material bonded together, with two conductive outer layers and a metal piece at the center (Lee and Santamarina, 2005; Rahman et al, 2016; Wang et al., 2016). A small-strain shear modulus is estimated by determining shear wave velocity using bender elements test based on the wave propagation theory (Shirley and Hampton, 1978). In spite of the difficulties in determining shear wave arrival time (Ibrahim et al., 2011; Cherian and Kumar, 2015), a soil sample can be subsequently tested for other soils characteristics, because the bender element tests do not disturb the soils samples, thus facilitating comparison with other results (Youn et al., 2008; Szilvagyi et al., 2016). As the characterizing behaviour of the specimens under dynamic loading becomes much more complex and expensive than that of specimens subjected to monotonic loading, only few researches have been carried out on correlating a dynamic test and a static test so far (Consoli et al., 2009; Flores et al., 2009). Thus, there is a need for an investigation of the comparison between dynamic tests and static tests. The unconfined compression (UC) test is by far the most popular technique of soil shear testing as it is one of the cheapest and fastest techniques of measuring shear strength. The technique is employed primarily for cohesive soils recovered from thin-walled sampling tubes (ASTM D 2166). To correlate q_u and G_{max} and using q_u to predict G_{max} of clay-sand mixtures, unconfined compression equipped with bender elements were conducted in this study

From the literature, it has been noted that there is no much information available on the experimental study of the clay-sand mixture using the bender element (BE) test and unconfined compression strength (UC) test. Although there have been several studies of the dynamic behaviour of sands, few studies have attempted to relate the shape and size of sand to the stiffness of clayey soil in the very small strain range. Hence, based on the existing relevant studies on soils, an attempt will be made to study the stiffness and strength properties of clayey soil mixed with three different sizes, two shapes and with five different contents of sand grains by the two test techniques. The stiffness differs extensively due it is a function of direction of loading and strain because of the soil is a non-linear material. Moreover, greater focusing has been located on soil behaviour at small strains. Studying the non-linear soil behaviour displayed by most natural soils and describing soil responses at the very small-strain range (γ_s < 0.001%) can be done using advanced measurement instruments and systems which became a necessary part of advanced laboratory testing (Tatsuoka et al., 2001). The use of internal instrumentation such as Linear Variable Differential Transformers (LVDTs) permits for shear strain determination as small as 0.002%.

The very small strain level corresponds to the range of strain less than the elastic threshold strain, approximately between 10^{-3} % and 10^{-2} %. Within this very small strain region, the soil exhibits linear-elastic behaviour and the shear modulus is independent of strain, approaching a nearly constant limiting value of the maximum shear modulus (G_{max}). The small strain range starts from elastic threshold strain to 1% where the shear modulus is highly non-linear and strain-dependent. The large strain range corresponds to strain generally larger than 1% (Sawangsuriya et al., 2005).

The triaxial test is one of the most versatile and widely geotechnical laboratory tests, allowing the shear strength and stiffness of soil to be determined for use in geotechnical design. Advantages over simpler procedures, such as the direct shear test, include the ability to control specimen drainage and take measurements of pore water pressures. Main parameters determined from the test may include the angle of internal friction (ϕ'), cohesion (c'), although other parameters such as the shear modulus (G), compression index (Cc), and permeability (k) may also be measured. Bender elements test is a nondestructive test because of the specimen it kept intact during the test (Callisto and Calabresi, 1998; Kuwano and Jardine, 2002; Cai et al., 2015). For this reason, small strain shear modulus of saturated soil can be measured using triaxial device equipped with bender elements (Finno and Cho, 2010; Styler and Howie, 2014). Bender elements improve the capabilities of triaxial testing instruments throughout both static and dynamic parameters of soils undergone to axisymmetric stress conditions can be determined. This study emphases on connecting the stiffness of clay-sand mixtures at very small and small strains using triaxial compression device equipped with bender elements. This study includes 39 isotropically consolidated undrained triaxial compression tests on samples of clayey soil and clay-sand mixtures at different sand contents, sand shapes, sand sizes, and confining stresses.

1.2 Aims and Objectives

The objective of this thesis is to determine the geotechnical properties of clayey soil mixed with different sizes and shapes of sand grains using a triaxial apparatus equipped with bender elements. To attain this aim, bender elements are mounted in the base pedestal and top cap of a triaxial machine to study the effect of sand grains size and shape and to measure the stiffness of clay-sand mixtures at very small strains and link it with large strain behaviour of these mixtures.

The experimental work of this research is aimed:

1- To study the effect of sand grains size and shape on shear modulus and unconfined compressive strength of clay-sand mixtures and evaluate the relationship between q_u and G_{max} of these mixtures using triaxial machine without cell equipped with bender elements.

2- To investigate the influence of frequency on shear wave velocity and G_{max} of clayey soil and clay-sand mixtures using bender elements test.

3- To determine the effect of sand grains size and shape on shear strength parameters of clay-sand mixtures using triaxial compression test.

4- To find the relationship between G_{max}, void ratio and effective stress of clay-sand mixtures by triaxial compression machine equipped with bender elements.

5- To normalize G with G_{max} of clay-sand mixtures obtained from triaxial compression apparatus equipped with bender elements.

1.3 Layout of the Thesis

This thesis is composed of five chapters as follows:

Chapter 1 presents the general introduction and the aim of this study.

Chapter 2 deals with the literature reviews and previous works of the stiffness of soil mixtures, bender elements, unconfined compression strength equipped with bender elements, triaxial equipped with bender elements, the shear strength of soil mixtures, and particle shape and size.

Chapter 3 covers the materials, testing machines, and methods of testing that used in this study.

Chapter 4 describes the results of G_{max} and q_u of clayey soil and clay-sand mixtures using unconfined compression device equipped with bender elements, and the results of G_{max} and shear strength parameters of clayey soil and clay-sand mixtures using triaxial compression device equipped with bender elements.

Chapter 5 displays the main conclusions of this study and the recommendations for future studies.

CHAPTER 2

REVIEW OF LITERATURE

2.1 Introduction

This chapter presents a literature review of subjects related to the study of the effect of shape and size of sand grains on engineering properties, especially dynamic properties of clay-sand mixtures using a conventional triaxial testing apparatus equipped with bender elements. Section 2.2 presents a review of stiffness of soil and soil mixtures. The chapter then moves on to describe bender elements testing and display some of the studies that used this test in the experimental work (section 2.3). Sections 2.4 and 2.5 concentrate specifically on the review of unconfined compression strength equipped with bender element and triaxial equipped with bender element, respectively. In section 2.6 emphasis is placed on the review of shear strength of soil mixtures studies. Finally, in Section 2.7, the particle shape and size of sand and review of its effects on engineering properties of soil is discussed.

2.2 Shear Modulus of Soil and Soil Mixtures

The stiffness of soil is one of the most important dynamic properties of soil and it is used in the design of geotechnical structures that subjected to dynamic loadings. Soil stiffness exhibits a clear nonlinear behaviour in the stress-strain relationship. For a safe design of geotechnical structures, the strains in the soil of these structures that must be taken into considerations are the small strains. Hence, the understanding of behaviour of stiffness parameters at small and very small strain is essential for accurate estimates of soil movements that may influence the performance of the geotechnical structures.

The small strain shear modulus is the shear modulus of soil within a narrow range of shear strain ($\gamma_s < 0.001\%$), and often denoted as G_{max}. The small-strain or maximum shear modulus (G_{max}) provide useful information about stiffness of soil. G_{max} is a significant factor in characterizing the dynamic properties of soil. It is an essential physical property related to the analysis and the design in seismic engineering, liquefaction assessment, and design of deep geotechnical structures (Kramer 1996; Zhou et al. 2005; Yang and Gu 2013; Luke et al. 2013). Furthermore, G_{max} is used to measure the stiffness of soil in geoenvironmental engineering (Tang et al. 2011; Hoyos et al. 2015). The G_{max} value is evaluated from shear wave velocity (Vs) of soil. The determination of Vs can be achieved from laboratory tests such as: bender elements (BE) test (Dyvik and Madshus, 1985; Brignoli et al., 1996; Pennington et al., 2001; Chang and Heymann, 2005; Lee et al., 2007; Ferreira et al., 2007; Teachavorasinskun and Lukkanaprasit,2008; Chan et al., 2010; Clayton, 2011), resonant column (RC) test (Thomann and Hryciw, 1990; Souto et al., 1994; Macari and Ko, 1994; Mancuso et al., 2002; Chien and Oh, 2002; Fam et al., 2002; Wichtmann and Triantafyllidis, 2009) and torsional shear test (Yamada et al., 2008; Youn et al., 2008).

Seed et al. (1986) studied G_{max} of sandy and gravelly soils and defined the relationship between G_{max} and mean effective confining pressure as follows:

$$G_{max}=1000\ (K_2)_{max}(\sigma_o')^{n_G} \tag{2.1}$$

σ_o': mean effective confining pressure. In this equation G_{max} and σ_o' are in units of psf, n_G is constant that its value mostly about 0.5 and $(K_2)_{max}$ is a non-dimensional factor which is a function of type of the soil and relative density of this soil. Table 2.1 illustrates $(K_2)_{max}$ values for different types of materials.

Ishihara and Koseki (1989) investigated the influence of fines content on the dynamic properties of soil using cyclic triaxial apparattus. The authors found that the relative density is not a suitable factor to expect the cyclic resistance of soil when the fines content of soil exceeds 50%. They found that the fine’s plasticity index (PI) is the most significant factor affecting the cyclic stiffness of the mixture. The cyclic stiffness of the soil increases when the plasticity index of fines containing sand increases. Nevertheless, the authors found that when PI below around 10% there was a little change in the cyclic stiffness.

Macari and Ko (1994) studied the anisotropic features of G_{max} and damping ratio of a silt that has been uniaxially consolidated. The test program followed in the study consisted of RC experiments to obtain the G_{max} and damping characteristics of silty soil samples. From this study, it was recognized that natural soil deposits are commonly an isotropically consolidated and their behaviour in both stiffness and strength were an isotropic in nature.

Tanaka et al. (1994) studied the dynamic properties of gravelly soil using cyclic triaxial test and travel time method by measuring the Vs of soil at small strain range. The comparison between Vs calculated from cyclic triaxial test with that evaluated by impacting the specimen at one end and observing the shear wave arrival on an accelerometer at the other end. The authors found that Vs evaluated by the travel time method is often higher than that found by a cyclic triaxial test and proposed that the variance may be because of the bedding error. This error can happen when local nonhomogeneity in a specimen results in a stiffer travel path through the specimen because of the stronger particles have intact skeleton (this influence is captured by a travel-time measurement while it is not fully captured using cyclic triaxial test because the cyclic triaxial device measures the average stiffness of the specimen). The fines content changed the ratio of Vs estimated using triaxial test (Vs*) to that evaluated using direct travel time. This difference is presented in Figure 2.1. Figure 2.1 shows that the minimum of Vs*/Vs ratio takes place at about 10% fines content, proposing that specimenes with about this fines content for this soil have the highest amount of local nonhomogeneity.

Chien and Oh (2002) carried out RC tests on sand quarried from Yunlin, Taiwan. The authors compared the G_{max} values obtained from tests with that predicted values that estimated from Hardin equation built in the paper. When the stress ratio increased from one to three, G_{max} increased considerably, and at the stress ratio of three the increment was about 32% under 196 kPa of confining pressure, as revealed in Figure 2.2.

Tao et al. (2004) investigated the influence of fines content on liquefaction resistance using thin hollow cylindrical samples of sand and non-plastic fines mixtures by conducting cyclic torsional shear tests. The G_{max} decreased as fines content increasing up to 28%, but when fines content exceeds, G_{max} increased as fines content increases. Figure 2.3 shows this relationship. A similar trend was discovered for the relataionship between liquefaction resistance and the fines content when the relative density is constant. Below the threshold fines content, as the fines content increasing in the soil the voids in the sand skeleton are filled but without increasing the number of interparticle contacts and thus the stiffness or strength does not increase. From viewpoint of particles contact, if samples are made at constant void ratio, specimens with lower fines contents are denser than the specimens with higher fines content up to a threshold value where fines begin to fill the contacts generated by the larger particles. Hence, they made comparsion between the liquefaction resistance of a soil sample and the void ratio of sand and they discocvered that a better key is the void ratio of sand to expect the stiffness or strength of soil when the fines content is lower than the fines content threshold.

Yamada et al. (2008) performed undrained tests using a cyclic torsional simple shear device on Ariake clay and silica sand mixtures. In the study of the variation of G/G_o with frequency two various mixtures were used. The normalized shear modulus is affected by frequency at the point when the behaviour is starting to become nonlinear at a strain above 0.01%. They found that between 0.1 and 1% strain amplitude, the increase is of 6% for pure Ariake clay and 9% for 30% mixture of Ariake clay silica sand at 0.1% strain amplitude, and the increase is of 21% for pure Ariake clay and of 13% for 30% Ariake clay silica sand mixture at 1% strain amplitude. Figure 2.4 shows The results of other amplitudes of strain which the pure Ariake clay denoted as (ACC100) and 30% Ariake clay-sand mixture denoted as (ACC30).

Wichtmann and Triantafyllidis (2009) studied the influence of size of quartz sand on G_{max} using RC devices on various grain size distribution of this sand. The authors observed that G_{max} is not a function of the mean grain size (d_{50}) at the same void ratio in the studied range (0.1 mm $\leq d_{50} \leq$ 6 mm, $1.5 \leq C_u = d_{60}/d_{10} \leq 8$). Furthermore, they found that G_{max} reduces remarkably as coefficient of uniformity (C_u) increasing as revealed in Figure 2.5.

Hsiao et al. (2015) studied the effect of silt content on sands using consolidation, triaxial compression, and cyclic triaxial tests at three various states which are: constant relative density, constant void ratio, and constant peak deviator stress. The silt percentages that investigated in this experimental study were 0%, 15%, 30%, 40%, 50% and 60% by weight. For silt percentage up to 40-50%, the increment of silt percentage results in a decrease in the cyclic resistance ratio (CRR), and then results in an increment of the CRR with the increment of silt percentage. For constant void ratio, as the silt percentage increased up to 50% the CRR values decreased and then increased with the increment of silt percentage. For constant deviator stress, at 40% of silt percentage the CRR value decreased to a minimum value.

Liu et al. (2016) made comparison between a volcanic granular soil quarried from northeastern Japan and two quartz sands (Toyoura sand and Fujian sand) by measuring the initial shear modulus (G_0) of these materials using the RC test with various densities and confining stresses. Compared with volcanic soil, for all confining stresses studied, the G_0 values of Toyoura sand are the highest. The existence of fines particles which its size (<63 μm) in the volcanic soil resulted in this remarkable difference. G_0 of volcanic soil increased markedly when the fines removed under same testing conditions. The removing coarse particles (>2 mm) and fines from volcanic soil which has the same gradation with that of Fujian sand gave initial shear modulus values slightly lower than those of Fujian sand. The difference in initial shear modulus values between these materials because of the difference in minerals and due to the grain shape influence. Figure 2.6 shows comparison between the predicted and measured values of G_0 for original volcanic (Volcanic_O), volcanic without fines (Volcanic_NF), volcanic without both coarse and fines (Volcanic_X) and two quartz sands.

Payan et al. (2017) investigated the effect of content of fines (silica non-plastic silt) on G_{max} and damping ratio (D_{min}) of various sizes and shapes of clean sands using torsional resonant column tests. At the same confining pressure, the values of G_{max} reduced when the fines content increased. Because of the different properties of the sand part in the mixtures of sand-fines, a substantial variance is found in the maximum shear modulus and damping ratio values of the different specimens at low fines content. At high fines content, the behaviour was entirely silt-dominant and the mixture of various types of sand with silt exhibited approximate values of G_{max} and D_{min}.

Sas et al. (2017) measured G_0 of cohesive soils from two different sites in Warsaw, Poland using RC test with various mean effective stresses (p′), void ratios (e) and PI. The soil from first site classified as normally consolidated soil, whereas the soil from second site characterized as lightly overconsolidated soil. The authors found that the initial shear modulus of both soils is affected by the mean effective stress, while there was no obvious trend identified for the marked influence of void ratios and plasticity indices. The study suggested the next relations between G_0 and the mean effective stress of normally consolidated and lightly overconsolidated soils, respectively:

$$G_0=3.02\ p'^{0.68} \tag{2.2}$$

$$G_0=0.82\ p'^{0.96} \tag{2.3}$$

2.3 Bender Elements

The BE test is a nondestructive test that has gained popularity in the evaluation of the G_{max}. The simple process of this test, together with their small size, has encouraged their use in a big set of geotechnical equipment since their first appearance (Shirley and Hampton, 1978). Also, the number of samples required is very minimal, because of the same sample can be tested at various intervals. The BE are piezo-electrical transducers, that involve two thin piezo-ceramic pieces, attached together with a conductive metal sheet at the center. Figure 2.7 presents the connection of BE (Lings and Greening, 2001). When an input wave is applied to the transmitter BE, one of the piezo-ceramic piece contracts and the other extends, causing of the transmitter to bend and produce a shear wave. When the shear wave arrives the receiver bends, and an electrical signal propagating that can be captured by a data acquisition. BE have been widely utilized to evaluate Vs at low strain levels, shear strain (γ_s) <0.001% (Camacho-Tauta et al., 2015). The BE were first presented by Shirley (1978) and Shirley and Hampton (1978) to measure soil properties, and as a result of its capability to estimate Vs of soil in a small-strain level, and in a wide variety of stress conditions. The BE have been becoming a conventional dynamic laboratory instrument, and many laboratory devices have been equipped with it, such as triaxial (Brignoliet al., 1996; Jovicic and Coop, 1998; Kuwano et al., 1999; Fioravante and Capoferri, 2001; Pennington et al., 2001; Styler and Howie, 2014), oedometers (Dyvik and Olsen, 1991; Sukolrat, 2007), RC devices (Ferreira et al., 2007; Gu et al., 2013). The BE were applied to calculate G_{max}, but with the passing the time and their greater usages, it is utilized to estimate P-wave velocity (V_P), to study structure and fabric, in cementation, also the degree of saturation or anisotropy, to assess the quality of sample (Airey and Mohsin, 2013).

BE testing is not a standard yet, because of the inconsistency of its results in comparison with standard RC testing (Camacho-Tauta et al., 2015). The accuracy of BE test is affected by various parameters, such as near-field effects (Sanchez-Salinero et al., 1986), travel distance (Brignoli et al., 1996), directivity (Airey and Mohsin, 2013), sample geometry and size (Arroyo et al., 2006), boundary effects (Arulnathan et al., 1998), cross-talking (Lee and Santamarina, 2005). The difficulty lies as well in accurately estimating the travel time (t) of theshear wave from a transmitter BE to a receiver BE, while a distance between elements (L), accepted as the tip-to-tip distance, can be precisely measured.

The near-field effect is the mixed of rays of shear (S) and compression (P) waves; this effect has been widely investigated and examined as the fundamental source of measurement errors (Sanchez-Salinero et al., 1986; Jovicic et al., 1996; Arroyo et al., 2003). It is responsible for the difficulty in the detection of the shear wave's arrival time. It has a significant contribution close to the source and therefore if the receiver is too close to the transmitter, the shear wave arrival is masked by this effect. This undesirable effect reducesas the frequency (f) of the shear waveincreased, which increases the ratio of the path length of the wave (travel distance (L)) to wavelength (λ) (Gordon and Clayton, 1997; Viggiani and Atkinson, 1995; Jovicic et al., 1996; Kumar and Madhusudhan, 2010). Arulnathan et al. (1998) stated that the near-field effect disappears as the ratio of L/λ become more than 1. Pennington et al. (2001) mentioned that when L/λ ratio between 2 and 10, a good signal can be achieved. Leong et al. (2005) suggested a value of this ratio as 3.33 to improve the signal interpretation. Wang et al. (2007) favoured this ratio is equal to or greater than 2 to avoid this effect. Many researchers recommended a range of $2<L/\lambda<9$ (Sanchez-Salinero et al., 1986; Arulnathan et al., 1998; Arroyo et al., 2003; Gajo et al., 1997; Pennington et al., 2001; Wang et al., 2007).

In spite of the popularity of using BE, complications of signal interpretation of its test, espically in the measuring of the arrival time are existing. Various procedures for the signal interpretation were mentioned (Lee and Santamarina, 2005; Arroyo et al., 2010), but nobody has been widely realized as a standard. Actually, the wave propagation in a soil which is a complex phenomena obstructs the measurement of the arrival time objectively and accurately (Camacho-Tauta et al., 2013). Generally, the selected frequency in most researchs is between 1 and 30 kHz for soils with low stiffness which represent most materials that tested by BE (Youn et al., 2008; Leong et al., 2009).

The Vs can be estimated from travel time (t) and the travel length between BE as tip-to-tip (L) by the following relationship (Viggiani and Atkinson, 1995):

$$V_S = L/t \tag{2.4}$$

The G_{max} depending on the theory of propagation of the shear wave can be evaluated as follows:

$$G_{max} = \rho V_S^2 \tag{2.5}$$

Where ρ is the soil density.

The progress of geophysical field tests lead to interpretation of BE tests by taking practice and interest of the knowledge (Viana da Fonseca et al., 2006).

Strassburger (1982) established piezo-electric transducers to evaluate V_S and V_P in the sand. The transducers were piezoelectric compression crystals, piezoelectric shear crystals, and piezoelectric benders. The transducerswere inserted in a test cell, which was filled with soil. The test cell was an aluminium cylinder whose measurements were 11 inches (28 cm) in height, 8.28 inches (21 cm) in diameter and 3/16 inches (0.48 cm) inches thickness. The loading system inside the cell consisted of a bladder filled with de-aried water. Also, strain gauges were attached to the outside of the cylinder to measure the hoop stresses.

Thomann and Hryciw (1990) used RC device equipped with BE and conducted tests to verify the accuracy of the BE on two cohesionless soils: Ottawa 100-200 and Glacier way silt. The confining stress was increased, and G_{max} was measured again for one day. They performed tests on five samples with confining stress running from 34.5 kPa (5 psi) to 345 kPa (50 psi). The BE results show a slightly higher stiffness than RC results. They believe that this small discrepancy is due to the slight variance in shear strain levels in the two tests as presented in Figure 2.8.

A special type of RC setup was developed by Souto et al. (1994) to study the limits of test conditions using piezo-crystals in coarse-grained soils in comparison with the

RC tests. The RC was a fixed free (fixed end, spring tops) type of equipment. The triaxial cell was the main part of the equipment; an oscillator was mounted on the upper part of the cell within the reaction mass. Both the bottom pedestal and top cap of the triaxial sample were equipped with piezo-crystals. For crushed materials with grain size greater than 8 mm, the results of G_{max} from BE are a little greater than the results from RC test as shown in Figure 2.9.

Fam et al. (2002) investigate the influence of salt on the Vs of the sand by using RC device equipped with BE. They performed RC tests on two specimens and taking Vs readings during particle dissolution using BE installed in the bottom and top of the device. One of the samples is prepared from pure sand (without salt), and the other specimen is prepared from sand-salt mixture with salt content of 5%. Good agreement was obtained from Vs results using RC apparatus and BE for dry and saturated samples as displayed in Figure 2.10.

Chang and Heymann (2005) investigated the influence of particle shape on gold tailings which composed of fine platy and rotund particles by evaluating Vs by carrying out BE test. They found that the gold tailings have a somewhat low G_{max} because of the gold tailings particles containing particles with platy shape.

Lee et al. (2007) investigated the influence of mica on Ottawa sand by measuring Vs of these mixtures with different mica to sand size ratios (L_{mica}/D_{sand} = 0.33, 1, 3) using an oedometer device fitted with BE. The authors proposed that Vs reduces, and becomes more affected by effective stress with increasing of mica content for $L_{mica}/D_{sand} \geq 1$ as shown in Figure 2.11. They observed that the normalized G_{max} values for the mixtures are considerably lower. The reason of low G_{max} values for the mixtures might be due to the combined influences of platy shape and size of mica particles. Nevertheless, the influence of void ratio was not considered. Also, the size of the sand grains was somewhat small when compared with that of the mica. The void ratios values of the mixture considerably increased resulted from bridge packing of the mica as presented in Figure 2.12. In this state, the influence of particle shape on Vs might be due to the altering in the void ratio as proposed by Hardin (1961). The susceptibility of effective stress, in this state, might also be due to the variation in the void ratio because of mica is highly deformable material. When the mica content is increased, the void ratio of the mixture increased, hence when the effective stress increased the volume changes are increased. So, in qualifying the influence of particle shape on G_0, the influence of void ratio should be considered.

Ferreira et al. (2007) performed simultaneous RC test equipped with BE on Porto granitic residual soils to measure G_0. The researchers used two interpretation methods (time domain (TD) and frequency domain (FD)) to determine travel time by BE test. Figure 2.13 shows the comparison of G_0 values evaluated by RC test with that measured by the two methods of BE. This Figure shows that the results of the time domain method deviate by 2% in average from RC test results. The results of frequency domain method of G_0 values deviate from results of RC test by 1% on an average.

Cai et al. (2015) studied the effect of fines content on G_{max} of three types of sand (i.e., Fujian sand, Hangzhou sand, and Nanjing sand) in saturated conditions with different void ratios and confining pressures using RC, torsional shear (TS), and BE tests. The study showed that the measurement of travel time in BE tests is influenced by the excitation frequency. The near-field effect is decreased as the excitation frequency increasing, but very high frequency leads to only little effect. The frequency between 10 and 20 kHz is the suitable frequency because the ratio between travel distances to wavelength (L/λ) ranged between 3 and 8 approximately. The difference between the Vs values that evaluated by BE tests compared with that measured by RC and TS tests is about 5-10% for saturated Fujian and Hangzhou sands, while this difference is decreased to about 3% for saturated Nanjing sand. Figure 2.14 shows that the G_{max} decreased with increasing of fines content under various confining pressures and similar void ratio.

Qiu et al. (2015) studied the concept of effective density and its effects on G_{max} of glass beads, coarse sand, Ottawa sand 20-30, and fine to medium sand in dry and saturated conditions using RC tests and BE tests. The authors made comparison between G_{max} values for dry condition with G_{max} values for saturated condition, which are estimated using effective density and saturated density. The errors in G_{max} values were about 28% when using saturated density, while the errors caused by using of effective density were not more than 5% using BE tests as shown in Figure 2.15. Because of the influence of mass polar moment of inertia and the range of frequency is smaller, the errors in the G_{max} of RC tests were smaller than that measured by BE tests.

Yang and Liu (2016) studied the influence of crushed silica fines content on the Vs and G_0 of clean quartz sand using the RC and BE tests. The fines content that investigated in this study were 5, 10, 20 and 30% by mass. The study displayed that when the fines content increased G_0 values decreased for both tests. They observed that the G_0 values evaluated by BE tests is larger than that evaluated by RC tests by approximately 20% for clean sand and sand-fines mixtures as shown in Figure 2.16. The reasons for this difference are the strain level covered by RC test is relatively higher than that covered by BE test, and the stiffness that evaluated by BE test representing the stiffness of central part of the sample between the transmitter and the receiver, while the stiffness evaluated by RC test representing the stiffness of whole sample.

2.4 Unconfined Compression Apparatus Equipped with Bender Element

The principle of this technique is based on the using of BE device to determine G_{max} and the conventional unconfined compression machine to evaluate the strength of soil samples. The unconfined compression (UC) tests and BE tests were conducted to study the relationship between q_u and G_{max} values. The UC test is used for measuring the undrained shear strength of cohesive soils because of simplicity of the test technique. The BE test is a nondestructive test that has gained popularity in the laboratory to measure G_{max}. From the literature, it has been noted that there is not much information available on the experimental study of the using the BE test and UC test.

Consoli et al. (2009) investigated the influence of the cement content and porosity (voids/cement ratio) (V_υ/V_{ce}) on G_0, q_u and effective strength parameters (c',ϕ') of cemented sand by using BE set up in the triaxial compression test. They found a correlation between the ratio of G_0 to q_u (G_0/q_u) as a function of (V_υ/V_{ce}) and observed that as the values of (V_υ/V_{ce}) increases the values of q_u, c', ϕ' and G_0 decreases. The change in G_0 with (V_υ/V_{ce}) is revealed in Figure 2.17.

Flores et al. (2009) studied the relation between q_u and G_0 of a Kaolin clay mixed with Portland cement and blast furnace slag cement at various contents to observe the hardening of cement-treated Kaolin clay with time. The G_0 is calculated using BE test. They found that the increase of G_0 and the increase of q_u of cement-treated soil are closely related as shown in Figure 2.18.

2.5 Triaxial Machine Equipped with Bender Element

Brignoli et al. (1996) added piezoelectric discs as compression wave transducers and two types of shear wave transducers (BE and shear-plates) to a triaxial chamber were executed with different confining pressures of Ticino sand. The authors presented various types of shear wave arrivals and provide procedures for selecting arrival time depending on the commonly produced variety of signals. It is noticed that it is difficult sometimes to receive a clear S-wave arrival. Possible states are that the first arrival of energy does not identify the right polarity or that the amplitude of the firstarrivalis not correlated to the largest in the received waveform. Figure 2.19 presents this comparison and shows that the largest values of Vs are determined using BE, followed by Vs values calculated by shear-plate and, finally, the lowest values of Vs corresponding to those measured by RC device.

Jovicic and Coop (1998) used a triaxial apparatus with BE attached to the specimen to study the influence of anisotropy on G_{max} in clay samples. The authors measured shear moduli, G_{vh}, $G_{hv,}$ and G_{hh} of natural and reconstituted London Clay in a triaxial cell with a pair of vertically mounted BE. It was necessary to cut samples in different directions because of the shear waves only propagate vertically in this configuration. The ratio of G_{hh}/G_{hv} was 1.24 for the normally consolidated reconstituted samples at isotropic stress while G_{vh}/G_{hv} and G_{hh}/G_{hv} for the natural samples were around 1.0 and 1.5, respectively. The over-consolidated samples displayed G_{hh}/G_{hv} is 1.5, similar to the natural samples. Since their experiments were conducted at isotropic stresses, the results for the natural samples may have been subjected to some change of anisotropy from the in-situ case. In this study, the measurable elastic moduli were limited, because of only a single pair of BE was employed along the longitudinal axis of a sample.

Fioravante (2000) installed BE and piezoelectric disks (PD) transducers in a triaxial device. This arrangement of transducers allows measurement of body waves in the representative vertical direction. However, BEs were also set up on the sides of the sample to estimate polarized shear and compression waves in horizontal and oblique directions. The main objective was to determine the influence of the anisotropy on the constrained modulus (M_{max}) and G_{max} of Ticino and Kenya sands.

Finno and Cho (2010) investigated the influences of recent stress history (RSH) on G_{max} of overconsolidated Chicago glacial clay using triaxial device equipped with BE. The RSH influences at very small strains can be computed only by BE results because of the apparatus that utilized in this work could not evaluate shear strains smaller than 0.002% precisely. By observing the results of BE test, the authors found that the stiffness in very small strain zone (γ_s< 0.001%) were not influenced by RSH. The results of shear modulus (G_{vh}) values that obtained by BE tests that mounted on soil samples during K_0 reconsolidation and unloading are presented in Figure 2.20.

Giang et al. (2017) studied the effects of particle shape and coefficient of uniformity (C_u) on the maximum shear modulus (G_{max}) of calcareous sand and silica sand using triaxial equipped with BE test. Silica sand is more spherical (less angular) than calcareous sand. The study showed that the G_{max} values of silica sand smaller than that of calcareous sand. The major parameter that influencing the maximum shear modulus of calcareous sand is particle shape. The decreasing of C_u resulted in an increase of maximum shear modulus.

2.6 Shear Strength of Soil Mixtures

Holtz and Willard (1956) were the first researchers to study the influence of gravel contents ranged between 0% and 65% on clayey soil using triaxial compression test. They observed that the apparent cohesion decreased with the increasing of gravel content, while the angle of shearing resistance increased as shown in Figure 2.21. The influence of the granular part of the mixture was the controlling, when the gravel fraction exceeds 50%.

Miller and Sowers (1958) studied the influences of the contents of fine and coarse grains of soils on the clay-sand mixtures by performing unconsolidated undrained (UU) triaxial tests. The clayey soil used in the study is a low plasticity sandy clay. To obtain the clay-sand mixtures different contents of sand and clay were used. They found that the angle of internal friction remained nearly constant until the fines content reduced to about 33%. For fines contents between 26% and 33%, a sharp alteration happened in the soil behaviour, where the cohesion decreased considerably, and the angle of shearing resistance increased markedly as presented in Figure 2.22.

Thevanayagam (1998) conducted consolidated undrained (CU) triaxial tests on mixtures of coarse and fine materials. The properties of coarse materials which were a sand with 2% non-plastic fines were: e_{min}= 0.6, e_{max}= 0.98, d_{50}= 0.25 mm, d_{10}= 0.16 mm, C_u= 1.77, C_c= 0.88. The fines materials were either kaolin silt or ground silica. The CU tests were conducted on the sand, mixtures of 10% and 25% kaolin silt with sand, and of 10% ground silica with sand to obtain specimens with high void ratio, low fines void ratio with high intergranular void ratio (e_s), and low e_s with high fines void ratio. These three cases were tested at range of confining stresses. In general, dense specimens or loose specimens tested at low confining stresses showed dilative or contractive-dilative trends, while specimens with high void ratio tested at high confining stresses displayed contractive trends. Undrained shear strength is taken as the strength at 20-25% strain because of this range in behaviour and continued volume-change tendency at moderate-large strains. The large strain shear strength of sand specimen prepared with void ratio $e=e_s$ was nearly the same as silty-sand specimens prepared with intergranular void ratio. The relationships between e with mean effective stress (P) and steady-state undrained shear strength (s_u) are presented in Figure 2.23.

Yin (1999) investigated the influence of clay on the properties of Hong Kong marine deposits which are denoted as (HKMD-1) with various clay contents 6, 10, 20 and 27.5% using CU triaxial tests on these samples. Figure 2.24 shows that the increase in PI decreases the friction angle of Hong Kong marine deposits. As effective confining pressure increased, the values of Young's modulus (E_{50}) were increased, while E_{50} values reduced as clay content increased.

Wood and Kumar (2000) studied the influence of sand on the properties of kaolin clay by carrying out undrained and drained triaxial tests on overconsolidated and consolidated mixtures of coarse sand and kaolin clay. The authors observed that the deviator stress, pore water pressure, and volumetric strain were affected by the addition of the sand when the sand content exceeded 60%.

Thevanayagam et al. (2002) tested mixtures of silica sand and non-plastic fines using triaxial test. They showed that the undrained response is based on collapse potential and is governed by inter-grain contacts. Results indicate that the silty-sand mixtures still be prone to undrained collapse because fines separate the coarse matrix in spite of these mixtures have low global void ratios.

Jafari and Shafiee (2004) conducted a monotonic and cyclic triaxial tests on mixtures of sand-clay and gravel-clay to study the influences of aggregate on the mechanical behaviour of these mixtures. As aggregate content increase, the angle of shearing resistance increased from compression monotonic test results. Also, pore pressure increased in both monotonic and cyclic tests when the aggregate content increased. Also, it was found that the formation of a nonhomogenous density in the clayey fraction of the sand-clay mixtures because of the existence of aggregates within a cohesive matrix.

Prakasha and Chandrasekaran (2005) carried out an investigation on Indian marine soils with various contents of sand and clay using static and cyclic triaxial. The authors observed that the addition of sand into clay resulted in a decrease in void ratio and increment in friction and pore pressure causing a reduction in the undrained shear strength of the sand and clay mixtures. They advanced a factor which is the effective void ratio (EVR) which is known as the ratio between the volume of voids to the volume of effective soil part. They found a unique correlation between the effective void ratio and vertical consolidation stress (σ'_{vc}) in logarithm scale.

Kim et al. (2006) performed CU triaxial tests on mixtures of Mikawa silica sand and Iwakuni clay with 2% coarse particles, the properties for Mikawa silica sand were e_{max}= 0.85, e_{min}= 0.524, d_{50}= 0.88 mm, C_u= 3.79 and for Iwakuni clay were PI= 48, G_s= 2.61, the clay contents were 0, 10, 15, and 17% of mixtures. They detected that when the clay content is less than 20%, the mixtures are non-plastic. Their CU triaxial data proposed that peak deviator stress was the same for 0 and 10% clay content, and was larger for 15 and 17% clay content for constant compaction energy during sample preparation. Nevertheless, peak deviatoric stress decreases with increasing clay content as the compaction energy is increased about 19-fold, as shown in Figure 2.25. Peak deviator stress increases as fines content increasing if the intergranular void ratio is instead held constant (by changing the compaction energy). They conclude that the peak strength and large strain response are governed by fines content and resulting coarse fraction skeleton. For undrained conditions, the strength increased due to fines content increasing if the intergranular void ratio is constant and lower than the maximum granular void ratio. However, the strength-strain response is dominated by the clay if the intergranular void ratio becomes higher than the maximum granular void ratio.

Monkul and Ozden (2007) investigated the compression behaviour of clayey sand and transitional fines contents using oedometer apparatus. They concluded that the compressional behaviour of clayey sand could be evaluated by and by the intergranular void ratio rather than the global void ratio. They observed that the coarse part of clayey sand soil controlled the compression up to fines fraction which is termed as 'transitional fines content'. While the fine part of clayey sand soil controlled the compression when the soil containing fines higher than transitional fines content. They found that the minimum void ratio was not the parameter that affected the transition fines content. They observed that the lower limits and upper limits of transition fines content are 19% and 34%, respectively. The relationship between the shear stress (τ_{max}) and fines content (FC) is presented in Figure 2.26. It is noticed from this Figure that there is no considerable variation in the shear strength of the soil up to specific value of fines content and then reduces. The values of transition fines content for the corresponding stress levels are represented by dashed lines in this Figure.

Cubrinovski and Rees (2008) investigated mixtures of silica sand and non-plastic fines using triaxial device and state that the addition of fines increases flow potential and moves the steady-state line down in the e-p' plane as presented in Figure 2.27.

2.7 Particle Shape and Size of Sand

Comprehension the influences of particle shape and size on the properties and behaviour of soil supports acheivemnet and interpretation the results of geotechnical laboratory tests (Kakou et al. 2001). Many studies have treated the features of different particle shape and size mixtures, but the effect of various particle shape and size contents on soil properties is still controversy (Vallejo and Zhou 1994; Cho et al. 2006).

Grain shape is determined by chemical and mechanical operations once it is released from the matrix (Margolis and Krinsley, 1974). Particle shape is characterized by three independent properties (Wadell, 1932; Krumbein, 1941; Krumbein and Sloss, 1963) which are: sphericity (S), roundness (R) and smoothness. Sphericity is quantified as the diameter of the largest inscribed sphere relative to the diameter of the smallest circumscribed sphere. Roundnessis defined as the average radius of curvature of surface features proportional to the radius of the maximum sphere that can be inscribed in the particle. Figures 2.28-2.30 characterize roundness, sphericity and a chart to compare between them to evaluate the particle shape parameters (Krumbein, 1941; Powers, 1953; Santamarina and Cho, 2004; Muszynski and Vitton, 2012).

Cho et al. (2006) studied the effects of particle shape on packing density, stiffness, and strength on natural and crushed sands using oedometer apparatus equipped with BE. They found that e_{min}, e_{max} and their difference which is (e_{max}-e_{min}) increased as roundness and sphericity decreased, this increasing is happened because of the particles mobility and their capability to achieve dense packing arrangements are blocked by irregularity. For stiffness, the influence of particle shape on small strain stiffness is investigated by estimating Vs during sample loading and unloading. The influences of history of loading and packing density are captured by the parameters α and β. They concluded that when sphericity, roundness, and regularity parameters decreased, the parameter α decreased. On the other hand, β exponent increased when these parameters decreased. These trends are determined by two influences. The two influences are: (a) the irregularity causes the packing of soil to be looser as shown in Figure 2.31, leads to smaller number of coordination between soil grains, and hence the matrix of soil become softer, (b) the contacts between irregular soil grains are more susceptible to deformation. The observed smaller stiffness (smaller value of α) and larger stiffness sensitivity to the stress condition (larger value of β exponent) are produced by these two influences of irregularity. The inverse correlation that previously found for many types of soils which is β=0.36-α /700 is satisfied by evaluated values of α and β (Santamarina et al., 2001). The effecte of particle shape on the modulus that measured by oedometer apparatus at zero-lateral strain is examined using these results. The results showed that the increased irregularity of soil particles causes the compression and decompression indices become larger.

Clayton et al. (2009) found that the particle shape, and form in particular, has a substantial influence on the properties of granular materials during compression and shear. The methods currently available for measuring form are either two-dimensional, or impractical for sand-sized particles and below, or cannot differentiate sufficiently between bulky and platy materials.

Cabalar and Hasan (2013) investigated the effect of fines content on the compressional behaviour of different size and shape of sand-clay mixtures using odometer device equipped with a linear displacement sensor. They used two types of sand which are Trakya Sand (TS) and Crushed Stone Sand (CSS). They related the various size fractions (0.3-0.6 mm; 1.0-2.0 mm) and shapes (rounded and angular) of sands with clay in various viscosity pore fluids (0.94 mm^2/s, 10.65 mm^2/s) to compressional behaviour. They found that the granular compression index (C_{c-s}) parameter which is used by (Monkul and Ozden, 2005) decreaeses with increasing of sphericity (S) and roundness (R) and with increasing of sand size as presented in Figures 2.32 and 2.33, respectively.

Table 2.1 Values of $(K_2)_{max}$ of sandy and gravelly soils (Seed et al.,1986)

	Soil description	Location	Depth (ft)	$(K_2)_{max}$
Sandy soils	Loose moist sand	Minnesota	10	34
	Dense dry sand	Washington	10	44
	Dense saturated sand	So. California	50	58
	Dense saturated sand	Georgia	200	60
	Dense saturated silty sand	Georgia	60	65
	Dense saturated sand	So. California	300	72
	Extermely dense silty sand	So. California	125	86
Gravel soils	Sand, gravel, and cobbles with little clay	Caracas	200	90
	Dense sand and gravel	Washington	150	122
	Sand, gravel, and cobbles with little clay	Caracas	255	123
	Dense sand and sandy gravel	So. California	175	188

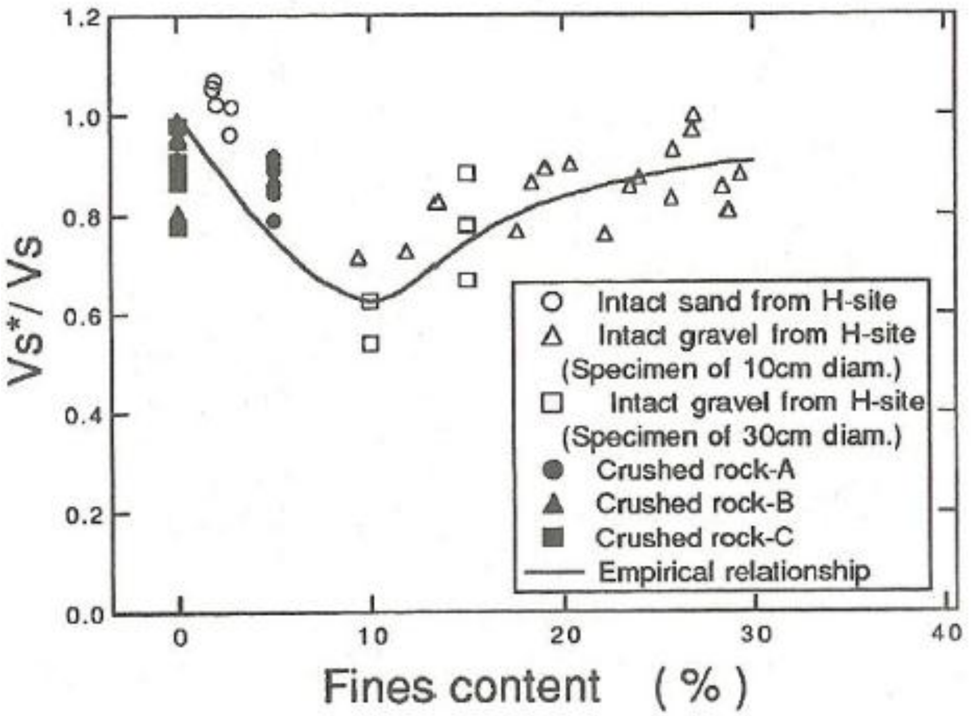

Figure 2.1 Relationship between the ratio of shear wave velocity evaluated by cyclic triaxial test (Vs*) to that by travel times (Vs) with fines content (Tanaka et al., 1994).

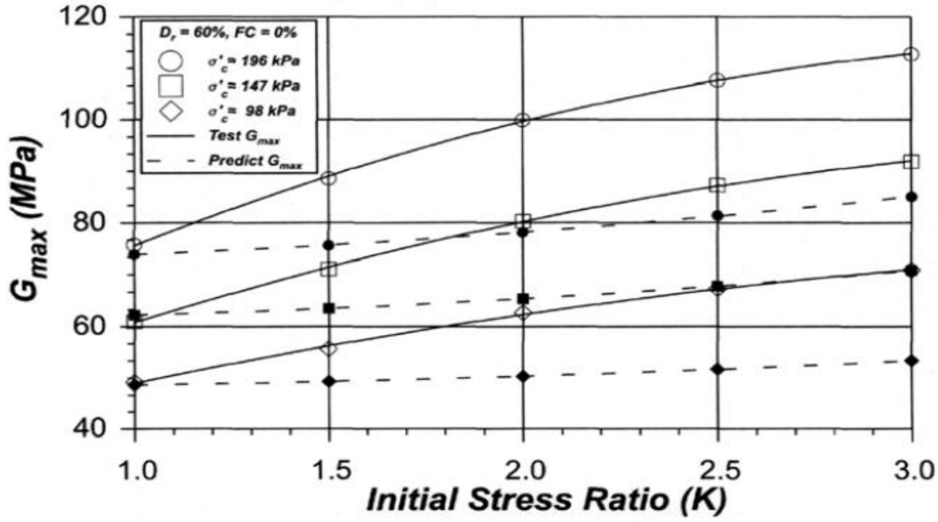

Figure 2.2 Variation in small strain shear modulus (G_{max}) with initial stress ratio (K) (Chien and Oh, 2002).

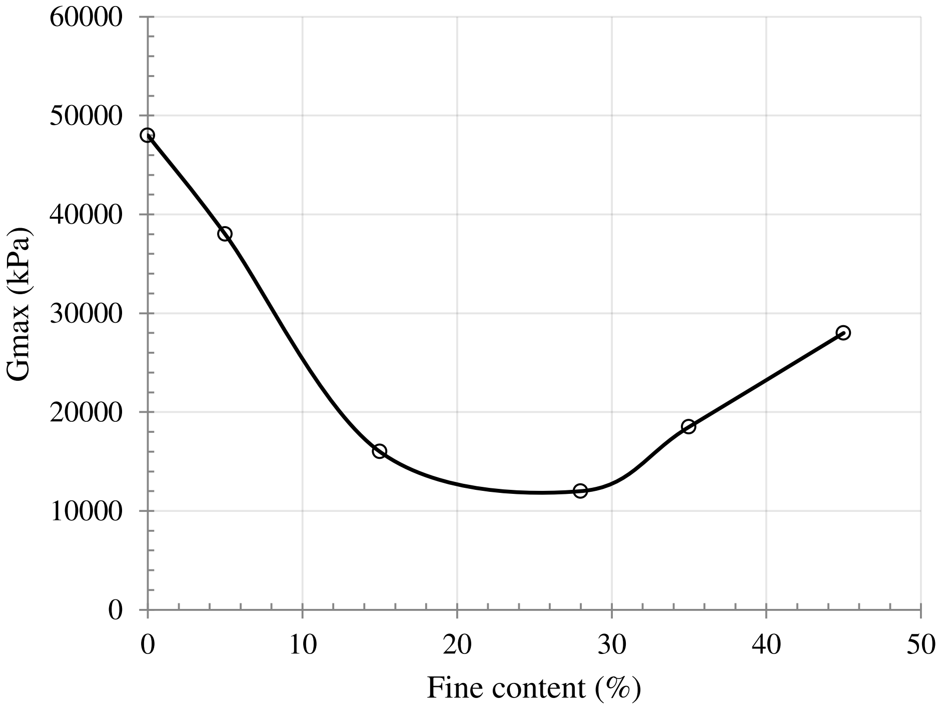

Figure 2.3 Change in maximum shear modulus (G_{max}) with fines content for a silty sand at the same relative density (D_r= 50%, σ_o' = 124.1 kPa) (Tao et al., 2004).

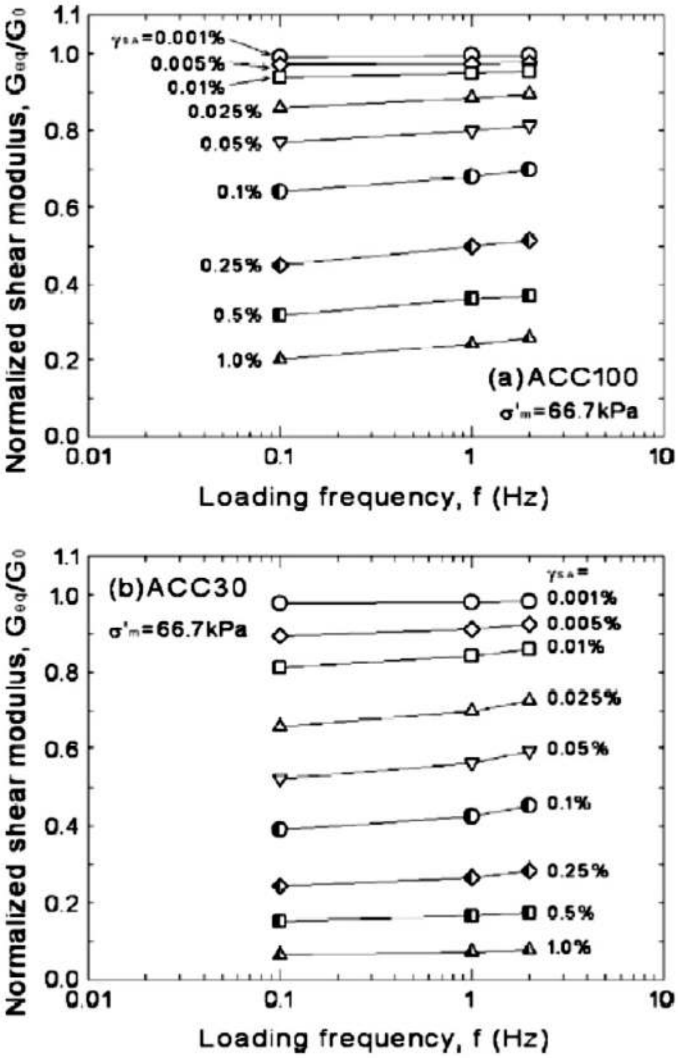

Figure 2.4 Relationship between normalized shear modulus and loading frequency for different strain amplitudes for (a) ACC 100 and (b) ACC30 (Yamada et al., 2008).

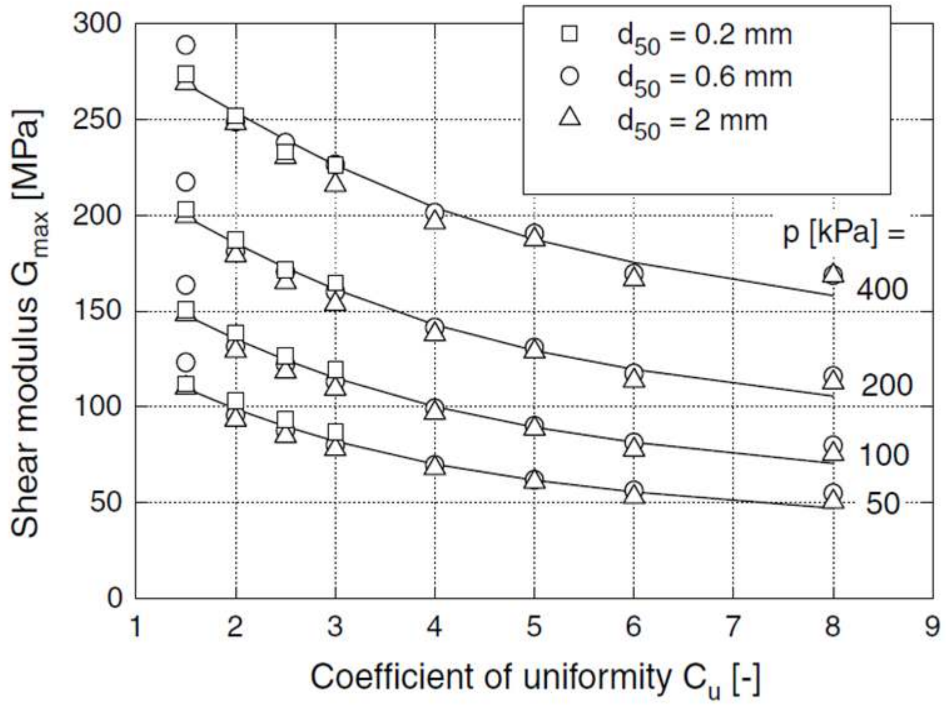

Figure 2.5 Maximum shear modulus (G_{max}) versus coefficient of uniformity (C_u) at e= 0.55 for different pressures (p) (Wichtmann and Triantafyllidis, 2009)

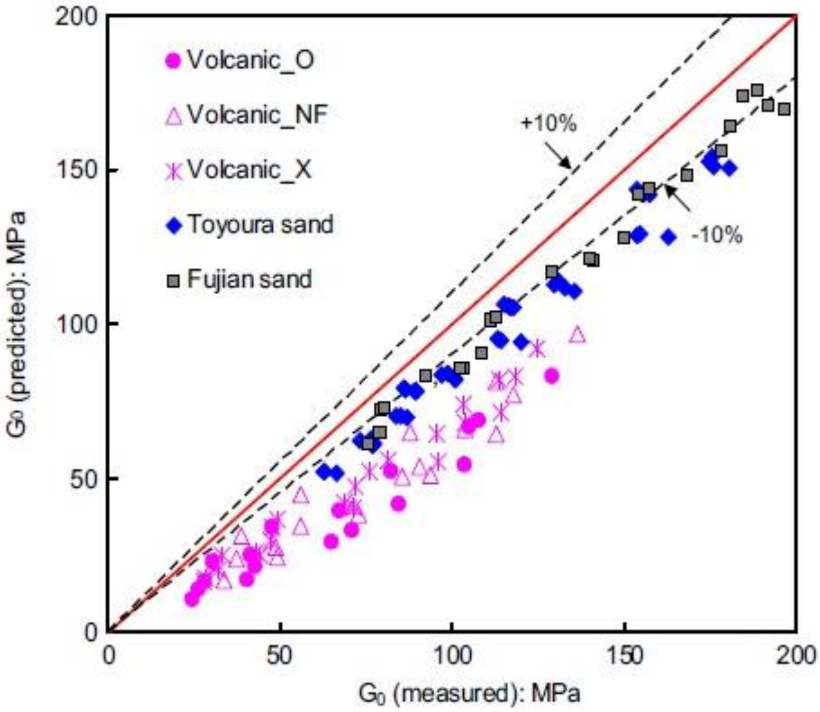

Figure 2.6 Comparison between the predicted and measured values of initial shear modulus of tested materials (Liu et al., 2016).

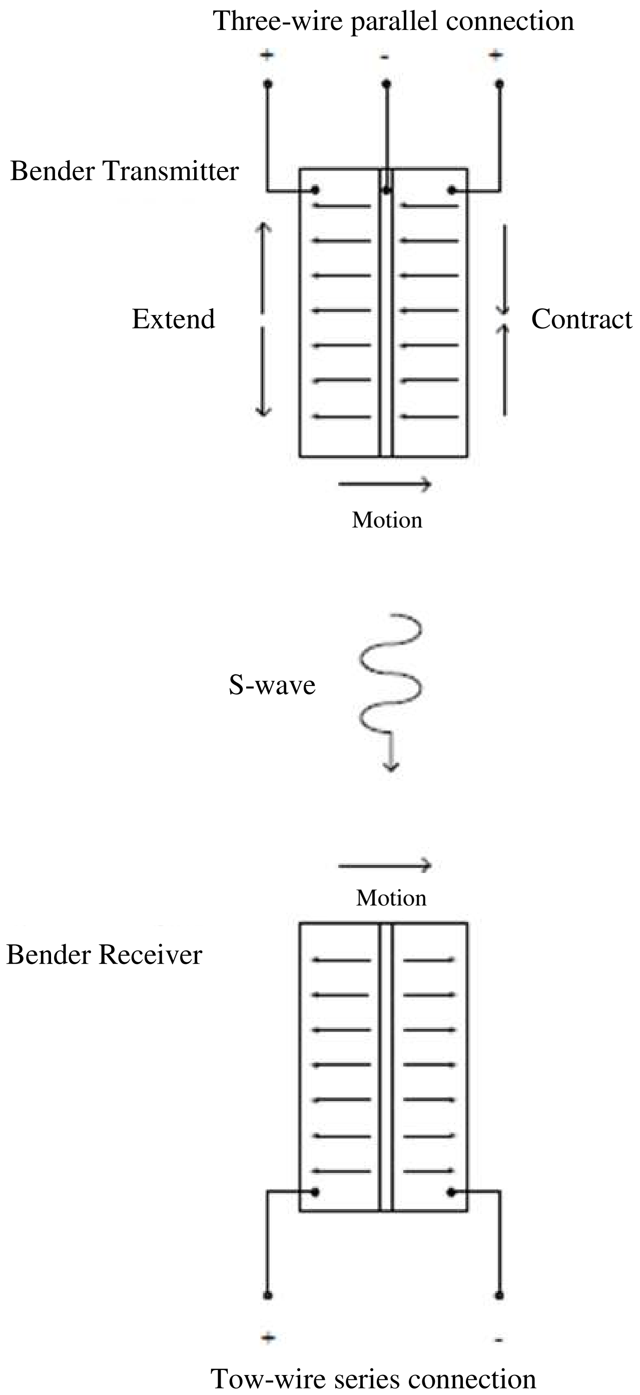

Figure 2.7 Sketch of bender elements connection (Lings and Greening, 2001).

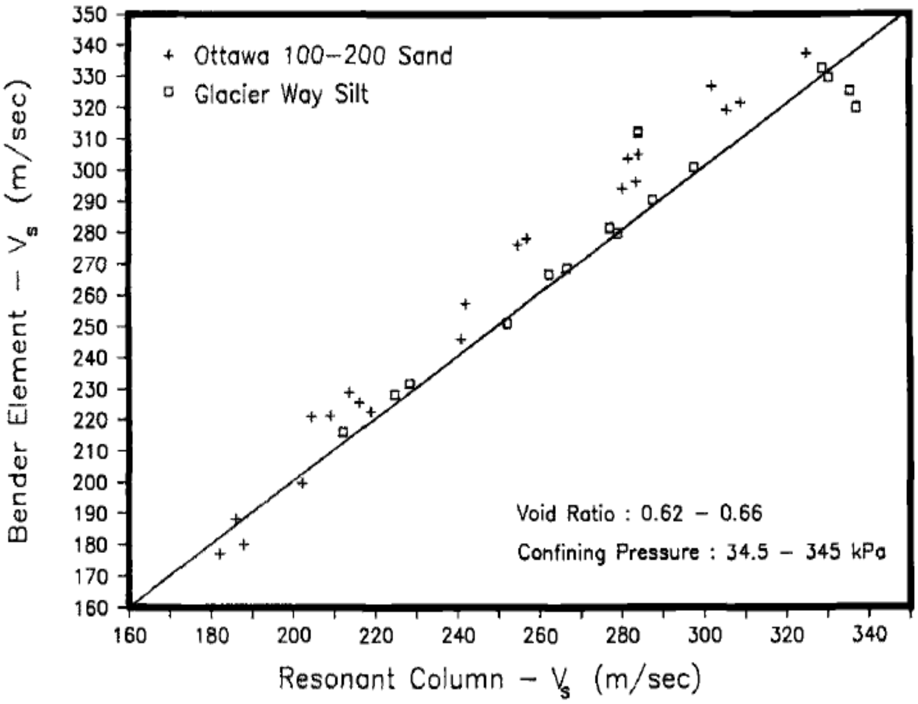

Figure 2.8 Comparison of shear wave velocity from resonant column (RC) and bender elements (BE) (Thomann and Hryciw,1990)

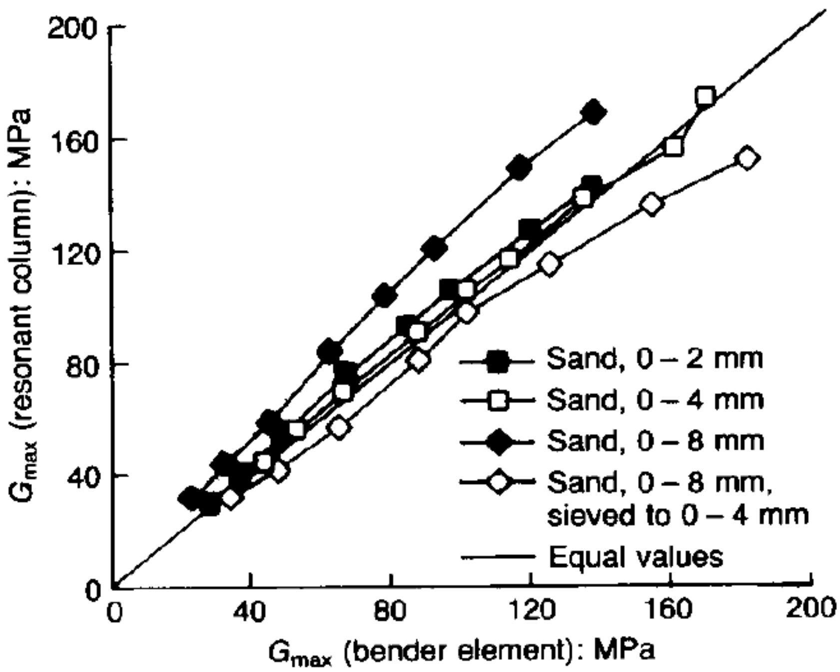

Figure 2.9 Comparison of maximum shear modulus (G_{max}) of sands evaluated by resonant column and bender elements tests (Souto et al., 1994)

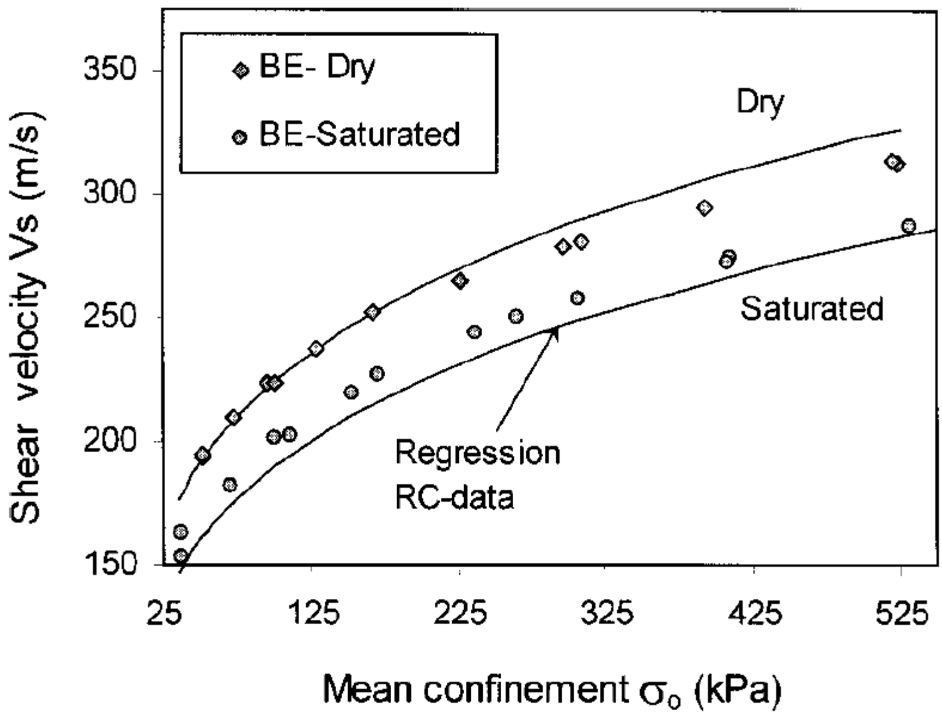

Figure 2.10 Shear velocity measured by resonant column (RC) and bender elements (BE) tests (Fam et al., 2002).

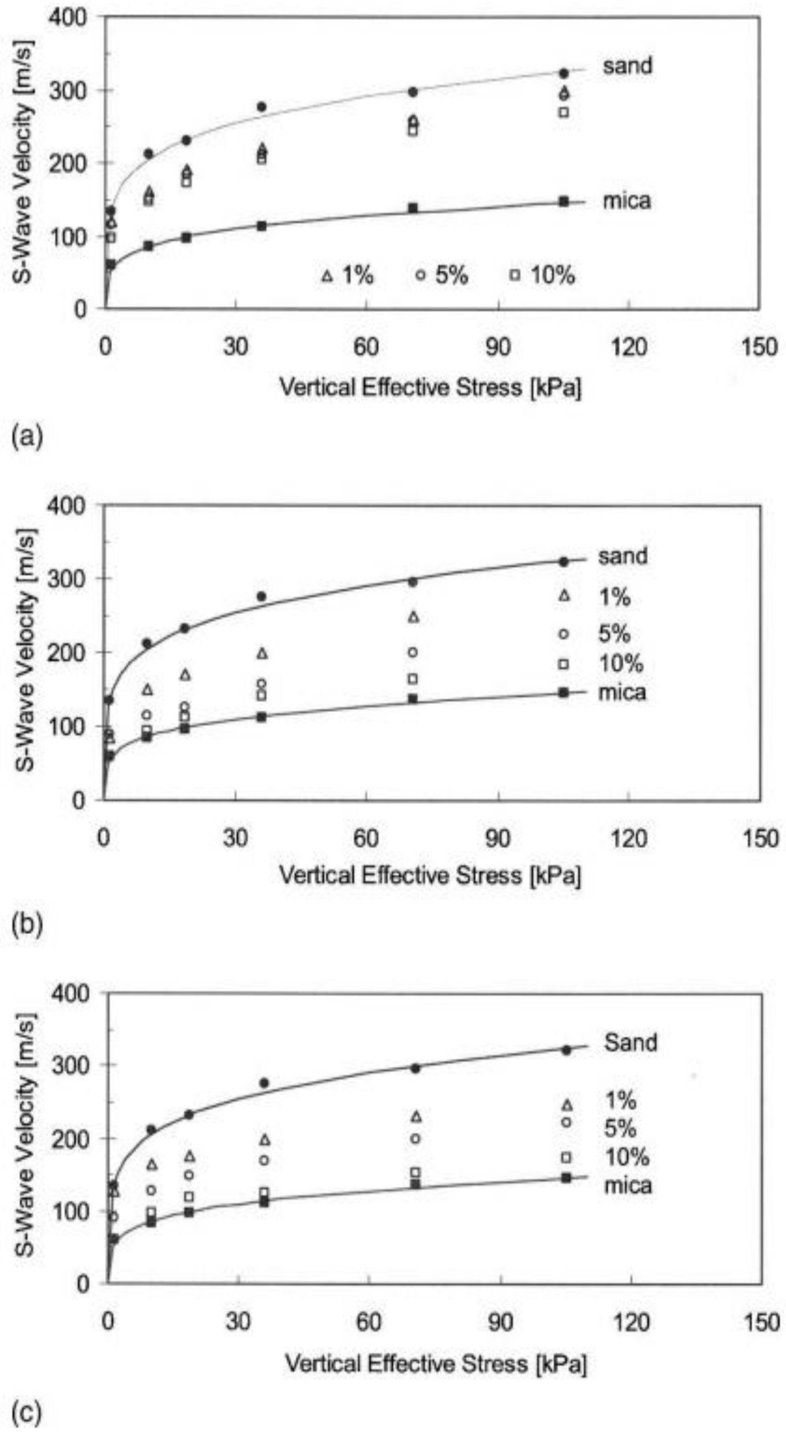

Figure 2.11 Variation of shear wave velocity with vertical effective stress for Ottawa sand-mica mixtures. (a) L_{mica}/D_{sand}= 0.33; (b) L_{mica}/D_{sand}= 1; (c) L_{mica}/D_{sand}=3 (Lee et al., 2007)

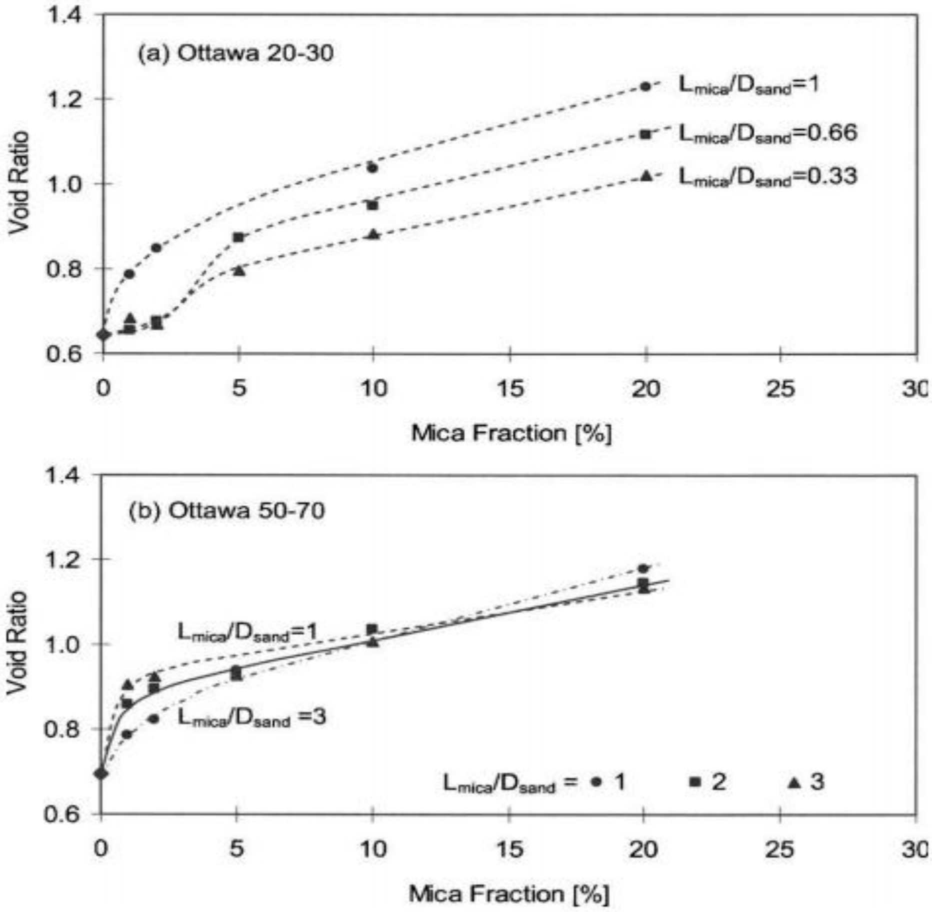

Figure 2.12 Relationship between void ratio and mica content (Lee et al., 2007)

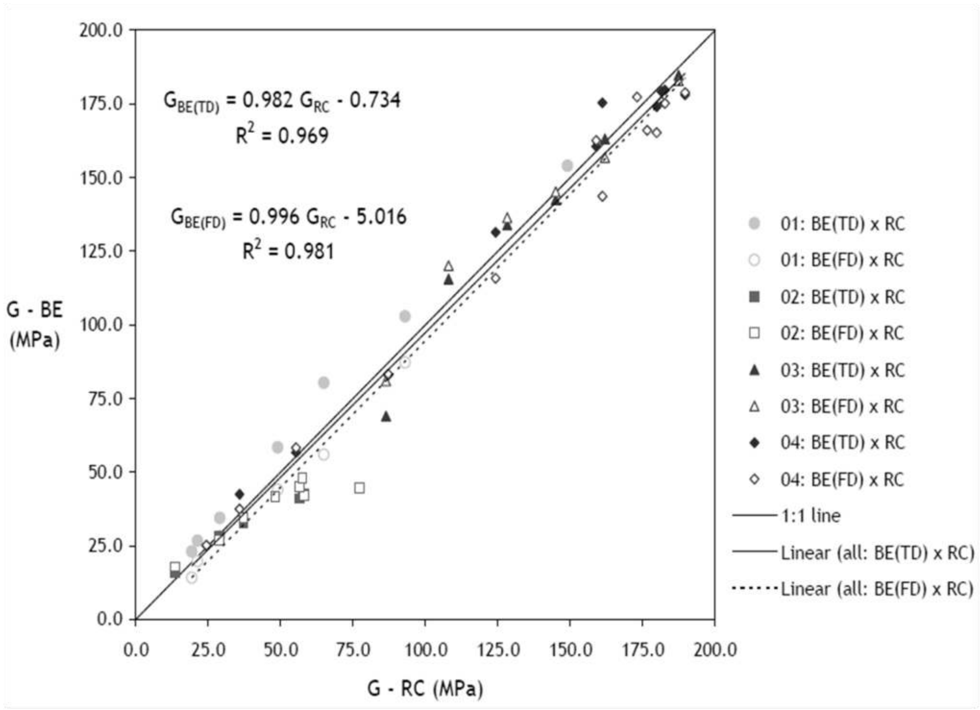

Figure 2.13 G_0 results measured by the RC compared with that evaluated by the two BE methods (Ferreira et al., 2007)

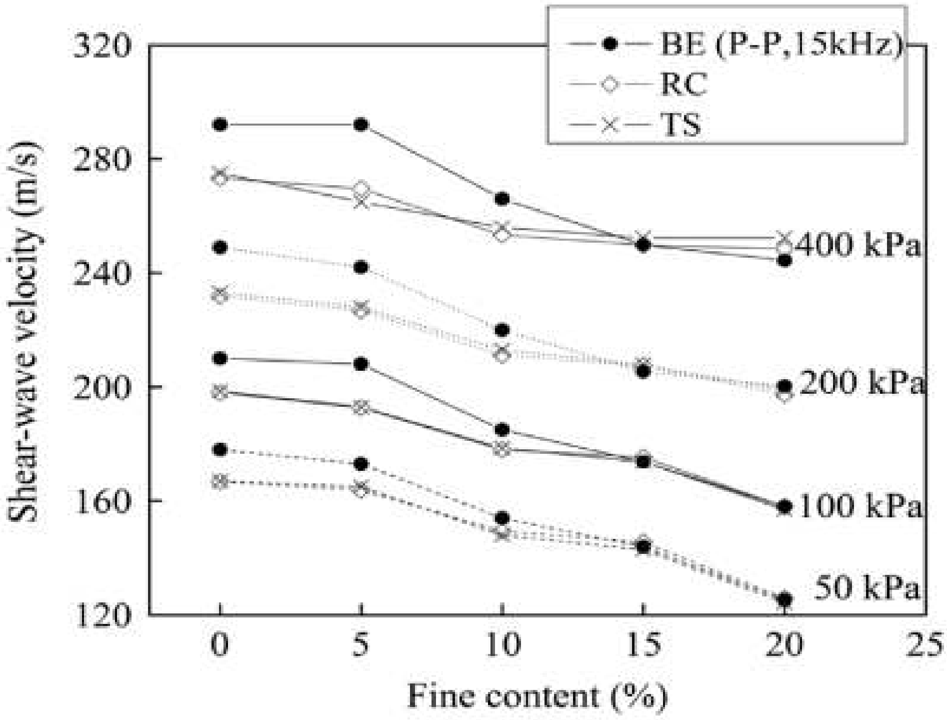

Figure 2.14 Change in maximum shear modulus with fines content under various confining pressures and similar void ratio (Cai et al., 2015).

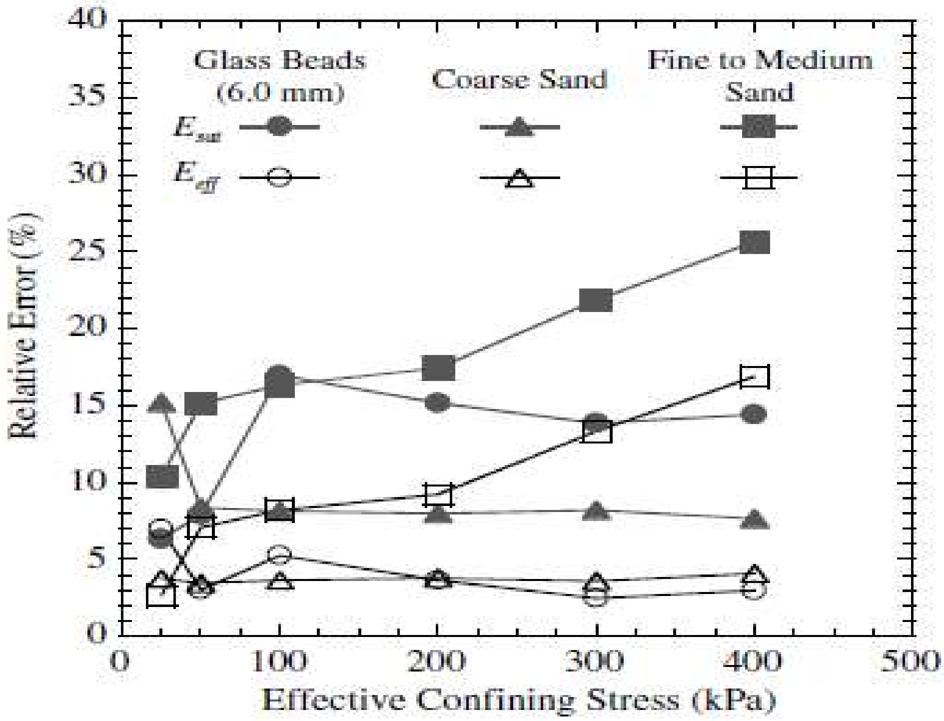

Figure 2.15 Relationship between relative errors of G_{max} and effective confining stress for bender elements tests in saturated conditions (Qiu et al., 2015).

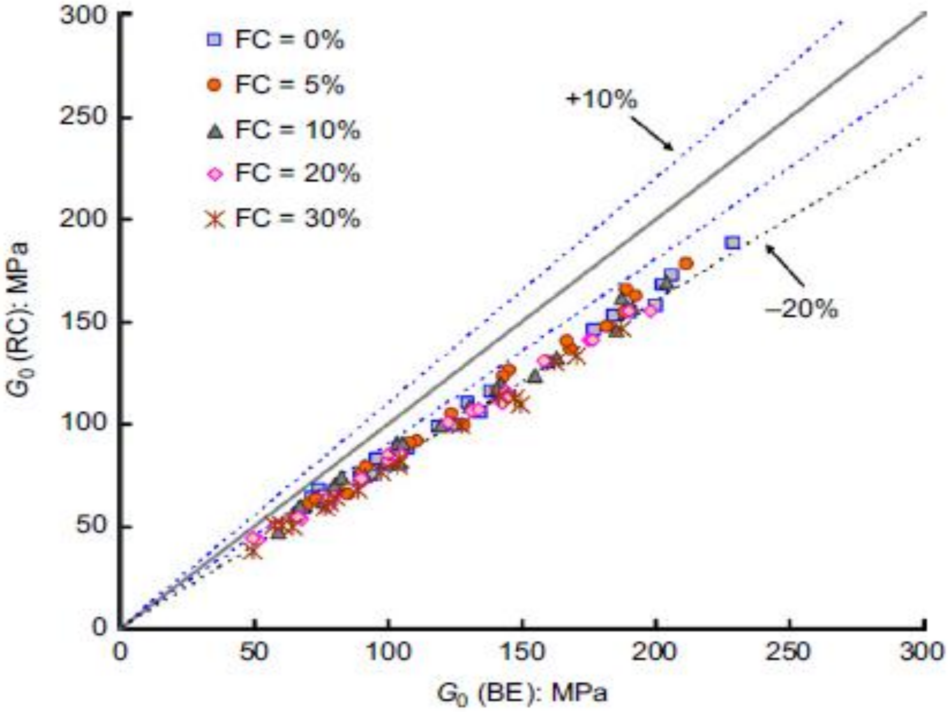

Figure 2.16 Comparison of G_0 values that evaluated by bender element and resonant column tests of clean sand and sand-fines mixtures(Yang and Liu, 2016).

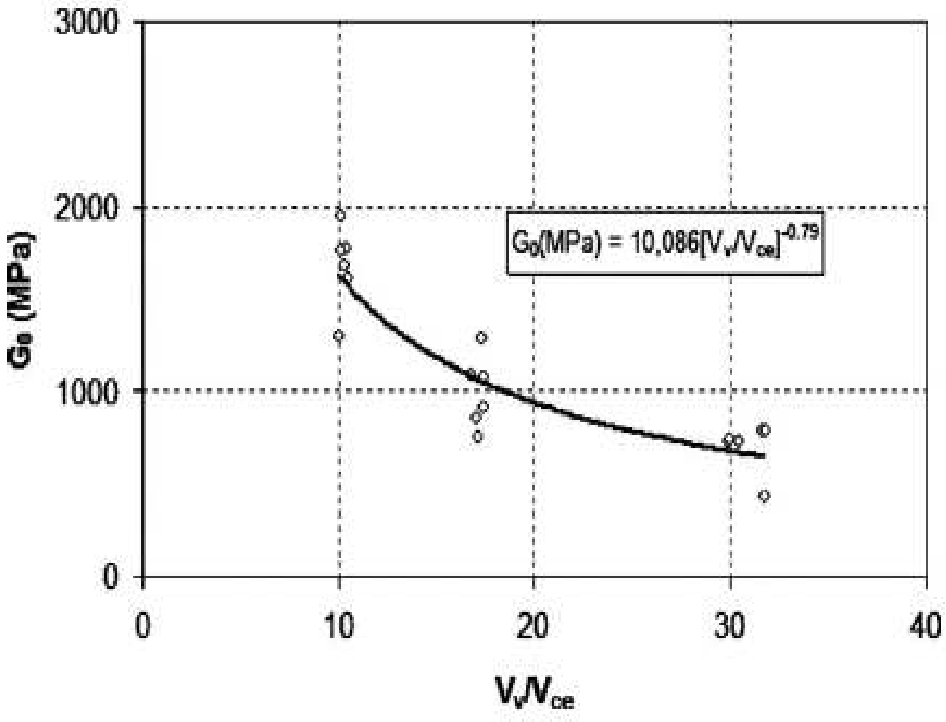

Figure 2.17 Change in small-strain shear modulus (G_0) with voids/cement ratio(V_υ/V_{ce}) (Consoli et al., 2009)

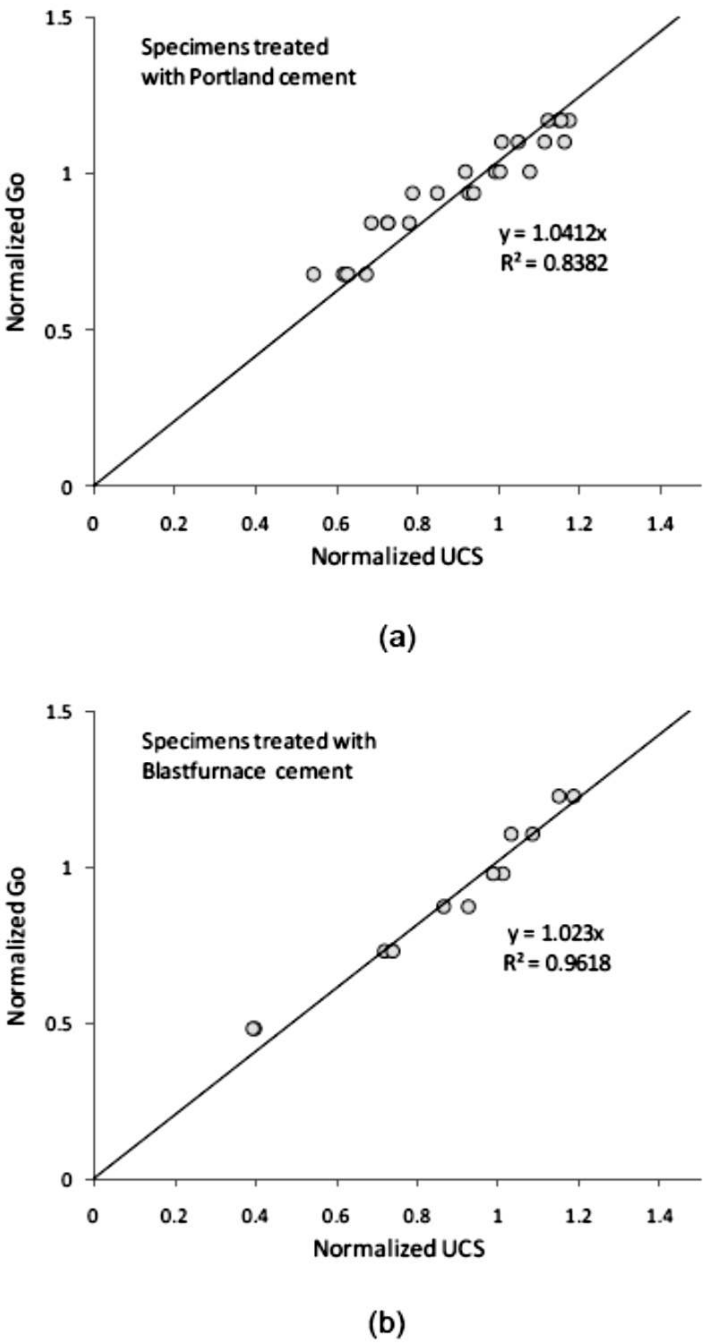

Figure 2.18 Variation of normalized G_0 with normalized UCS: (a) sample treated with Portland cement (b) sample treated with blast furnace slag cement (Flores et al., 2009).

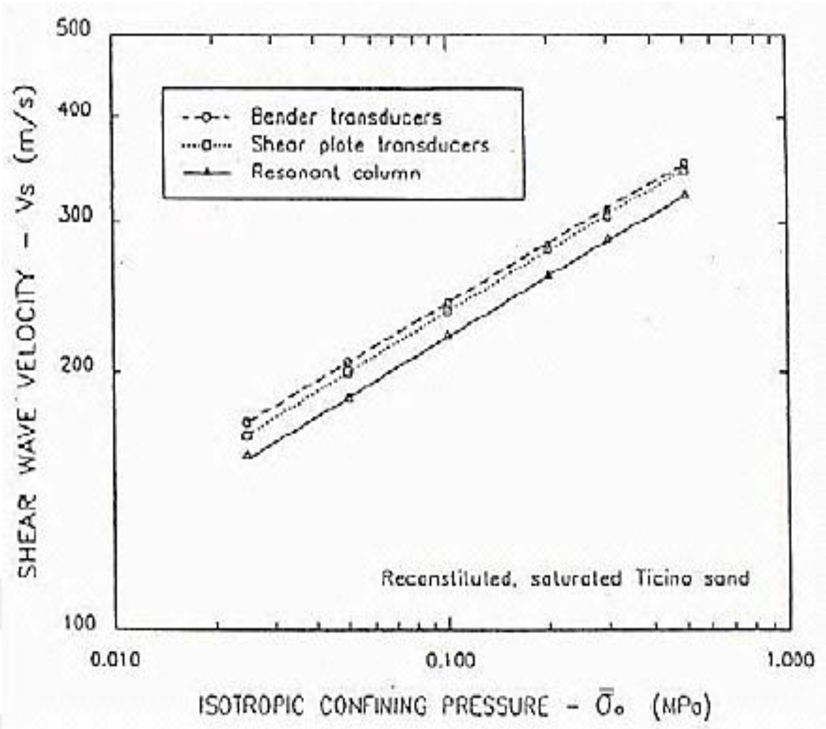

Figure 2.19 Comparison of variations of the Vs with confining pressure measured using different methods (Brignoli et al., 1994).

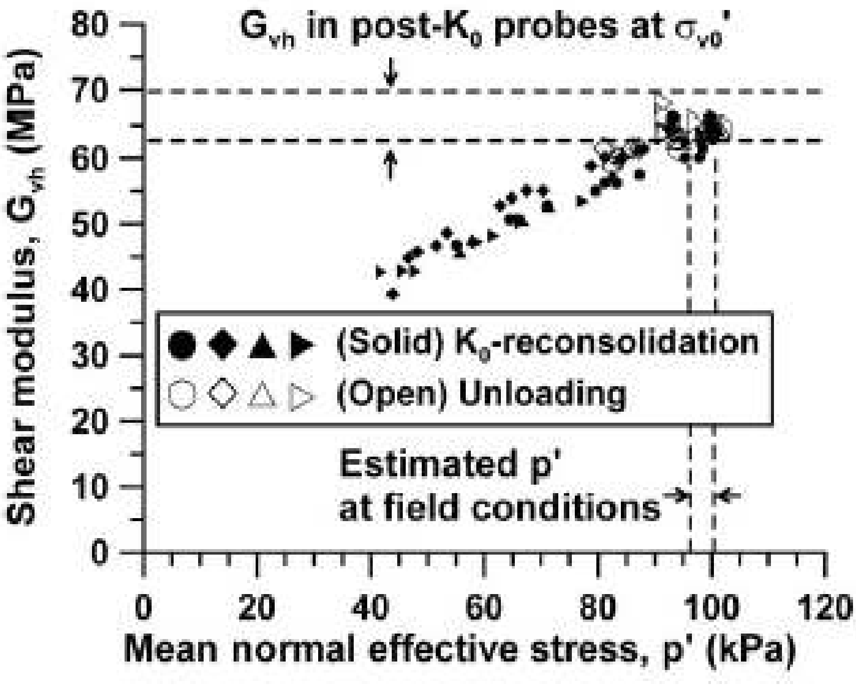

Figure 2.20 Relationship between shear modulus (G_{vh}) and mean normal effective stress (p′) during K_0 reconsolidation and unloading (Finno and Cho, 2010).

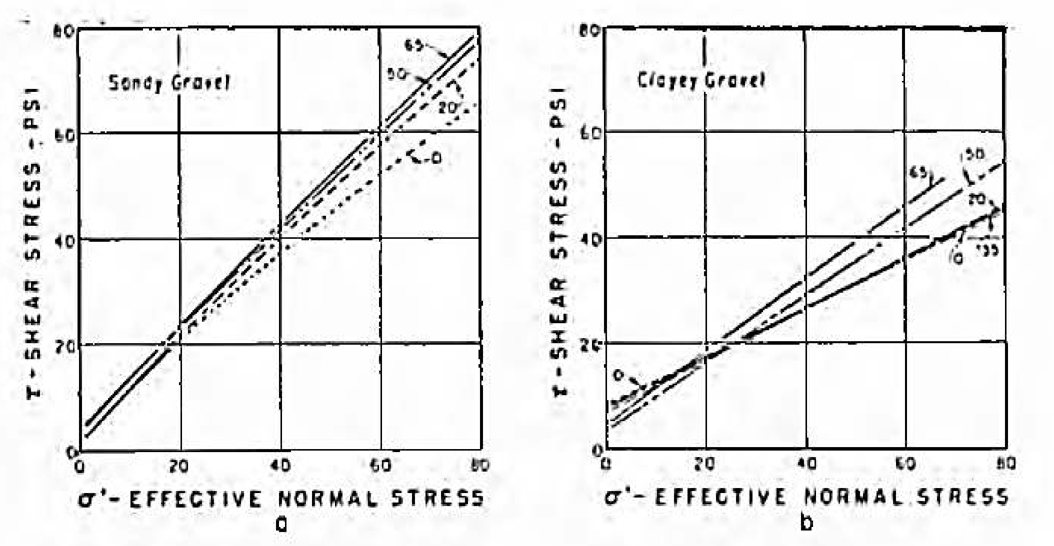

Figure 2.21 Summary of shear test results for sandy and clayey gravel soils (Holtz and Willard, 1956).

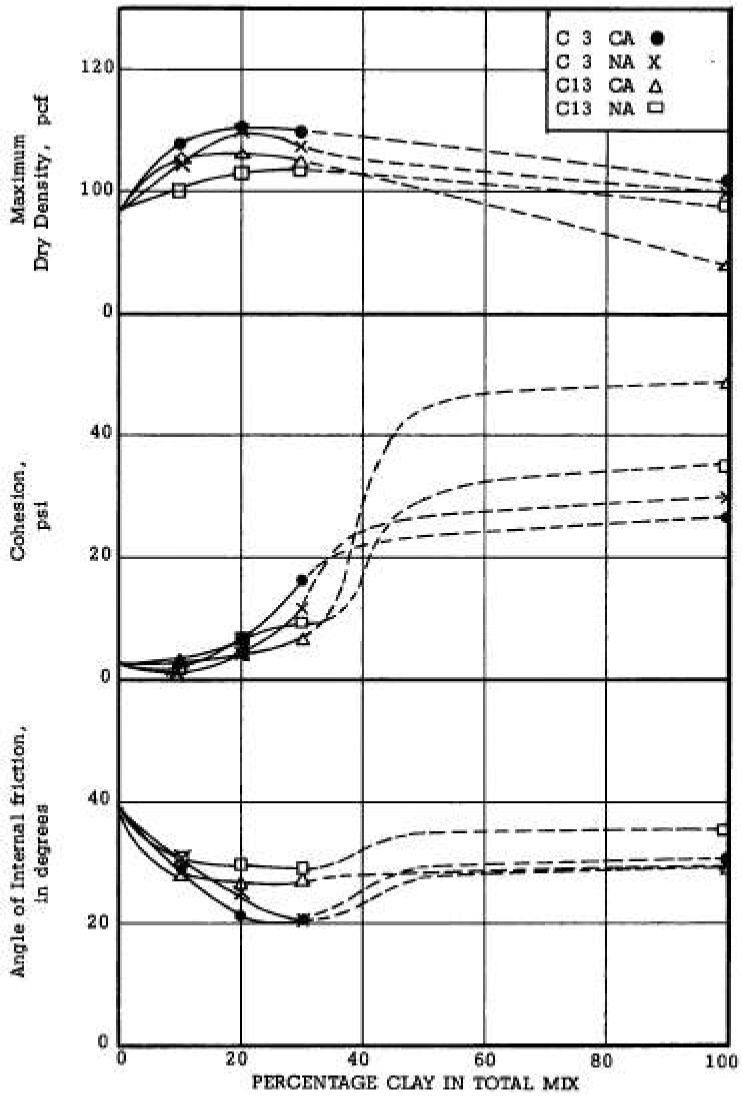

Figure 2.22 Effect of clay percentage on maximum dry density, cohesion and angle of internal friction (Miller and Sowers, 1958).

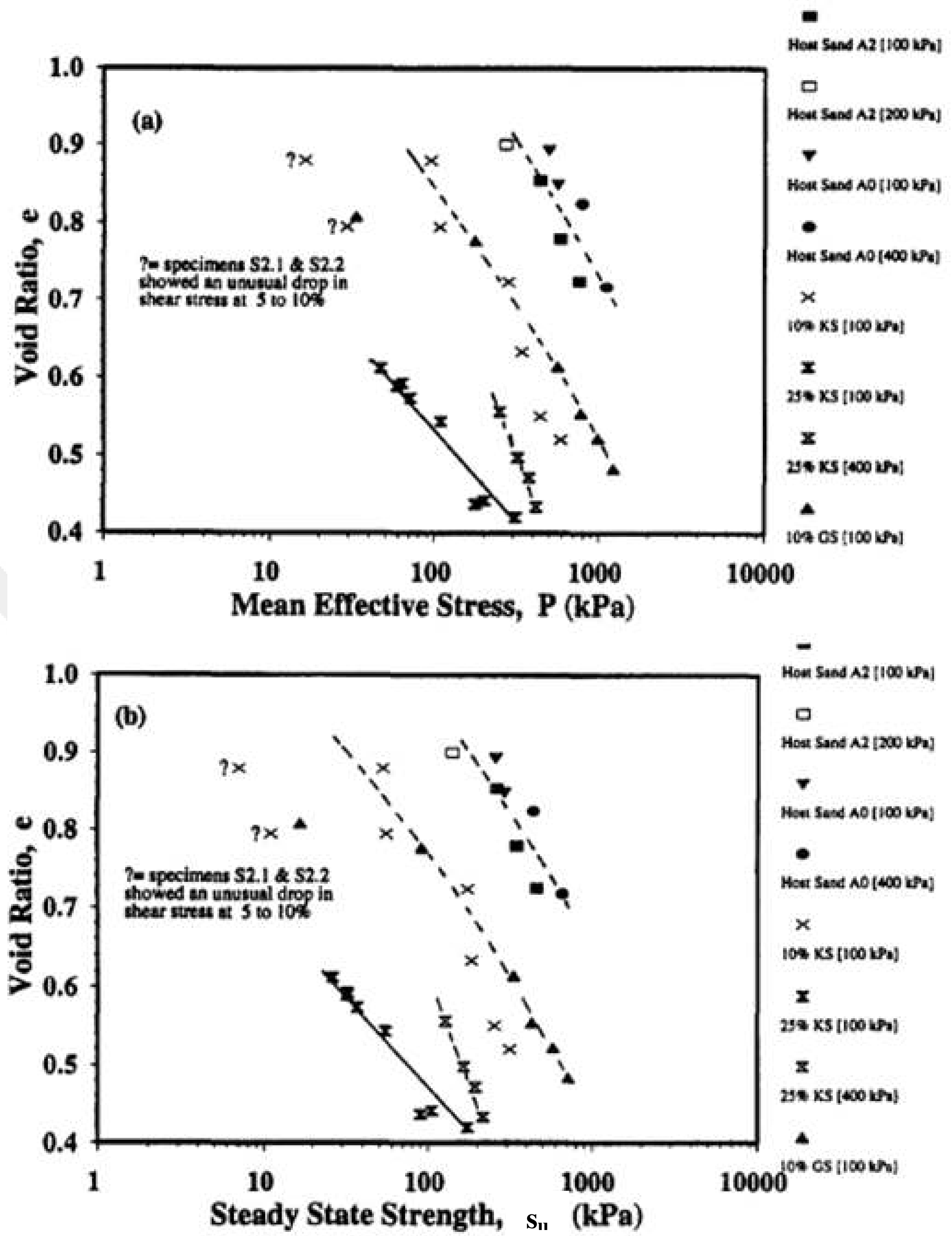

Figure 2.23 Steady-state data (a) e versus p; (b) e versus s_u (Thevanayagam, 1998)

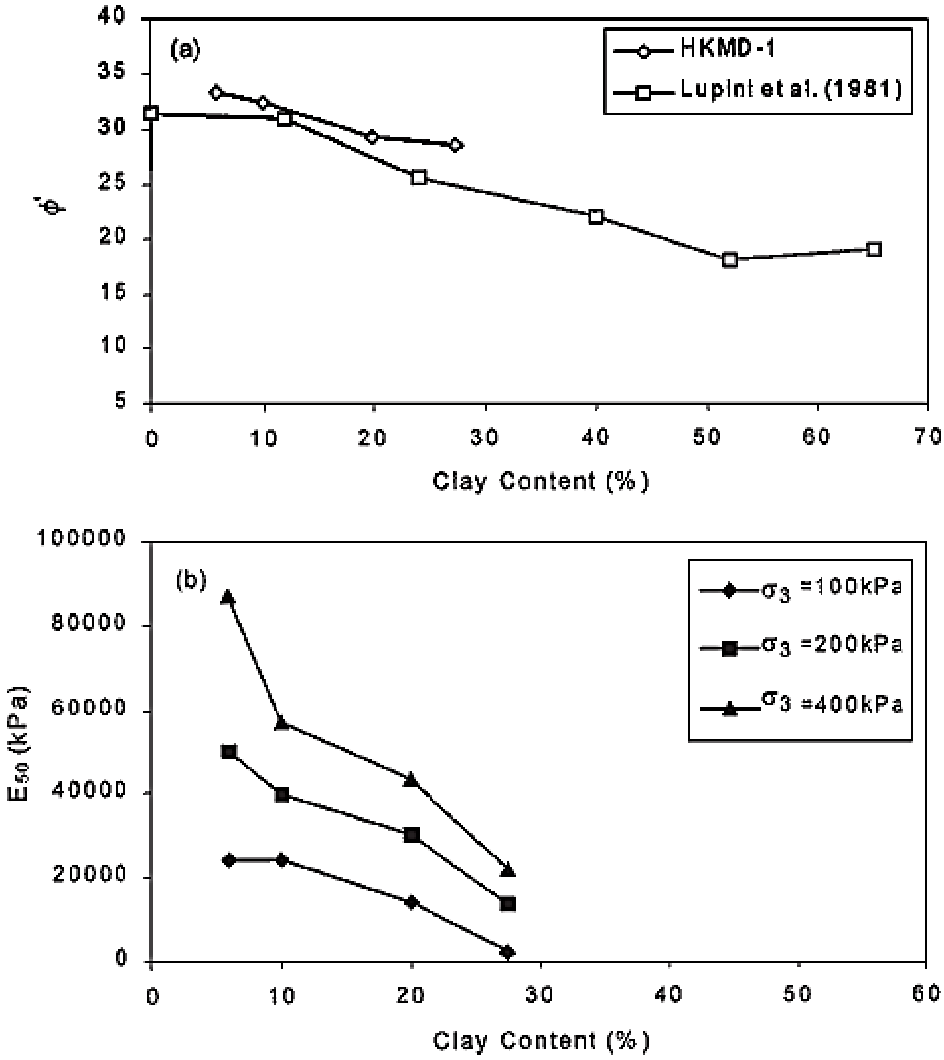

Figure 2.24 (a) Relationship between effective friction angle (ϕ′) and clay content for HKMD-1 and a sand-bentonite mixture (from Lupini et al. 1981). (b) Relationship between Young's modulus *E*50 and clay content for HKMD-1(Yin, 1999).

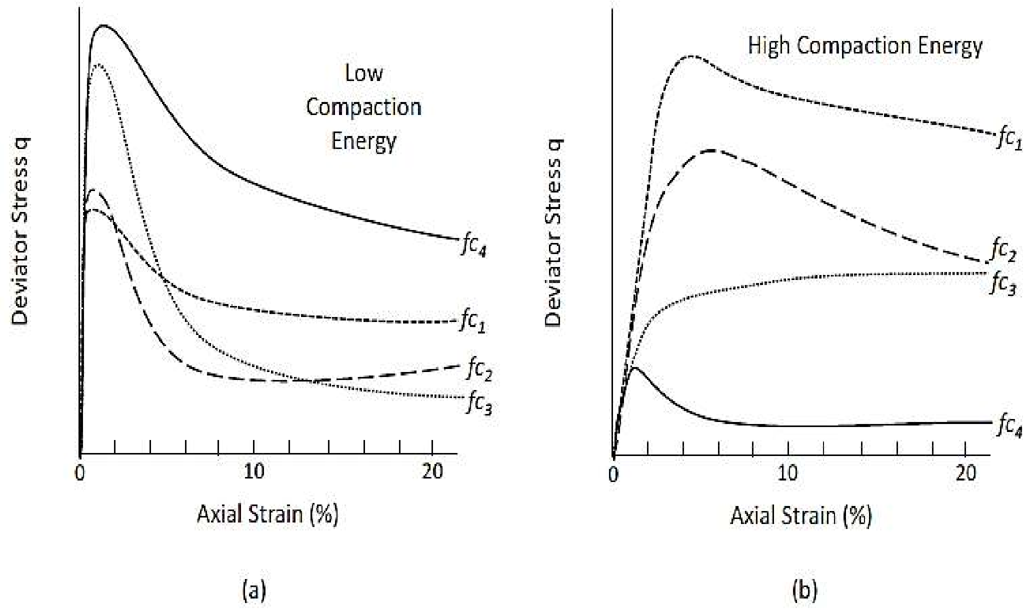

Figure 2.25 Generalized influence of plastic fines content on monotonic shear behavior with *fc* representing fine fraction by mass with $fc_1 < fc_2 < fc_3 < fc_4 < fc_{plastic}$ and $fc_{plastic}$ denoting the fines content when mixture transitions from non-plastic to plastic behavior (Kim et al., 2006).

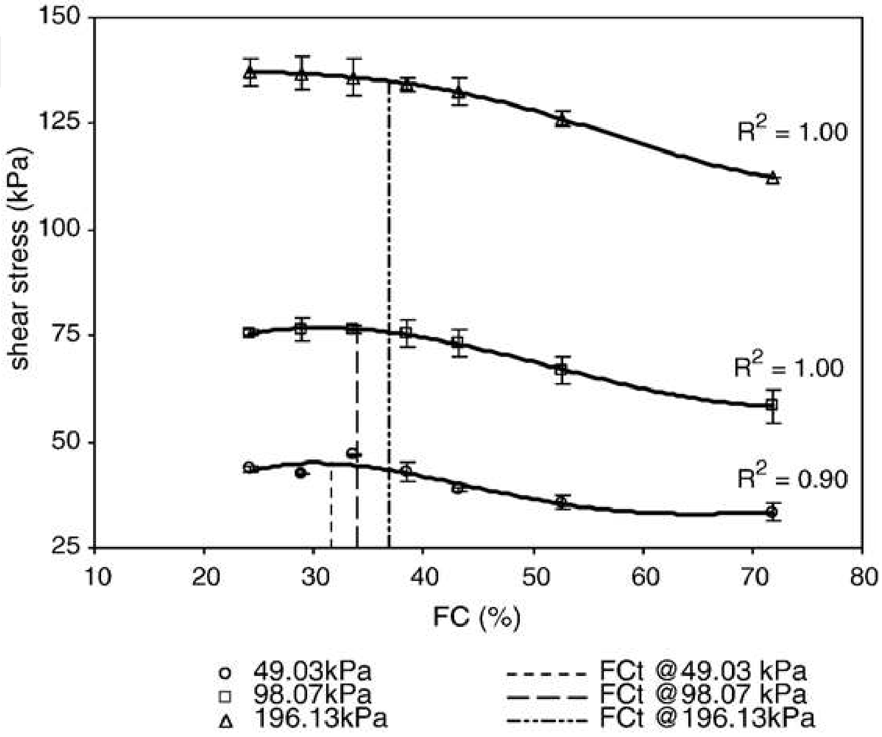

Figure 2.26 Relationship of shear strength and fines content with various normal stresses (Monkul and Ozden, 2007).

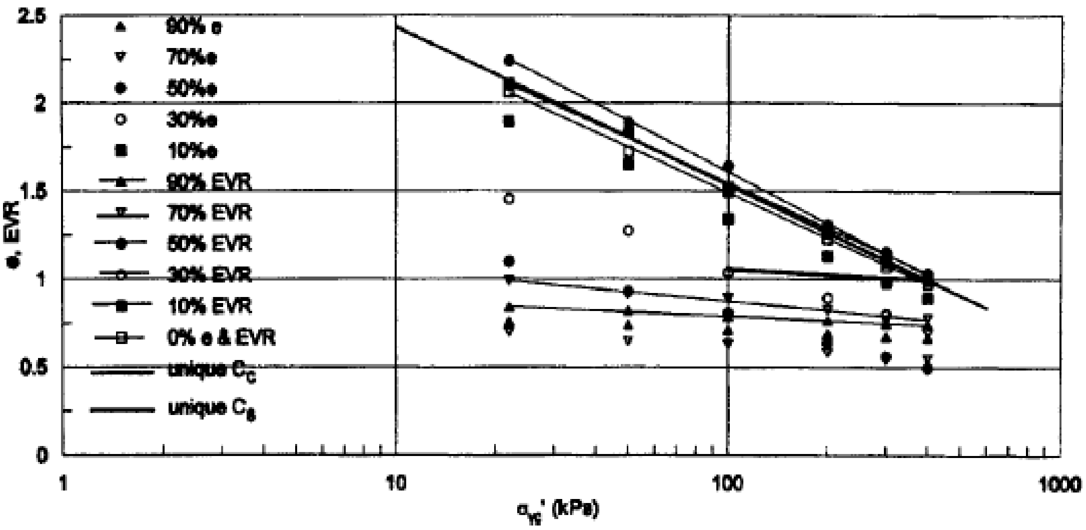

Figure 2.27 Influence of fines content on monotonic shear behavior with $fc_1 < fc_2 < fc_3$ (Cubrinovski and Rees, 2008).

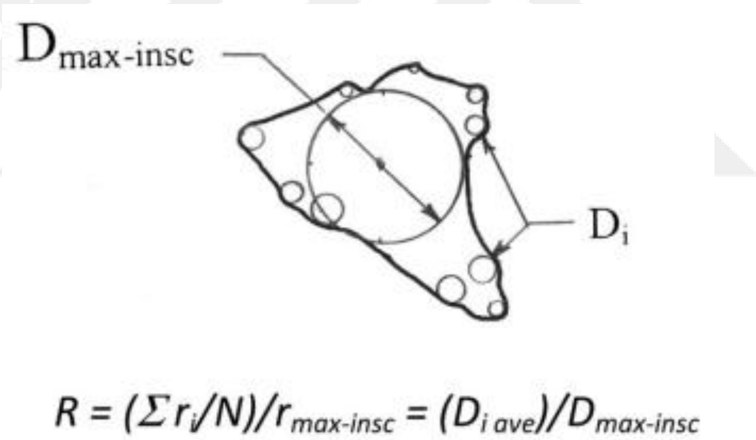

Figure 2.28 Graphical representation of roundness (R) (Muszynski and Vitton, 2012).

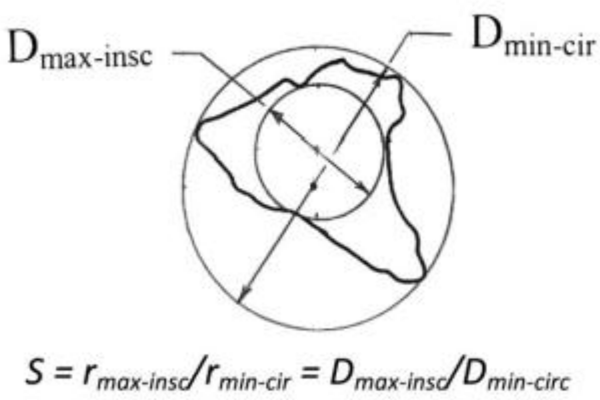

Figure 2.29 Graphical representation of sphericity (S) (Muszynski and Vitton, 2012).

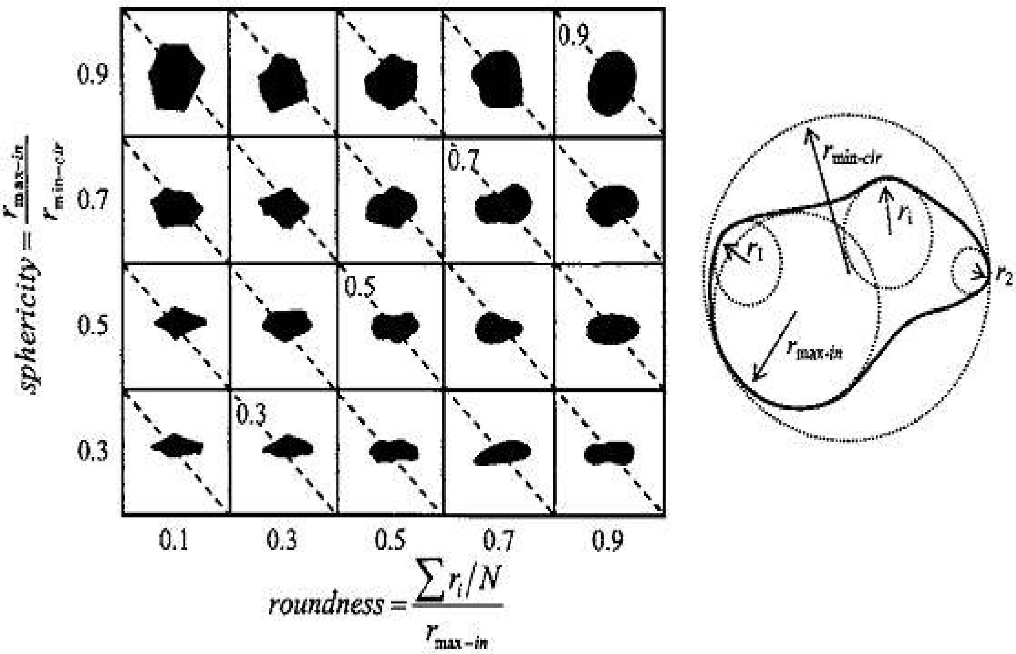

Figure 2.30 Chart of comparison for particle shape parameters (Santamarina and Cho, 2004).

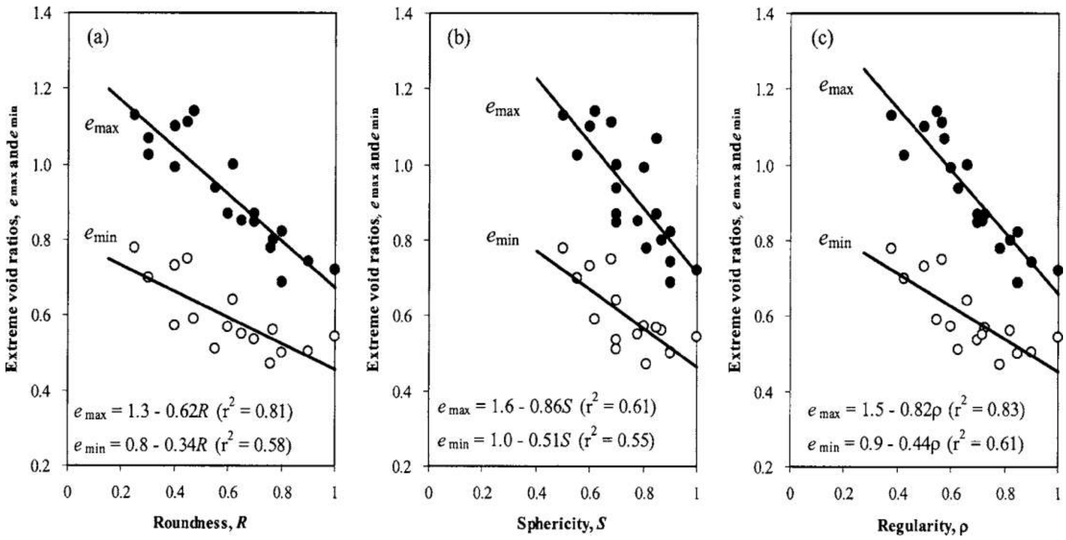

Figure 2.31 Correlation between particle shape parameters and extreme void ratios (natural sands of $C_u \leq 2.5$) (Cho et al., 2006).

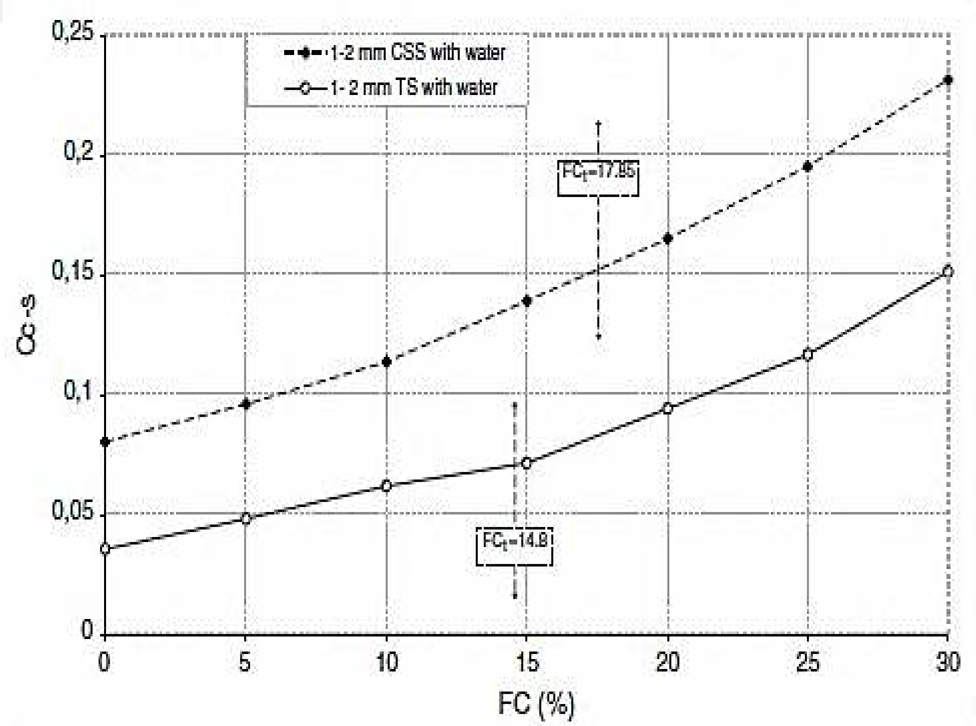

Figure 2.32 Relationship between granular compression index and fines content of TS and CSS (Cabalar and Hasan, 2013).

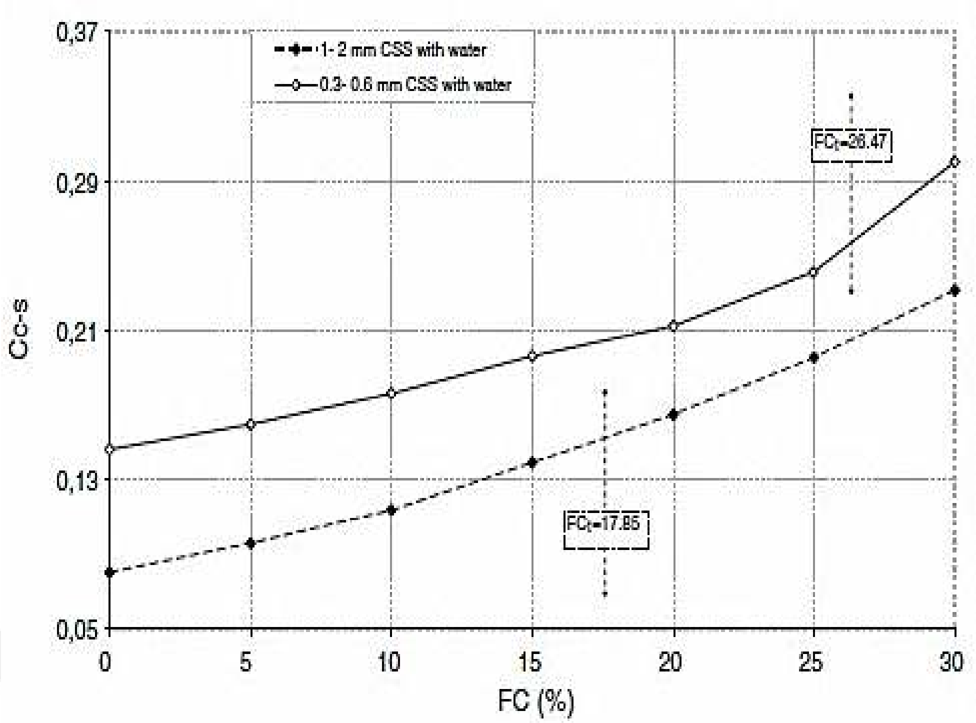

Figure 2.33 Change in granular compression index with fines content with various sizes of CSS (Cabalar and Hasan, 2013).

CHAPTER 3

EXPERIMENTAL STUDY

3.1 Materials

The materials used in the experimental work of this study were clay, Narli Sand (NS) and Crushed Stone Sand (CSS).

Clay

The soil used in this study was a clayey soil which was quarried from the Gaziantep University Campus. The liquid limit of this clay is 41, and its plastic limit is 23 in accordance with ASTM D4318. Depending on Unified Soil Classification System (USCS), this type of soil is classified as 'low plasticity clay' which is denoted as CL. The specific gravity (G_s) of the clay is 2.61. The modified proctor test was performed according to ASTM D1557 standards to compute the maximum dry unit weight (γ_{drymax}) and optimum moisture content (w_{opt}) values, which were found to be 17.12 kN/m^3 and 18.4%, respectively.

Narli Sand and Crushed Stone Sand

Narli Sand representing a rounded sand, was quarried from Kahramanmaras city in southern-central of Turkey. Crushed Stone Sand with an angular shaped sand grains which is a commercially available was obtained from southern-central Turkey. It is vastly used in earthworks in certain regions of Turkey. The Gs of the sand grains was found to be 2.65 for Narli Sand, and 2.68 for Crushed Stone Sand. Three different gradations of these sands ranged between 0.6 mm and 0.3 mm, 1.0 mm and 0.6 mm, and 2.0 mm and 1.0 mm were chosen to obtain uniform specimens for classification purposes. Figure 3.1 shows the grain size distribution of these sizes of sand. The Roundness (R) estimates for CSS and NS were obtained as 0.16 and 0.43, while the sphericity (S) estimates were found to be 0.55 and 0.67, respectively. Table 3.1 shows roundness (R) and sphericity (S) estimates made depend on the study by Muszynski and Vitton (2012) and coefficients of grain size.

Clay-sand mixtures

A series of clay-sand mixtures were studied at different sand contents, shapes and sizes to investigate the effect of sand grains shape and size on the engineering properties of clayey soil. Five percentages by dry weight of clay-sand (90-10, 80-20, 70-30, 60-40 and 50-50) of three grain sizes of sand (2.0-1.0 mm, 1.0-0.6 mm and 0.6-0.3 mm) of two shapes of sand (angular and rounded) were studied. Clay and sand were mixed manually, and the amount was computed on the oven-dried base. Table 3.2 shows the γ_{drymax} and w_{opt} values of clay and all the clay-sand mixtures tested.

The testing plan of this study is presented in Table 3.3.

3.2 Testing Devices

3.2.1 Bender Elements

Bender elements (BE) are piezo-ceramic sheets inserted in either a top cap or pedestal. In the top caps, the inserts are manufactured from titanium to give high rigidity and to reduce the insert weight to half of the stainless steel insert manufactured for the base pedestal. This reduces the applied axial load. The bender element system consists of the following components:

- Two bender elements with adapted top cap and pedestal as shown in Figure 3.2
- External control box
- High-speed PC data acquisition and control card
- Windows based Bender Element System control and acquisition software (GDSBES) (www.gdsinstruments.com).

The bender elements are manufactured to be mounted in the top cap and pedestal of triaxial device (Giang et al. 2017). This allows to replace them easily and to used them with a many types of the triaxial cells. When carrying out the bender element test, the phase orientation of the elements is significant. A consistent phase relationship between source and receive signals makes post processing more intuitive, and therefore simpler. There are several functions can be obtained from the external control box supplied with the GDS Bender elements, which are:

- Power supply system
- Signal conditioning
- The source signal amplification
- Shear and compression wave velocity tests can be switched between them easily.

Because of the insufficiency of suitable standards for determining the travel times using bender element test, the GDS company developed a new tool which is GDS Bender Element Analysis Tool (GDS BEAT). It is a series of Add-Ins compatible with Microsoft Office program of version not less than 2007 that permit to compute travel times from bender element test results (www.gdsinstruments.com).

3.2.2 Triaxial Compression

Triaxial tests equipped with bender elements were conducted on clayey soil samples and clay-sand mixtures samples using a triaxial machine manufactured by ELE company with a 70 mm diameter and a load capacity of 50 kN. The testing system of the triaxial equipped with bender elements is presented in Figure 3.3. As can be seen from this figure, the triaxial system consists of loading frame, step motor, load cell, an external linear displacement sensor (LDS), linear variable differential transformers (LVDTs), pore pressure transducers, pressure volume controllers, and data acquisition system. The loading frame has a maximum load of 50 kN. The maximum load of this device is mostly restricted by the tensile resistance of the two main columns, which support the upper beam, and by the step motor, which applies a constant strain rate. The step motor permits for upwards or downwards movement of the base plate of the device, thus permitting for applying a constant rate of strain. A front panel permits the choice of the strain rate through a strain rate control switch, two buttons for the upwards and downwards direction, one stop button and two buttons for quick base plate movement.

The loading frame is companied by a triaxial cell. The triaxial cell which is manufactured by a local company has an inner diameter of 280 mm and height of 470 mm, and a design pressure of 1700 kPa. The wall of this cell is made by Perspex material to provide maximum visibility. The cell was manufactured in such a size to give a good clearness between the local instrumentation such as internal LVDTs and bender elements connections inside the cell. The pedestal of the triaxial cell is a circular on which the chamber is firmly screwed on by six external tie rods. The water tightness of the pedestal and the chamber is achieved through an O-ring, which is placed in a circular groove, on the pedestal. There are three pressure lines of water connected with the base plate. The first pressure line is used to fill the chamber with water. This line is connected to a pressure volume control which is used for applying and measuring the cell pressure. The next (second) pressure line is connected to the sample at the pedestal, and is used either to flush water into the sample, or allow drainage from the sample. At the same time it can be connected to the other pressure volume control which is used to apply back pressure on the sample and to measure the pore water pressure. Finally, the third pressure line is connected to the pressure volume control which is used to apply the suction on sample for saturation. This line is connected to a pipe which in turn connected from other side to a valve on the receiver bender element that is used to take out the water from the top of sample during the saturation process.

In the upper part of the chamber, a de-airing valve allows the user to extract air trapped in the upper part of the chamber. Such de-airing valve may prove to be of great importance because of the cell must be fully filled with water and no air is allowed to stay in the cell. A strain arm as a mounting block is installed on the upper part of the cell, for global measurement of axial displacement of the sample by displacement transducer which is attached to the strain arm. A LDS mounted on the vertical rods of the frame, while its spindle comes into contact with the upper part of the cell by the strain arm. A loading ram is also allowed to slide in the triaxial cell along a hole in the top of the cell. The loading ram is fitted into the cell with a low friction, low leakage assembly. The water tightness of the contact between the load ram and the hole is achieved through an O-ring. The loading ram applies the axial force to the top of receiver bender element that located on the top of the sample during a triaxial test. The axial force measured by a submersible load cell. This load cell is designed for use fully submerged in the water at maximum pressures of 7000 kPa. It is used in pressurized triaxial chambers for determining the shear strength parameters (cohesion and angle of internal friction). The submersible load cell is fixed on the lower part of the loading ram in the triaxial cell to give a more accurate measurement of the axial force applied to the sample.

3.3 Calibration of Devices

3.3.1 Calibration of Bender Elements

Before testing soil in the bender elements, it is important to conduct a series of test for the calibration of this system. Because of the time delay arising from coating materials, ceramics and electronics, the measured travel time between transmitted and received signals is larger than the travel time (t) across the soil sample (Brignoli et al., 1996). The time delay is evaluated by measuring a travel time between transmitted and received signals when the transmitter and receiver elements are placed directly in contact as shown in Figure 3.4. In theory, the time delay should be null, since the tips of the elements are in contact, that is, at null travel distance (Camacho-Tauta et al., 2012). The travel time, t (which is used to calculate wave velocity Vs as in Equation 2.4) is computed by subtracting the delay time from the measured travel time. The time delay value was 0.0014 ms during measurement of shear wave velocity using a sinusoidal signal as presented in Figure 3.5. The absence of wave transmission paths, other than through the soil sample, was checked as well by placing the two elements without any soil and without contact and ensuring that no wave arrival was recorded by the receiver when pulses were generated by the transmitter.

3.3.2 Calibration of Triaxial

The calibration graphs of a submersible load cell, a linear displacement sensor (LDS), cell and back pressure transducers and submersible linear variable differential transformers (LVDTs) are presented in Figures 3.6-3.11, respectively.

3.4 Specimen Preparation and Test Methods

3.4.1 Unconfined Compression Apparatus Equipped with Bender Elements

Bender element tests were conducted on the different clay-sand mixtures to evaluate the shear wave velocity at various frequencies, sand contents, grain shapes and grain sizes, thus to calculate the maximum shear modulus (G_{max}). The tests were carried out just before applying a uniaxial load to the compacted specimens taken out from the two-part split mold with a 70 mm in diameter and 147 mm height. The samples were prepared at γ_{drymax} and w_{opt} values. The shear wave velocity measurements were performed by a pair of bender elements, one of which was installed on the pedestal, and the other one was placed in the top cap. The bender element on the pedestal was used as a transmitter, while the other in top cap was used as a receiver to measure the shear wave propagated through a specimen. Software package for data acquisition as well as the BE testing equipment used during the experimental works is a product of GDS Instruments Limited. The Vs estimates were achieved by employing a sinusoidal wave input with a magnitude of 10 V, and periods of 0.01 mV. Acquisition of the received wave was obtained using a sampling frequency of 5, 10, 15, 20, and 25 kHz to study the effect of frequency on G_{max} of clay-sand mixtures, and a sampling interval of 15 ms. The shear wave velocity transmitted through the specimens was estimated using 'tip-to-tip' distance between the bender elements (Viggiani and Atkinson, 1995), consequently wave travel time was evaluated. To obtain the arrival time value, the first major peak-to-peak method was employed. The arrival time in this method was defined as the time measured between the peak of the source signal and the first major peak of the received signal.

The unconfined compression (UC) test, which is used for determining the undrained shear strength of cohesive soils because of simplicity of the test technique, was employed on various clay-sand specimens compacted in a mold with a 70 mm in diameter and 147 mm height (ASTM D2166). The cylindrical soil specimens were compacted by static compaction in a mold at a γ_{drymax} and w_{opt}. All samples were compacted in three equal layers, with each layer statically compacted in a compression frame at a fixed displacement rate of 1.27 mm/min. The behaviour of the samples was studied with the clay, and clay mixed with sand at the mixture contents of 10%, 20%, 30%, 40%, and 50% by dry weight of the samples. Amount of each constituent in a mixture was determined by employing compaction test to prepare the specimens at the γ_{drymax} and w_{opt} values. In this experimental work, the required amount of sand, clay, and water was weighed and thereafter mixed until a homogeneous mixture reached. The specimens were kept in plastic bags during 24 hours to avoid the loss of moisture, and to obtain a homogeneous paste. A mixture to be tested was then statically compacted into a two-part cylindrical mold (70 mm x 147 mm) in three layers. Then, the samples were extracted from the mold, trimmed out, and placed on to the UC testing equipment to estimate the shear wave velocity first, and then the q_u value for each specimen. The rate of strain employed in the UC tests was 0.7 mm/min. Figure 3.12 presents the equipment used for experimental determination of both G_{max} and q_u values.

3.4.2 Triaxial Machine Equipped with Bender Elements

The triaxial equipped with bender elements tests were carried out on three percentages by weight of clay-sand (90-10, 70-30, and 50-50) of two particle sizes of sand (2.0-1.0 mm and 0.6-0.3 mm) of two shapes of sand (angular, CSS, and rounded, NS). The type of triaxial test used in this study was consolidated undrained (CU) test to study the soil behavior in the undrained conditions and to investigate the effect of sand content, shape and size on the change in pore water pressure with strain.

After preparing the sample by the same method that was used in the unconfined compression testing device equipped with bender elements, both of the height and the diameter of the compacted sample were measured at three various positions using a digital caliper. The pedestal flushed with de-aired water before a filter paper is placed on the pedestal to avoid trapping air between the base and the sample. Then, a filter paper was placed on the pedestal fitted with the transmitter bender element. The transmitter bender element inserted in the soil sample by pushing the sample in the bender element without disturbing the sample. A special mold containing hole connected to an elastic pipe is used to position the membrane around the sample (Figure 3.13). The membrane is placed inside the special mold and the top and bottom of the membrane was folded back over the mold. The air pulled out of the special mold using the elastic pipe to make the membrane stacked to the walls of the special mold (Figure 3.14). To position the membrane around the sample, the special mold with the stacked membrane is placed around the sample. When the air blows inside the mold, the membrane is stacked around the sample. After that, two O-rings were pushed into place over the membrane at the bottom using an O-ring stretcher (Figure 3.15). A two-part split mold with two O-rings at the top was placed around the sample with membrane. The filter paper is placed on the top of the sample. Top of the membrane was folded back over the mold and the receiver bender element inserted in the top of soil sample without disturbing the sample. Top part of the membrane was pulled off the split mold, stretched around the receiver bender element and was tighted by two O-rings without disturbing the sample. The two part split-mold was carefully removed after that (Figure 3.16). The vacuum applied to the sample was about 20 kPa. This vacuum was kept by identifying a target pressure of -20 kPa to the pressure volume controller that connected to the third pressure line. The LVDT brackets were glued to the membrane with super glue. The two LVDTs were fixed to the sample sides in the same position in the middle third of the sample (Figure 3.17).

Saturation of soil sample was made by introducing the water to the sample through second pressure line, the water was flushed from the bottom to the top until the water seep up through the sample from the top of sample next day. The triaxial cell was located on the circular groove of the base plate around the sample; the load ram was attached to the top of the receiver bender element. The tie rods were placed on its position on the triaxial cell to prevent water to seep outside especially when the water being under pressure when increasing cell pressure, then the cell was filled with water (Figure 3.18). Back pressure inside the sample was increased at small increments until the desired pressure values were achieved (350 kPa back pressure) to remove the air trapped between the soil particles, this value of back pressure is located within the range (300-600 kPa) that investigated in the previous studies. The sample was kept under the specified pressures for about 24 hours for consolidation. B-value was estimated by closing the valve that connected to the second pressure line, whilst the cell pressure is increased of 10 kPa, then the change in sample pore pressure resulted by the change in confining pressure is measured. After the B-value is checked, the cell pressure was decreased of 10 kPa, then the valve was opened again. The B-value was found to be between 96 and 97 % (Skempton, 1954).

After consolidation process completed, bender elements test was conducted to evaluate the shear wave velocity, thus the maximum shear modulus. The Vs estimates were achieved by employing a sinusoidal wave input with a magnitude of 10 V, and periods of 0.01 mV. Acquisition of the received wave was obtained using a sampling frequency of 5 kHz, and a sampling interval of 15 ms which were selected to provide a received signal with optimal resolution. The stage of shearing test was started after measuring the shear wave velocity using bender elements.

The shearing stage of test for clay and clay-sand mixtures were started after completing the sample preparation, saturation and consolidation of sample. The drainage valve to the sample (back pressure channel) was closed. The load ram has been attached to the top of receiver bender element. The zero reading was set for the reading of the submersible load cell, internal LVDTs and external LDS. A standard machine rate of displacement equal to 0.03 mm/min was used throughout the testing to study soil behavior at small strains. During shear, deviatoric load, external axial strain, local strain by internal LVDTs, and pore pressure were recorded at 5 seconds intervals. The sample was tested under shearing until the axial strain value of about 15% which is the maximum strain can be measured.

3.5 Scanning Electron Microscopy (SEM)

The microscopic pictures of the materials used in the study (clay, NS and CSS) were conducted using a scanning electron microscope that produced by JEOL limited (joel 6390 LV, operating at 15 kV accelerating voltage) in the University of Gaziantep. Figure 3.19 presents SEM pictures of the materials that used in the study.

Table 3.1 Some properties of the sands used in the experimental study.

Gradation (mm)	D_{10} (mm)	D_{30} (mm)	D_{50} (mm)	D_{60} (mm)	c_u	c_c	R		S	
							NS	CSS	NS	CSS
0.6-0.3	0.33	0.39	0.45	0.48	1.45	0.96	0.43	0.16	0.67	0.55
1.0-0.6	0.64	0.72	0.80	0.84	1.31	0.96				
2.0-1.0	1.10	1.30	1.50	1.60	1.45	0.96				

Table 3.2 Some properties of the clay-sand mixtures used in the experimental study.

Sand Size (mm)	Sand content (%)	NS		CSS	
		γ_{drymax} (kN/m^3)	w_{opt} (%)	γ_{drymax} (kN/m^3)	w_{opt} (%)
---	0	17.12	18.4	17.12	18.4
0.6-0.3	10	17.41	16.8	17.24	16.3
	20	17.83	15.8	17.65	15.3
	30	18.25	14.6	18.02	14.2
	40	18.59	13.5	18.41	13.1
	50	18.93	12.7	18.74	12.3
1.0-0.6	10	17.58	16.2	17.44	15.7
	20	18.04	15.2	17.86	14.8
	30	18.57	14.3	18.39	13.9
	40	18.88	13.4	18.69	13.0
	50	19.12	12.6	18.93	12.3
2.0-1.0	10	17.76	15.5	17.58	15.1
	20	18.23	14.6	18.08	14.2
	30	18.76	13.8	18.57	13.4
	40	19.07	12.9	18.90	12.5
	50	19.31	12.2	19.16	11.8

Table 3.3 Testing plan of the study.

Test	Materials	Sand Shape	Sand Size (mm)	Sand content (%)
Unconfined Compression Machine Equipped with Bender Elements	Clay, Sand	Rounded, Angular	0.6-0.3, 1.0-0.6, 2.0-1.0	10, 20, 30, 40, 50
Triaxial Compression Machine Equipped with Bender Elements	Clay, Sand	Rounded, Angular	0.6-0.3, 2.0-1.0	10, 30, 50

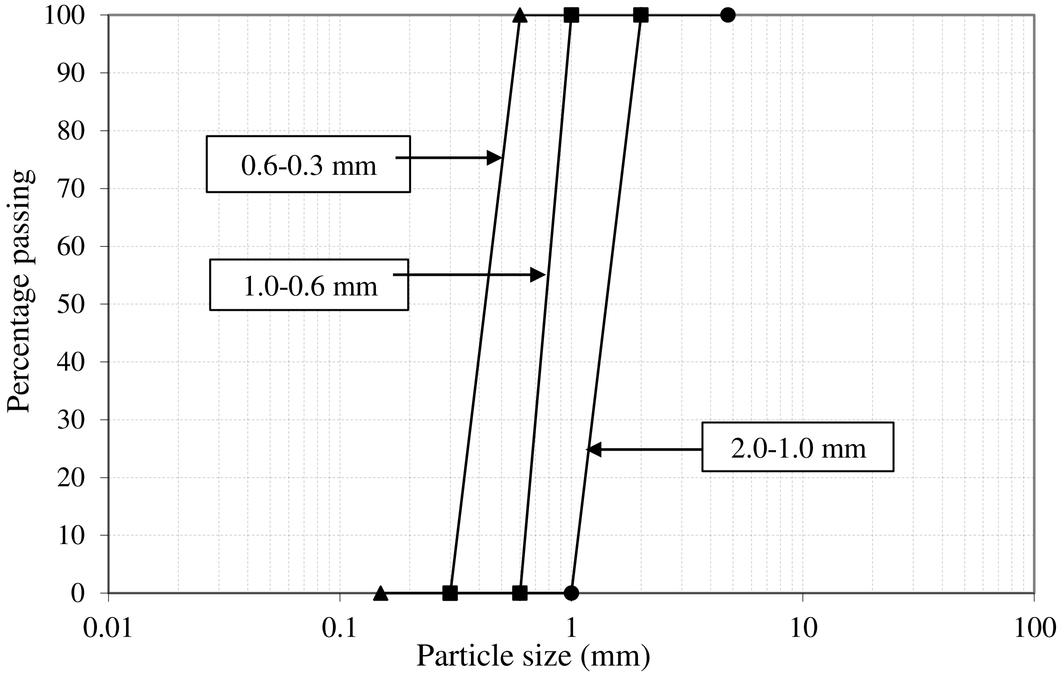

Figure 3.1 Particle size distributions of the sands used in the experimental study.

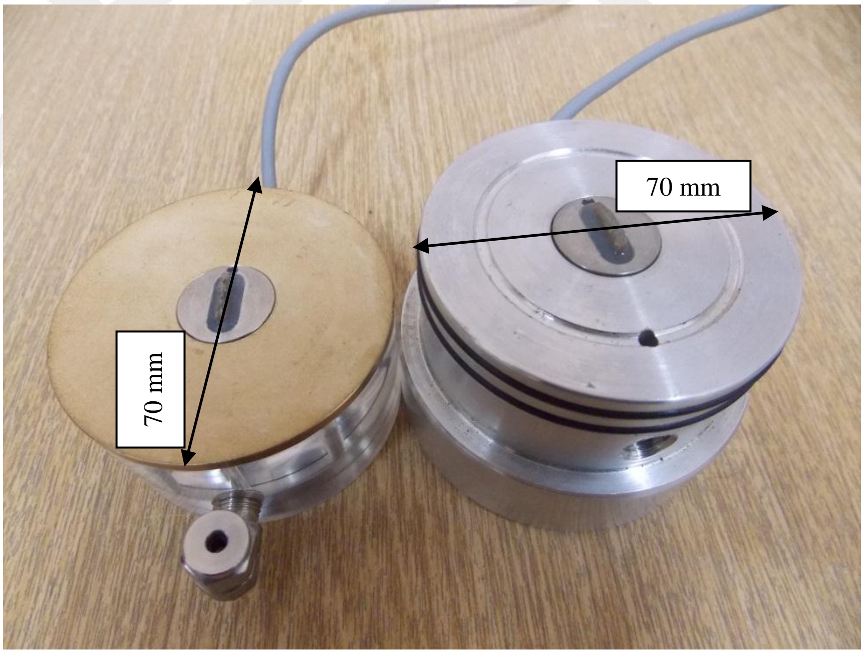

Figure 3.2 Bender elements device used during the test.

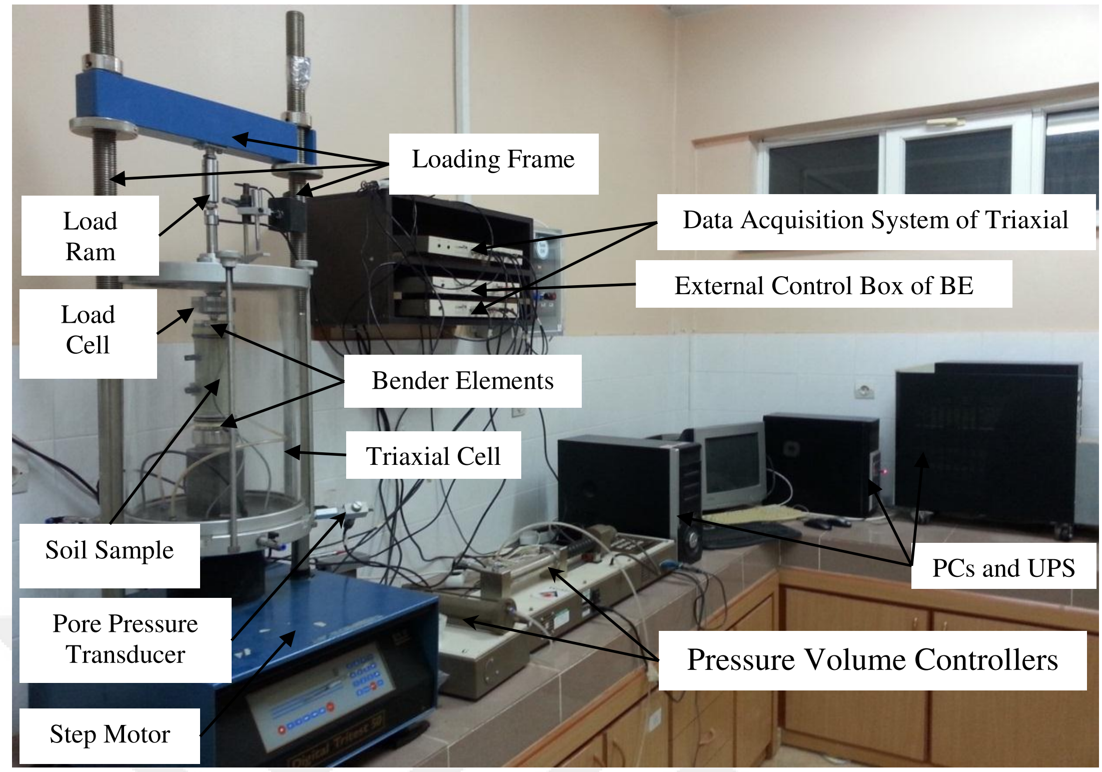

Figure 3.3 An overview of the triaxial equipped with bender elements system.

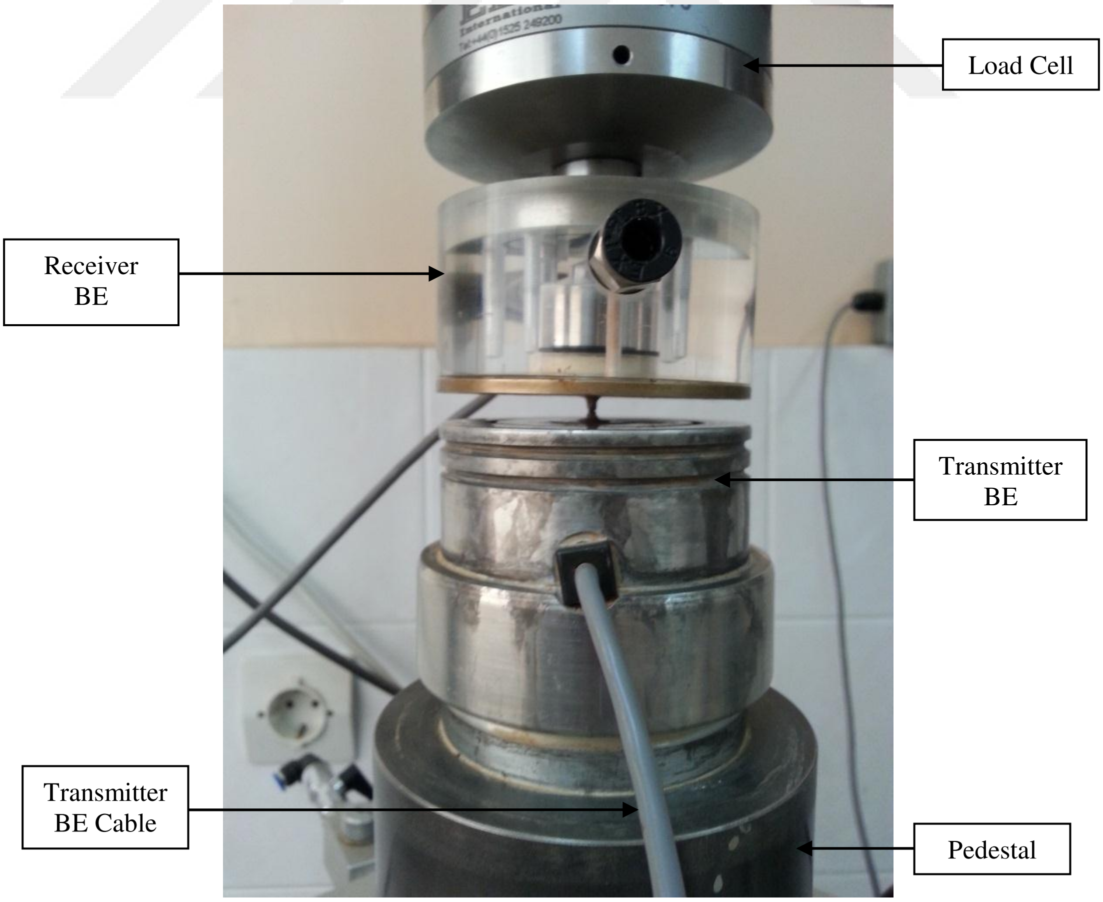

Figure 3.4 Calibration of bender elements by direct contact method.

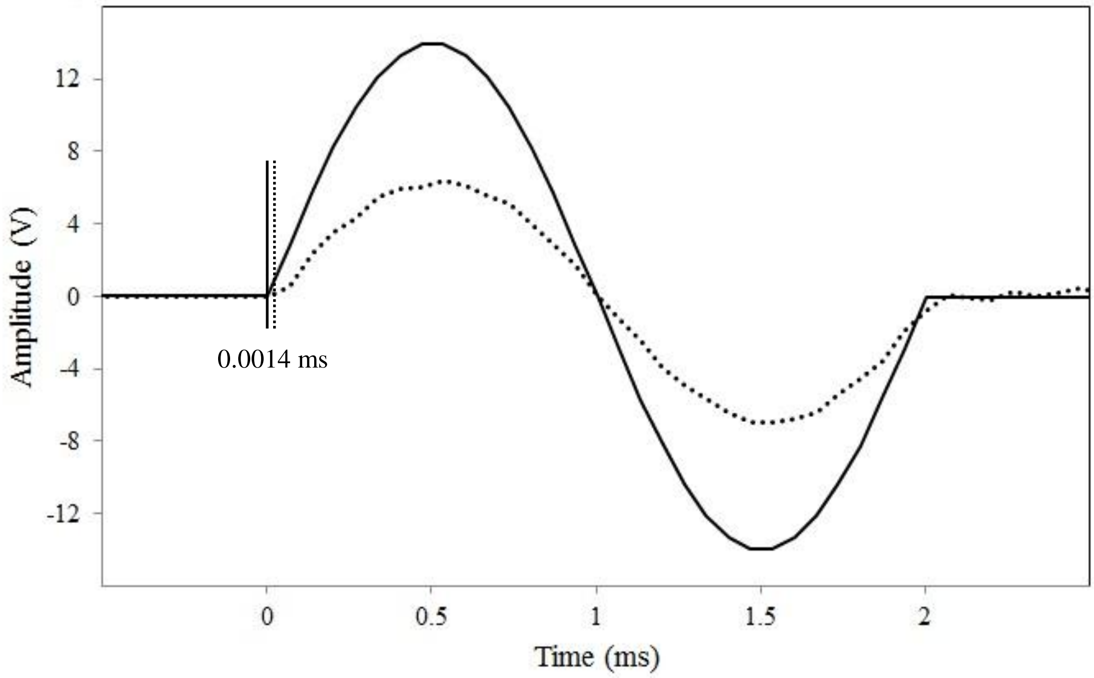

Figure 3.5 Delay time measurement for bender elements calibration.

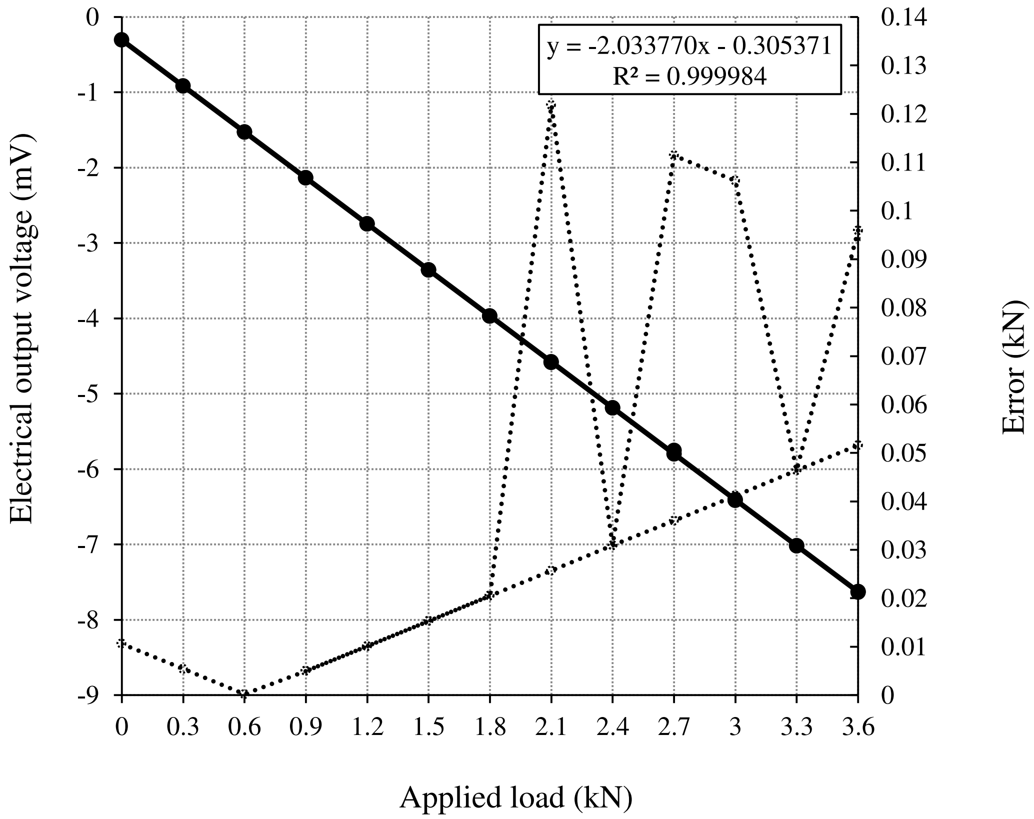

Figure 3.6 Calibration of the 10-kN submersible load cell, ELE Type.

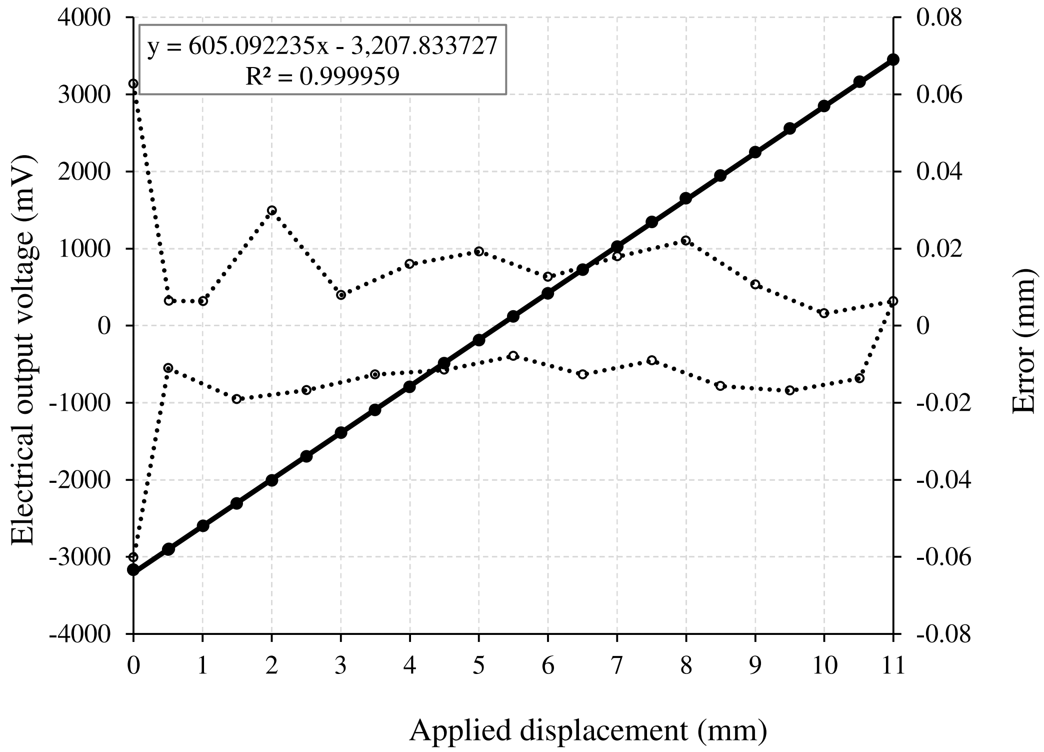

Figure 3.7 Calibration of the external LDS, ELE type.

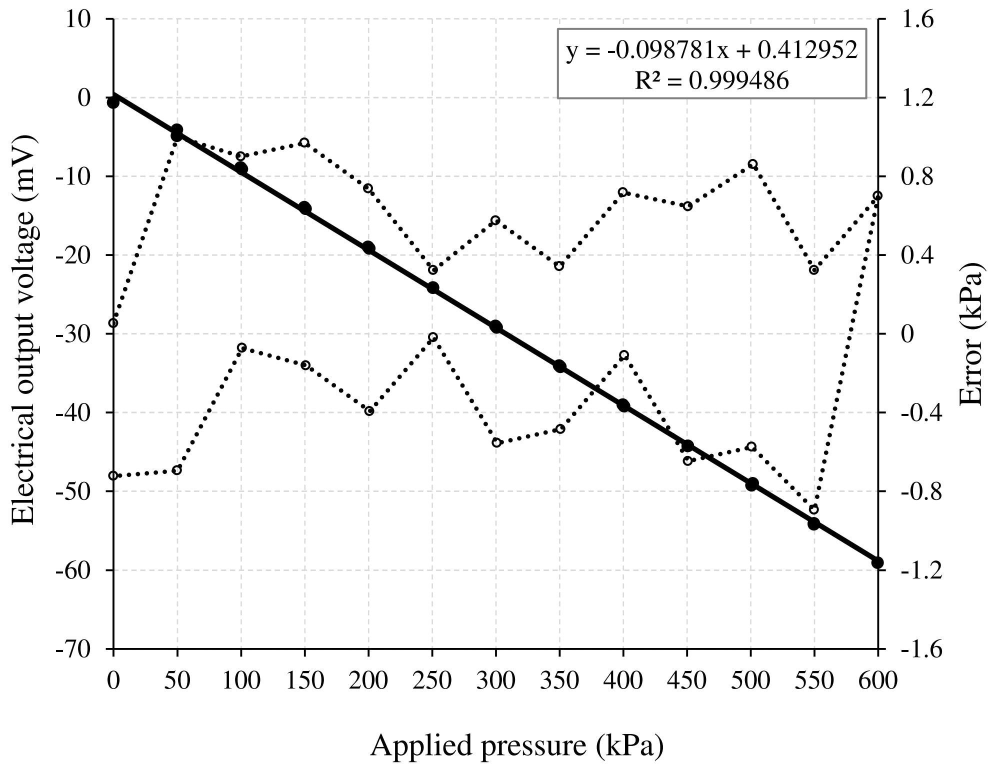

Figure 3.8 Calibration of the cell pressure transducer, PDCR 810.

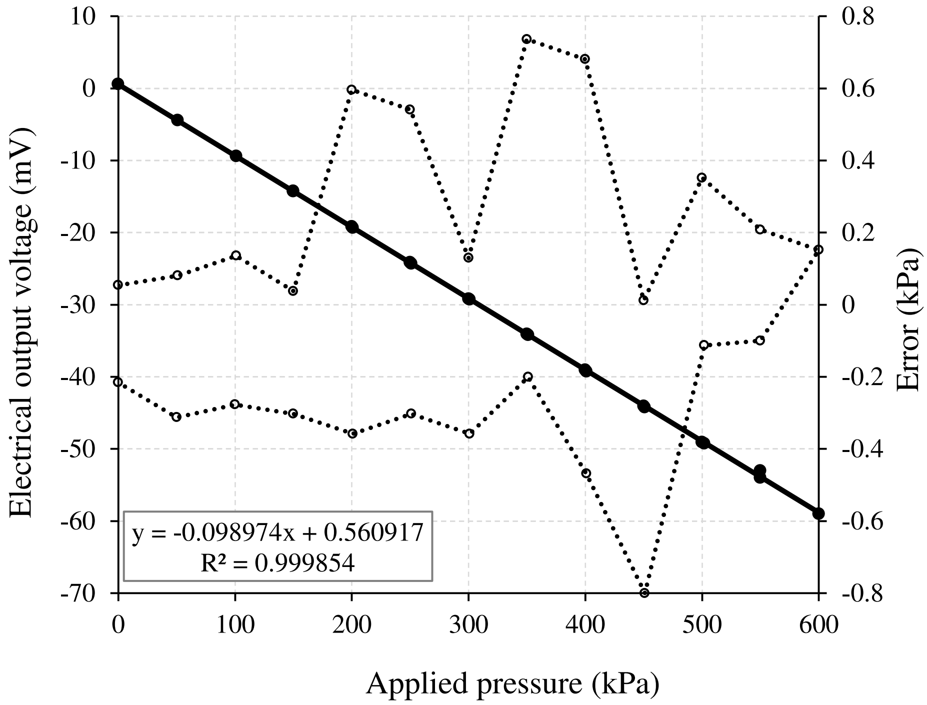

Figure 3.9 Calibration of the pore pressure transducer, PDCR 810.

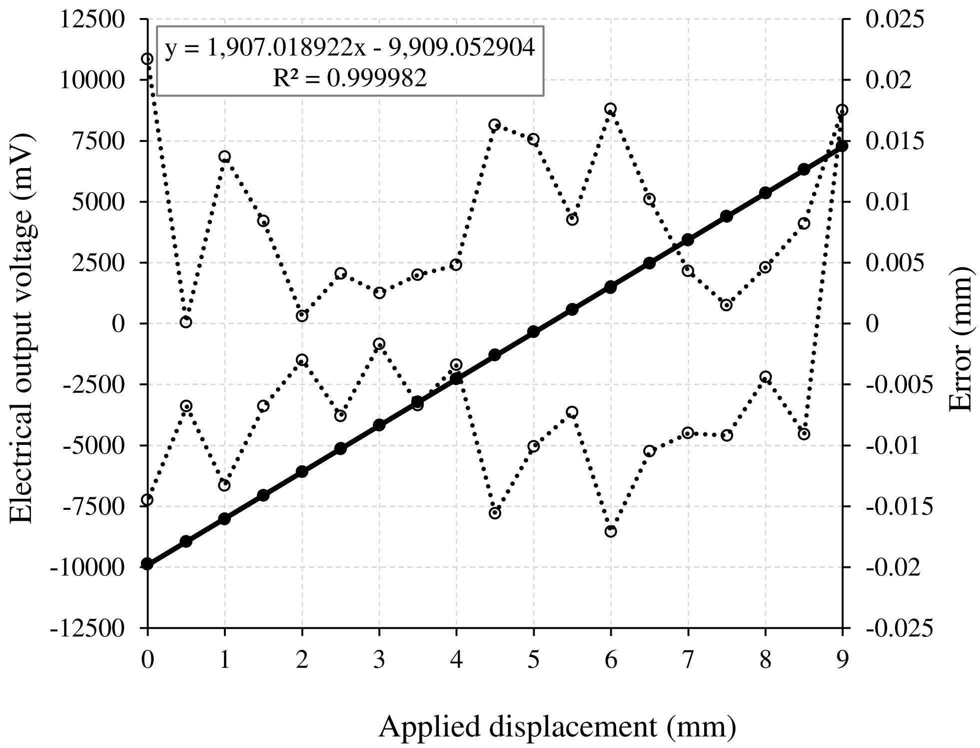

Figure 3.10 Calibration of the internal LVDT1, GDS Ltd.

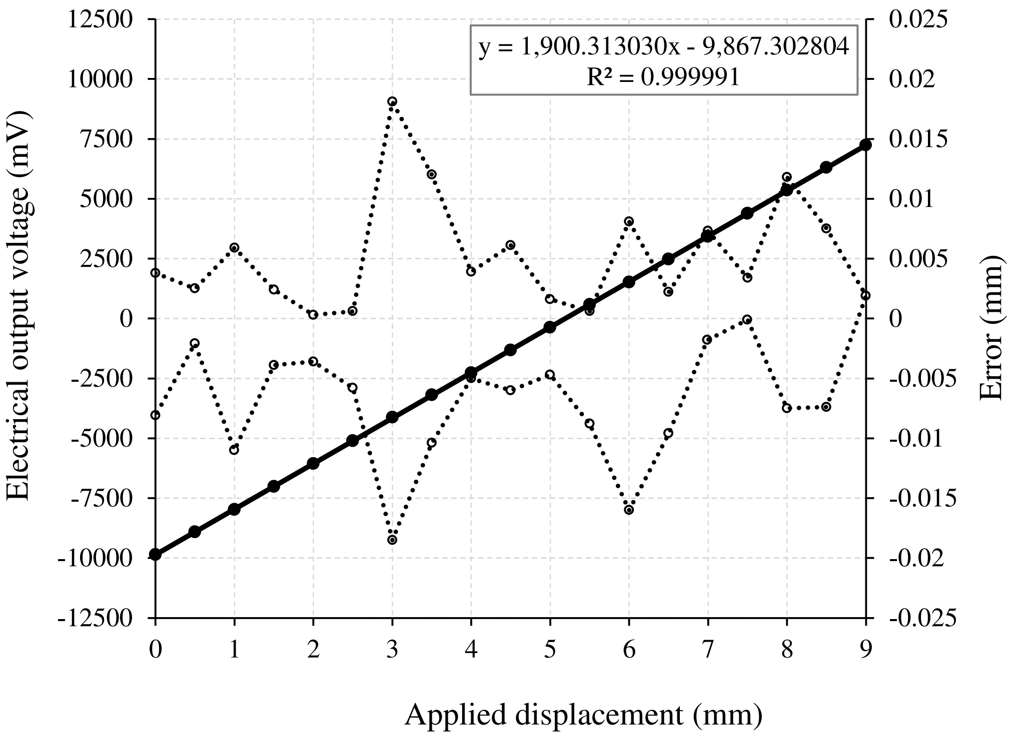

Figure 3.11 Calibration of the internal LVDT2, GDS Ltd.

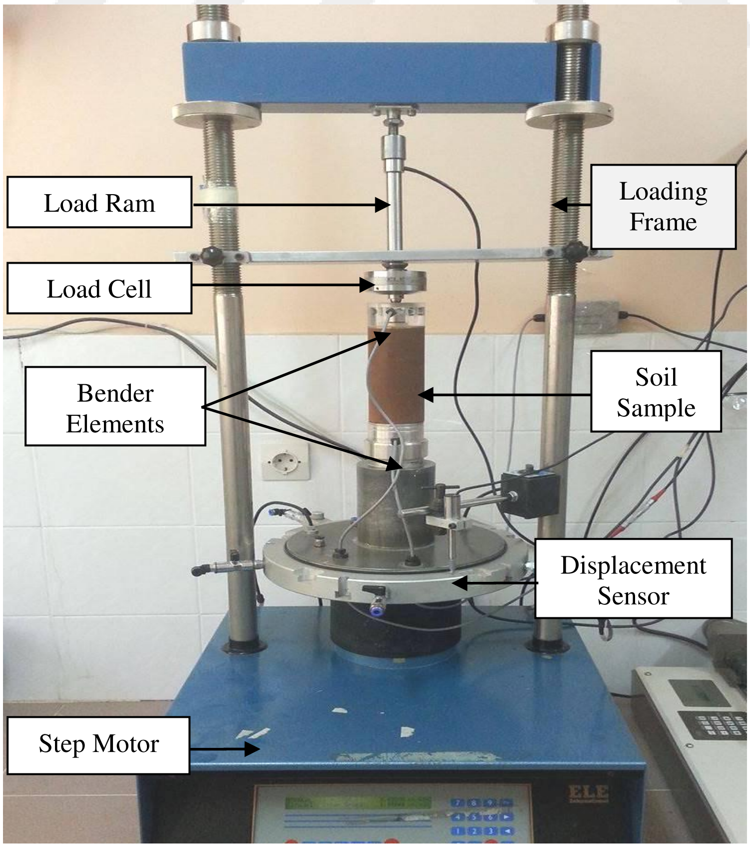

Figure 3.12 Device used for unconfined equipped with bender elements tests.

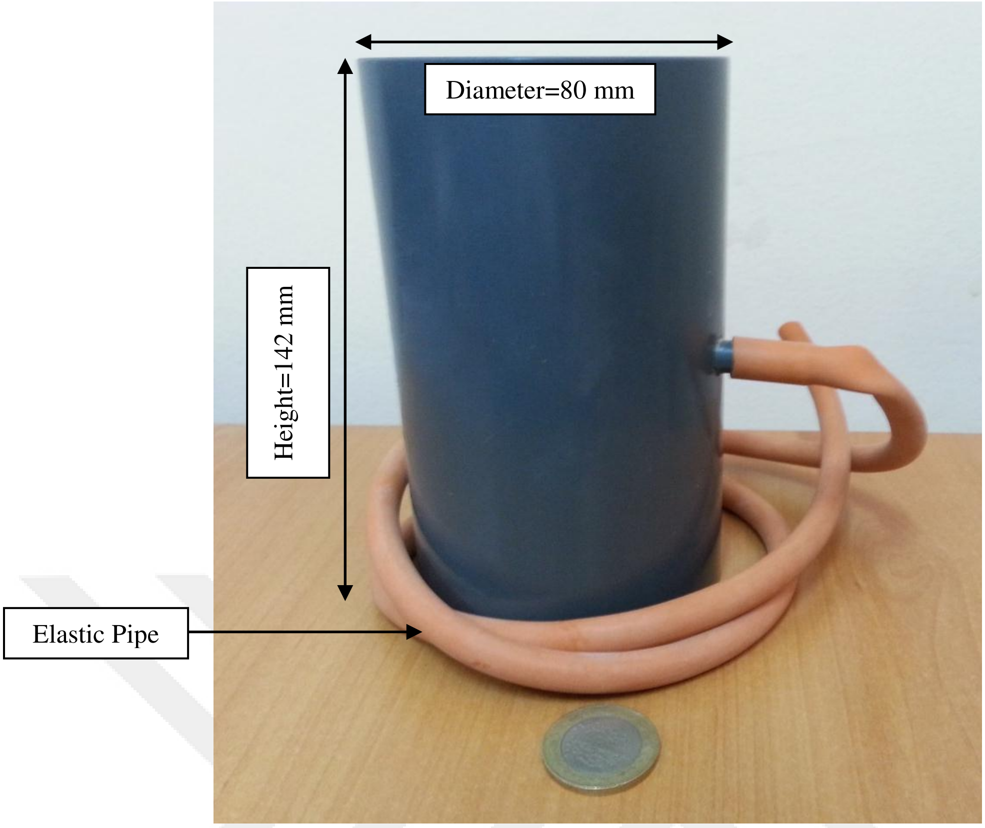

Figure 3.13 A special mold used to position the membrane around the sample.

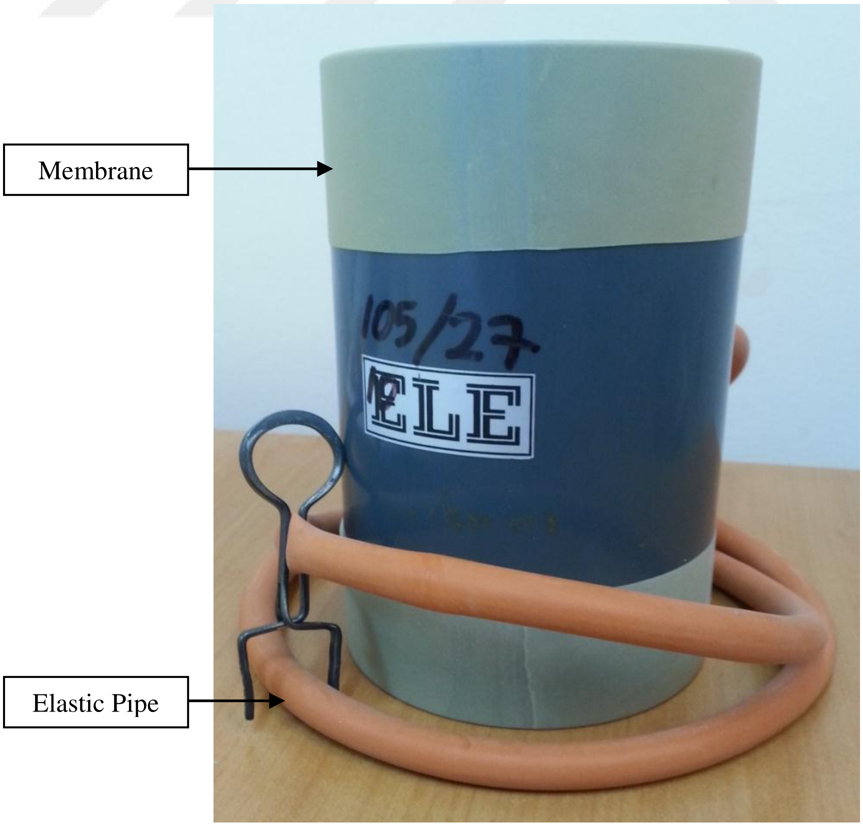

Figure 3.14 The membrane stacked to the special mold.

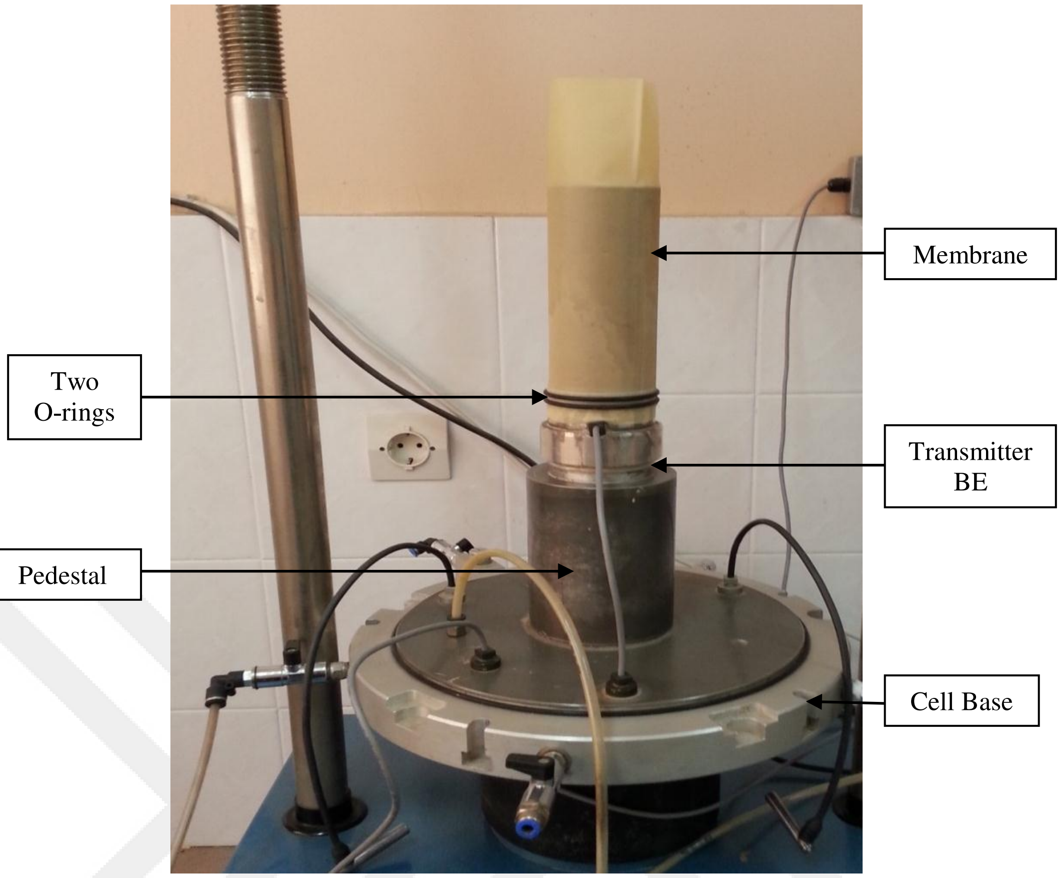

Figure 3.15 Positioning the membrane around sample by two O-rings in pedestal.

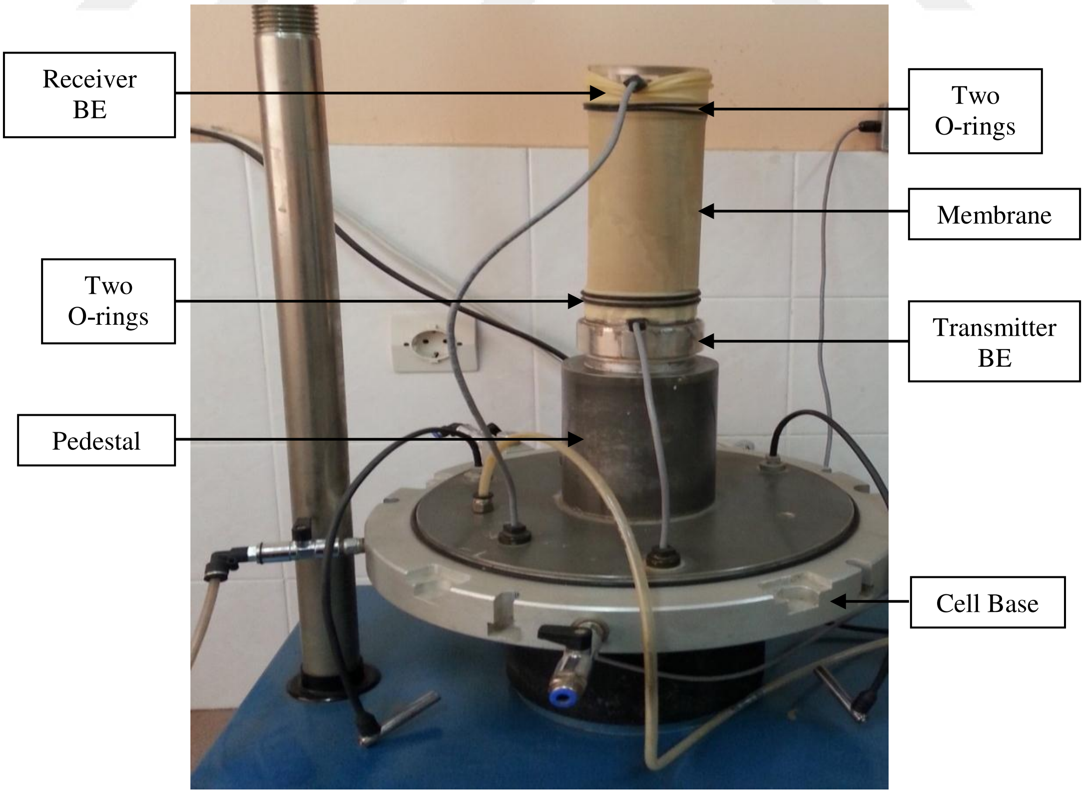

Figure 3.16 Receiver bender elements placed above sample with two O-rings on top.

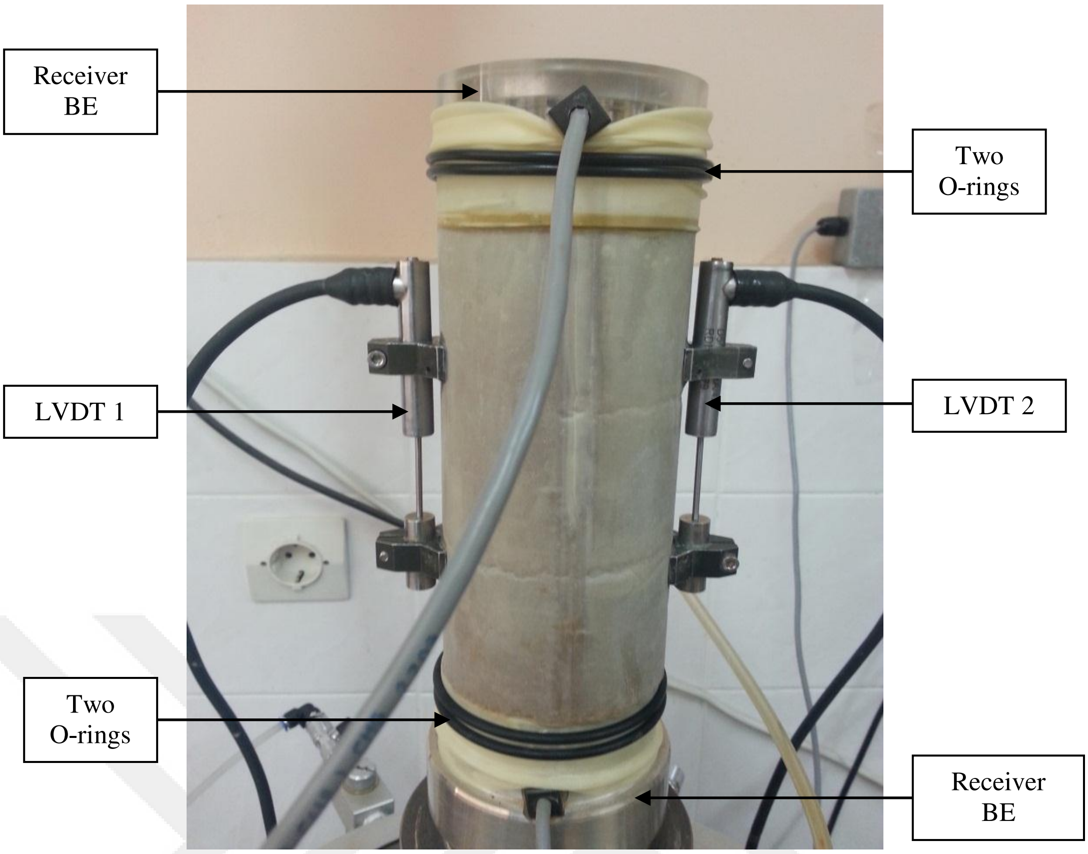

Figure 3.17 Internal LVDTs mounted on the soil sample.

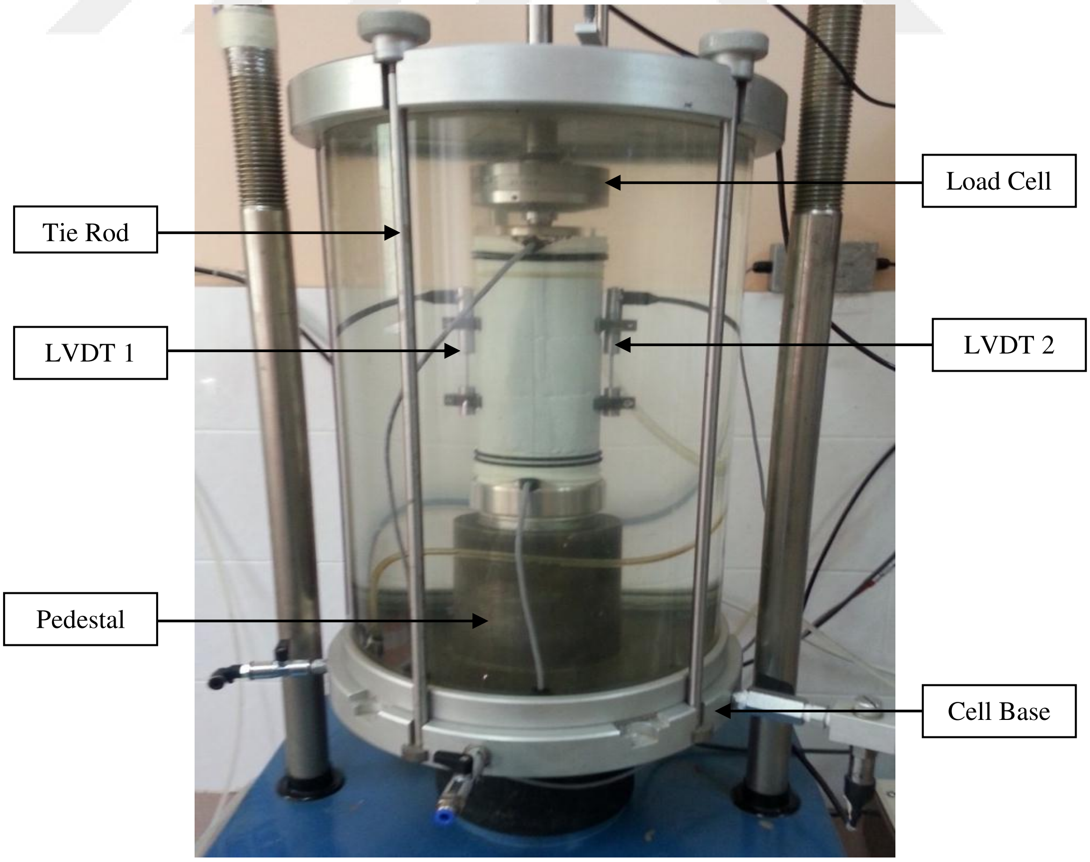

Figure 3.18 Triaxial cell contained soil sample and filled with water.

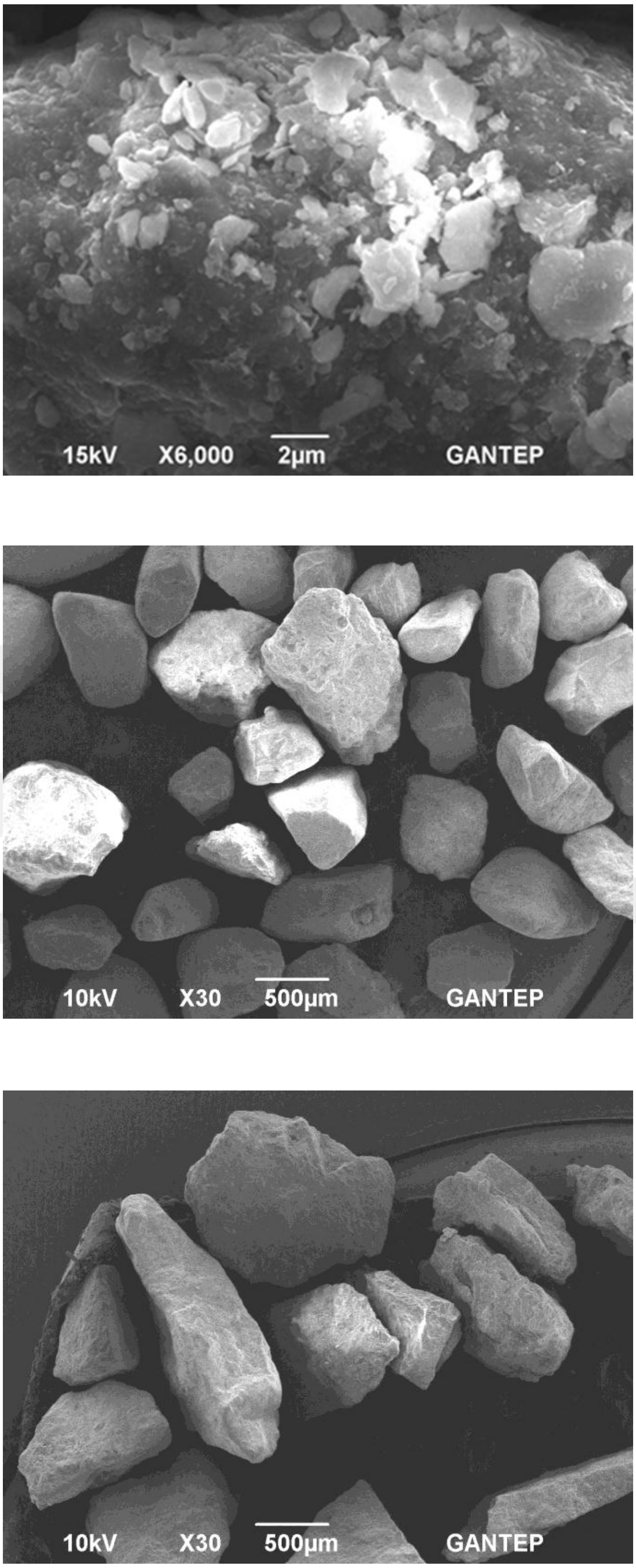

Figure 3.19 SEM pictures of the materials used during the experimental study (top) clay, (middle) NS, (bottom) CSS.

CHAPTER 4

RESULTS AND DISCUSSION

Bender elements are widely used for measuring the shear modulus of the soil at small strains. Dyvik and Madshus (1985) stated that the maximum shear strain to be estimated by bender elements is less than 10^{-3} %, so that the shear modulus measured is maximum shear modulus (G_{max}), corresponding to small strains (Viggiani and Atkinson, 1995). Bender elements can be installed in some geotechnical laboratory devices, but they are in particular suitable with the triaxial apparatus. G_{max} of the soil is computed from the shear wave velocity (Vs) using the following relationship:

$$G_{max}=\rho\ Vs^2=\rho\left(\frac{L^2}{t^2}\right) \tag{4.1}$$

where ρ: soil mass density; L: the length between the bender elements measured from tip to tip; and t: travel time between the source and receiver bender elements.

In this chapter, section 4.1 presents the results of unconfined compression equipped with bender elements tests through evaluating the G_{max} of clay-sand mixtures which is denoted $G_{max(Unc)}$ as a function of unconfined compressive strength and the effects of shape, size and content of sand on the G_{max} and the unconfined compressive strength values, the effect of frequency on the G_{max} values also presented in this section. Section 4.2 shows the results of triaxial equipped with bender elements to indicate the effects of shape, size and content of sand on the G_{max} which is denoted $G_{max(Tri)}$, shear strength parameters (cohesion and angle of internal friction) and another properties of clay-sand mixtures that could be obtained from the triaxial test.

4.1 Unconfined Compression Apparatus Equipped with Bender Elements

4.1.1 Effect of Frequency

The near-field effect is the mixed of rays of shear and compression waves. The existence of the near field-effect influences the shape of the output signal, and it generates a difficulty in measuring the travel time of the shear wave in the bender elements tests effectively (Schultheiss, 1981; Sanchez-Salinero et al., 1986; Gu et al., 2013; Yang and Gu, 2013). This undesirable effect reduces as the frequency (f) of the shear wave increased. Jovicic et al. (1996) and Brignoli et al. (1996) mentioned that the near-field effect were minimized when the frequency of the input signal is increased. Near-field effects are measured regarding the ratio of the wave path length (L) to the wavelength (λ) (Schultheiss, 1981; Leong et al. 2009). Sanchez-Salinero et al. (1986) indicated that the near-field effects stay critical when the value of L/λ is less than one, and it would not be substantial if L/λ is more than two. Arulnathan et al. (1998) showed that the receiver signal was deteriorated as this ratio is increased and it was stated that the near-field effect disappeared when the ratio is more than one. Pennington et al. (2001) stated that the range of the ratio must be between 2 and 10. Arroyo et al. (2003) mentioned that when L/λ is more than 1.6 the near-field effect do not exceed 5%. Leong et al. (2005) found that this ratio should be not less than 3.33 utilizing a 16 kHz signal. Thus, in the present study, to investigate the influence of frequency, bender elements tests at five various values of the input frequencies, which are 5, 10, 15, 20 and 25 kHz have been performed. For several tests conducted in this experimental study, the values of L/λ associated with an input signal of 5 kHz is presented in Table 4.1. Where L= 143 mm, λ= Vs/f. It can be noticed that for the present study, the value of L/λ is 5.98 for clean clay, it lies between 4.42 and 4.83 for clay-sand mixtures of NS sand and between 4.46 and 4.83 for clay-sand mixtures of CSS sand.

Figure 4.1 presents the change of shear wave velocity measured from bender element tests with frequency. The velocities determined from bender element tests are frequency dependent. For all frequencies, there is a trend that the increasing of frequency leads to a decrease in velocity. It can be noticed that the L/λ resulted from a frequency of 5 kHz gives better results than other frequencies because L/λ values within the range 1 to 9. Therefore, the frequency of 5 kHz is used to compute the shear wave velocity by bender element tests.

4.1.2 Effect of Sand Size

The sands used during the experimental study have the same classification, SP, although they have different gradation curves. The grain size distribution of cohesionless materials used in the tests plays a significant role in determining q_u from the UC testing results. It was realized that the smaller size of sand grains the specimens have, the less the q_u (Figure 4.2). For example, the specimens with 30% angular sand grains have 206 kPa, 222 kPa, and 237 kPa for the size of 0.6-0.3 mm, 1.0-0.6 mm, and 2.0-1.0 mm, respectively. The soil grains have much less contact points in the specimens prepared with smaller size sand grains than those with larger sand grains, hence the overall strength behavior of the specimens is mainly governed by the void ratio (e).

To investigate the influence of size of sand grains on the G_{max} values, results obtained for the same shape of both sand grains with different amount of clay were compared. For example, the G_{max} values for the specimen prepared with 40% angular sand between 0.6 mm and 0.3 mm, 1.0 mm and 0.6 mm, and 2.0 mm and 1.0 mm are 50 MPa, 51 MPa, and 52 MPa, respectively. Actually, the G_{max} values for the clay with smaller grains were found to be always lower than those with larger sand grains. It was seen that the difference in G_{max} values of the 2.0-1.0 mm and 1.0-0.6 mm specimens with same shape sand grains is generally more than 5%, and those of the 0.6-0.3 mm and 2.0-1.0 mm is more than 10%, which means that the grain size of the sands used in the mixtures has primary importance. Similar to the observations made by Hardin and Kalinski (2005), that the G_{max} increases with increase in the mean effective grain size, D_{50} (Figure 4.3).

4.1.3 Effect of Sand Shape

The shape of sand grains in mixtures is of great importance to the undrained shear strength behavior of mixtures tested in UC tests. As can be seen from the Figure 4.2, the q_u obtained for the clay with CSS grains between 0.6 mm and 0.3 mm have the minimal values, while the q_u obtained for the clay with NS grains between 2.0 mm and 1.0 mm have the maximal values. Actually, the mixtures with angular shaped grains (CSS) at all three gradations exhibited a much lower q_u values for all content of sands. For instance, the q_u values of the specimens with 30% rounded sand content (NS) were found to be 221 kPa, 246 kPa, and 254 kPa, while those with same amount of angular sand content (CSS) were 206 kPa, 222 kPa, and 237 kPa for the cohesionless materials between 0.6-0.3 mm, 1.0-0.6 mm, and 2.0-1.0 mm, respectively. In the light of the papers by Rothenburg and Bathurst (1989), Thornton

(2000), Cho et al. (2006), Cabalar et al. (2013), Cabalar (2015), it is likely because of open fabric structure in the specimens with angular sand grains (CSS). Hence, based on the grain fabric taking place in the specimens, the contact points (coordination number) among soil grains decrease, the overall behaviour of the mixture is controlled by the void ratio (e) as presented in Table 4.2. Table 4.2 shows q_u values of clay-sand mixtures with voids ratio values corresponding to each of them. It has been a long understood that the void ratio (e) of a soil matrix is the ratio of voids to the volume of solid grains. The resulting void ratio by the clean angular sand grains are larger than those for clean rounded grains (Santamarina and Cho, 2004; Cho et al., 2006).

The grains of both angular (CSS) and rounded (NS) sands used in the present study are considered as floating in the clay matrix. Then, it was seen that the clay with angular sand grains (CSS) resulted in lower q_u values in UC tests, since random packing of angular grains resulting void ratios are larger than those of rounded grains (NS). Thus, it was concluded that the less angularity in sand grains the more q_u values obtained in the clay-sand mixtures.

It was realized that the difference in G_{max} values of the specimens with same size sand grains is generally less than 5%, which means that the difference observed should not be primarily because of the difference in the grain shape of the sands used in the mixtures. Because they have similar values for coefficient of uniformity (cu), and coefficient of curvature (c_c), besides the mean particle size (D_{50}) has an ignorable influence on the elastic modulus (Wichtmann and Triantafyllidis, 2010; Yang and Gu, 2013). Otsubo et al. (2015) determined the shear modulus of borosilicate glass beads (ballotini) indicated that the stiffness decreased with increasing of surface roughness. However, the sand grains of both angular (CSS) and rounded (NS) sands in the present study are thought to be covered with clay grains, then they do not contact to each other directly. Therefore, it is postulated that the mineralogy or the surface roughness of sand grains seems to be beyond the scope of this study.

4.1.4 Effect of Sand Content and the Relationship Between q_u and G_{max}

To study the relationship between q_u and G_{max} values for different clay-sand mixtures, the unconfined compression tests and bender element tests were conducted. Table 4.2 gives the UC testing results reported here. From the tests with both clay and clay-sand mixtures compacted at w_{opt} and γ_{drymax}, the unconfined compressive strength (q_u) values were observed to be significantly affected by the addition of sands. The q_u values decreased as the amount of sand content increased in all size, shape, and content of the sand grains. Similar results were also reported by Stavridakis (2005) for investigation of problematic soils.

As Hardin (1978) stated the void ratio is also influential on the shear modulus (G_{max}). Ghayoomi et al. (2017) supported Hardin (1978) considering the statement of void ratio dependence on G_{max} estimates. As several other researchers have also indicated (Santagata et al., 2005; Chen et al., 2017; Asadi et al., 2018), the effect of increasing G_{max} with decreasing void ratio (e). An analysis of the results of the bender element tests on clay only and clay with various types of sands indicated that the G_{max} tended to increase at several levels by adding different amount of sands (Table 4.3). Therefore, the G_{max} estimates in each condition should be investigated individually. For example, the G_{max} value of clay only increased sharply from 29 MPa to 48 MPa by adding 10% rounded sand at 2.0-1.0 mm grain size interval. However, the increment observed for the clay with angular sand at both same amount and grain size interval was found to be slightly lower, 46 MPa.

The amount of the cohesionless material in the mixtures has an obvious influence on the overall behaviour as well as G_{max} of such mixtures (Ni et al., 2004; Monkul and Ozden, 2007; Yamada et al., 2008; Cabalar and Mustafa, 2015, 2017) (Figure 4.4). The evaluated G_{max} values for the mixtures have been almost doubled when the clay is mixed with 50% sand addition at any size and shape. The G_{max} of mixtures show significant changes at sand content of 10%, which suggests that the threshold value of sand content at which the trend changing e_{max} of the mixtures with clay content should be at less than 10%. The void ratio values, strongly effective on the shear modulus, were found to be changed from 0.577 to 0.385 by adding 50% sand rounded between 2.0-1.0 mm size. Such decrease in void ratio has resulted in an increase in G_{max} from 29 MPa to 56 MPa. Figure 4.5 reveals that the G_{max} decreased with the increase of void ratio for all sizes and both shape of grains in clay-sand mixtures. The reason of decrease in the G_{max} is mainly attributed to the increase in void ratio, which changes based on the size and shape characteristic of soil grains (Cubrinovski and Ishihara, 2002; Clayton, 2011; Ching et al., 2017). The packing features of soil control the void ratio and fabric, which represents grains orientation, and contact patterns of grains (Lo Presti et al., 1997; Cubrinovski and Ishihara, 2002). The shear waves propagate through a soil matrix with maximum influence from the contact network. The variation of void ratio may change the travel length for wave. The larger the void ratio is, the more travel length is created. Actually, a more travel time would be spent in the contact network of loose sample. Conversely, a dense specimen would create a more stable connection, and thus avoids the micro-rotation of grains. Such as, well graded soils with wide range of grain sizes tend to have smaller average void ratios, and exhibit larger values of Vs. Hence, the present study has pointed out that the G_{max} is dependent on void ratio controlled by grain contents and characteristics including size, shape, gradation, and roughness.

The differences between the G_{max} and q_u values are influenced by different conditions under which the dynamic (BE) and static (UC) tests are carried out. The values of q_u in UC tests are of several hundred of kPa, while the G_{max} at BE tests does not exceed the value of 60 MPa (Figures 4.6-4.7). The loading at UC tests can produce the micro-cracks, that results in the growth of deformation and consequently to the failure of the specimen. However, the BE tests do not change the structure of the material, which is the biggest advantage of their use. The time of applying stress is also different, it lasts several minutes at the UC tests whilst it lasts only several microseconds at the BE tests. The fact is that purpose of methods for determining the q_u and G_{max} differs based on demands in practice. If requirement of determining the q_u is formulated by a long termed loading point of view, such as the problem of stability at building works, mining works etc., the qu values can be obtained from the UC tests. Conversely, if the loading is short termed, such as the blasting works, earthquakes, etc., the determination of the G_{max} is required. The measurements of G_{max} can be made using relatively sophisticated, that is why an alternative method of its determination could be beneficial. Based on the above discussion, the following derived empirical formulas for estimating the G_{max} from the UC tests is suggested for the mixtures of clay-angular sand (R^2=0.77), and clay-rounded sand (R^2=0.66), respectively.

$$G_{max}=-97.7q_u+70012 \tag{4.2}$$

$$G_{max}=-97.5q_u+72877 \tag{4.3}$$

Where G_{max} and q_u values are to be found in kPa.

Figure 4.8 presents the values of G_{max} with q_u values corresponding of them for clay-NS sand and clay-CSS sand of clay mixtures for all contents and size of sand used in this study. Figures 4.9-4.10 show the effect of sand size on the correlation between q_u and G_{max} for clay-NS sand and clay-CSS sand mixtures. The effect of sand shape on the correlation between q_u and G_{max} for clay-NS sand and clay-CSS sand mixtures with size of 0.6-0.3, 1.0-0.6, 2.0-1.0 mm are presented in Figures 4.11-4.13, respectively.

4.2 Triaxial Equipped with Bender Elements

4.2.1 Deviatoric Stress

The results on NS sand and the CSS sand of the clay-sand mixtures indicate that the properties of the mixtures tested is affected by including the sand grains in the samples that tested using triaxial compression test. As can be seen from the Figures 4.14-4.19, it was found that the presence of NS and CSS sand (10%, 30%, and 50%) in the specimens tested had a marked influence on the deviatoric stress versus strain. The same findings of this study can be observed by Fei (2016). Fei (2016) studied the effect of coarse content on the behaviour of clay-aggregate mixtures using odometer and triaxial compression tests. The author suggests that sand grains separate the clay grains. Based on the content of sand grains present, the clay particles are in contact with each other and the behaviour of specimens tested are controlled by the clay grains. When the contacts between the clay grains reduce by infilling sand grains, the behaviour of the specimens starts to change. Therefore, a remarkable increase in deviatoric stress can be observed when the amount of sand grain increases. As the axial strain increase the deviatoric stress increases to a maximum value, and then stays constant approximately for all effective stresses studied. Also, the deviatoric stress increases as the effective stress increased.

4.2.1.1 Effect of Sand Content

Figures 4.14-4.19 show the deviatoric stress versus axial strain of the clay and clay with different contents of sand (10, 30 and 50%) at various effective stresses. The clayey specimens responses to triaxial loading was served as a reference line from which the adding of sand content could be compared with it. Figures 4.14-4.19

present results of different experiments, which are the clayey specimens, clay with 10% sand, clay with 30% sand, and clay with 50% sand of two sand sizes of two sand shapes. It is seen that the addition of sand causes a significant effect on the deviatoric stress. As can be seen from these Figures, the higher sand content of the clay-sand mixtures, the higher deviatoric stress. There is a peak shear stress values observed in all the specimens. As the sand content increases, the deviatoric stress values increases. Wood and Kumar (2000) investigated the effect of sand content on the behaviour of kaolin clay by conducting undrained and drained triaxial tests on clay-coarse sand mixtures. They indicated that the deviatoric stress were affected positively by the addition of the sand when the sand content exceeded 60%. The energy absorption increase by shifting the deviatoric stress upward with increasing of sand content. Energy absorption can be measured by computing the area under the stress-axial strain curve (Hamidi and Hooresfand, 2013; Cabalar et al., 2018). On the other hand, for all effective stresses the deviatoric stress increased as the sand content increases. The effect of sand content is significantly lower in low effective stress. The deviatoric stress values of the clay-sand mixtures ranged from 67 kPa of 0.6-0.3 mm sand size with 10 % angular sand content (CSS) at effective stress of 50 kPa to 273 kPa of 2.0-1.0 mm sand size with 50 % rounded sand content (NS) at effective stress of 200 kPa.

4.2.1.2 Effect of Sand Shape

The shape of sand grains in the clay-sand mixtures plays a role in the shear behavior of these mixtures. The deviatoric stress values of the clay and clay-sand mixtures with NS sand and CSS sand are presented in Table 4.4. As can be seen from this Table, the deviatoric stress of clay-sand mixtures with NS sand higher than the deviatoric stress value of clay-sand mixtures with CSS sand. This behaviour is similar for all effective stresses. The deviatoric stress increase as the roundness and sphericity of the sand grains increases in the clay-sand mixtures that investigated in this study. This increment in deviatoric stress is occurred due to the decrease in void ratio of these mixtures with the increase of the roundness and sphericity of the sand grains as shown in Table 4.5. The results of this study is consistent with the experimental study of Cabalar et al. (2013). Cabalar et al. (2013) investigated the effect of particle shape on the behaviour of different type of sands using triaxial and cyclic direct shear testing devices, the authors stated that the deviatoric stress increased with increasing of roundness and sphericity of sand. For instance, the maximum deviatoric stress values of the specimens with 30% rounded sand content (NS) at effective stress of 100 kPa were found to be 120 kPa, and 131 kPa, while those with same amount of angular sand content (CSS) and same effective stress were 117 kPa, and 125 kPa of the clay-sand mixtures with sizes of 0.6-0.3 mm, and 2.0-1.0 mm, respectively.

4.2.1.3 Effect of Sand Size

The effect of sand size on the deviatoric stress versus axial strain responses of the clay-sand mixtures are shown in Figures 4.20-4.25. As the clayey specimens, the clay-sand mixtures specimens have peak deviatoric stress values. It can be shown that the deviatoric stress increases with the increase of the size of sand grains for all the cases studied as presented in these Figures. The deviatoric stress values increase as the size of sand grains increases because of the void ratio of larger soil grains less than that of smaller grains. For the same volume of soil, larger soil grains have less surface area when compared to that of smaller soil grains. Hence the voids created between the smaller grains are more as compared to larger grains. Contrary to this study, Fei (2016) indicated that the soil mixtures with smaller-sized steel beads exhibit a slightly higher deviotric stress by small percentage.

4.2.2 Pore Water Pressure

Figures 4.26-4.31 show the variation of the pore water pressure generation versus axial strain for clay and clay-sand mixtures at three different effective stresses (50, 100 and 200 kPa). As can be seen from these Figures, as the axial strain increases, the pore water pressure increases to a maximum value at a specific value of strain, and then starts to decrease with increasing of axial strain. Here there is a shift in pore water pressure versus axial strain upward as the effective stress increase.

4.2.2.1 Effect of Sand Content

Figures 4.26-4.31 show the pore water pressure behaviour of clay and clay-sand mixtures as a function of axial strain for the specimens. It is seen that the clay generates the highest values of pore water pressure and the pore water pressure generation decreases as the sand content increase in the clay-sand mixtures for all cases investigated in this study. This behaviour may be attributed to the increase in the area of contact between the soil grains that lead to increase in frictional resistance among them. These results are in an agreement with the experimental test results indicated by Najjar et al. (2010), the authors conducted consolidated undrained triaxial tests to study the effect of sand columns on soft clays, they reported that when the column penetration ratio and area replacement ratio increased, the pore water pressure decreased. Same observations were found by McKelvey et al. (2004), Sivakumar et al. (2004), Black et al. (2007). Furhermore, Wood and Kumar (2000) stated that the pore water pressures are unaffected by the inclusion of the sand in clay tested in undrained conditions. The results in this study are in the contrast with the results were obtained by Prakasha and Chandrasekaran (2005). They studied the behaviour of Indian marine soils with different contents of sand and clay using static and cyclic triaxial. They reported that the addition of sand to the clayey soil led to increase the pore water of these mixtures. The higher sand content of the clay-sand mixtures, the lower pore water pressure, on the other hand, the higher sand content of the clay-sand mixtures, the higher deviatoric stress, which means that the behaviour of clay-sand mixtures is less compressive than clayey soil samples, and the compressibility be less and less with increasing sand content of the clay-sand mixtures. The pore water pressure values of the clay-sand mixtures ranged from about 375 kPa of 2.0-1.0 mm sand size with 50% rounded sand content (NS) at effective stress of 50 kPa to about 505 kPa of 0.6-0.3 mm sand size with 10% angular sand content (CSS) at effective stress of 200 kPa.

4.2.2.2 Effect of Sand Shape

Table 4.6 show the change in pore water pressure generation versus the axial strain of the clay and clay-sand mixtures with NS sand and CSS sand. It is seen that the shape of grains of NS and CSS sand in the clay-sand mixtures affected the pore water pressure generation of the mixtures investigated in this study. The pore water pressure values for the clay-sand mixtures of CSS sand are higher than their values for the clay-sand mixtures of NS sand. This behaviour is similar for all effective stresses. The pore water pressure increase as the roundness and sphericity of the sand grains decreases in the clay-sand mixtures that investigated in this study because of the voids ratio of rounded sand lower than angular sand in the clay-sand mixtures. The results of these tests in a good agreement with the results of the test carried by Karabash and Cabalar (2015), the authors studied the influence of sand grains shape on the properties of sand clay mixtures using consolidated undrained triaxial compression tests, they reported that the pore water pressure generation increased as the angularity of sand tested in the study increased. For example, for sizes of 0.6-0.3 mm and 2.0-1.0 mm of the clay-sand mixtures, the maximum pore water pressure values of the specimens with 50% angular sand content (CSS) at effective stress of 100 kPa were found to be about 407 kPa and 404 kPa, respectively, while those with same amount of angular sand content (CSS) and same effective stress were about 403 kPa and 402 kPa.

4.2.2.3 Effect of Sand Size

Figures 4.32-4.37 present the variation of the pore water pressure versus the axial strain. As the sand size of clay-sand mixtures increases the pore water pressure generation decreases for both types of sand (NS and CSS) and for all sand contents that studied, while, the deviatoric stress increased as the sand size of clay-sand mixtures increases. These behaviours might be due to the decrease in the void ratio and increasing in the density as the sand size of clay-sand mixtures increase in the specimens, high densities may lead to a better interlocking between the grains. Belkhatir (2014) investigated the influence of gradation on the pore water pressure behaviour of sand-silt mixtures. The results showed that the maximum positive excess pore water pressure decreases as the effective size and the mean grain size of sand increased. The results of this study is in a line with the investigation of Belkhatir (2014). The pore water pressure values for 0.6-0.3 mm sand size have reached about 505 kPa and 503 kPa for 0.6-0.3 mm sand size with 10% angular sand content (CSS) at effective stress of 200 kPa.

4.2.3 Stiffness

Figures 4.38-4.43 show the change in the stiffness of clay-sand mixtures with the strain for the samples tested under different effective stresses. Generally, the stiffness of clay-sand mixtures was decreased with increasing of strain. The samples that were tested at low effective stresses have lower stiffness value than the specimens at high effective stresses. This is belong to that the voids ratio of clay-sand mixtures decreased with increasing of effective stress for NS and CSS sand of clay-sand mixtures.

4.2.3.1 Effect of Sand Content

It has been observed that the inclusion of sand in the clayey soil causes a considerable increment in the stiffness of clay-sand mixtures. The values of stiffness increased with the increase of sand contents for NS and CSS sand of clay-sand mixtures for all sizes of sand and for all effective stress that investigated in this study as presented in Figures 4.38-4.43. The reason of this increasing belong to that the voids ratio decreased with increasing of sand content for NS and CSS sand of clay-sand mixtures.

4.2.3.2 Effect of Sand Shape

The stiffness values of the clay-sand mixtures with NS sand and CSS sand are presented in Table 4.7. As can be seen from this Table, the stiffness of clay-sand mixtures with NS sand higher than the stiffness value of clay-sand mixtures with CSS sand. This behaviour is similar for all effective stresses. The stiffness increased as the roundness and sphericity of the sand grains increased in the clay-sand mixtures that investigated in this study. This increment in stiffness is occurred due to the decrease in void ratio of these mixtures with the increase of the roundness and sphericity of the sand grains as shown in Table 4.5.

4.2.3.3 Effect of Sand Size

The effect of sand size on the stiffness versus strain responses of the clay-sand mixtures are shown in Figures 4.44-4.49. It can be seen that the stiffness decreased as the size of sand grains decreased for all the cases studied as presented in these Figures. The stiffness values decreased with decreasing of the size of sand grains because of the void ratio of smaller soil grains higher than that of larger grains. For the same volume of soil, smaller soil grains have more surface area when compared to that of larger soil grains. Hence, the voids created between the larger grains are less as compared to smaller grains.

4.2.4 Shear Strength Parameters

The Mohr circles and failure envelopes of the clay and clay-sand mixtures are plotted to measure the parameters of shear strength of soil (cohesion and angle of internal friction). The failure envelope and internal friction angle of the clay and clay-sand mixtures were determined for the CU condition based on effective stress. The addition of sand in various contents, shapes and sizes to a clay led to a considerable difference in the cohesion and angle of internal friction. Figures 4.50-4.62 present the Mohr circles and failure envelopes of the clayey specimens and clay-sand mixtures with different sand contents (10, 30 and 50%), two shapes of sand (rounded (NS) and angular (CSS)) and two sizes of sand (0.6-0.3 and 2.0-1.0 mm) in the CU condition based on effective stresses.

4.2.4.1 Effect of Sand Content

The shear strength parameters of clayey soil (cohesion and angle of internal friction) are significantly influenced by the sand content. The soil cohesion and angle of internal friction of clay with various sand contents for all sand sizes and both types of sand (NS and CSS) of clay-sand mixtures are shown in Figures 4.63-4.64, respectively. The cohesion of soil specimens with sand content is lower than that of clayey soil sample. The soil cohesion decreases with increasing sand contents for all sand contents, sand sizes and both types of sand (NS and CSS) of clay-sand mixtures. The soil friction angle of clayey samples with sand contents is higher than that of samples of clayey soil and it increases as sand content increased for all sand contents, sand sizes and both types of sand (NS and CSS) of clay-sand mixtures because of each sand grain replaces a group of clay particles and their corresponding voids, resulting in an increase in friction. The higher the sand content in the clay-sand mixture, the higher the angle of internal friction becomes, and thus the cohesion is lower. The results of this study present a good agreement with the results reported by Li (2013), the author investigated the influence of particle shape and size distribution on the shear strength behaviour of various soils, these soils were: mixtures of fines (clay and silt) and an ideal coarse fraction (glass sand and beads), and mixtures of fines and natural coarse fraction (river sand and crushed granite gravels). The results showed that as the content of coarse materials increased, the angle of internal friction of soil mixtures increased. The results from Chenari et al. (2015); Alshameri et al. (2016) are in line with this study.

From Figures 4.63 and 4.64 at 10 % of sand content of NS and CSS sand of clay-sand mixtures the percentage increased in the angle of internal friction was 9.2% and 6.7%, respectively. Based on experimental study the percentage decreased in cohesion of soil was found to be 32.5% and 38.75% at 10% of sand content of clay-sand mixtures for NS and CSS sand, respectively. From the test results, the frictional angle and cohesion is more in NS sand compared to CSS sand. The results given on Figures 4.50 through 4.62 and summarized in Table 4.8 show the effect of varying contents of sand in the clay soil matrix. The angle of internal friction of the soil with no sand was 11.9˚ and the cohesion 8 kPa. The angle of internal friction increased and the cohesion decreased when 10% of sand content was added, showing that there was very little large particle interference and, therefore, the soil had shear properties similar to the clay matrix. However, when the sand content was increased to 50%, the effect of the sand was readily apparent and the angle of internal friction value was increased to 15.7˚. A corresponding reduction in the cohesion of the soil was apparent as it became more granular. Thus, it can be stated that, as the sand content of a clay-sand mixtures is increased, a rather abrupt change in shear strength can be expected when sufficient sand is added.

4.2.4.2 Effect of Sand Shape

Particle shape was observed to affect the shear behavior of the clay-sand mixtures. To study the influence of the shape characteristics of sand grains, variations of the cohesion and angle of internal friction of the clay-sand mixtures of NS and CSS sand are shown in Figures 4.63 and 4.64, respectively. It is seen from these Figures that the clay-sand mixtures with NS sand have higher values of cohesion and angle of internal friction for all sizes and contents of sand. This behaviour is attributed to that the void ratio decreased as roundness and sphericity increase. The number of contacts per particle increased by decreasing the void ratio. If a soil has a higher packing density (the particles are more closely together), it should have a greater number of particle to particle contacts and a greater area of contact per particle. The same observations can be found in (Jia and Williams, 2001; Cubrinovski and Ishihara, 2002; Cho et. al., 2006; Lim et al., 2013). The reason of decreasing void ratio is the particle mobility and their ability to achieve minimum potential energy arrangements obstructed by irregularity (Cho et. al., 2006). The results showed that the maximum decrease in the cohesion is 3.8 kPa between the clayey soil samples and clay-sand mixtures with 50% sand content of 2.0-1.0 mm of CSS sand of clay-sand mixtures, while the maximum increase in the angle of internal friction was 4.9° between the clayey soil samples and clay-sand mixtures with 50% sand content of 2.0-1.0 mm of NS sand of clay-sand mixtures as presented in Table 4.8.

4.2.4.3 Effect of Sand Size

The effect of particle size distribution on the shear strength of soils has been well proven in the previous studies. The increment of gravel content of clay-gravel mixtures was found to decrease the cohesion and increase the shear resistance of these mixtures (Holtz and Willard, 1956; Shakoor and Cook, 1990; Liu et al., 2006; Li et al., 2011). It is commonly recognized that the increment of gravel content of sand-gravel mixtures results in increment in the peak strength and the constant volume strength of these mixtures (Holtz and Gibbs, 1956; Simoni and Houlsby, 2006). Using conventional triaxial test, Martinez (2003) reported that particle size affect the stress strain and volumetric strain behaviour of the granular materials. Katzenbach and Schmitt (2004), using 3D-DEM (PFC), conducted triaxial simulation to evaluate particle size effect and found that particle size distribution strongly alters the stress-strain behavior. Herbold et al. (2008) reported that the dynamic mechanical properties alter with the increase of particle size. Gupta (2009) investigated particle size (25, 50 and 80 mm) for Ranjit Sagar Rockfill Material (RSRM) and Purulia Rockfill Material (PRM) and found that for RSRM angle of internal friction increase with the increase of particle size for RSRM but for PRM angle of internal friction decrease with the increase of particle size for PRM. Islam (2009) using 3D-DEM (YADE) observed that particle size alters the strength characteristics. Omar and Sadrekarimi (2014) indicated that the increment in the mean particle size caused increment in peak shear strength and the mobilized friction angle for the same sandy soil density. In addition, Islam et al. (2011) indicated increment in the shear strength and friction angle with the increment of the particle size. Moreover, Kara et al. (2013) declared that the increment in the particle size led to the increment in the peak friction angle. Pitman et al. (1994) declared that the increment of the fine content to specific value (i.e. to fine content equals to 40%) led to the reduction or elimination of any contact between the coarse particles; consequently, reduced the friction angle.

From Figures 4.65 and 4.66, it is observed that for all the cases studied with the increment of grain size the angle of internal friction of clay-sand mixtures increases for all sand contents and for two shapes of sand (NS and CSS) which is similar to Vangla and Latha (2012) because of the increase in grain size will increase contact area, and contact force, leading to an increase in friction. While cohesion the of clay-sand mixtures decreases for all sand contents and for two shapes of sand (NS and CSS) as the grain size of sand increases.

4.2.5 Small Strain Shear Modulus (G_{max})

Small strain shear modulus (G_{max}) is a significant factor representing the small strain response of soils subjecting to a seismic load and an essential parameter in the design of foundations where only small deformation takes place. It is considerably affected by a range of parameters of which the main are shear strain amplitude, the void ratio (e), and mean effective stress (σ') (Hardin and Drnevich, 1972). The shear modulus of soil is dependent on the stress state, over consolidation ratio, density, void ratio, microstructure, anisotropy, the degree of saturation, aging, cementation, and temperature (Sawangsuriya, 2012). The mean effective stress (σ'_m), void ratio (e), the degree of saturation (Sr), maximum principal stress difference (σ_1-σ_3), soil grain characteristics (shape, size and mineralogy), and gradation are the parameters that affect the shear modulus of soil (Hardin and Black, 1969).

Voids ratio, which is directly related to packing features of soil, has a substantial effect on G_{max}. The increase in void ratio causing the decrease of G_{max} (Kallioglou et al., 2008; El Mosallamy et al. 2014; Liu et al., 2016; Panuska and Frankovska, 2016; Asadi et al., 2018; Mojezi et al., 2018; Shivaprakash and Dinesh, 2018). Void ratio affects shear wave velocity through the coordination number of the fabric (Santamarina and Fam, 2001). The void ratio range is controlled by particle shape and size. The structure which represents the particle orientations, contact patterns of soil (especially clays) is likewise controlled by the shape of the particles. The smaller particle fraction considerably influenced the void ratio range of two different sizes (Cubrinovski and Ishihara, 2002). The number of contacts per particle increased by decreasing the void ratio. The number of particle to particle contacts and the area of contact per particle should be more when the soil has a higher packing density (the particles are more closely together). Santamarina and Cascante (1998) showed that the increase of the average contact force is resulted by an increase in void ratio and the soil stiffness reduces with increasing void ratio. Iwasaki and Tatsuoka (1977) showed that G_{max} is strongly influenced by the grain size distribution at a constant void ratio but could not detect a considerable effect of the grain shape, and G_{max} was observed to be increasing with a decrease in void ratio. Hardin and Kalinski (2005) found that gravels had significantly larger shear modului than that for uniform sand using resonant column tests which indicates the increase in G_{max} with an increase in D_{50}. The study carried out by Senetakis et al. (2013) showed that G_{max} of granular soils is strongly dependent on the type of particles, which include both mineralogy and particles shape and size. The influence of particle shape on dynamic soil properties is still discussed. Some researchers believe that the effect is attributed to the variation in void ratio and not only due to the particle shape itself.

Figures 4.67 and 4.68 illustrate the relationship between measured G_{max} and the effective stress of NS and CSS sand for clay-sand mixtures, respectively. It can be seen from these Figures that the values of G_{max} increase with effective stress for all cases that studied in this study. These results are compatible with other studies (Bui et al., 2007; Wichtmann and Triantafyllidis, 2009; Szilvagyi, 2016; Chen et al., 2017). This increasing of G_{max} is attributed to that the voids ratio of clay-sand mixtures decreased with increasing of effective stress for NS and CSS sand of clay-sand mixtures as presented in Figures 4.55 and 4.56, respectively.

4.2.5.1 Effect of Sand Content

It has been observed that the addition of sand to the clayey soil leads to a substantial increase in G_{max} of these mixtures. This can be the main reason for the results shown in Figures 4.69 and 4.70 that G_{max} values of the clay-sand mixtures are significantly higher than those of clayey soil. The values of G_{max} increased with the increase of sand contents for NS and CSS sand of clay-sand mixtures for all sizes of sand and for all effective stress that investigated in this study as presented in Figures 4.69 and 4.70, respectively. The reason of this increasing belong to that the voids ratio decreased with increasing of sand content for NS and CSS sand of clay-sand mixtures as shown in Figures 4.71 and 4.72, respectively. The results of this study presents a good agreement with the study of Fei and Xu (2017). They investigated the influences of coarse particles on the dynamic behavior of clay-aggregate mixtures using cyclic triaxial tests on clay specimens with various glass bead contents They observed that the initial shear modulus increased with the increasing of coarse aggregate content. Figures 4.73 and 4.74 show that G_{max} increased with decreasing of voids ratio of NS and CSS sand of clay-sand mixtures, respectively. The G_{max} values of the clay-sand mixtures changed from 20.8 MPa of 0.6-0.3 mm sand size with 10

% of sand of 50 kPa effective stress to 53.8 MPa of 2.0-1.0 mm sand size with 50 % of sand of 200 kPa effective stress for the rounded sand (NS), while it ranged from 20.1 MPa of 0.6-0.3 mm sand size with 10 % of sand of 50 kPa effective stress to 51.6 MPa of 2.0-1.0 mm sand size with 50 % of sand of 200 kPa effective stress for the angular sand (CSS) as presented in Table 4.9.

4.2.5.2 Effect of Sand Shape

The shear wave velocity (Vs) of soil is affected by soil type. Soils with a wide range of grain sizes tend to have smaller average void ratios, therefore, exhibit larger values of Vs. Hardin and Drnevich (1972) observed that G_{max} is highly dependent on void ratio and hardly affected by grain characteristics, size, shape, gradation, and mineralogy. However, if wide ranges in the void ratio are employed with specifying soil type, the effect of soil type is reduced. The shear wave propagating in a granular material can be considered as a combination of the shear wave through the contact network and solid particle. The change of the void ratio may partly variation the length of wave travel. Furthermore, less travel time would be spent in the contact network for the dense sample. Compared to the loose specimen, the dense one would form a much more stable connectivity, and thus blocks the particle micro-rotation. Hardin (1961) concluded that grain shape influenced Vs through void ratio; the void ratio of the crushed quartz sand (angular grains), was greater than that of Ottawa sand (rounded grains), causing Vs to be higher in the rounded material. Hardin and Richart (1963) proposed that for uncemented soils, the controlling factor was a void ratio, and that particle shape was of minor significance and in soul only contributed to variations in void ratio, and effective strength envelope and the addition of fine, platy mica into round sand reduced the stiffness. The recent investigation by Payan et al. (2016) shows the importance of the influence of particle shape on the shear modulus of granular soils.

G_{max} values of NS sand of clay-sand mixtures are compared with those of CSS sand of clay-sand mixtures for different sand contents and for three effective stress levels for 0.6-0.3 mm and 2.0-1.0 mm, the results are presented in the Figures 4.75 and 4.76, respectively. The G_{max} reduced with the increase of voids ratio (e) for all sizes of sand and for all effective stresses for NS and CSS sand of clay-sand mixtures. The sand grains with angular shape have lower G_{max} values for all sizes and contents of sand of clay-sand mixtures. This behaviour is occurred because of the void ratio decreased as roundness and sphericity increased (e of rounded sand is lower than that of angular sand). Same findings can be observed in (Dyskin et al., 2001; Jia and Williams, 2001; Nakata et al., 2001; Guimaraes, 2002; Cubrinovski and Ishihara, 2002; Shin and Santamarina, 2013). Nevertheless, both NS and CSS sand of clay-sand mixtures exhibit higher G_{max} than clayey soil samples. The values of G_{max} of NS sand of clay-sand mixtures are approximately 3-7% higher than that of CSS sand of clay-sand mixtures. The observed difference is considered to be mainly related to the grain shape. Compared with the shape of NS sand grains which are rounded, while the CSS sand grains are angular. The effect of grain shape may have been largely attributed to the void ratio (Payan et al., 2016). For the NS sand of clay-sand mixtures with rounded grains the void ratios are lower, whereas for CSS sand of clay-sand mixtures with angular grains the void ratios are higher as shown in Table 4.98.

4.2.5.3 Effect of Sand Size

The measurements of G_{max} at three different effective stress levels (50, 100 and 200 kPa) are shown as a relationship with voids ratio for NS and CSS sand of clay-sand mixtures in Figures 4.73 and 4.74, respectively. Clearly, at a given effective stress the G_{max} decreases with increasing void ratio, and for a given void ratio the shear modulus increases with an increase in effective stress. The sand grains with larger sizes have higher G_{max} values than those with smaller sizes for both types of sand (NS and CSS) that form the clay-sand mixtures under study as presented in Figures 4.69 and 4.70. The main reason for this increment in G_{max} with increasing of size is because of decreasing of e with increasing of sand size as presented in Table 4.9, and the increase in particle size increased the contact area and contact force, and therefore an increase in friction strength and hence contact stiffness. Bui (2009) studied the influences of some particle characteristics such as particle size and particle shape on the small strain response of soils. Granular materials with different particle shapes, namely glass ballotini with various diameters, Leighton Buzzard sand fraction B and E, glass glitter, glass nugget, as well as mixtures of Leighton Buzzard sand fraction B and 0.1 mm mica, are tested using a fixed-free resonant column apparatus. They observed that G_{max} significantly increases with an increase in particle size. Enomoto et al. (2013) stated that the larger grain size the higher shear modulus of soil. This study is in a good agreement with the studies of Bui (2009) and Enomoto et al. (2013). As example, G_{max} value of the clay-sand mixtures with 30 % of sand of 100 kPa effective stress for the rounded sand (NS) with 0.6-0.3 mm sand size is 33 MPa, while it is 35.8 MPa with 2.0-1.0 mm sand size. In the same trend, G_{max} value of the clay-sand mixtures with 30 % of sand of 100 kPa effective stress for the angular sand (CSS) with 0.6-0.3 mm sand size is 31.6 MPa, while it is 33.8 MPa with 2.0-1.0 mm sand size. The values of G_{max} of 2.0-1.0 mm sand size are approximately 4-9 % higher than those of 0.6-0.3 mm sand size of clay-sand mixtures for NS sand, while these values of 2.0-1.0 mm sand size are about 3-8 % higher than those of 0.6-0.3 mm sand size of clay-sand mixtures for CSS sand.

4.2.5.4 Relationship Between Shear Modulus, Voids Ratio and Effective Stress

In Figures 4.65 and 4.66, the relationship between the G_{max} and effective stress for NS and CSS sand of clay-sand mixtures is presented. Results shown in this graph confirm the positive impact of stress on the G_{max}. In all the cases analyzed the values of G_{max} increase with the effective stress. Many investigators in this topic have confirmed in their papers the increase of the G_{max} with effective stress (Gryczmanski, 2009; El Mosallamy et al. 2014; Asadi et al., 2018). This conclusion is true also in the light of the authors' results. Presentation of these three variables (G_{max}, e and p) on a three dimensional graph allowed subsequently a common function describing all data to be found for clay, clay-NS sand and clay-CSS sand as presented in Figures 4.77 and 4.78, respectively. The empirical correlation between G_{max}, e and p′ of clay-rounded sand (R^2=0.99), and clay-angular sand (R^2=0.99), respectively have been found:

$$G_{max}=2.53\ p^{0.4}\ e^{-0.89} \tag{4.4}$$

$$G_{max}=2.16\ p^{0.43}\ e^{-0.92} \tag{4.5}$$

4.3 Normalized Shear Modulus (G/G_{max})

It is difficult to attain accurate measurement of soil stiffness in conventional geotechnical laboratory testing. The stiffness of a soil sample that obtained using conventional triaxial compression test is depended on external measurements of strain which include a number of irrelevant displacements. In the conventional triaxial test, surface friction arises between the unlubricated ends of the test specimen and the end platens of the test apparatus. Accordingly, the test specimen deforms non-uniformly with an increasing of axial deformation from zero at the ends to a maximum at the middle part of the sample. It is widely believed that triaxial test specimens have end zones which are more or less restrained while the middle third is more or less unrestrained. It is highly desirable therefore that axial deformations are measured locally in this region if realistic deformation moduli are to be found. The measurement of axial strain based on the relative movement between the top cap and the base pedestal is subject to bedding errors. These errors arise because of the difficulty in providing perfectly plane, parallel and smooth ends on the triaxial test specimen. The top cap can rest on surface asperities of the test specimen or make contact imperfectly. Due to this loading effect, rapid deformation will occur during the early stages of triaxial compression until the top cap is properly bedded down. Because of these reasons, the local strain measurement by internal LVDTs were used in this study for an accurate evaluation the stiffness behaviours of the clay-sand mixtures at small strain level.

The following researchers conducted their studies with LVDTs (Cabarkapa and Cuccovillo, 2006; Yimsiri et al., 2009; Jung et al., 2012; Surarak et al., 2012; Ratananikom et al., 2013; Likitlersuan et al., 2013; Nishimura, 2014; Gasparre et al., 2014; Kumar et al., 2016; Roshan et al., 2017; Wild et al., 2017). Depending on the investigations that carried out by the researchers (Bonal et al., 2012; Wu et al., 2014; Ackerley et al., 2016; Nishimura and Abdiel, 2017; Brosse et al., 2017), the following properties of the small strain measuring apparatuses are concluded: the ability to measure soil properties at strain of at least 10^{-2}% objectively and accurately, the ability to be mounted on samples with different dimensions, the ability to measure on the central one-third of the sample to avoid end restrained effects and capability of providing stable stress-strain measurement over long period of time.

A modulus reduction curve is used to represent the degradation of shear modulus with strain in terms of reduction in modulus ratio (G/G_{max}) to assess both the value of soil shear modulus for small strain and scheme of its degradation with increasing strain. The degradation in shear modulus of soils with increasing strain has a substantial influence on the analysis and design of a wide range in geotechnical engineering, such as soil-structure interaction, deep excavations and the dynamic response of soils under seismic loading (Likitlersuang et al., 2013; Yang and Gu, 2013). Experimental studies on the relationship between shear modulus reduction and the strain have found that the shear modulus varies greatly depending on soil type, initial density, stress history, loading cycles, and degree of saturation of soil (Alramahi et al., 2008; Khosravi and McCartney, 2012). A range of shear modulus degradation curves for various soils have been suggested, for clay (Darendeli, 2001; Vardanega et al., 2015), for sand (Oztoprak and Bolton, 2013) and for gravels (Menq, 2003). Published data on the shear modulus degradation curves of clay-sand mixtures are limited.

The shear modulus values from static triaxial compression tests were normalized by the G_{max} derived from the shear wave velocity measured using the Be tests to obtain the shear modulus degradation curves for clay-NS sand and clay-CSS sand mixtures at various effective stresses to study their variation in a range of strain levels as presented in Figures 4.79-4.84. It is observed from these Figures that the G/G_{max} values decreased with increasing of the strain and increased with the increasing of effective stresses. Same findings can be observed by (Rayhani and El Naggar, 2008; Vardanega et al., 2015; Yang, 2017). These Figures present a link between the stiffness at very small strains using bender element tests with the stiffness at small strains using internal LVDTs for local strain measurements in triaxial compression test. The values of shear modulus of clay-sand mixtures can be obtained at any strain level from the shear modulus degradation curves that presented in these Figures. Ishibashi et al. (1991) compared between the normalized shear modulus of glass spheres and Ottawa sand using resonant column apparatus. They found that both materials showed very similar behaviour and it may be concluded that the glass spheres can be effectively used in studying state and evolution of fabric of this type of granular materials.

4.4 Comparison Between $G_{max(Unc)}$ and $G_{max(Tri)}$

Figures 4.85-4.88 present the comparison between the values of G_{max} obtained from unconfined compression machine equipped with bender elements with that obtained from triaxial compression machine equipped with bender elements at different effective stresses for clay-NS sand with 0.6-0.3 and 2.0-1.0 mm size and clay-CSS sand with 0.6-0.3 and 2.0-1.0 mm size, respectively.

Table 4.1 The values of L/λ and Vs for clay-sand mixtures of frequency 5 kHz.

Sand Size (mm)	Sand Content (%)	NS		CSS	
		V_s (m/s)	L/λ	V_s (m/s)	L/λ
---	0	118.6	5.98	118.6	5.98
(0.6-0.3)	10	147.1	4.83	146.9	4.83
	20	150.7	4.71	150.1	4.73
	30	152.7	4.65	151.8	4.68
	40	155.8	4.56	155.1	4.58
	50	158.9	4.47	157.7	4.50
(1.0-0.6)	10	148.9	4.77	147.0	4.83
	20	152.0	4.67	150.7	4.71
	30	154.1	4.61	151.8	4.68
	40	156.4	4.54	155.6	4.56
	50	160.5	4.42	158.5	4.48
(2.0-1.0)	10	152.5	4.66	150.6	4.71
	20	154.7	4.59	152.1	4.67
	30	154.8	4.59	153.0	4.64
	40	157.2	4.52	156.9	4.53
	50	160.7	4.42	159.0	4.47

Table 4.2 q_u values (kPa) for the mixtures tested.

Sand Type	Sand Content (%)	0.6-0.3 mm	e	1.0-0.6 mm	e	2.0-1.0 mm	e
---	0	355	0.577	355	0.577	355	0.577
NS	10	278	0.548	295	0.533	314	0.518
	20	250	0.508	267	0.491	288	0.476
	30	221	0.471	246	0.446	254	0.431
	40	190	0.442	209	0.419	223	0.405
	50	163	0.413	174	0.399	187	0.385
CSS	10	266	0.565	280	0.547	296	0.535
	20	231	0.528	253	0.506	263	0.491
	30	206	0.495	222	0.465	237	0.451
	40	174	0.462	197	0.440	209	0.424
	50	151	0.435	163	0.421	176	0.404

Table 4.3 G_{max} values (MPa) for the mixtures tested.

Sand Type	Sand Content (%)	0.6-0.3 mm	e	1.0-0.6 mm	e	2.0-1.0 mm	e
---	0	29	0.577	29	0.577	29	0.577
NS	10	44	0.548	45	0.533	48	0.518
	20	47	0.508	48	0.491	50	0.476
	30	49	0.471	50	0.446	51	0.431
	40	51	0.442	52	0.419	53	0.405
	50	54	0.413	55	0.399	56	0.385
CSS	10	43	0.565	44	0.547	46	0.535
	20	46	0.528	47	0.506	48	0.491
	30	47	0.495	48	0.465	49	0.451
	40	50	0.462	51	0.440	52	0.424
	50	52	0.435	53	0.421	54	0.404

Table 4.4 Deviotric stress values (kPa) at various strains for the mixtures tested.

Effective Stress (kPa)	Sand Size (mm)	Sand Content (%)	NS			CSS		
			ε=0.01%	0.1%	1.0%	0.01%	0.1%	1.0%
50	---	0	2.3	13.4	50.8	2.3	13.4	50.8
	0.6-0.3	10	2.9	20.8	60.5	2.5	17.9	56.6
		30	3.1	23.4	62.7	2.7	21.1	60.6
		50	3.3	27.3	66.0	3.0	24.3	62.1
	2.0-1.0	10	3.0	20.9	62.9	2.8	19.8	61.1
		30	3.3	25.0	67.5	3.2	22.1	63.7
		50	4.2	32.1	73.6	3.8	28.2	68.2
100	---	0	3.8	23.2	87.8	3.9	23.2	87.8
	0.6-0.3	10	4.2	30.7	99.5	4.0	29.3	96.5
		30	4.4	36.2	105.3	4.2	33.5	100.9
		50	4.7	40.2	113.1	4.5	38.1	112.7
	2.0-1.0	10	4.3	33.6	106.6	4.1	32.1	99.7
		30	4.6	38.5	114.2	4.4	34.7	107.9
		50	5.7	47.6	119.6	5.3	43.4	118.2
200	---	0	4.1	31.8	148.3	4.1	31.8	148.3
	0.6-0.3	10	5.2	43.1	177.9	4.7	41.2	172.8
		30	5.7	51.2	200.1	5.3	46.9	191.4
		50	6.4	58.9	218.3	6.0	55.9	209.8
	2.0-1.0	10	5.6	47.9	195.3	5.1	43.1	176.2
		30	6.3	54.7	210.7	5.8	51.6	200.2
		50	7.6	63.2	227.3	6.9	58.5	217.4

Table 4.5 Values of voids ratio (e) of clay-sand mixtures.

Effective Stress (kPa)	Sand Content (%)	NS		CSS	
		0.6-0.3 mm	2.0-1.0 mm	0.6-0.3 mm	2.0-1.0 mm
50	0	0.560	0.560	0.560	0.560
	10	0.540	0.512	0.553	0.528
	30	0.466	0.427	0.479	0.442
	50	0.403	0.380	0.418	0.396
100	0	0.554	0.554	0.554	0.554
	10	0.528	0.499	0.545	0.517
	30	0.451	0.413	0.465	0.430
	50	0.384	0.369	0.401	0.384
200	0	0.541	0.541	0.541	0.541
	10	0.510	0.486	0.532	0.507
	30	0.440	0.402	0.458	0.425
	50	0.374	0.357	0.391	0.376

Table 4.6 Pore water pressure values (kPa) at various strains for the mixtures tested.

Effective Stress (kPa)	Sand Size (mm)	Sand Content (%)	NS			CSS		
			ε=0.01%	0.1%	1.0%	0.01%	0.1%	1.0%
50	---	0	351.8	357.5	378.3	351.8	357.5	378.3
	0.6-0.3	10	351.3	355.6	370.3	351.4	355.9	371.8
		30	350.5	353.8	367.0	350.7	354.4	369.3
		50	350.4	353.6	363.9	350.5	354.2	366.2
	2.0-1.0	10	350.7	355.2	370.1	350.8	355.7	371.3
		30	350.4	354.1	366.9	350.6	354.5	369.1
		50	350.3	354.0	363.6	350.5	354.3	366.0
100	---	0	352.0	360.7	393.4	352.0	360.7	393.4
	0.6-0.3	10	351.5	358.5	385.1	351.7	359.7	389.5
		30	351.0	357.0	380.7	351.2	357.6	383.9
		50	350.8	356.6	378.0	351.0	357.5	380.6
	2.0-1.0	10	351.2	358.3	384.7	351.3	359.5	389.2
		30	350.9	356.7	380.5	351.1	358.4	383.5
		50	350.7	356.4	377.8	350.9	358.2	380.3
200	---	0	352.3	366.1	424.1	352.3	366.1	424.1
	0.6-0.3	10	352.1	363.3	412.1	352.2	364.0	415.6
		30	351.9	360.6	402.1	352.0	361.9	407.2
		50	351.6	360.3	399.3	351.8	361.5	402.0
	2.0-1.0	10	352.0	360.1	411.7	352.1	363.8	414.9
		30	351.8	359.9	401.7	351.9	361.6	406.8
		50	351.5	359.8	399.0	351.6	361.3	401.6

Table 4.7 Stiffness values (MPa) at various strains for the mixtures tested.

Effective Stress (kPa)	Sand Size (mm)	Sand Content (%)	NS			CSS		
			ε=0.01%	0.1%	1.0%	0.01%	0.1%	1.0%
50	---	0	15.9	13.4	5.1	15.9	13.4	5.1
	0.6-0.3	10	25.1	19.6	5.6	23.3	19.1	5.5
		30	29.9	23.1	6.5	26.7	20.7	6.2
		50	36.1	27.3	6.6	31.6	24.3	6.4
	2.0-1.0	10	27.5	21.4	6.8	25.1	19.5	6.1
		30	32.9	25.4	6.9	29.2	22.7	6.5
		50	39.4	29.7	7.1	34.6	26.4	6.7
100	---	0	28.4	23.0	8.8	28.4	23.0	8.8
	0.6-0.3	10	38.1	30.6	9.9	36	29.3	9.6
		30	44.2	35.8	10.5	40.8	33.2	10.1
		50	51.6	40.7	11.4	46.8	38	11.0
	2.0-1.0	10	40.9	32.7	10.4	39.6	31.8	9.9
		30	48.9	40.1	11.6	44.4	36.3	11.2
		50	55.9	43.5	12.0	55.3	40.9	11.5
200	---	0	35.9	31.4	14.8	35.9	31.4	14.8
	0.6-0.3	10	50.6	42.3	17.7	47.4	40.8	17
		30	63.9	49.9	19.9	55.2	47.7	19.2
		50	68.8	57.7	21.8	65.1	55	20.8
	2.0-1.0	10	54.1	45.1	18.8	50.4	42.3	17.6
		30	64.4	55.4	21.1	58.8	49.7	19.9
		50	73.9	63.6	22.6	69.2	58.2	21.6

Table 4.8 Values of effective shear strength parameters of clay-sand mixtures.

Sand Size (mm)	Sand Content (%)	NS		CSS	
		c′ (kPa)	φ′ (degree)	c′ (kPa)	φ′ (degree)
---	0	8.0	11.9	8.0	11.9
0.6-0.3	10	6.4	13.0	5.9	12.7
	30	5.2	14.1	4.6	13.6
	50	4.0	15.1	3.4	14.7
2.0-1.0	10	6.1	13.5	5.6	13.1
	30	4.8	14.6	4.1	14.2
	50	3.7	15.7	3.1	15.2

Table 4.9 G_{max} values (MPa) of clay-sand mixtures.

Sand Type	Effective Stress (kPa)	Sand Content (%)	0.6-0.3 mm	e	2.0-1.0 mm	e
NS	50	0	18.4	0.560	18.4	0.560
		10	20.8	0.540	22.4	0.512
		30	24.2	0.466	26.2	0.427
		50	27.6	0.403	29.2	0.380
	100	0	25.2	0.554	25.2	0.554
		10	28.6	0.528	30.2	0.499
		30	33.0	0.451	35.9	0.413
		50	37.9	0.384	39.6	0.369
	200	0	34.9	0.541	34.9	0.541
		10	38.7	0.510	40.4	0.486
		30	44.8	0.440	48.0	0.402
		50	51.7	0.374	53.8	0.357
CSS	50	0	18.4	0.560	18.4	0.560
		10	20.1	0.553	21	0.528
		30	22.7	0.479	24.5	0.442
		50	25.8	0.418	27.3	0.396
	100	0	25.2	0.554	25.2	0.554
		10	27.2	0.545	28.8	0.517
		30	31.6	0.465	33.8	0.430
		50	36.4	0.401	37.8	0.384
	200	0	34.9	0.541	34.9	0.541
		10	37.5	0.532	39.3	0.507
		30	43.2	0.458	45.9	0.425
		50	50.1	0.391	51.6	0.376

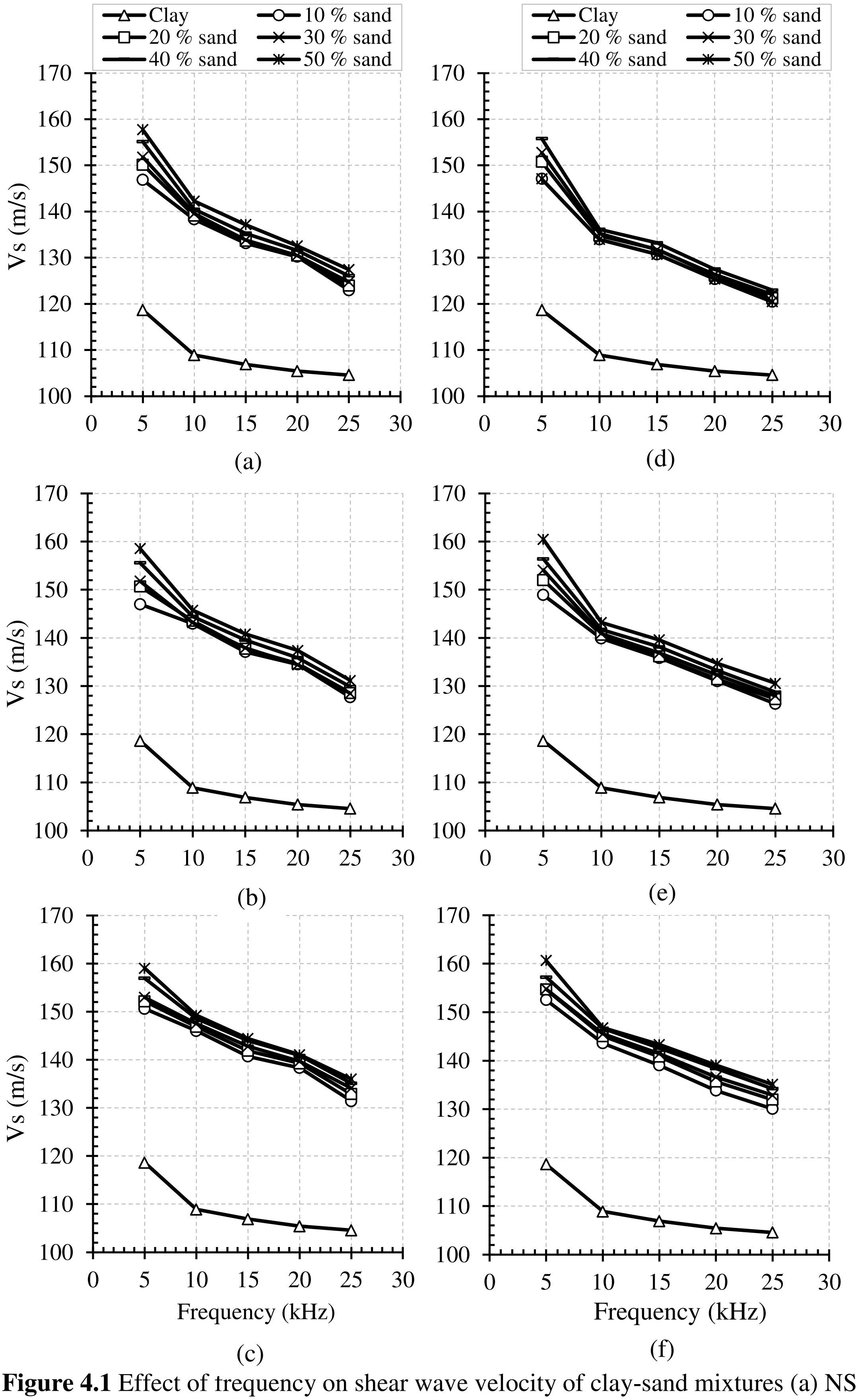

Figure 4.1 Effect of frequency on shear wave velocity of clay-sand mixtures (a) NS, (0.6-0.3) mm (b) NS, (1.0-0.6) mm. (c) NS, (2.0-1.0) mm. (d) CSS, (0.6-0.3) mm (e) CSS, (1.0-0.6) mm. (f) CSS, (2.0-1.0) mm.

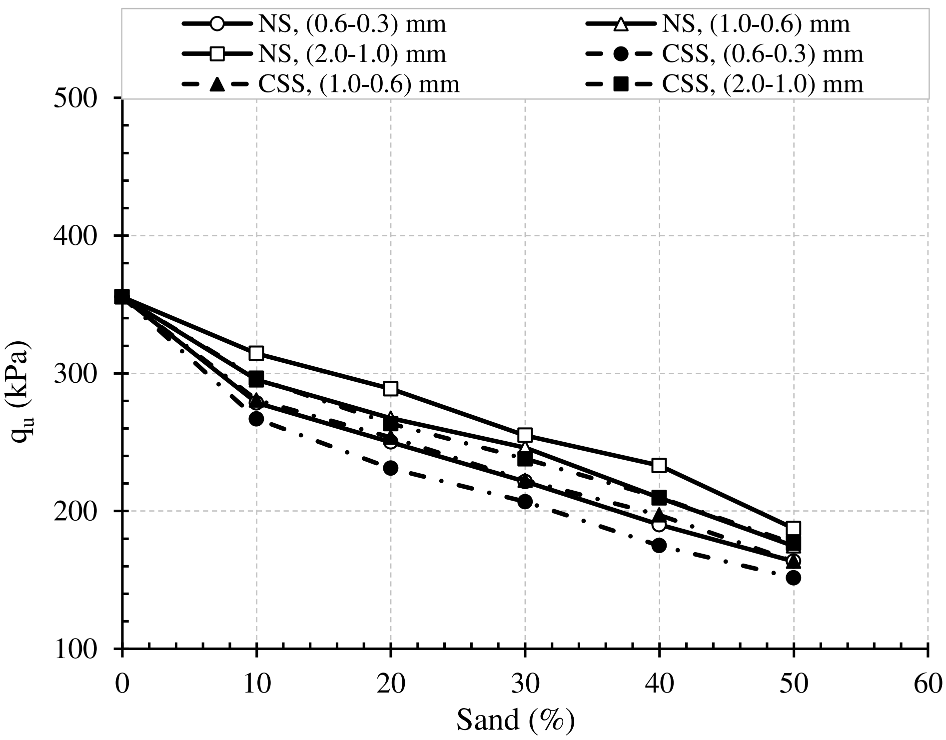

Figure 4.2 Change of q_u (kPa) with the sand content (%).

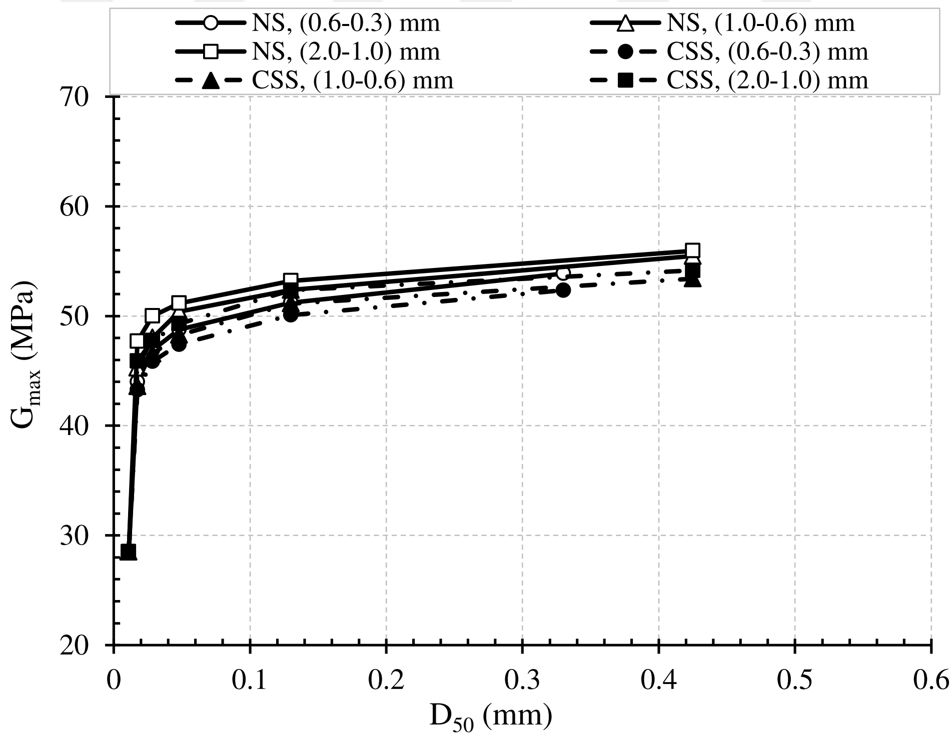

Figure 4.3 Relationship between G_{max} (MPa) and D_{50} (mm) for various sands in mixtures.

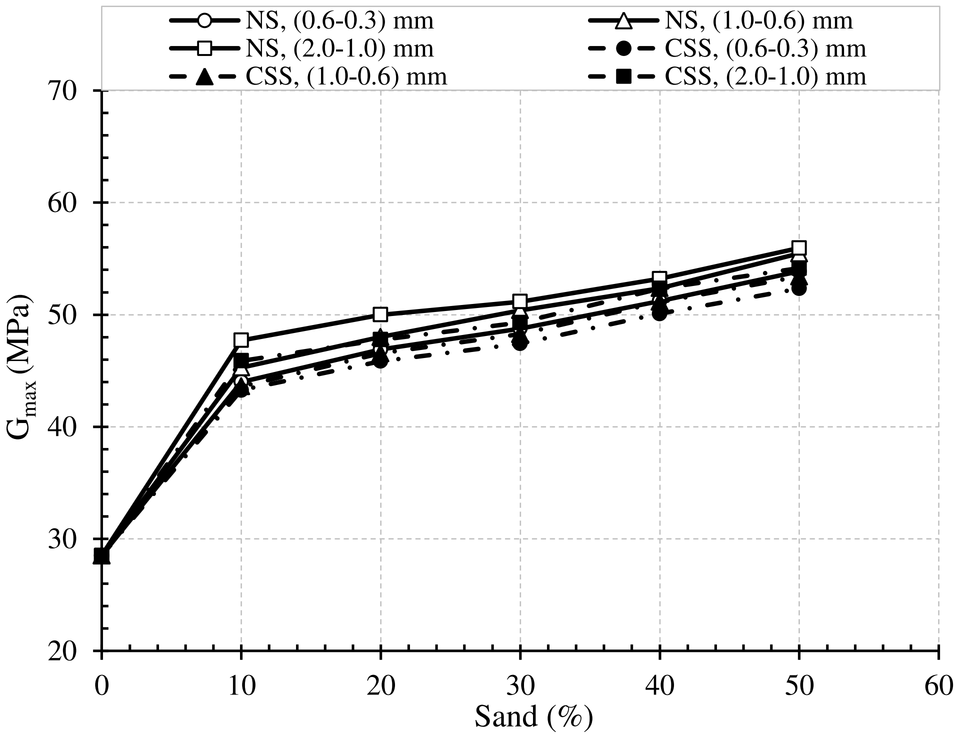

Figure 4.4 Relationship between G_{max} (MPa) and sand content (%).

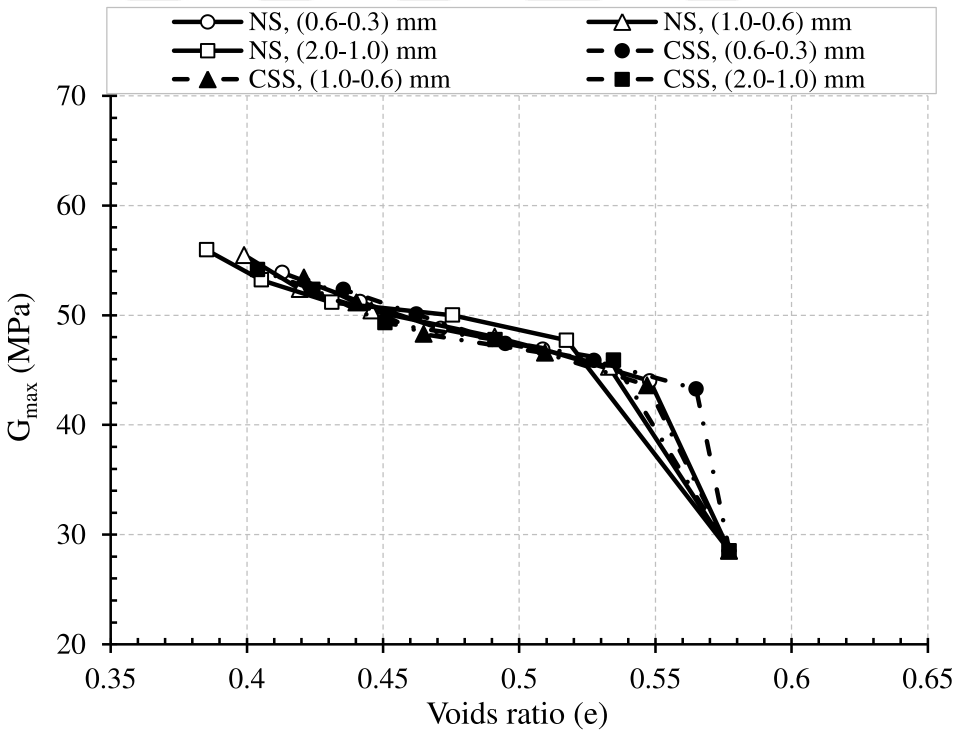

Figure 4.5 Effect of voids ratio (e) on the change of G_{max} (MPa).

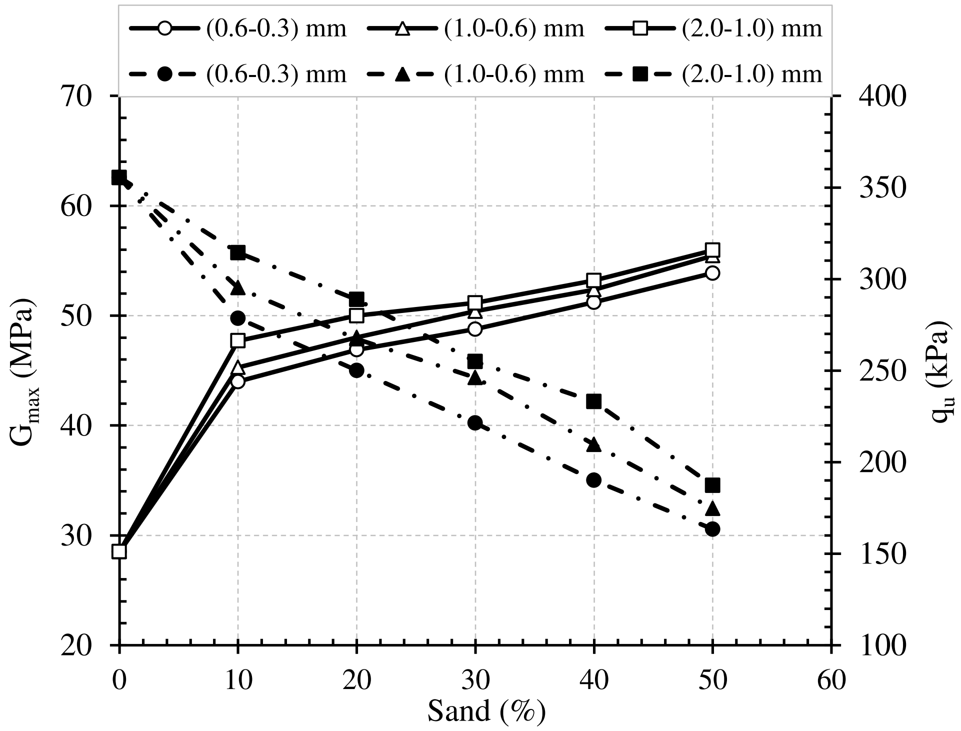

Figure 4.6 Comparison of G_{max} (MPa) and q_u (kPa) of the NS-clay mixtures.

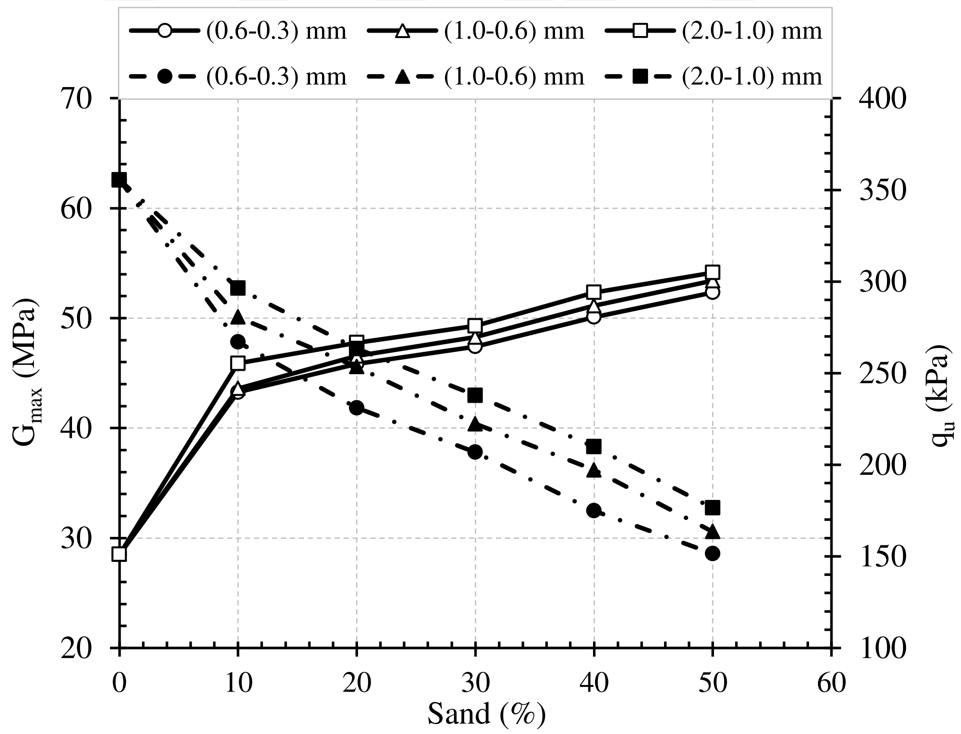

Figure 4.7 Comparison of G_{max} (MPa) and q_u (kPa) of the CSS-clay mixtures.

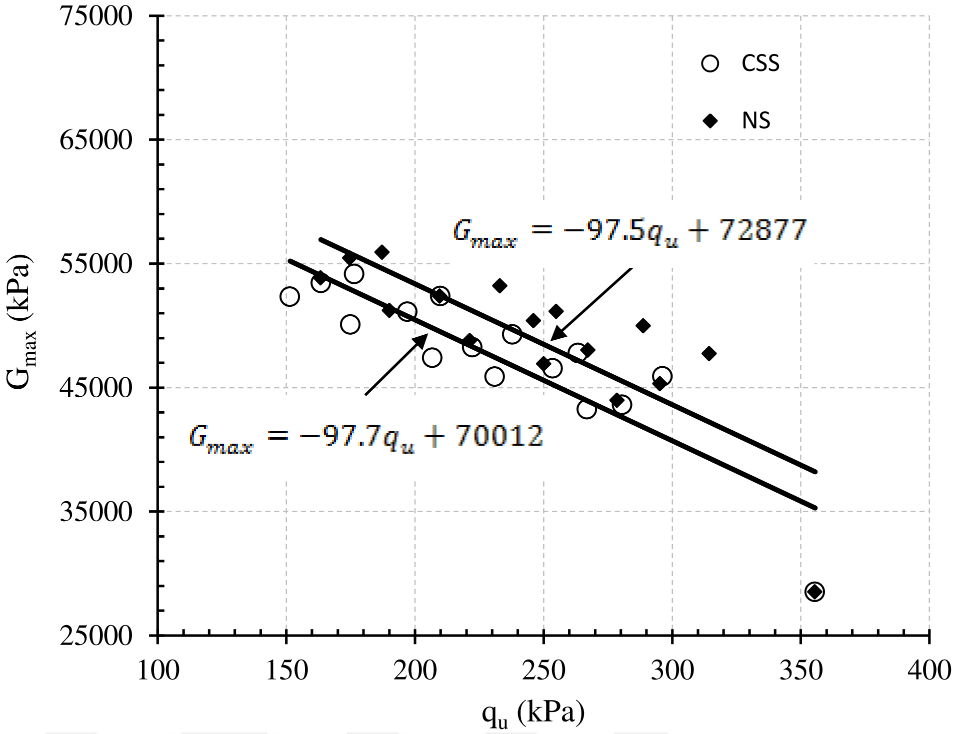

Figure 4.8 G_{max}-q_u correlation with sand content (%).

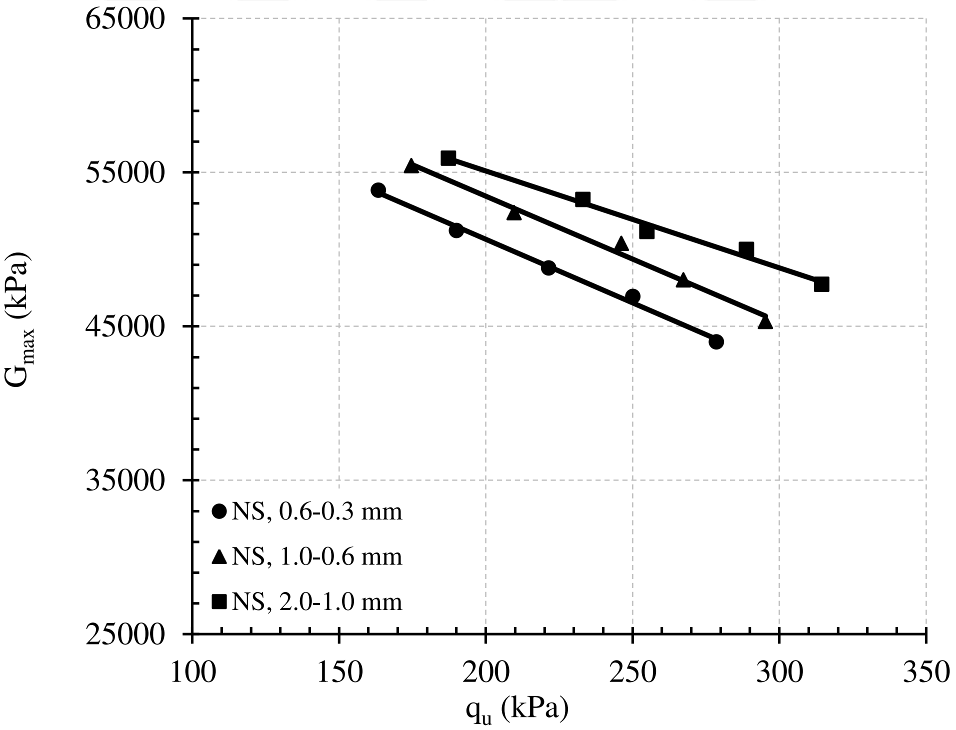

Figure 4.9 G_{max}-q_u correlation for clay-NS sand mixtures.

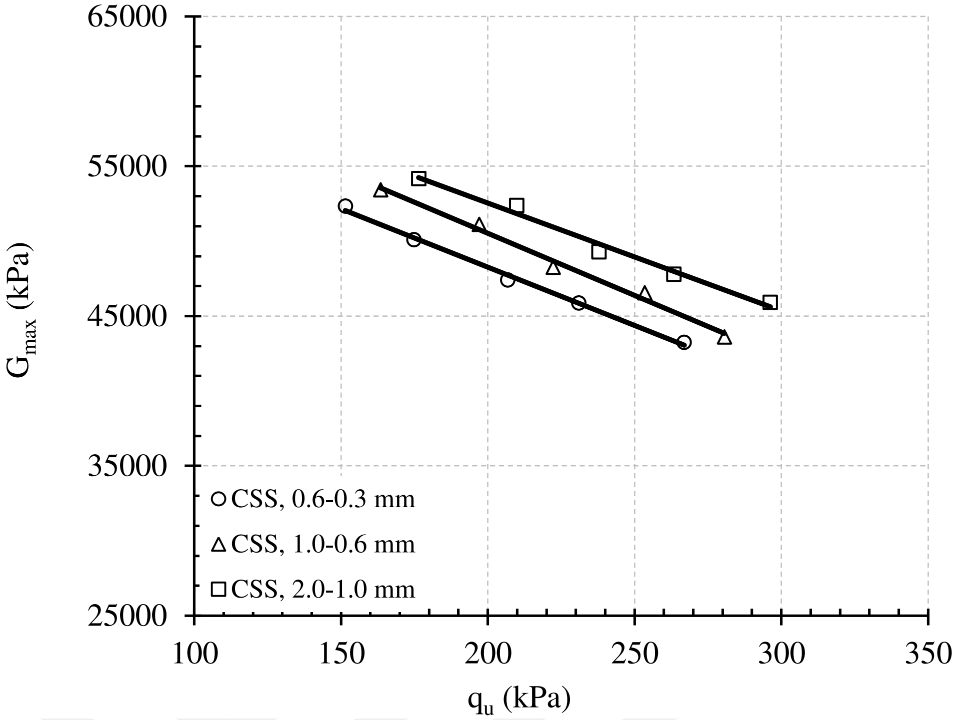

Figure 4.10 G_{max}-q_u correlation for clay-CSS sand mixtures.

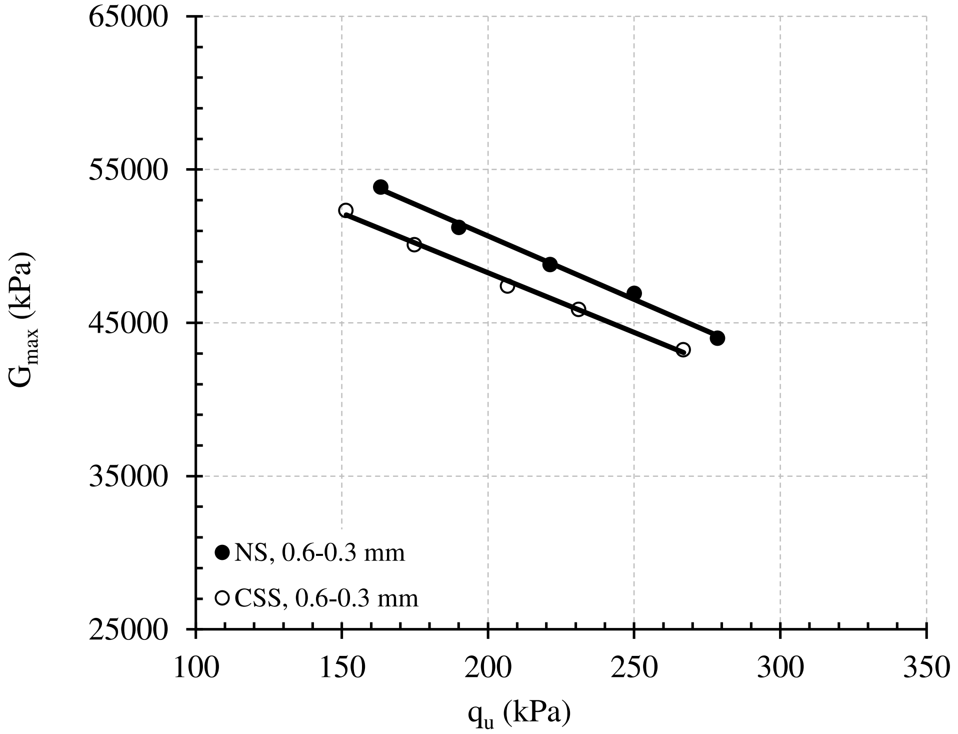

Figure 4.11 G_{max}-q_u correlation for clay-sand mixtures with size 0.6-0.3 mm.

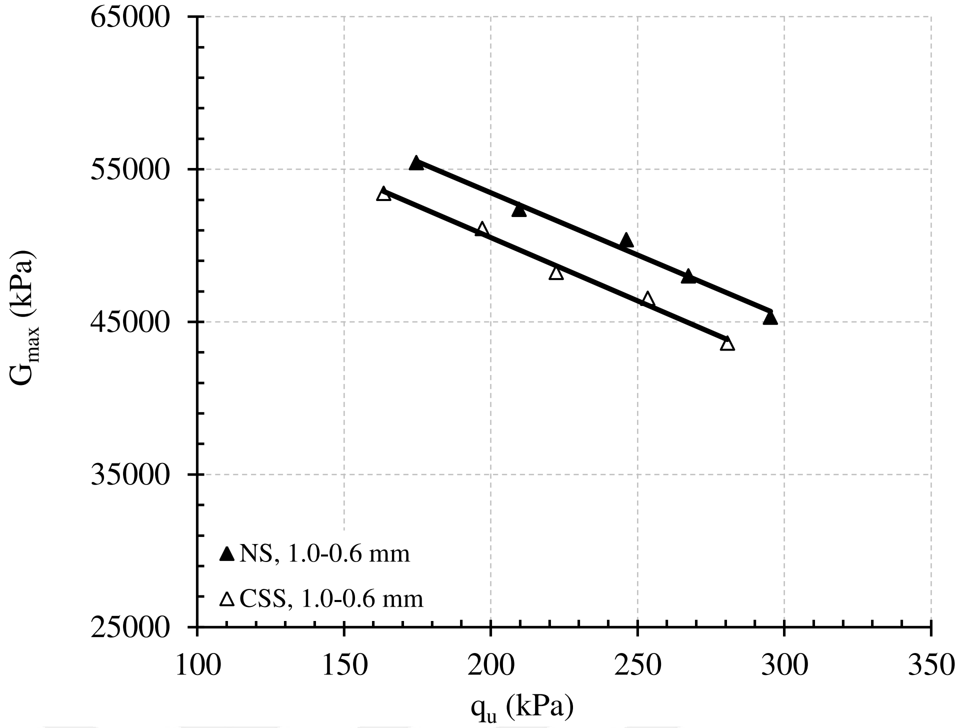

Figure 4.12 G_{max}-q_u correlation for clay-sand mixtures with size 1.0-0.6 mm.

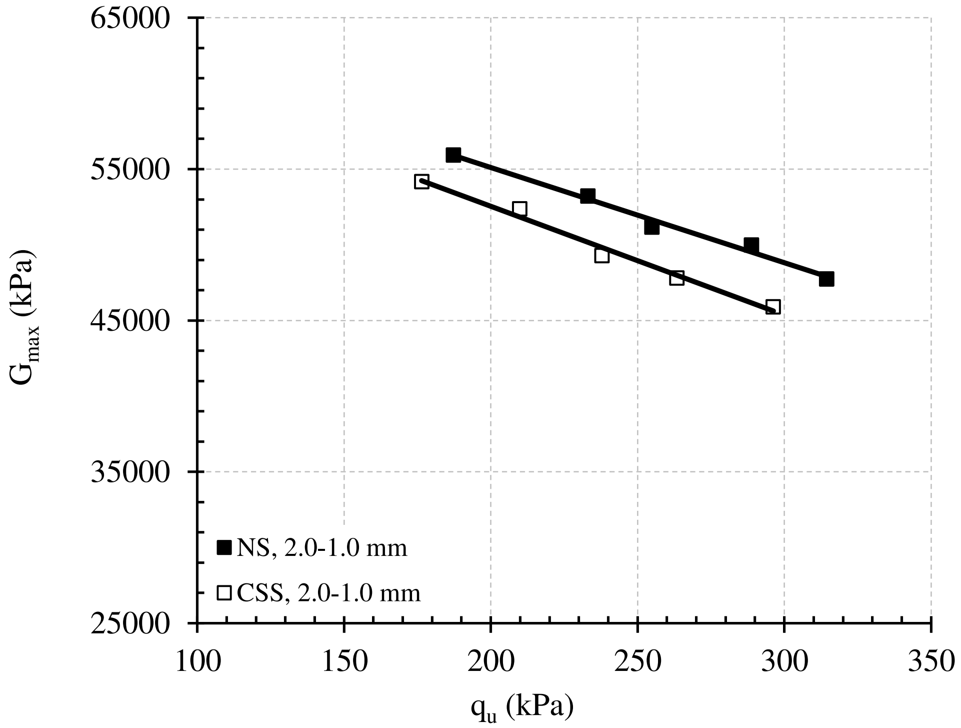

Figure 4.13 G_{max}-q_u correlation for clay-sand mixtures with size 2.0-1.0 mm.

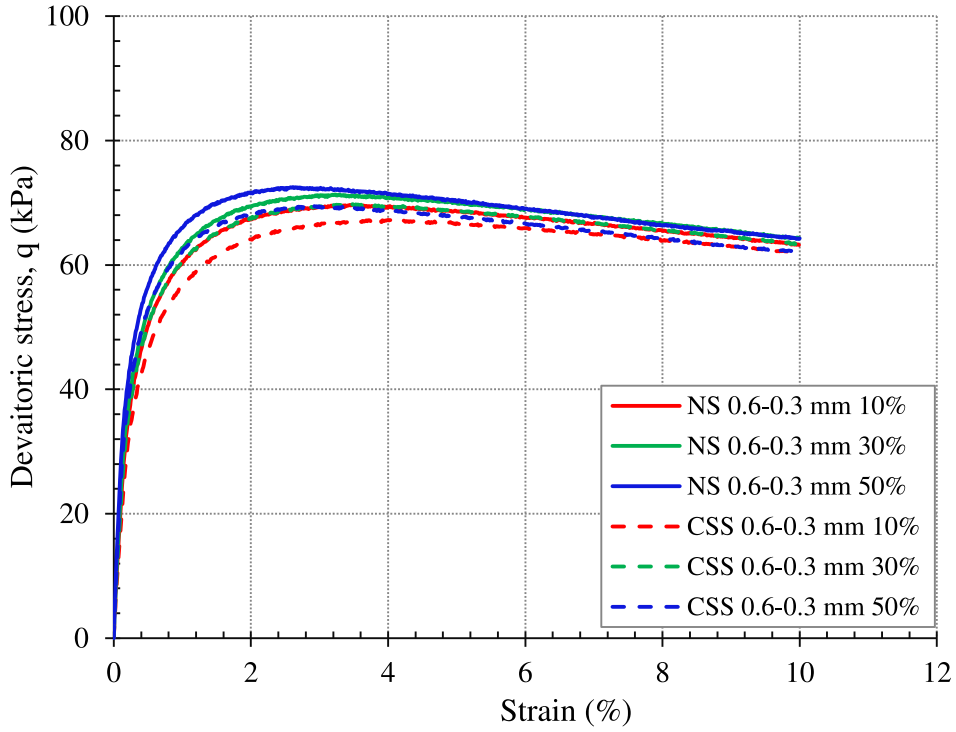

Figure 4.14 Deviotric stress versus strain for clay-NS and clay-CSS sands of 0.6-0.3 mm size with 50 kPa effective stress at different sand contents.

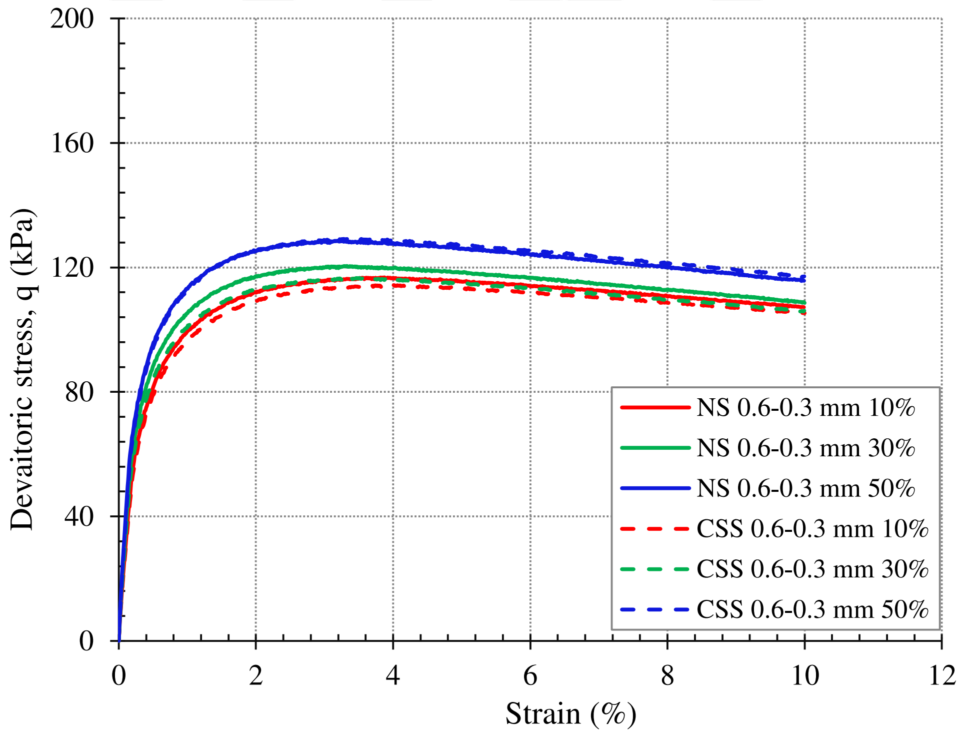

Figure 4.15 Deviotric stress versus strain for clay-NS and clay-CSS sands of 0.6-0.3 mm size with 100 kPa effective stress at different sand contents.

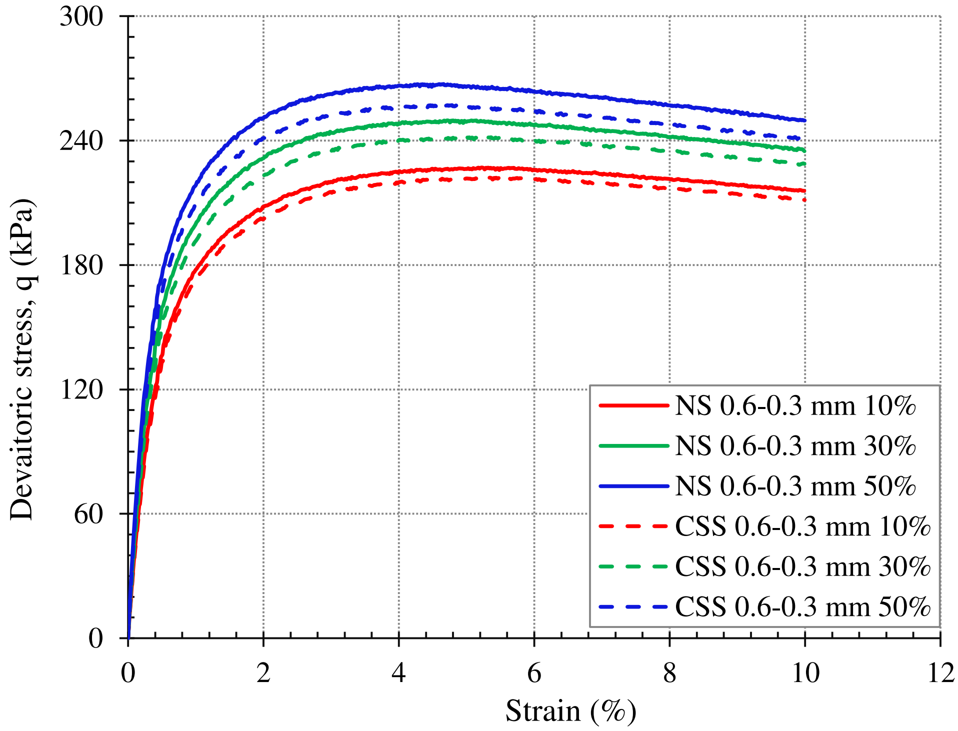

Figure 4.16 Deviotric stress versus strain for clay-NS and clay-CSS sands of 0.6-0.3 mm size with 200 kPa effective stress at different sand contents.

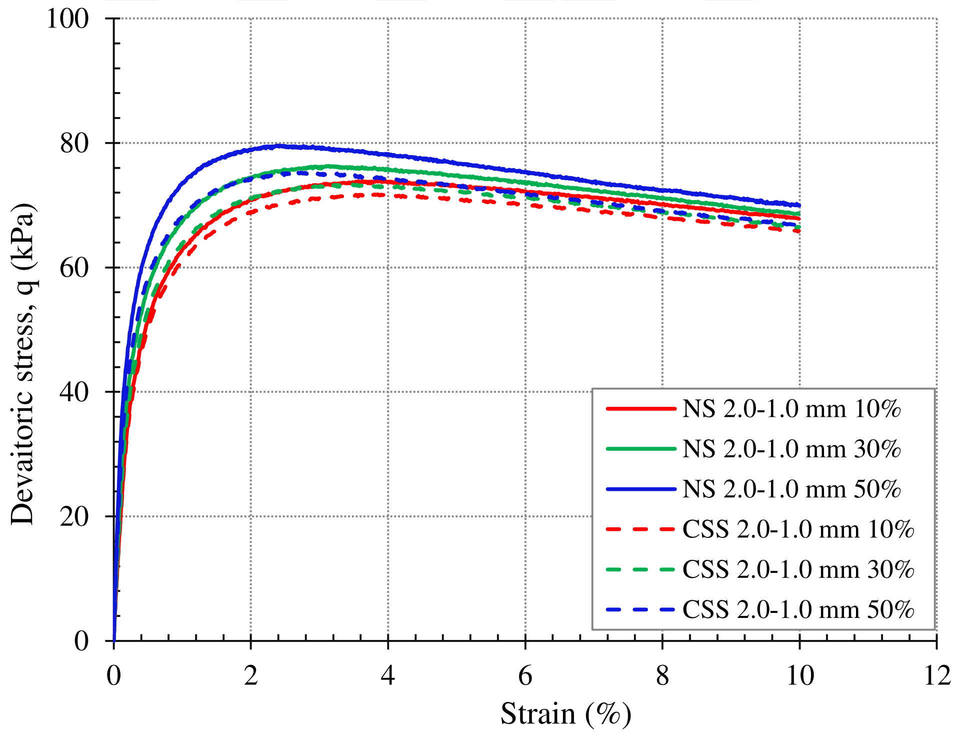

Figure 4.17 Deviotric stress versus strain for clay-NS and clay-CSS sands of 2.0-1.0 mm size with 50 kPa effective stress at different sand contents.

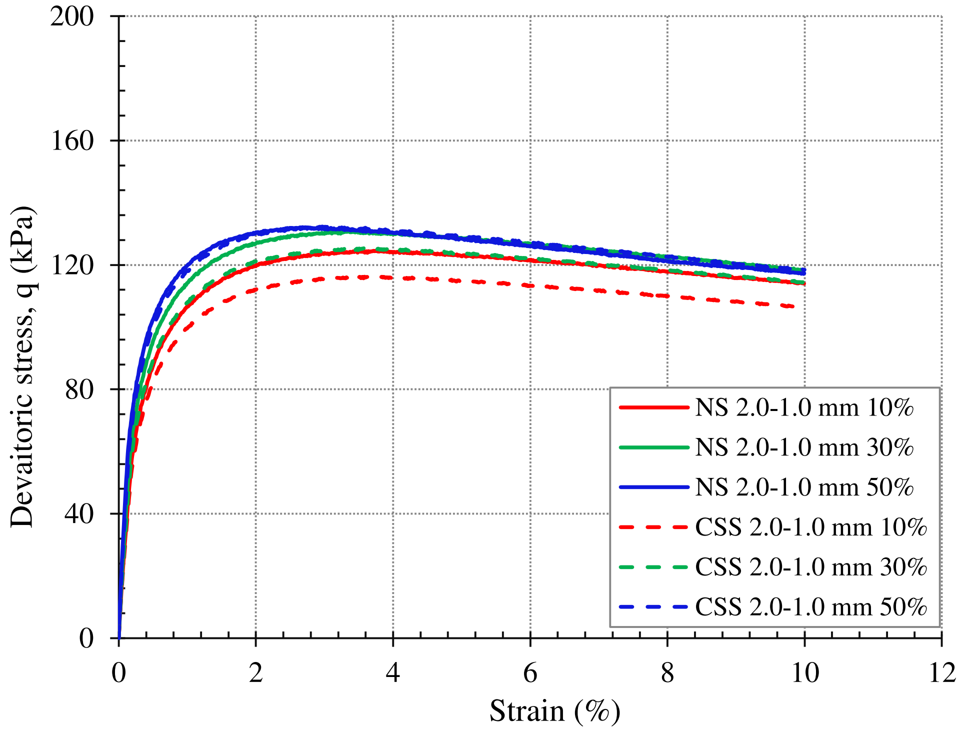

Figure 4.18 Deviotric stress versus strain for clay-NS and clay-CSS sands of 2.0-1.0 mm size with 100 kPa effective stress at different sand contents.

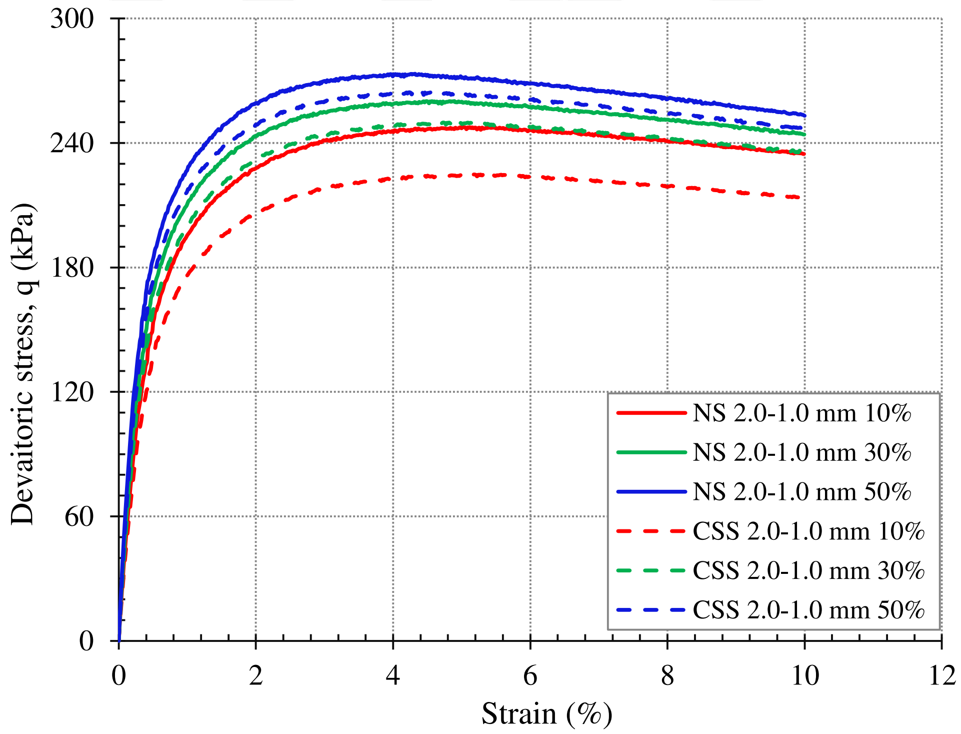

Figure 4.19 Deviotric stress versus strain for clay-NS and clay-CSS sands of 2.0-1.0 mm size with 200 kPa effective stress at different sand contents.

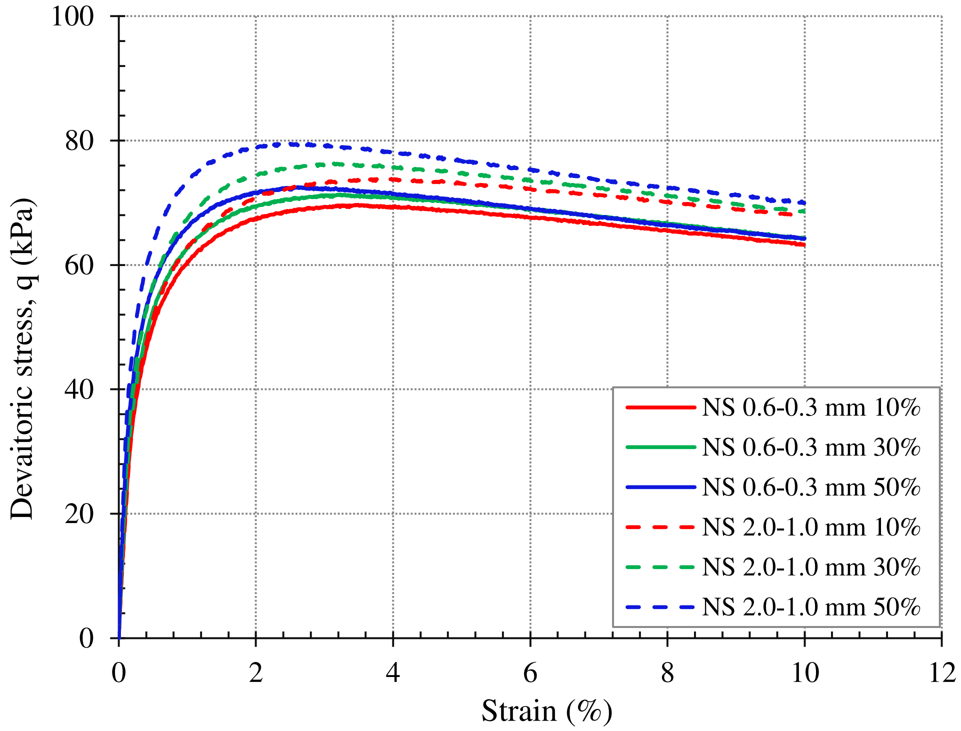

Figure 4.20 Deviotric stress versus strain for clay-NS sand of 0.6-0.3 mm and 2.0-1.0 mm size with 50 kPa effective stress at different sand contents.

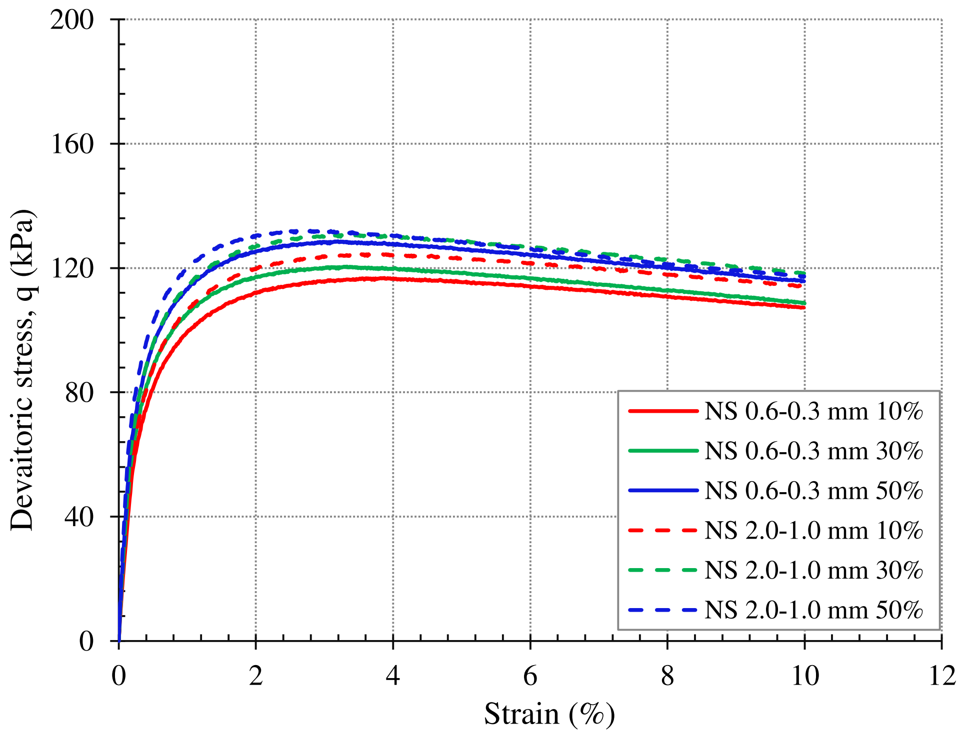

Figure 4.21 Deviotric stress versus strain for clay-NS sand of 0.6-0.3 mm and 2.0-1.0 mm size with 100 kPa effective stress at different sand contents.

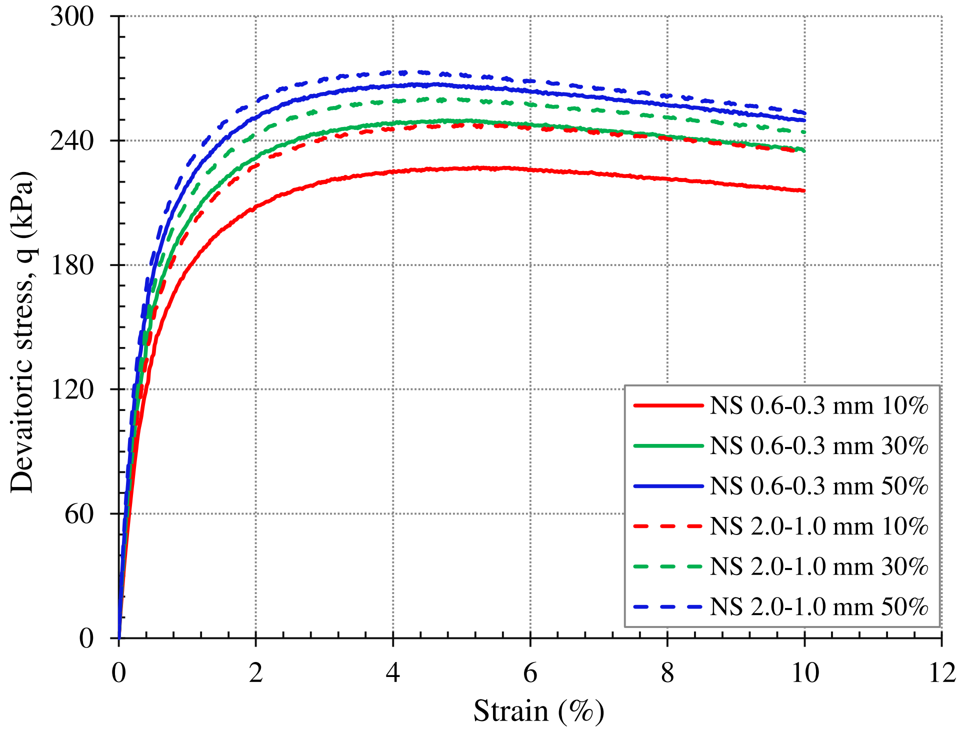

Figure 4.22 Deviotric stress versus strain for clay-NS sand of 0.6-0.3 mm and 2.0-1.0 mm size with 200 kPa effective stress at different sand contents.

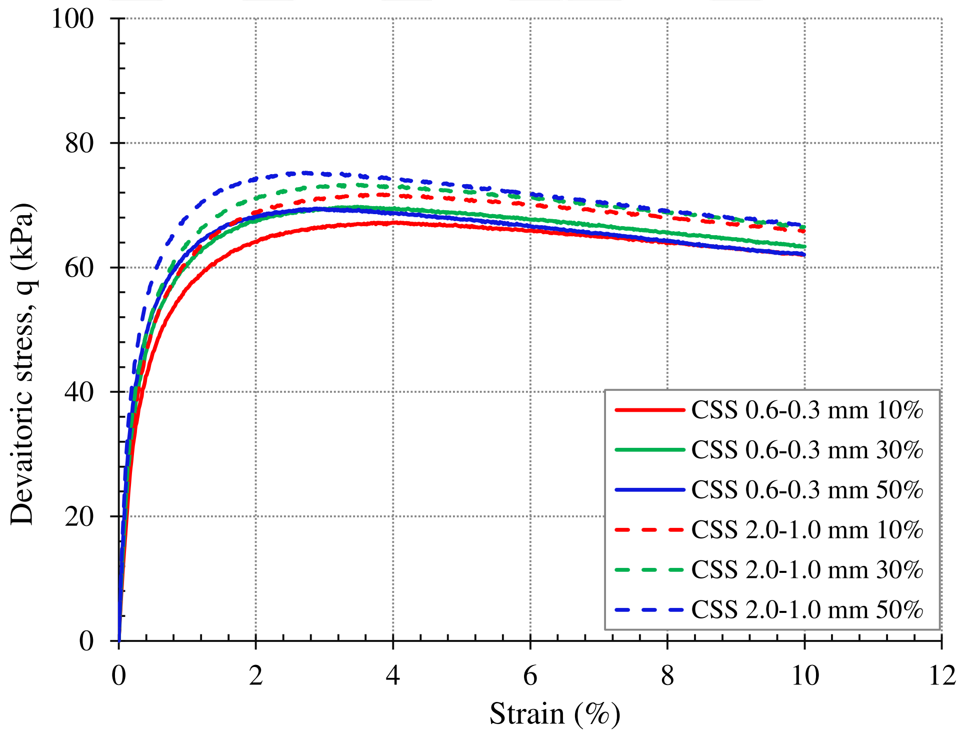

Figure 4.23 Deviotric stress versus strain for clay-CSS sand of 0.6-0.3 mm and 2.0-1.0 mm size with 50 kPa effective stress at different sand contents.

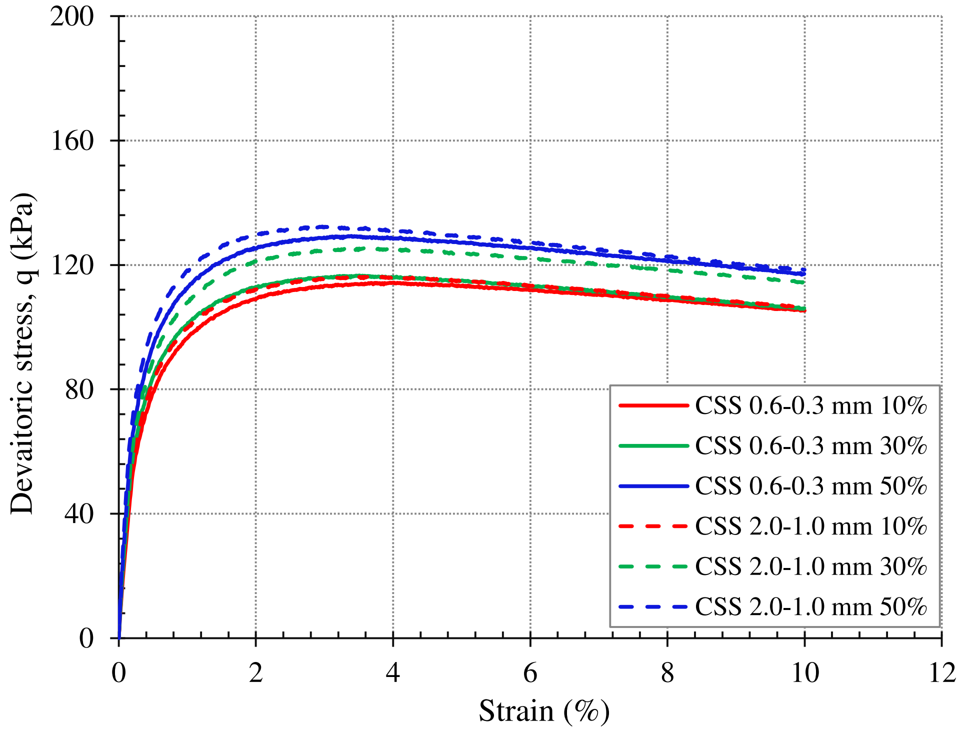

Figure 4.24 Deviotric stress versus strain for clay-CSS sand of 0.6-0.3 mm and 2.0-1.0 mm size with 100 kPa effective stress at different sand contents.

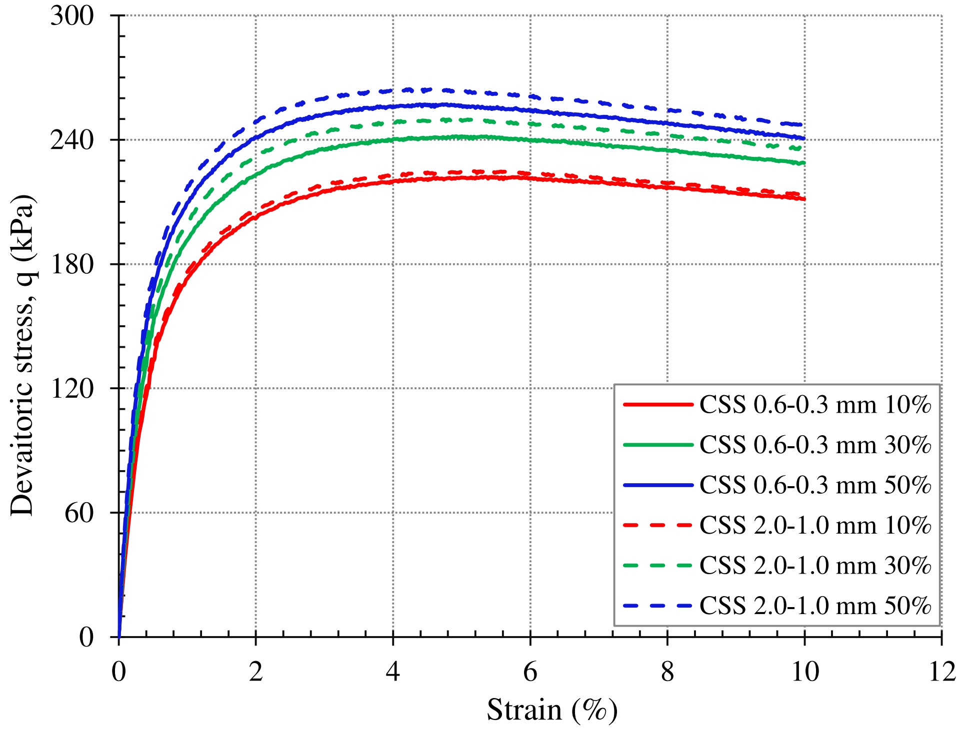

Figure 4.25 Deviotric stress versus strain for clay-CSS sand of 0.6-0.3 mm and 2.0-1.0 mm size with 200 kPa effective stress at different sand contents.

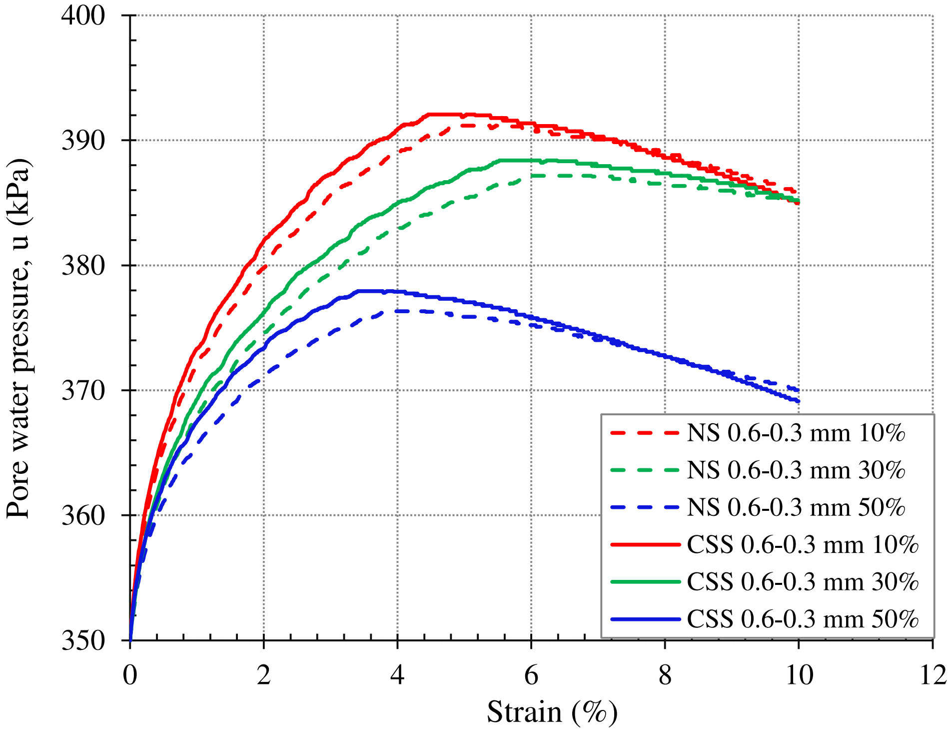

Figure 4.26 Pore water pressure versus strain for clay-NS and clay-CSS sands of 0.6-0.3 mm size with 50 kPa effective stress at different sand contents.

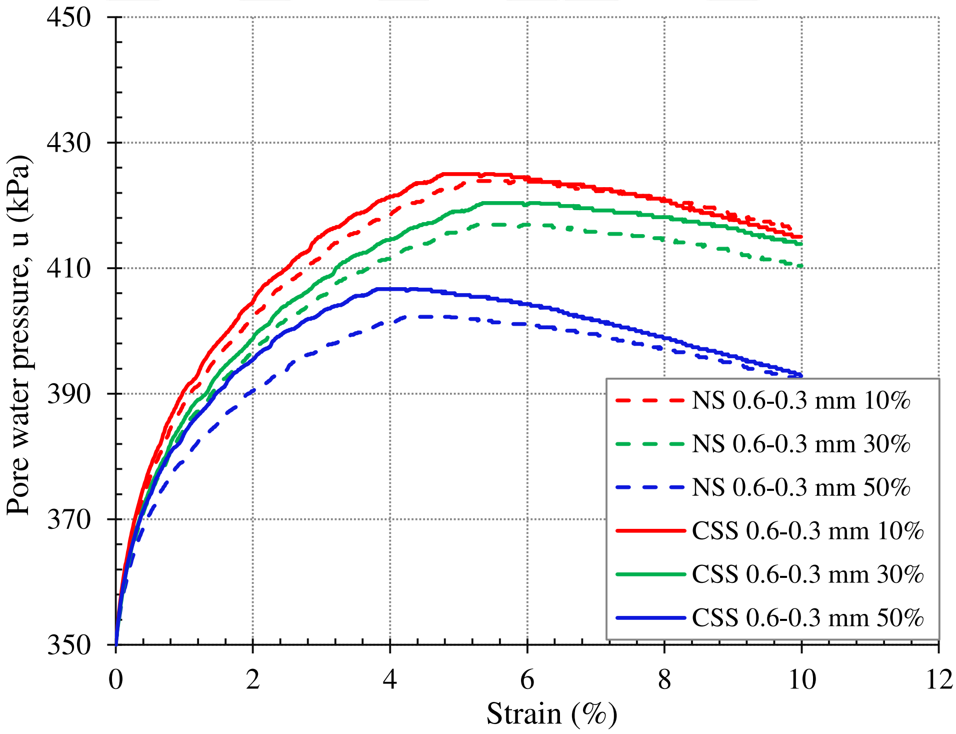

Figure 4.27 Pore water pressure versus strain for clay-NS and clay-CSS sands of 0.6-0.3 mm size with 100 kPa effective stress at different sand contents.

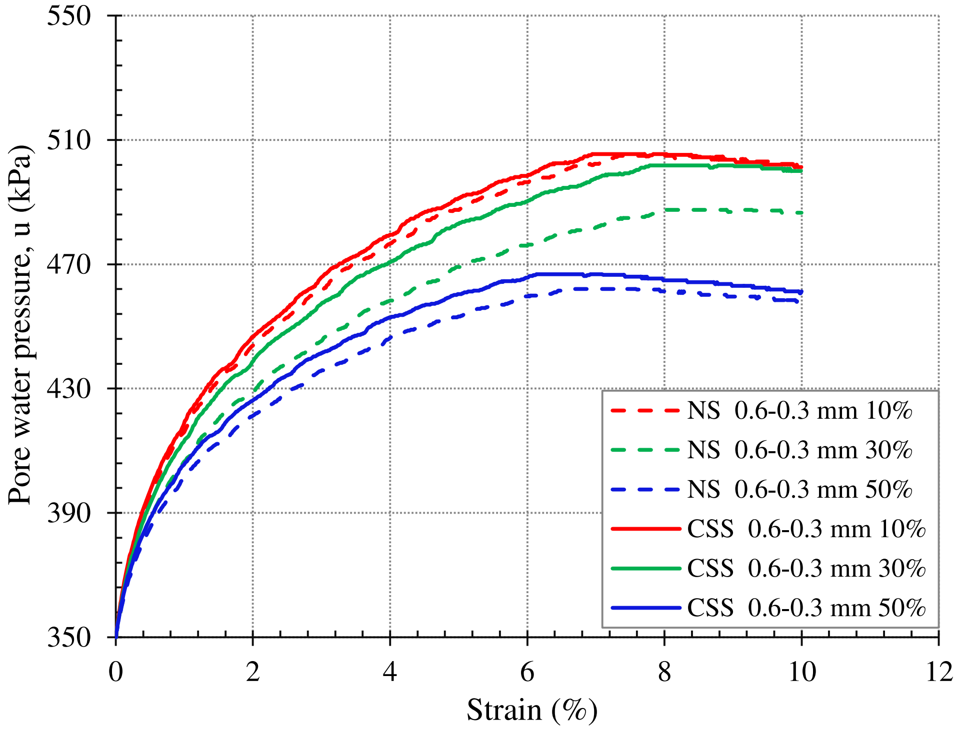

Figure 4.28 Pore water pressure versus strain for clay-NS and clay-CSS sands of 0.6-0.3 mm size with 200 kPa effective stress at different sand contents.

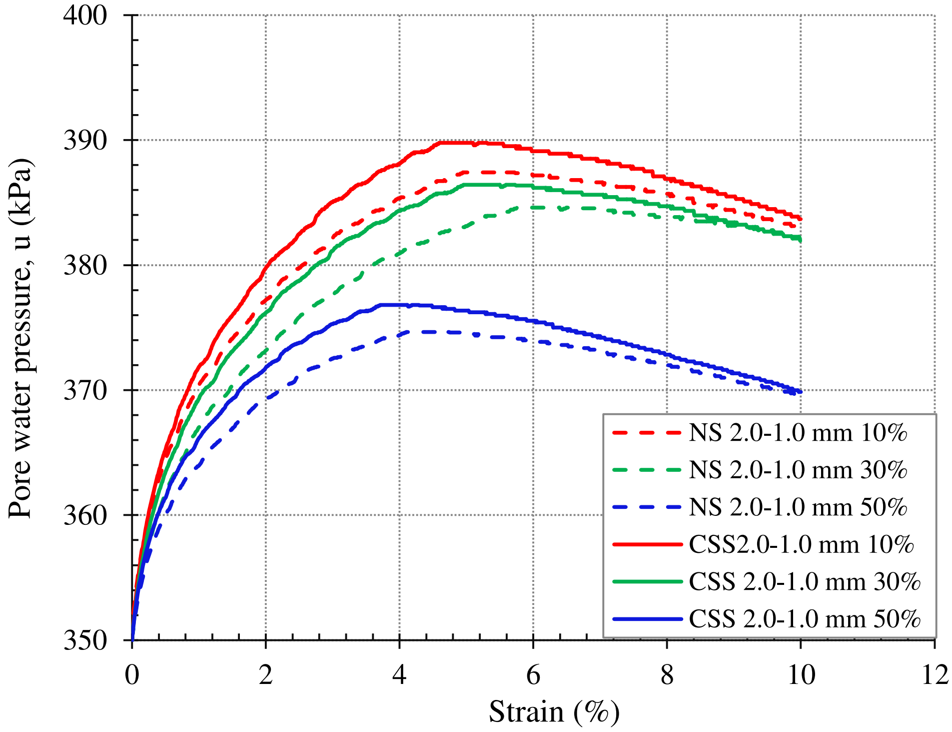

Figure 4.29 Pore water pressure versus strain for clay-NS and clay-CSS sands of 2.0-1.0 mm size with 50 kPa effective stress at different sand contents.

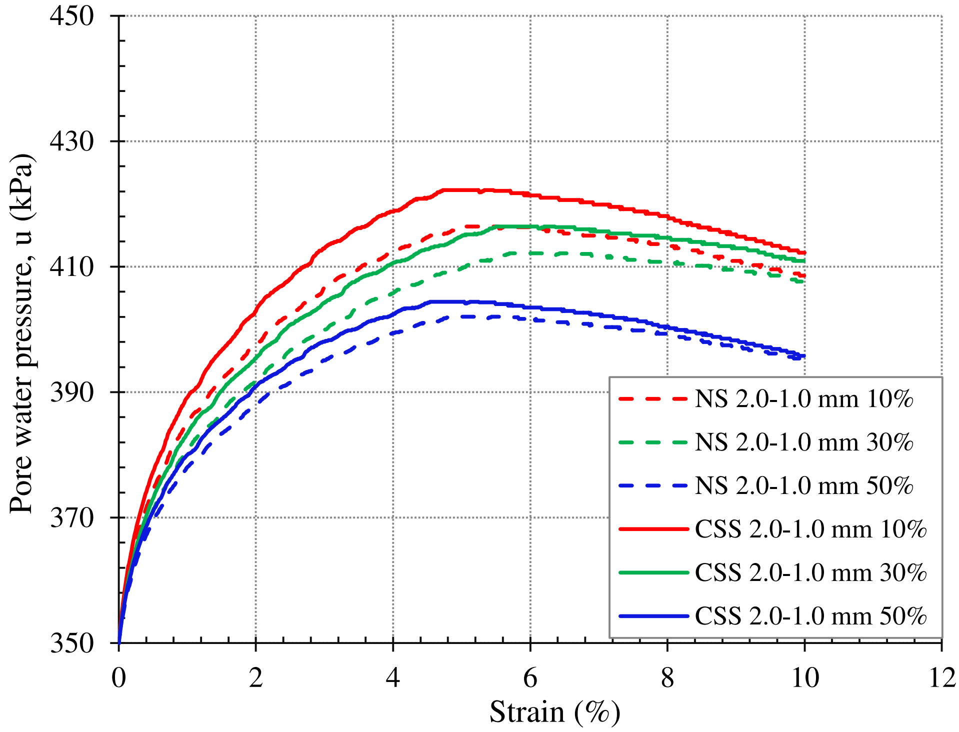

Figure 4.30 Pore water pressure versus strain for clay-NS and clay-CSS sands of 2.0-1.0 mm size with 100 kPa effective stress at different sand contents.

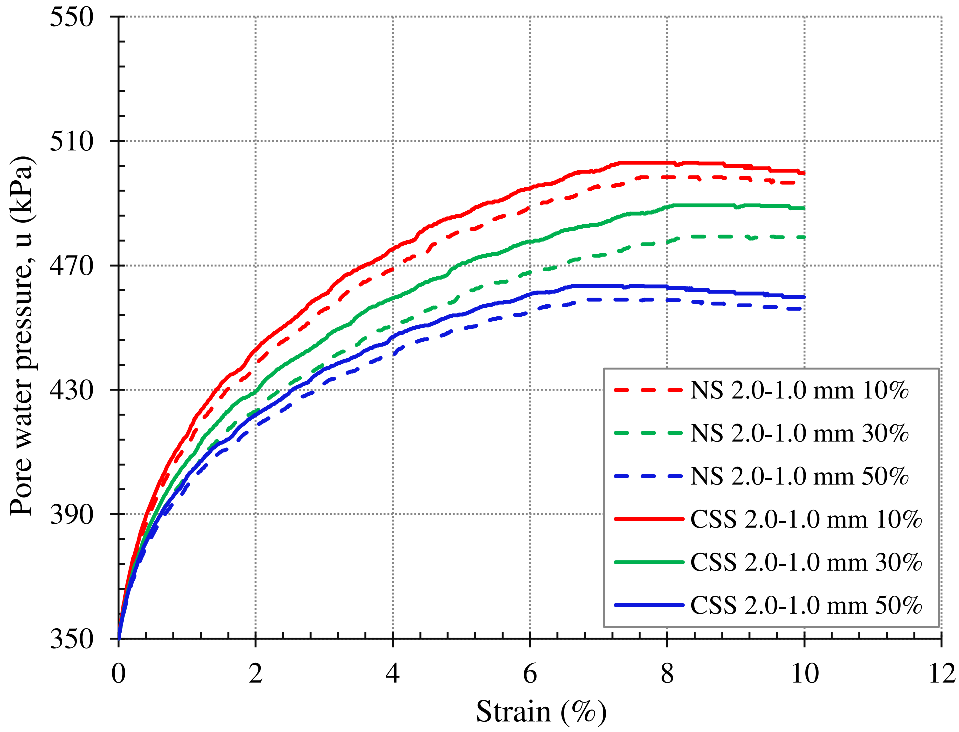

Figure 4.31 Pore water pressure versus strain for clay-NS and clay-CSS sands of 2.0-1.0 mm size with 200 kPa effective stress at different sand contents.

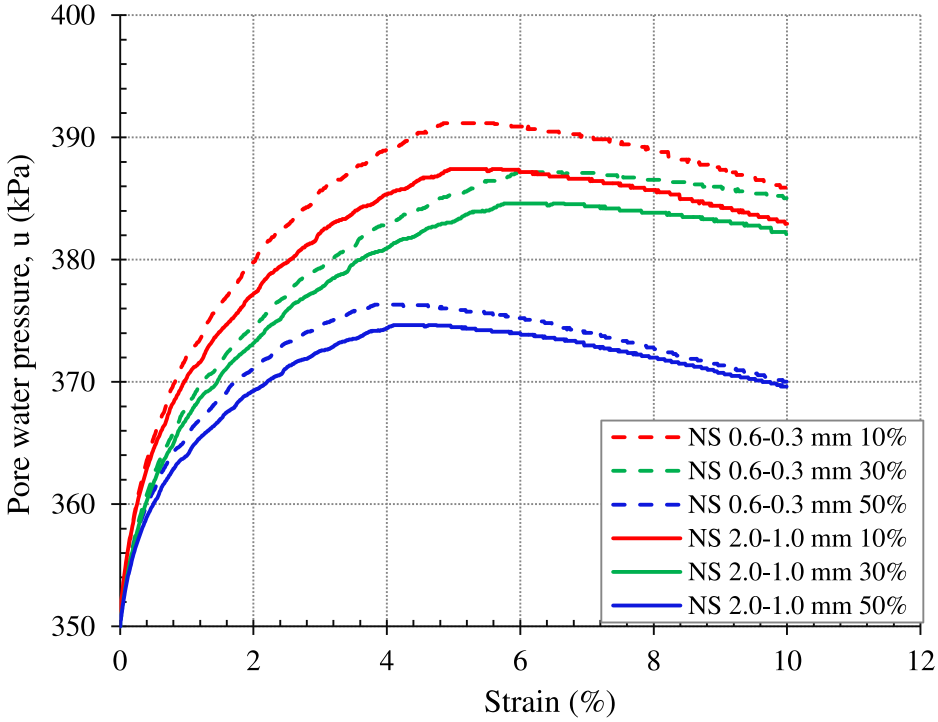

Figure 4.32 Pore water pressure versus strain for clay-NS sand of 0.6-0.3 mm and 2.0-1.0 mm size with 50 kPa effective stress at different sand contents.

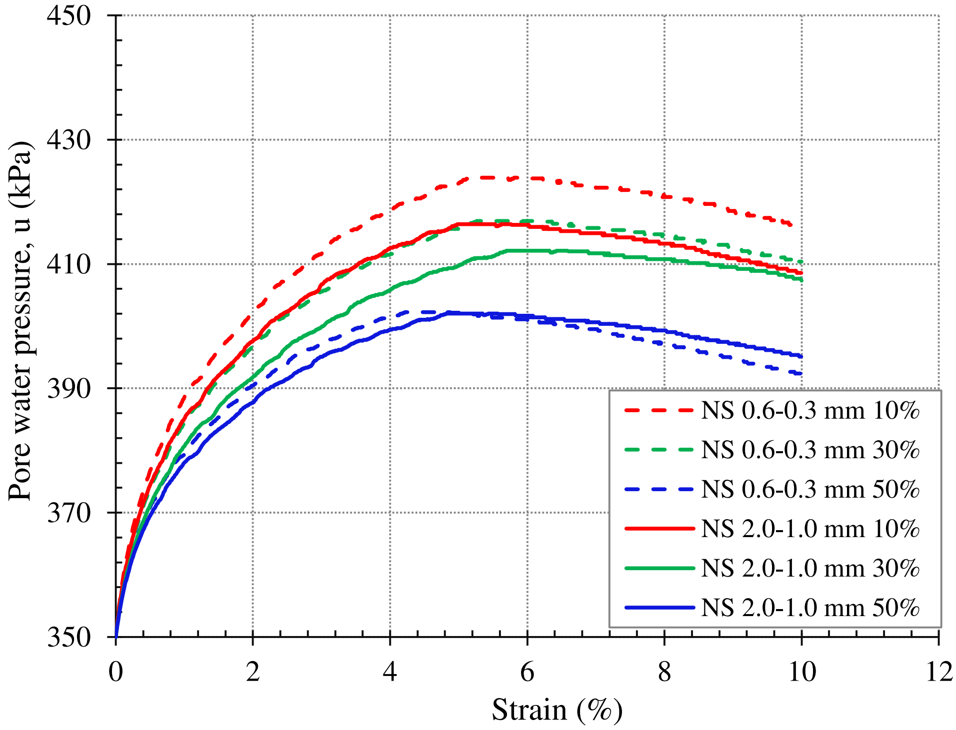

Figure 4.33 Pore water pressure versus strain for clay-NS sand of 0.6-0.3 mm and 2.0-1.0 mm size with 100 kPa effective stress at different sand contents.

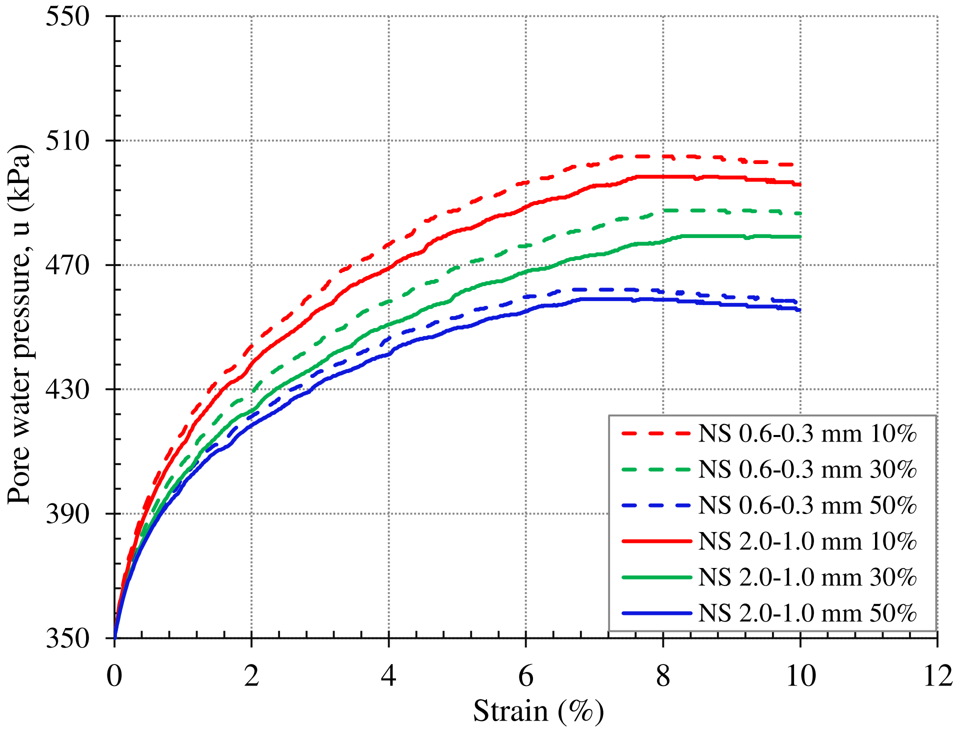

Figure 4.34 Pore water pressure versus strain for clay-NS sand of 0.6-0.3 mm and 2.0-1.0 mm size with 200 kPa effective stress at different sand contents.

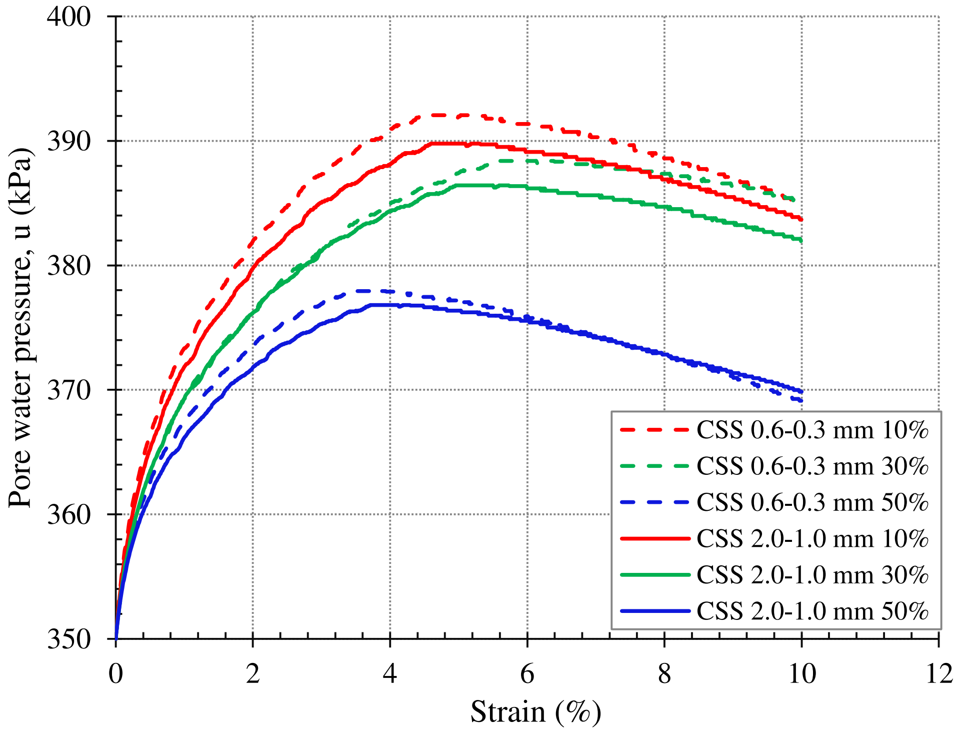

Figure 4.35 Pore water pressure versus strain for clay-CSS sand of 0.6-0.3 mm and 2.0-1.0 mm size with 50 kPa effective stress at different sand contents.

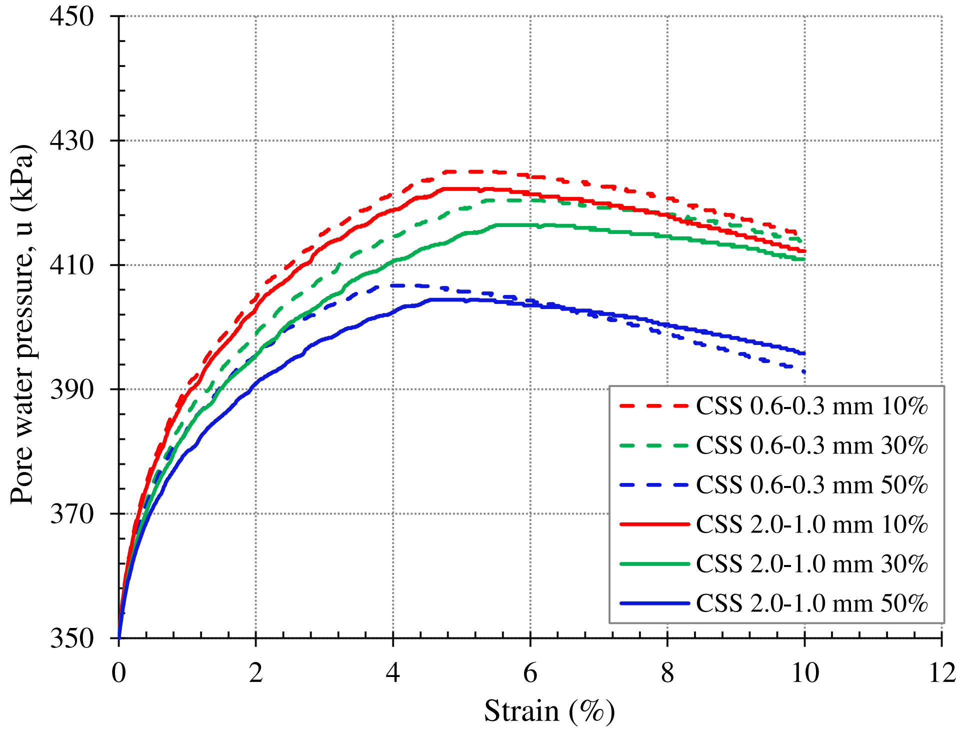

Figure 4.36 Pore water pressure versus strain for clay-CSS sand of 0.6-0.3 mm and 2.0-1.0 mm size with 100 kPa effective stress at different sand contents.

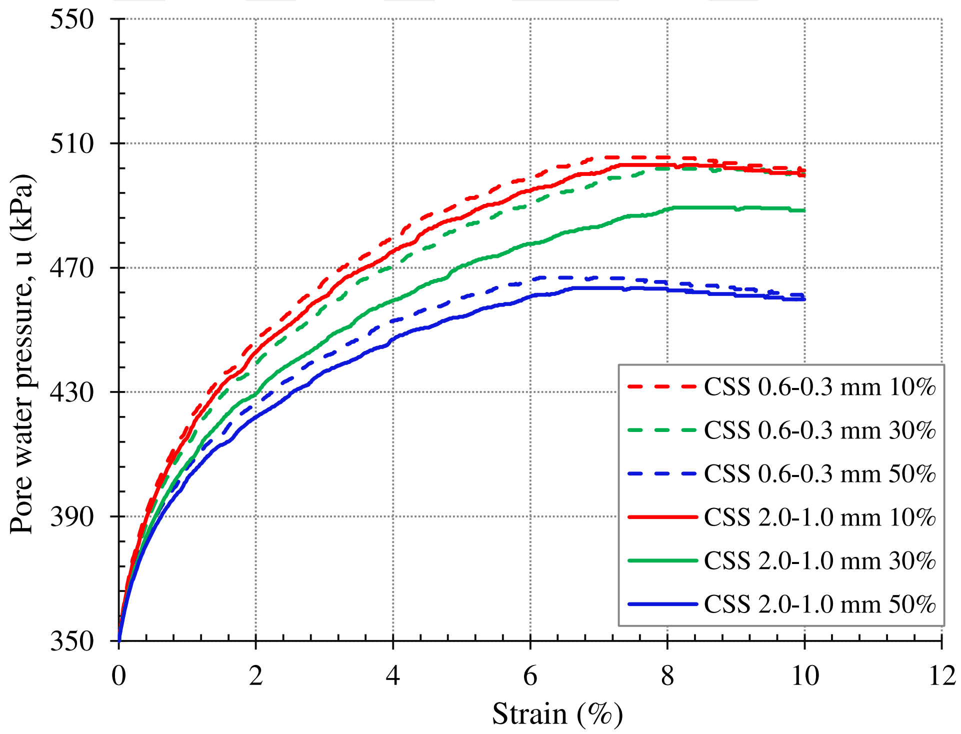

Figure 4.37 Pore water pressure versus strain for clay-CSS sand of 0.6-0.3 mm and 2.0-1.0 mm size with 200 kPa effective stress at different sand contents.

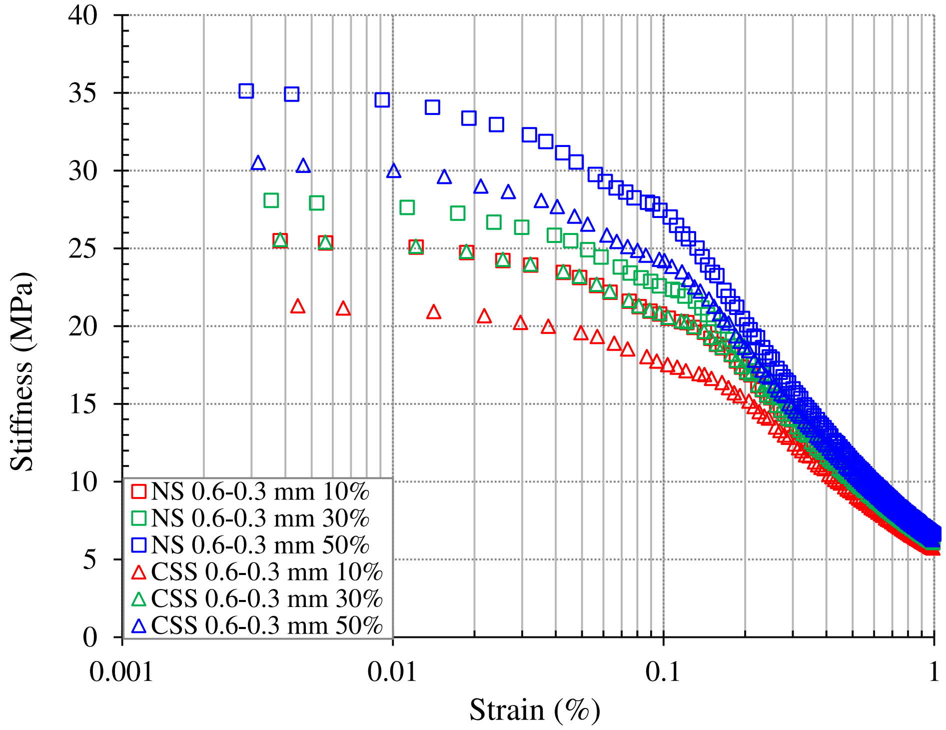

Figure 4.38 Stiffness versus strain for clay-NS and clay-CSS sands of 0.6-0.3 mm size with 50 kPa effective stress at different sand contents.

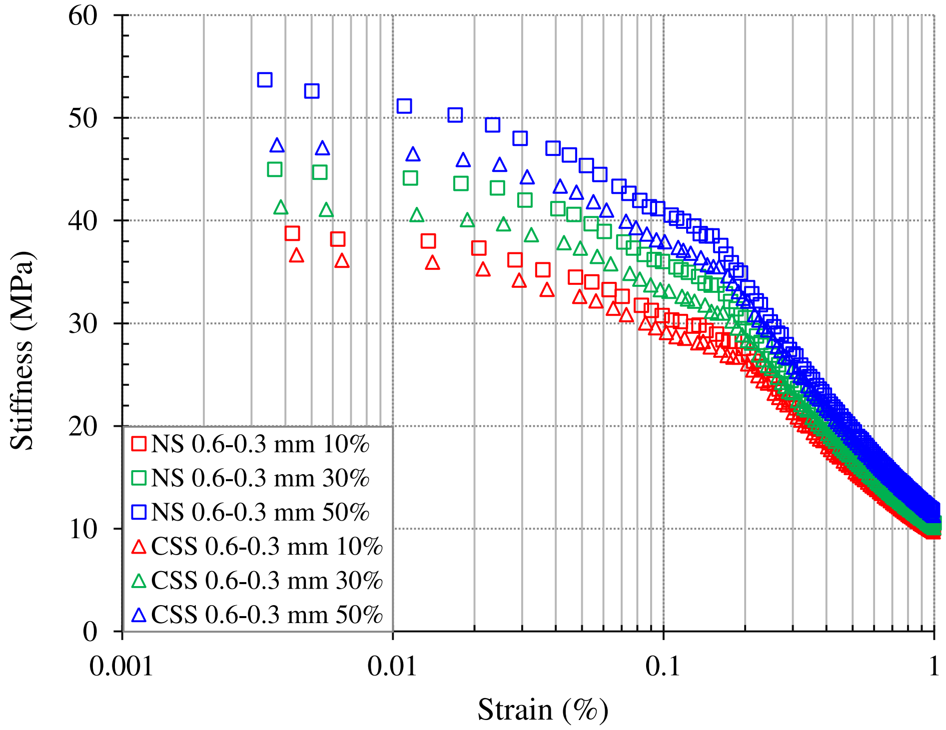

Figure 4.39 Stiffness versus strain for clay-NS and clay-CSS sands of 0.6-0.3 mm size with 100 kPa effective stress at different sand contents.

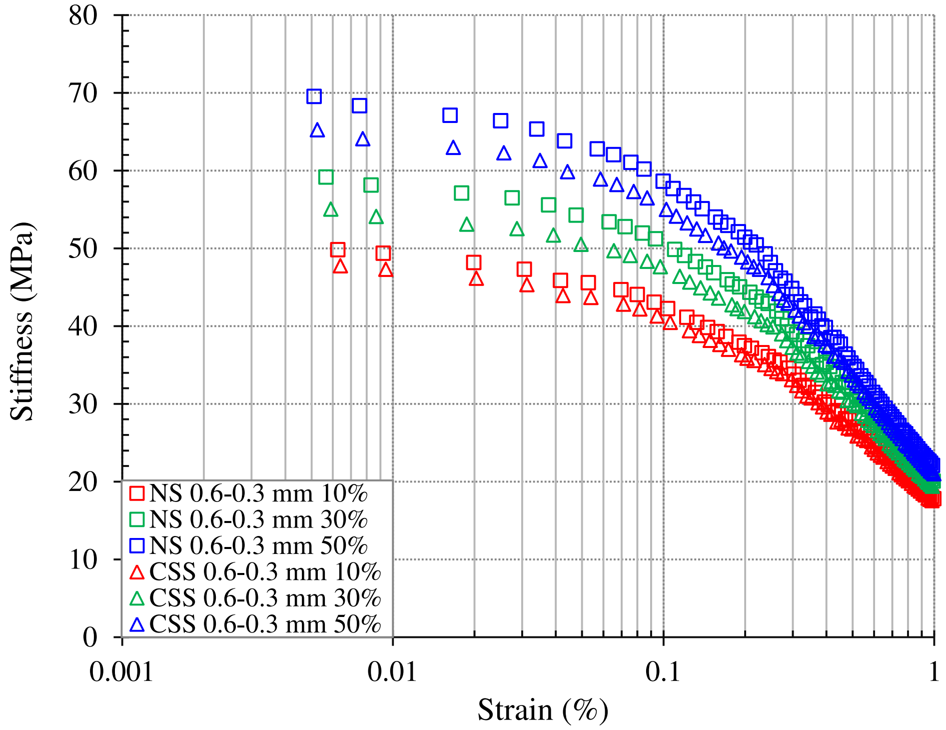

Figure 4.40 Stiffness versus strain for clay-NS and clay-CSS sands of 0.6-0.3 mm size with 200 kPa effective stress at different sand contents.

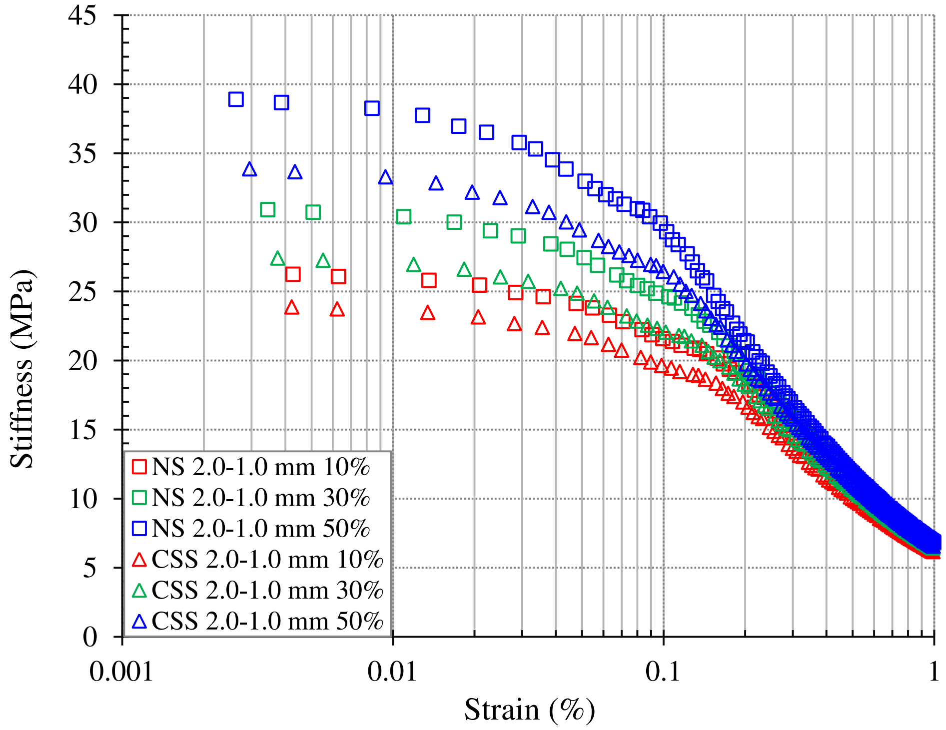

Figure 4.41 Stiffness versus strain for clay-NS and clay-CSS sands of 2.0-1.0 mm size with 50 kPa effective stress at different sand contents.

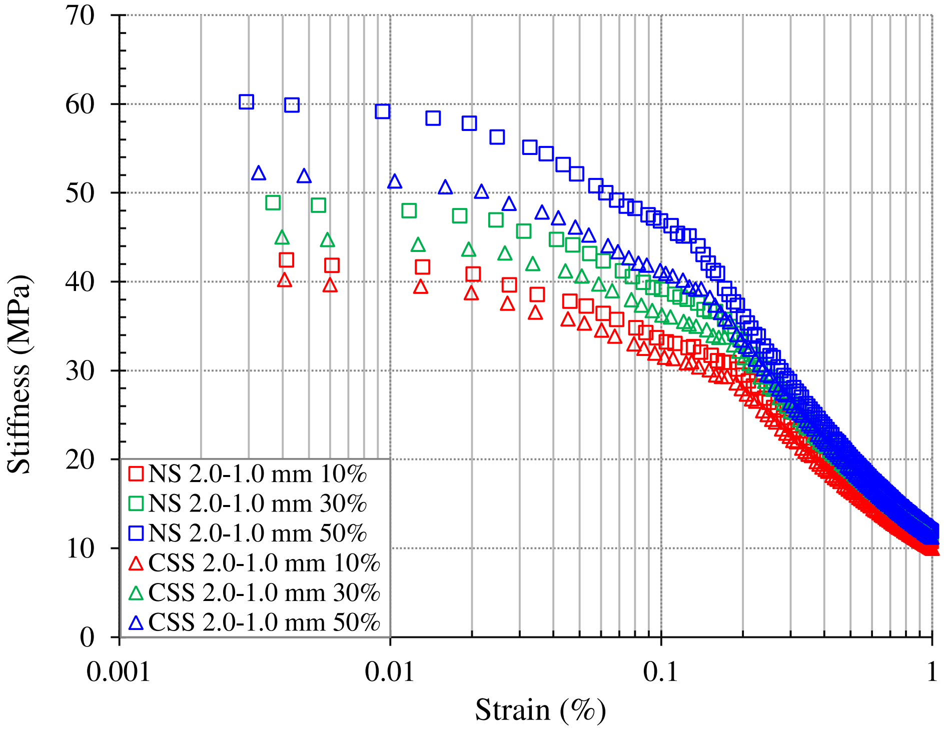

Figure 4.42 Stiffness versus strain for clay-NS and clay-CSS sands of 2.0-1.0 mm size with 100 kPa effective stress at different sand contents.

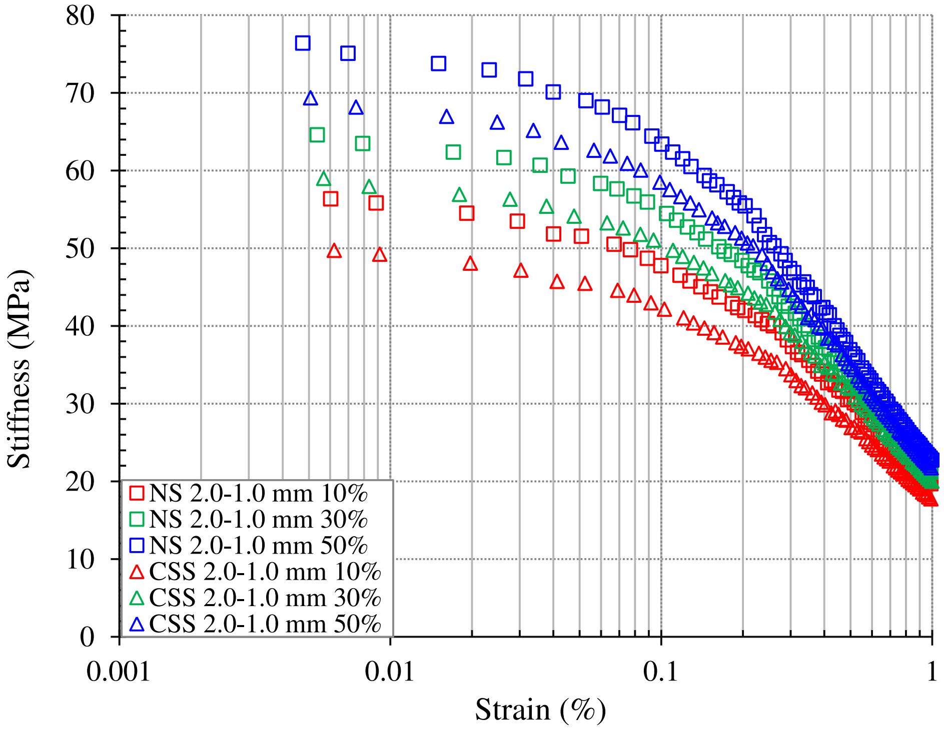

Figure 4.43 Stiffness versus strain for clay-NS and clay-CSS sands of 2.0-1.0 mm size with 200 kPa effective stress at different sand contents.

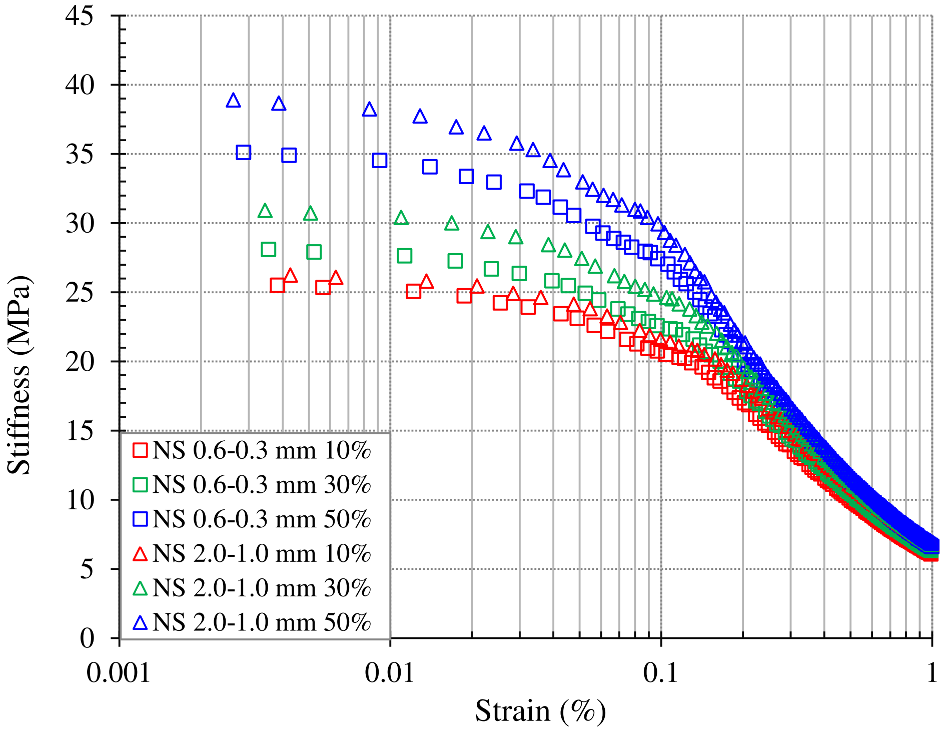

Figure 4.44 Stiffness versus strain for clay-NS sand of 0.6-0.3 mm and 2.0-1.0 mm size with 50 kPa effective stress at different sand contents.

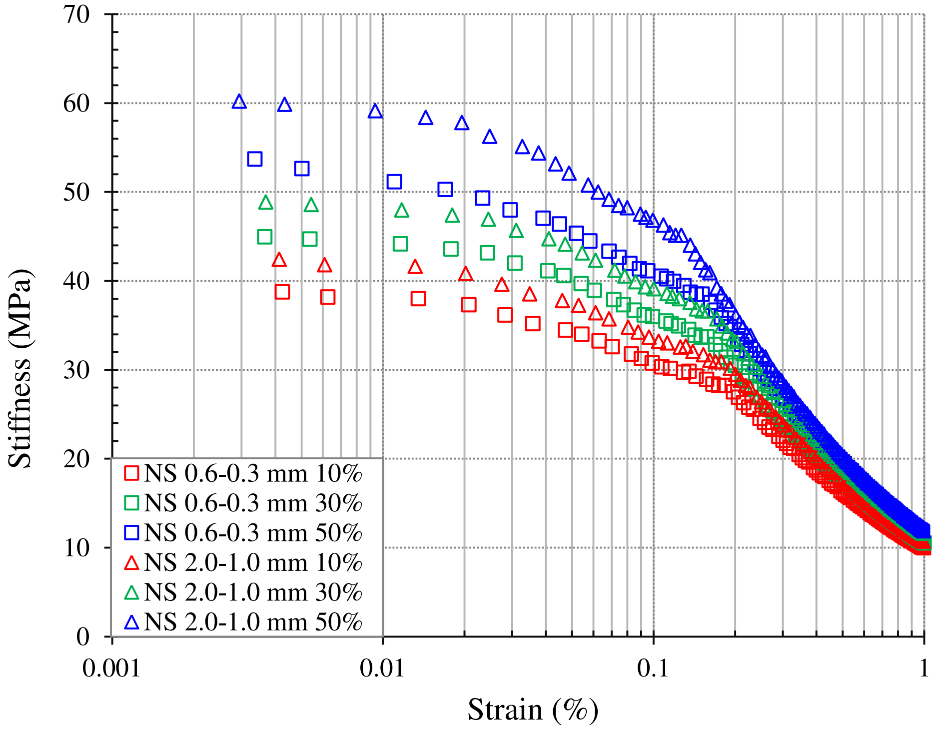

Figure 4.45 Stiffness versus strain for clay-NS sand of 0.6-0.3 mm and 2.0-1.0 mm size with 100 kPa effective stress at different sand contents.

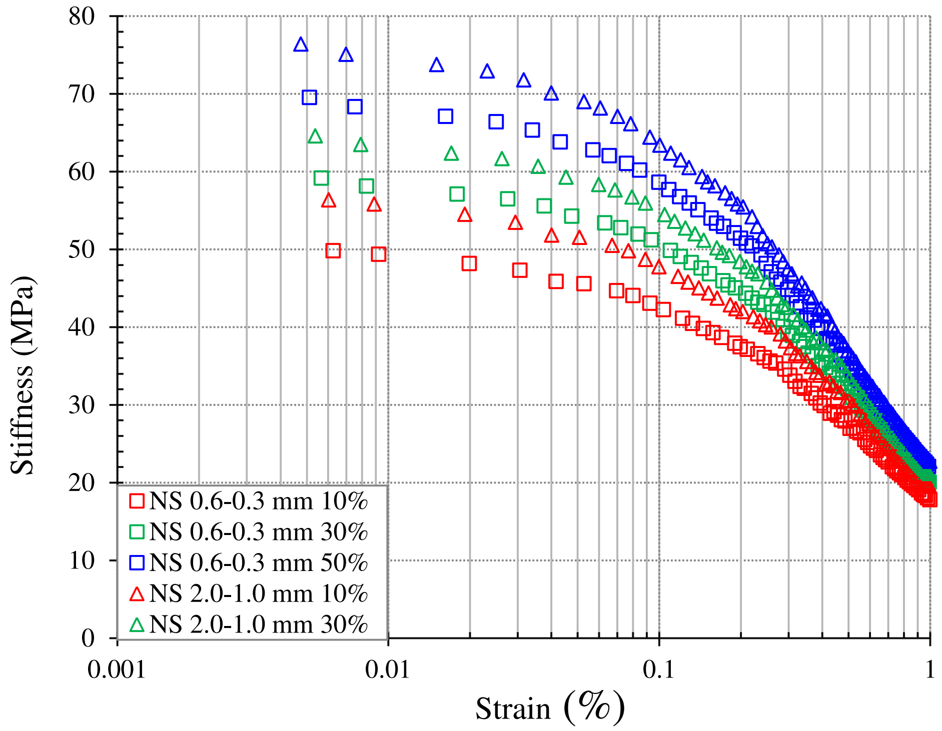

Figure 4.46 Stiffness versus strain for clay-NS sand of 0.6-0.3 mm and 2.0-1.0 mm size with 200 kPa effective stress at different sand contents.

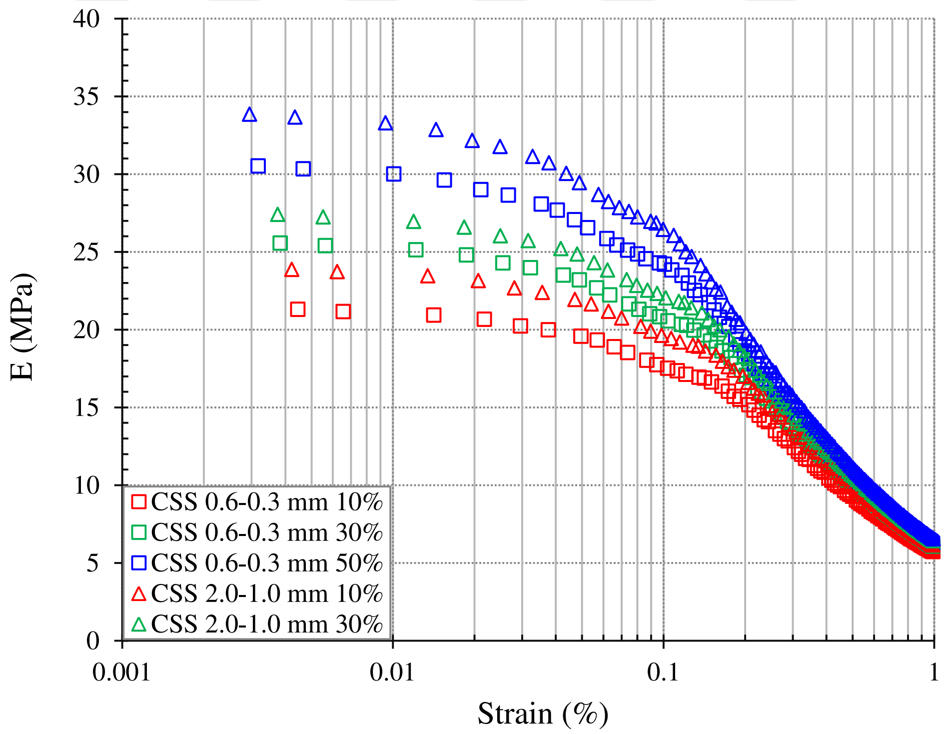

Figure 4.47 Stiffness versus strain for clay-CSS sand of 0.6-0.3 mm and 2.0-1.0 mm size with 50 kPa effective stress at different sand contents.

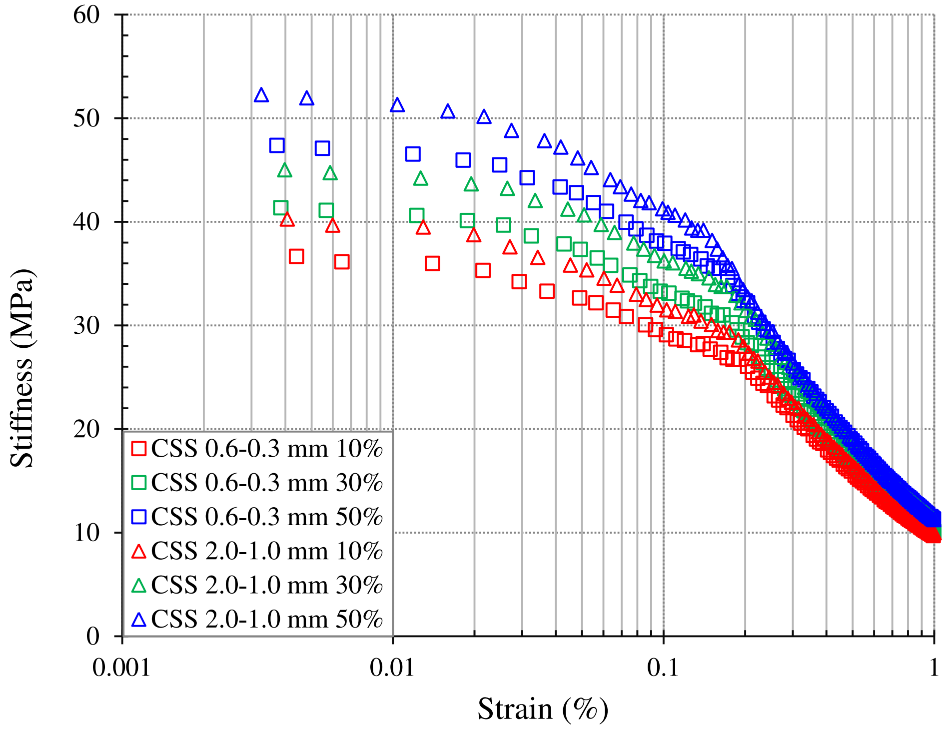

Figure 4.48 Stiffness versus strain for clay-CSS sand of 0.6-0.3 mm and 2.0-1.0 mm size with 100 kPa effective stress at different sand contents.

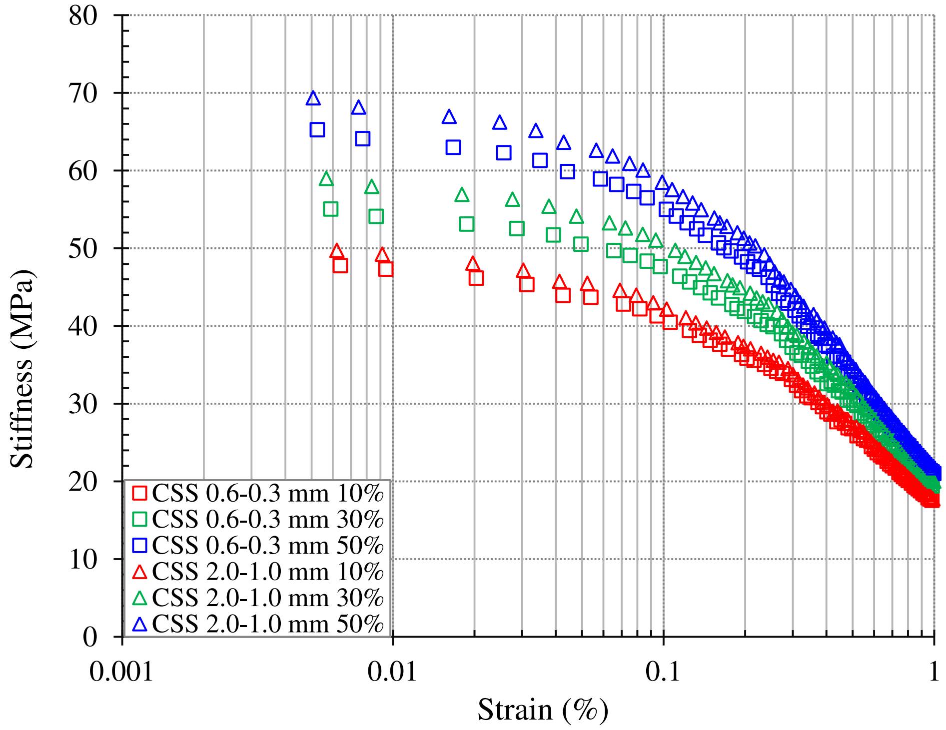

Figure 4.49 Stiffness versus strain for clay-CSS sand of 0.6-0.3 mm and 2.0-1.0 mm size with 200 kPa effective stress at different sand contents.

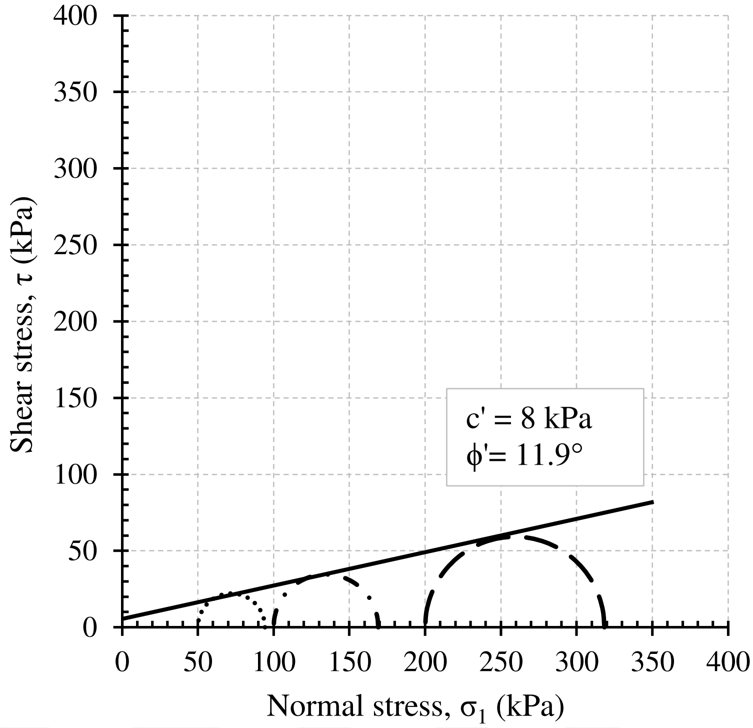

Figure 4.50 Mohr circles and failure envelope of clayey soil tested in CU conditions, (effective stresses).

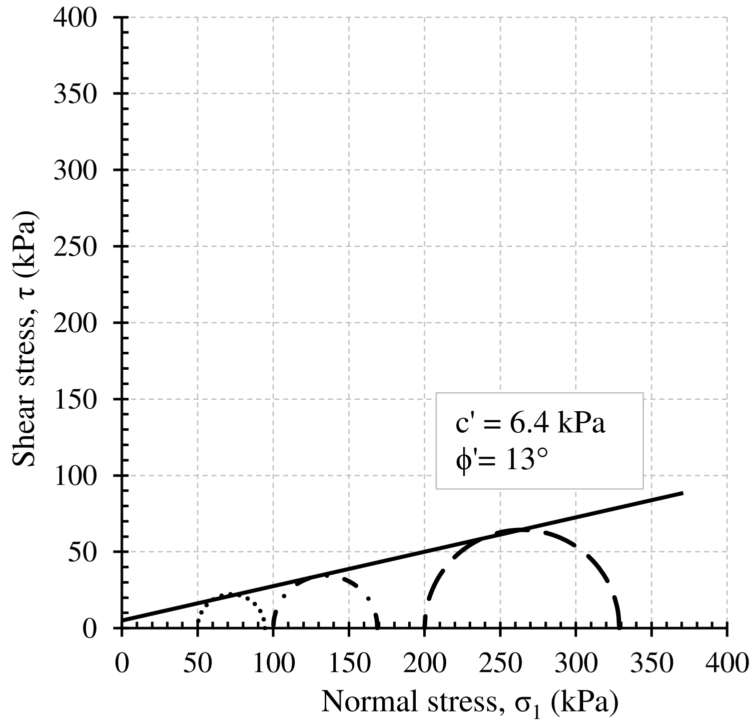

Figure 4.51 Mohr circles and failure envelope of 10% NS sand with 0.6-0.3 mm size of clay-sand mixtures tested in CU conditions, (effective stresses).

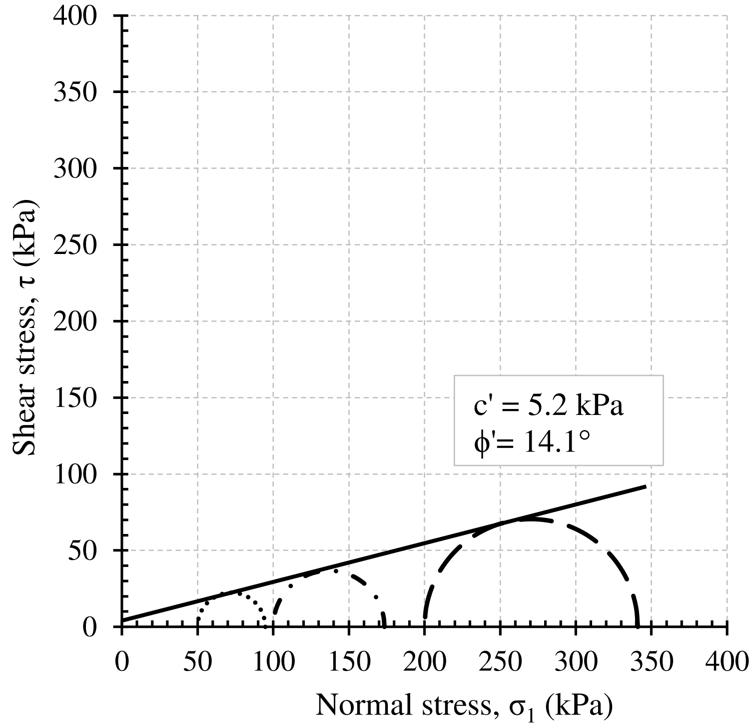

Figure 4.52 Mohr circles and failure envelope of 30% NS sand with 0.6-0.3 mm size of clay-sand mixtures tested in CU conditions, (effective stresses).

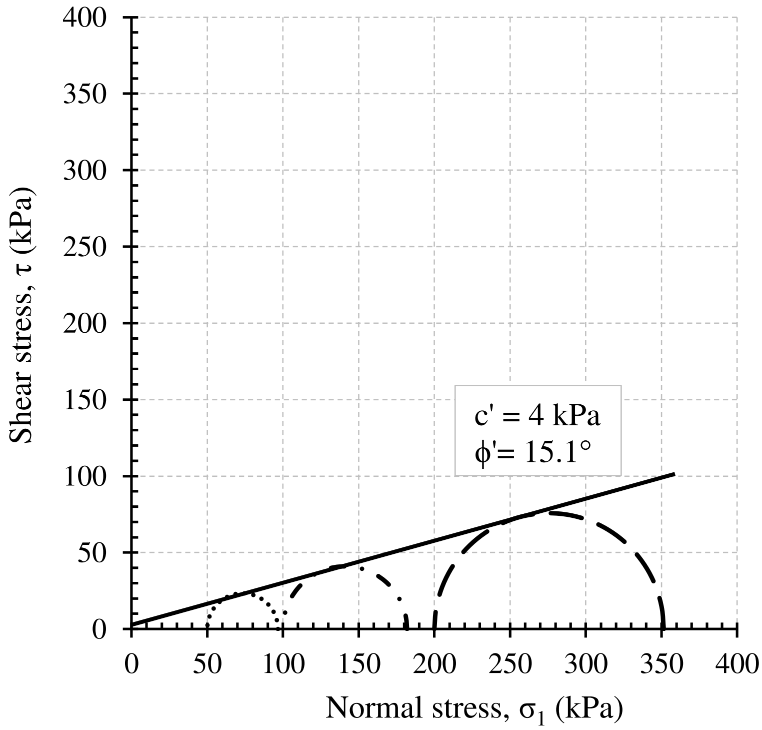

Figure 4.53 Mohr circles and failure envelope of 50% NS sand with 0.6-0.3 mm size of clay-sand mixtures tested in CU conditions, (effective stresses).

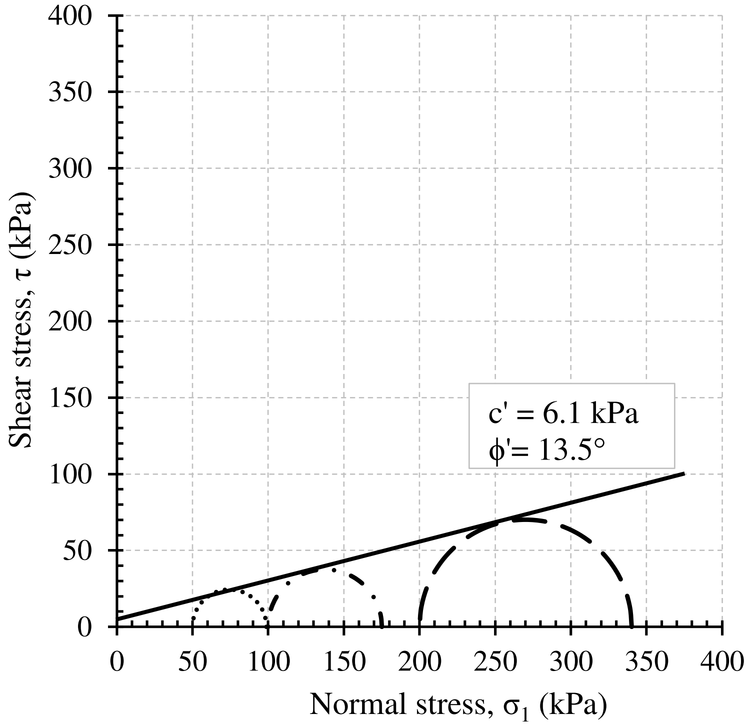

Figure 4.54 Mohr circles and failure envelope of 10% NS sand with 2.0-1.0 mm size of clay-sand mixtures tested in CU conditions, (effective stresses).

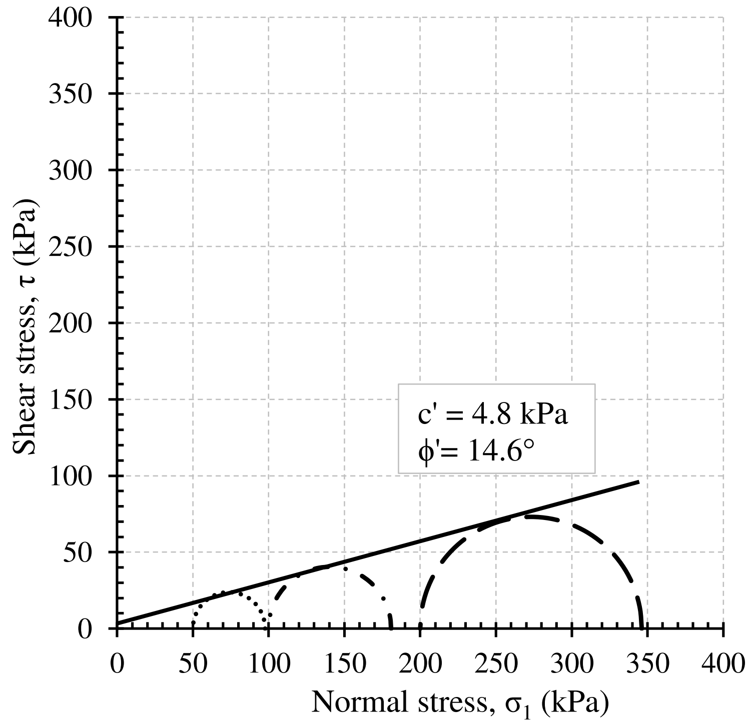

Figure 4.55 Mohr circles and failure envelope of 30% NS sand with 2.0-1.0 mm size of clay-sand mixtures tested in CU conditions, (effective stresses).

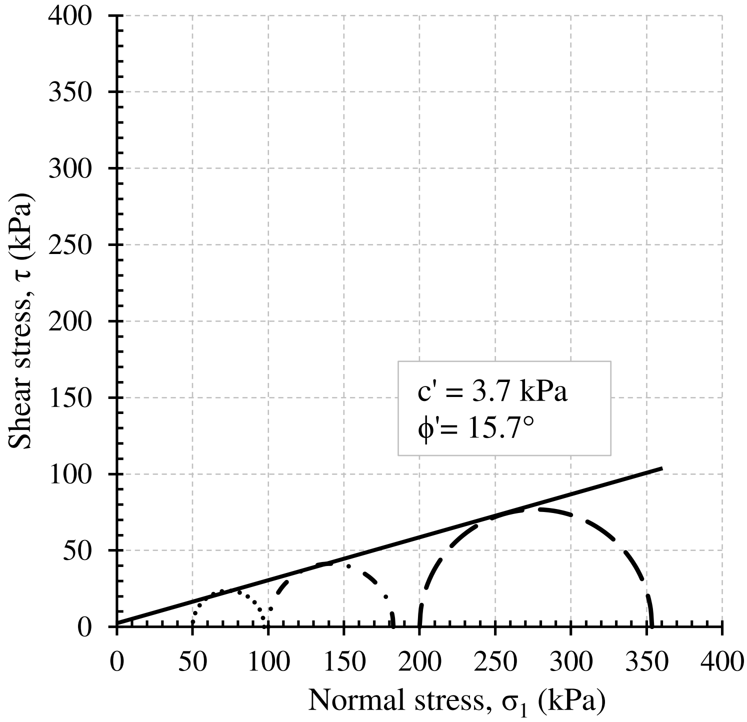

Figure 4.56 Mohr circles and failure envelope of 50% NS sand with 2.0-1.0 mm size of clay-sand mixtures tested in CU conditions, (effective stresses).

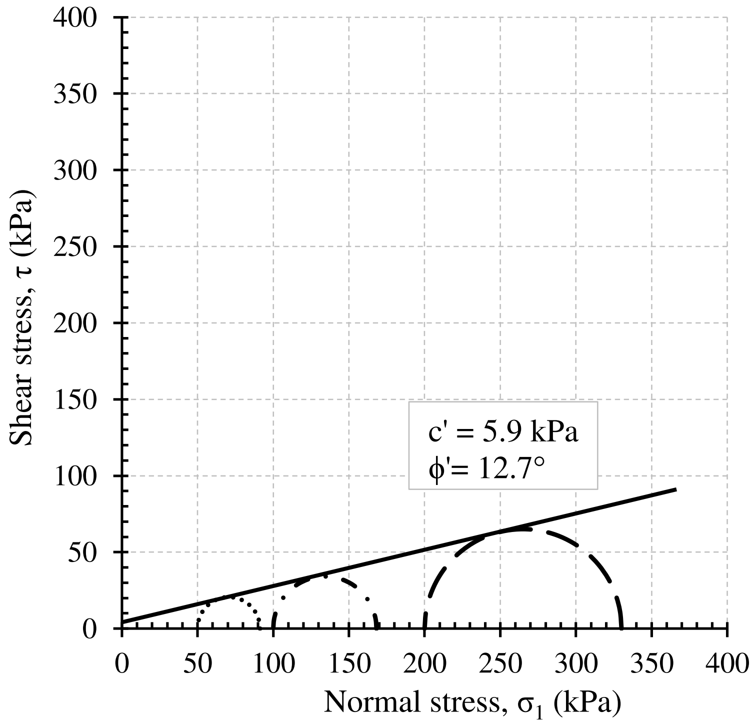

Figure 4.57 Mohr circles and failure envelope of 10% CSS sand with 0.6-0.3 mm size of clay-sand mixtures tested in CU conditions, (effective stresses).

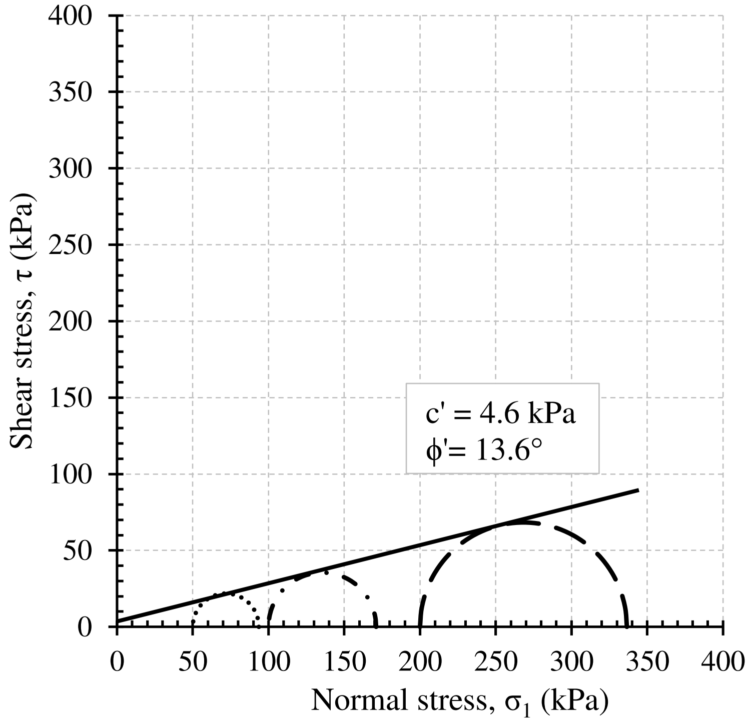

Figure 4.58 Mohr circles and failure envelope of 30% CSS sand with 0.6-0.3 mm size of clay-sand mixtures tested in CU conditions, (effective stresses).

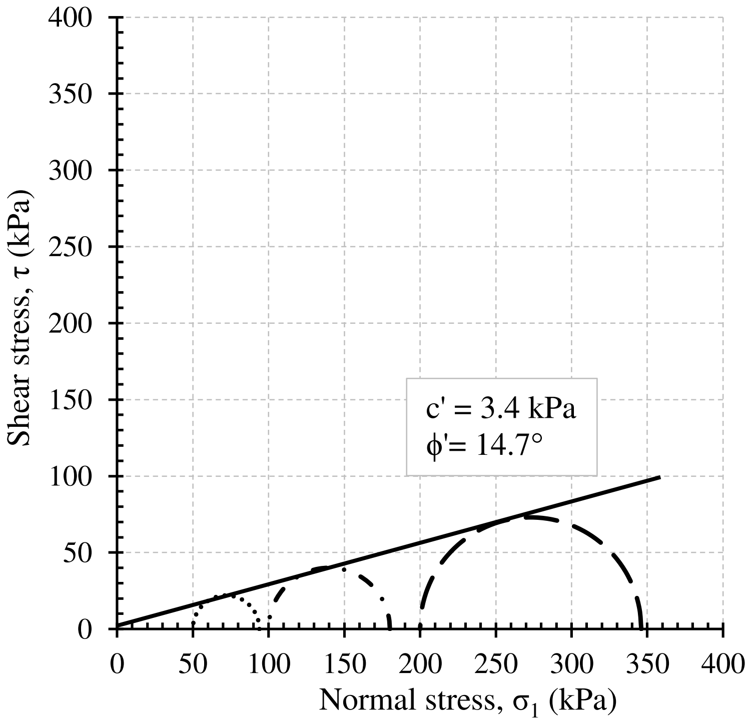

Figure 4.59 Mohr circles and failure envelope of 50% CSS sand with 0.6-0.3 mm size of clay-sand mixtures tested in CU conditions, (effective stresses).

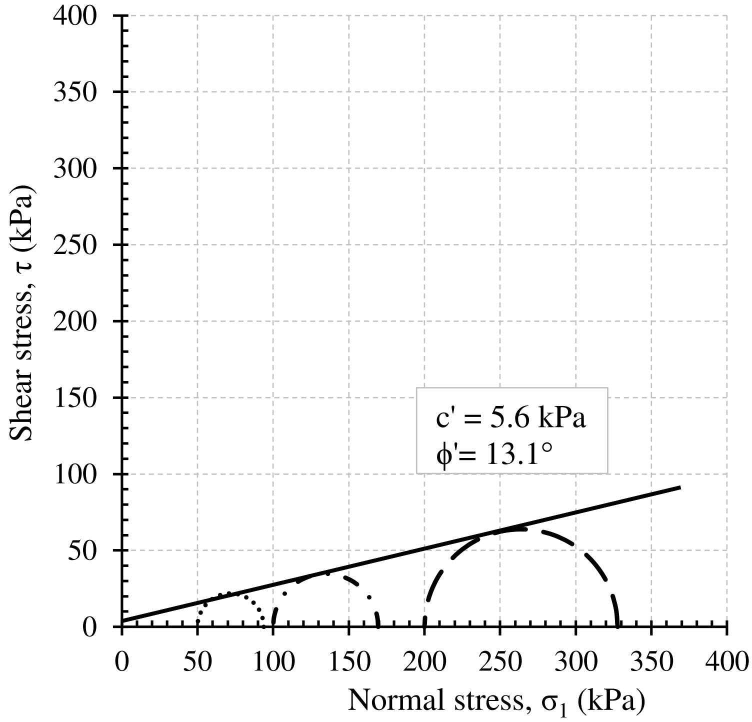

Figure 4.60 Mohr circles and failure envelope of 10% CSS sand with 2.0-1.0 mm size of clay-sand mixtures tested in CU conditions, (effective stresses).

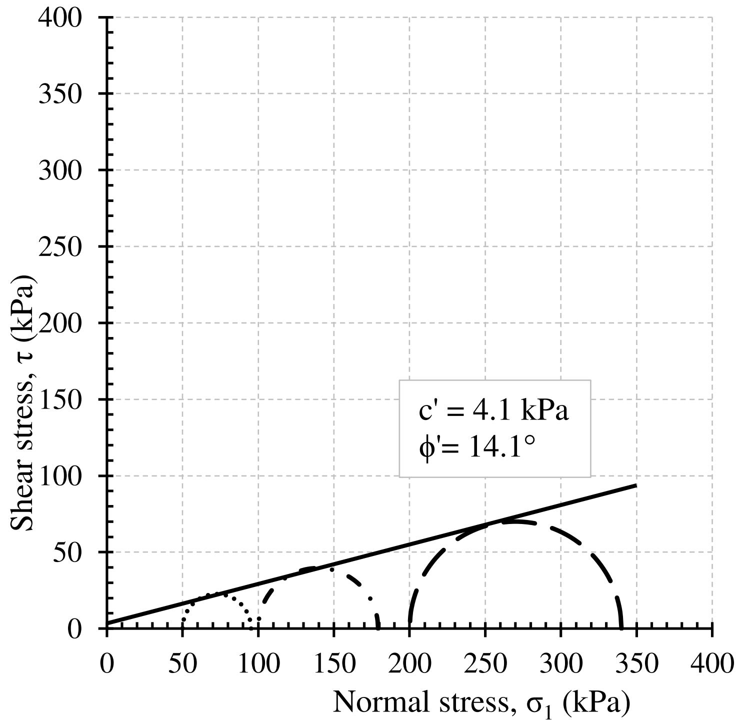

Figure 4.61 Mohr circles and failure envelope of 30% CSS sand with 2.0-1.0 mm size of clay-sand mixtures tested in CU conditions, (effective stresses).

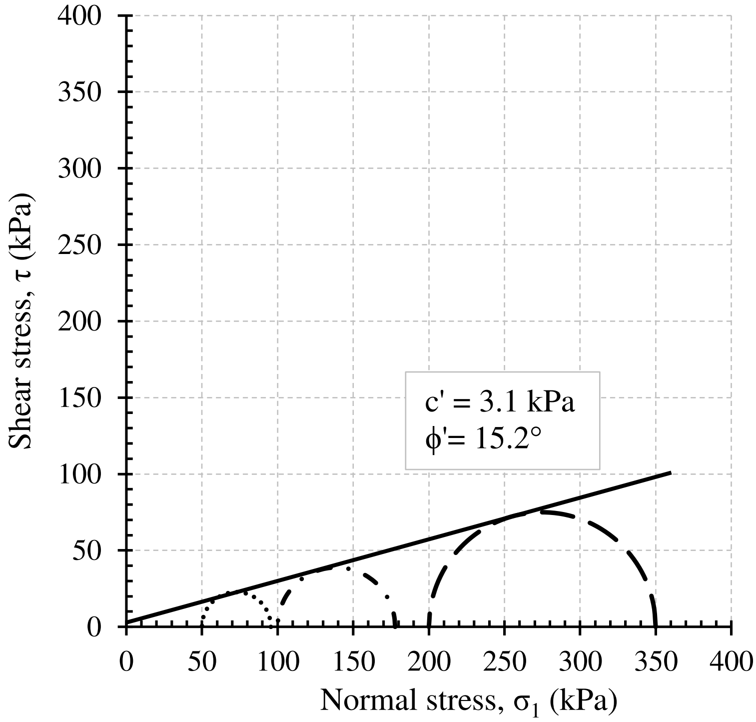

Figure 4.62 Mohr circles and failure envelope of 50% CSS sand with 2.0-1.0 mm size of clay-sand mixtures tested in CU conditions, (effective stresses).

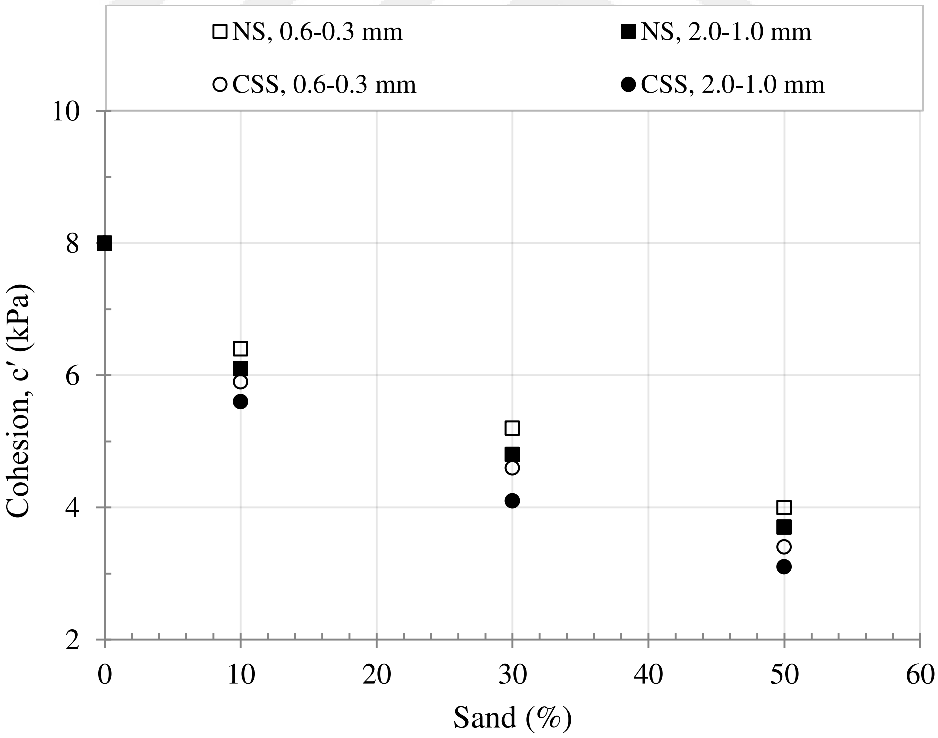

Figure 4.63 Variation of effective cohesion with sand content of clay-sand mixtures.

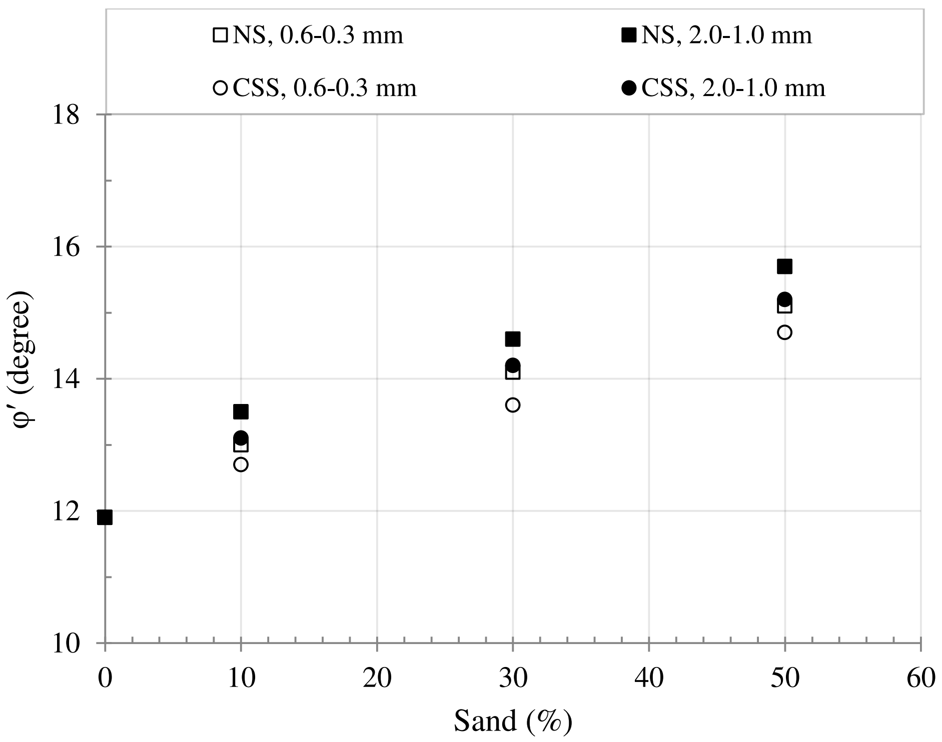

Figure 4.64 Variation of effective internal angle of friction with sand content of clay-sand mixtures.

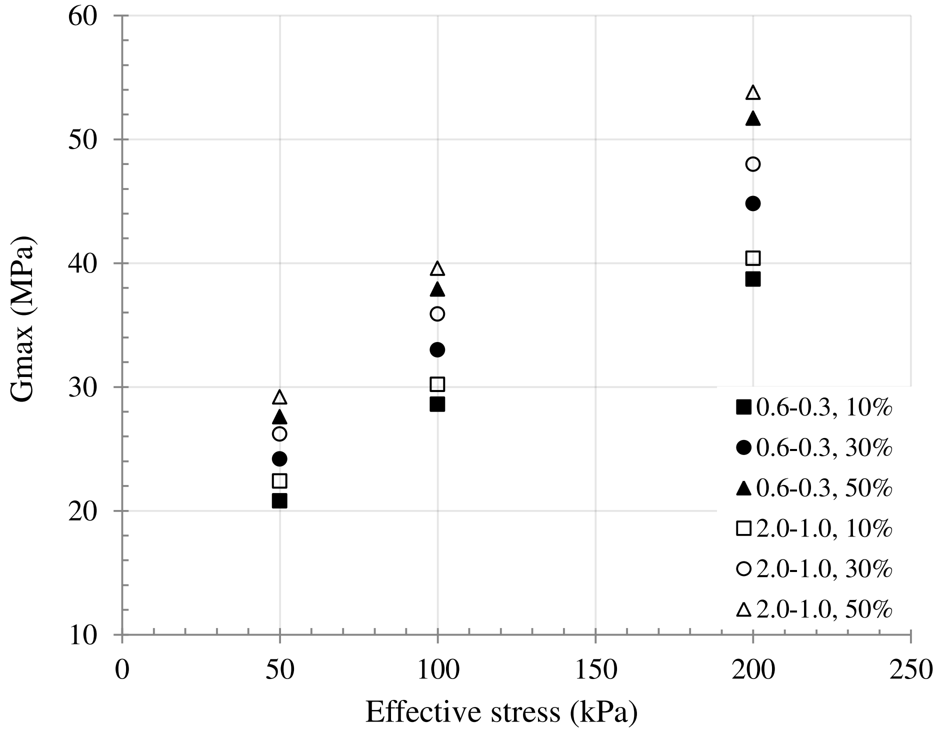

Figure 4.65 Change in G_{max} with effective stress of clay-NS sand at different sand contents.

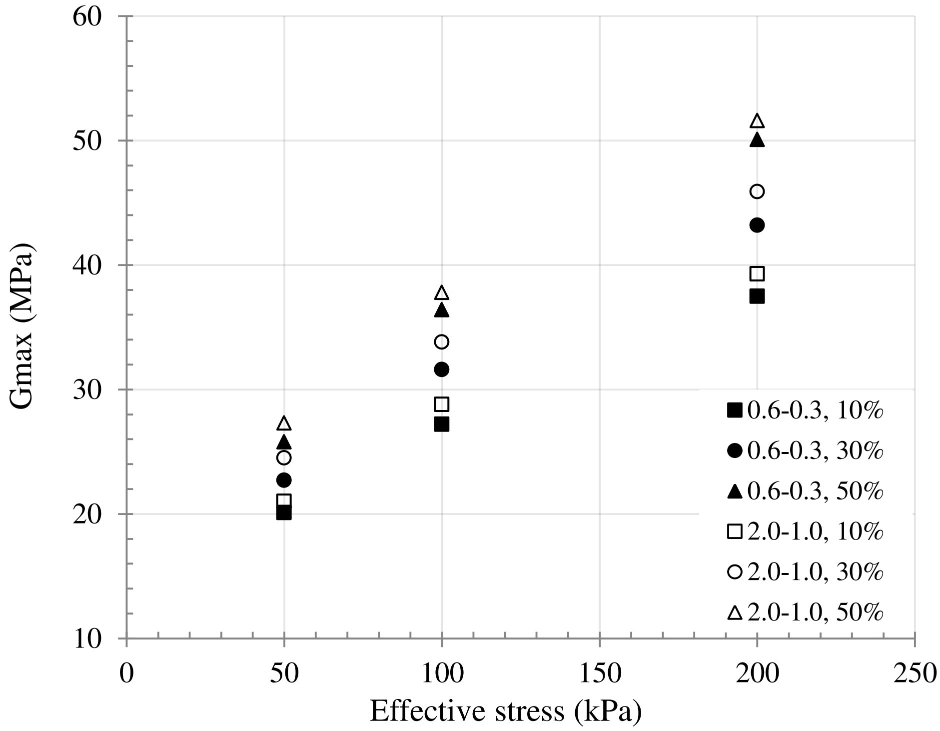

Figure 4.66 Change in G_{max} with effective stress of clay-CSS sand at different sand contents.

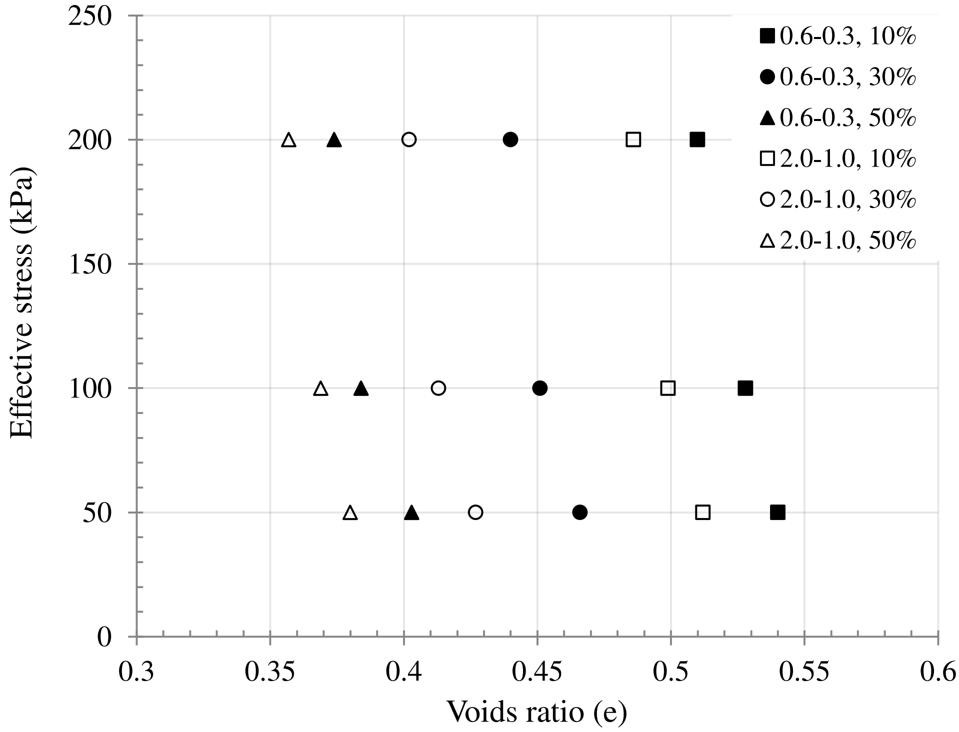

Figure 4.67 Change in effective stress with voids ratio of clay-NS sand at different sand contents.

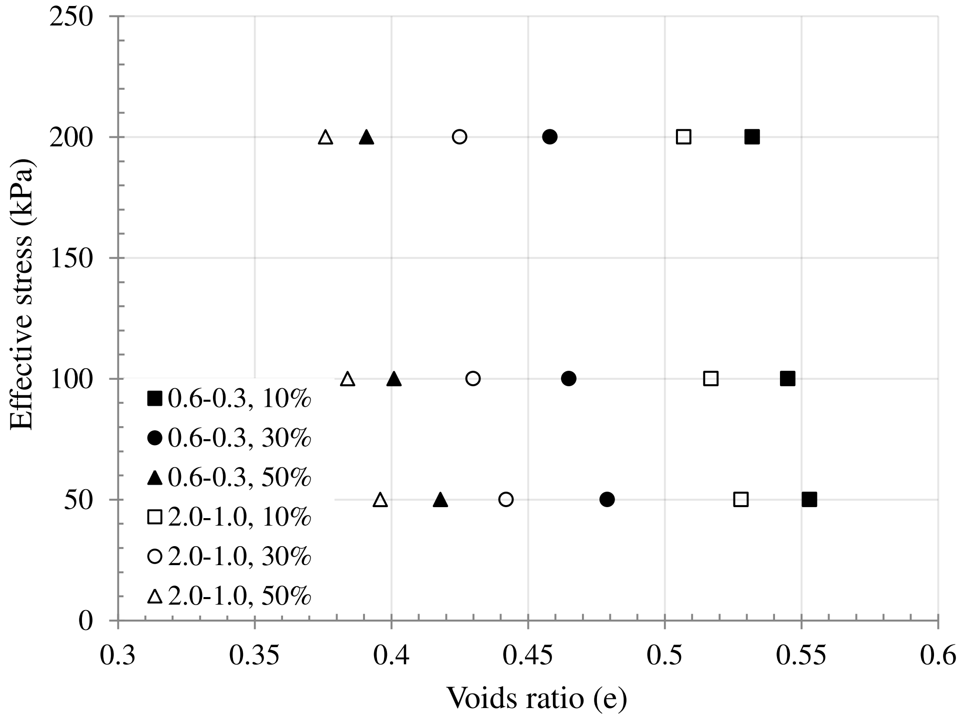

Figure 4.68 Change in effective stress with voids ratio of clay-CSS sand at different sand contents.

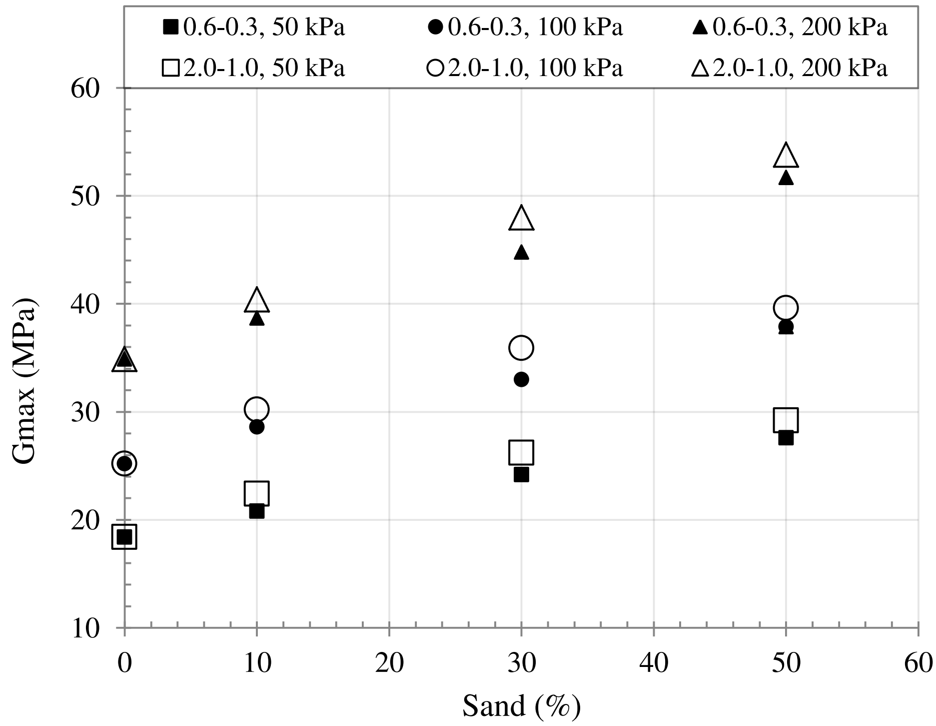

Figure 4.69 Change in G_{max} with sand content of clay-NS sand at different effective stresses.

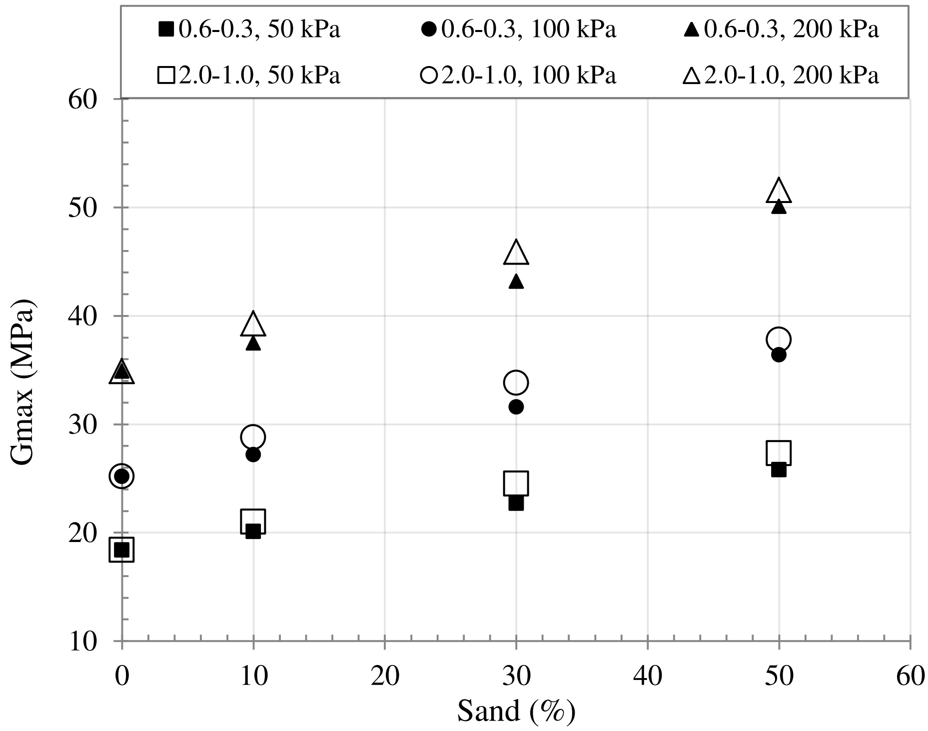

Figure 4.70 Change in G_{max} with sand content of clay-CSS sand at different effective stresses.

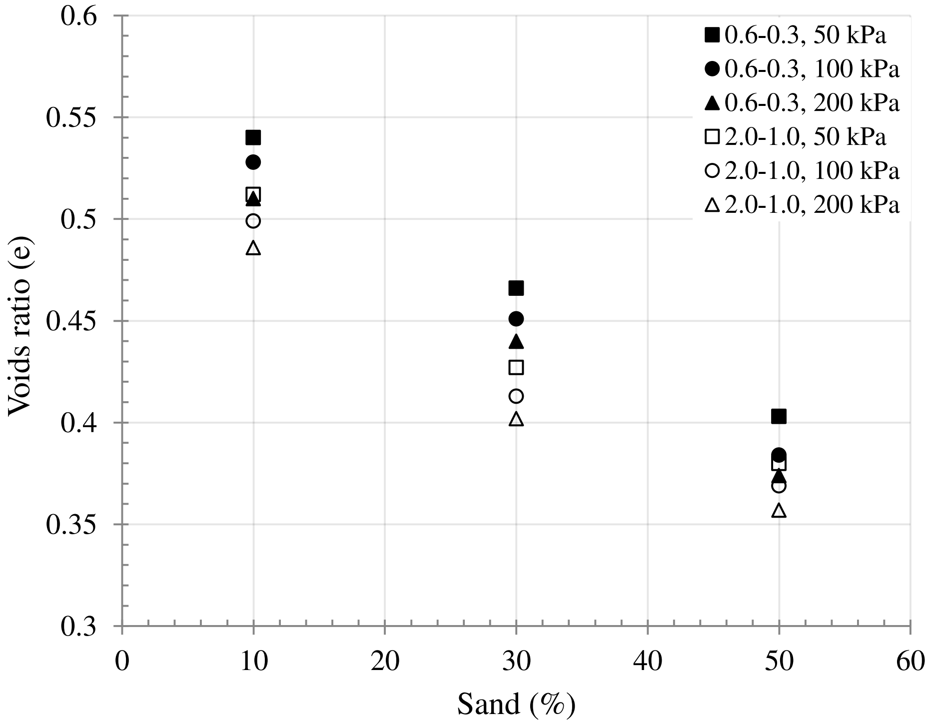

Figure 4.71 Change in voids ratio with sand content of clay-NS sand at different effective stresses.

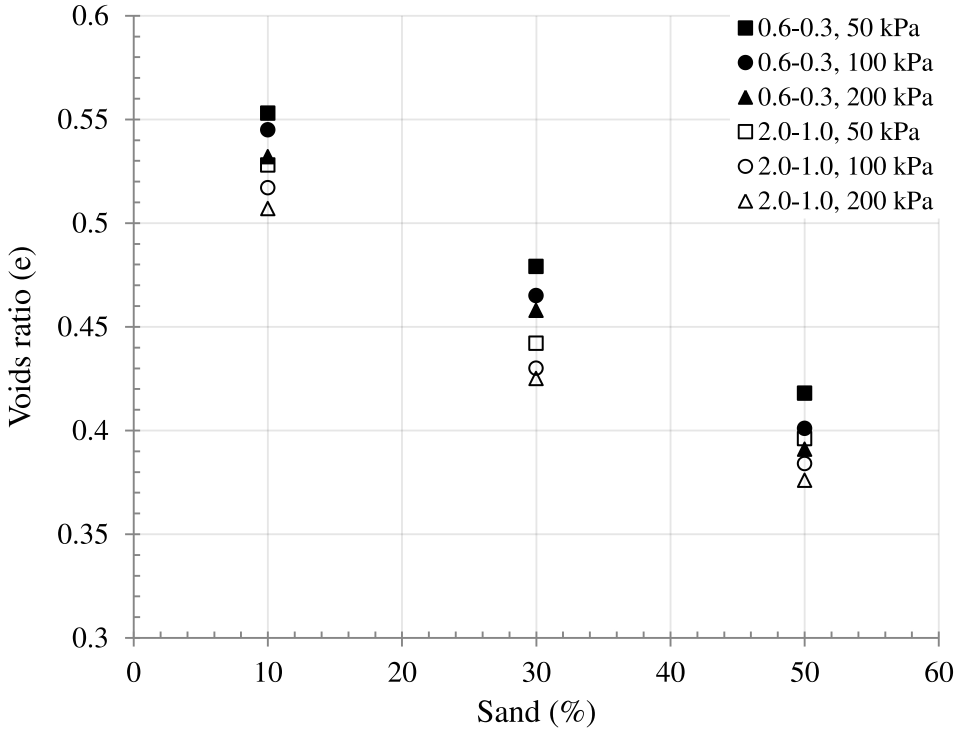

Figure 4.72 Change in voids ratio with sand content of clay-CSS sand at different effective stresses.

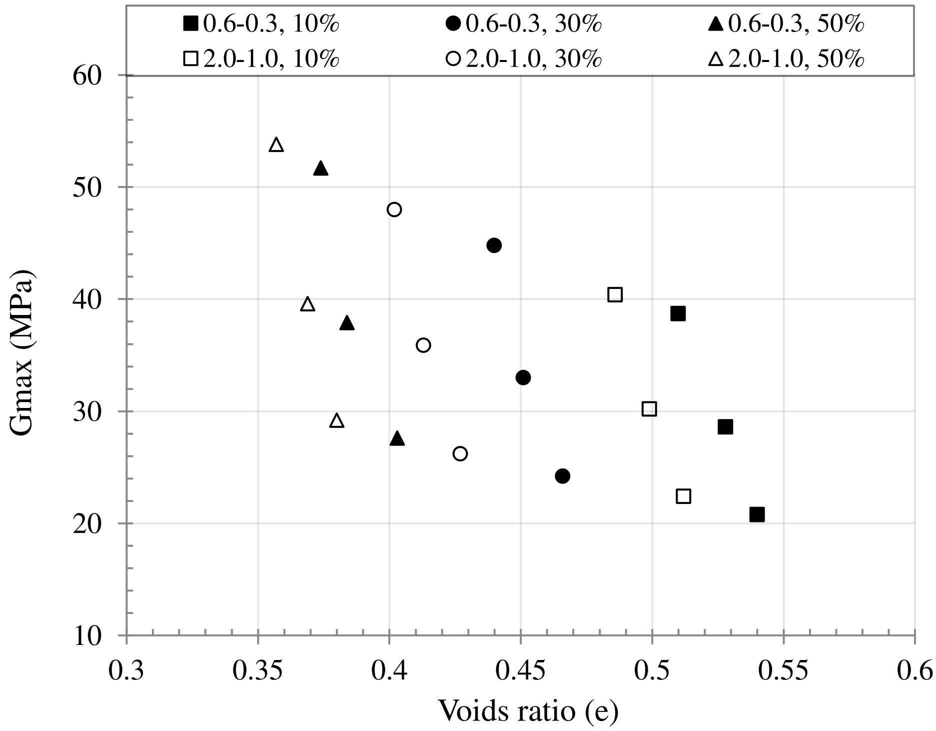

Figure 4.73 Change in G_{max} with voids ratio of clay-NS sand at different sand contents.

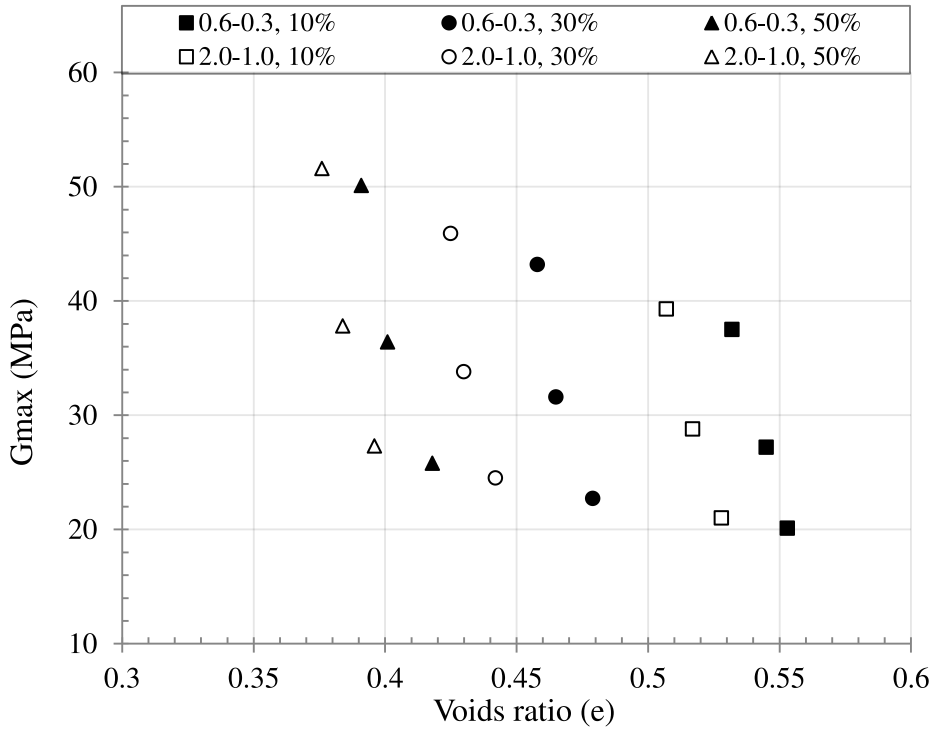

Figure 4.74 Change in G_{max} with voids ratio of clay-CSS sand at different sand contents.

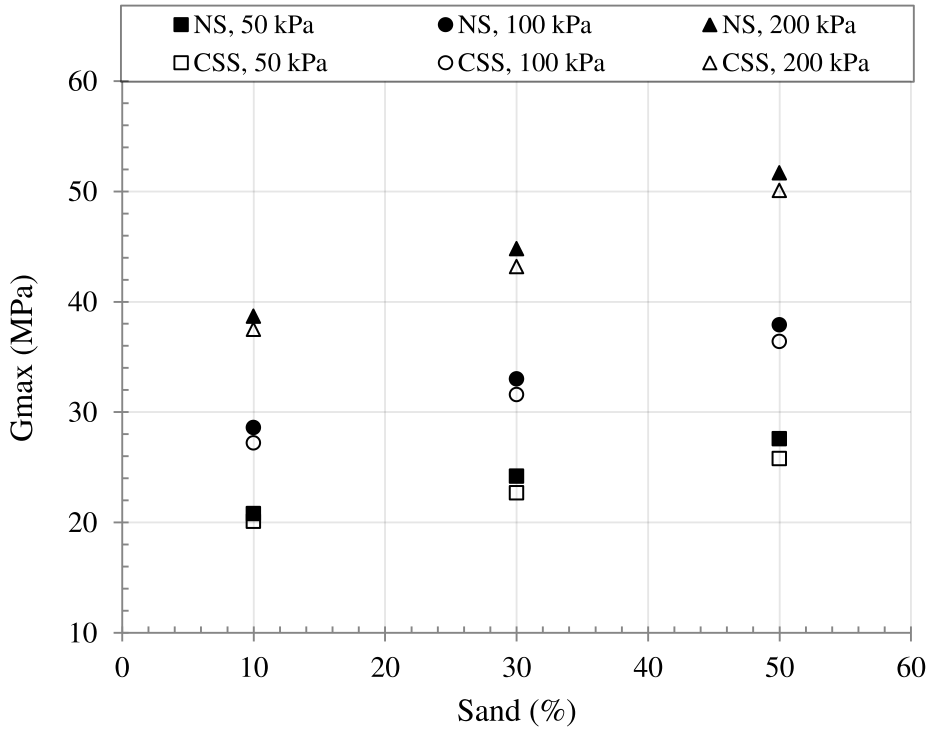

Figure 4.75 Comparison of G_{max} for 0.6-0.3 mm of clay-sand mixtures with NS and CSS sand at different effective stresses.

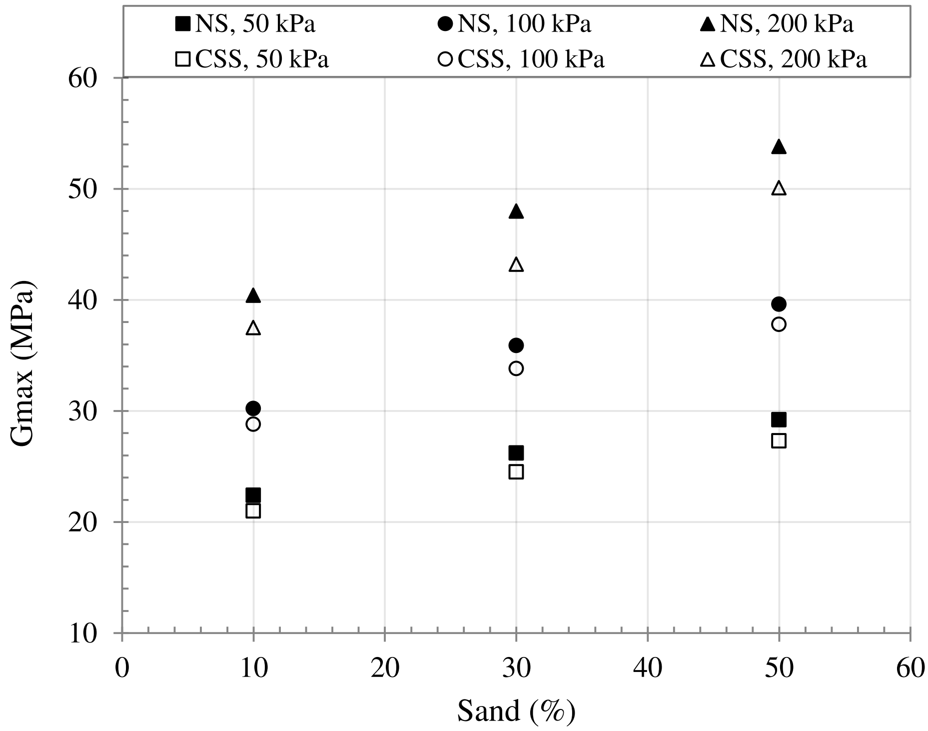

Figure 4.76 Comparison of G_{max} for 2.0-1.0 mm of clay-sand mixtures with NS and CSS sand at different effective stresses.

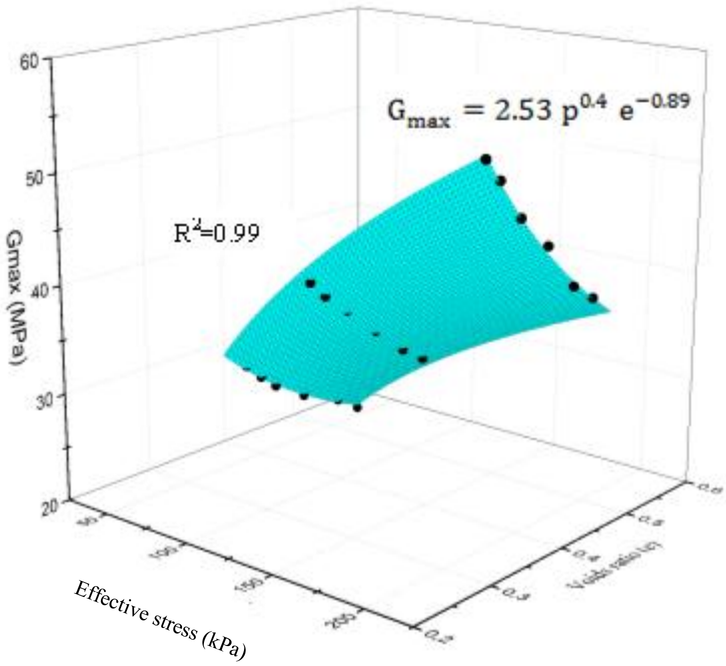

Figure 4.77 Relationship between G_{max}, voids ratio and effective stress of clay-NS sand mixtures.

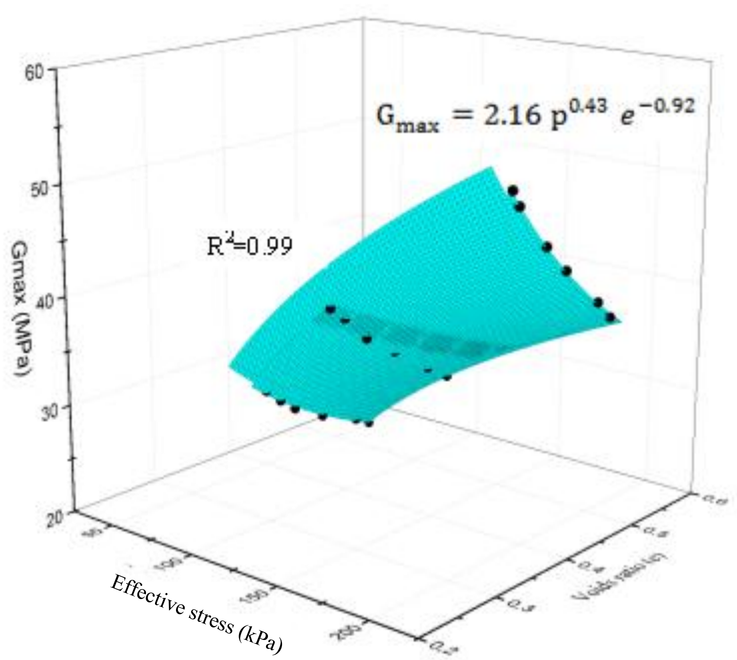

Figure 4.78 Relationship between G_{max}, voids ratio and effective stress of clay-CSS sand mixtures.

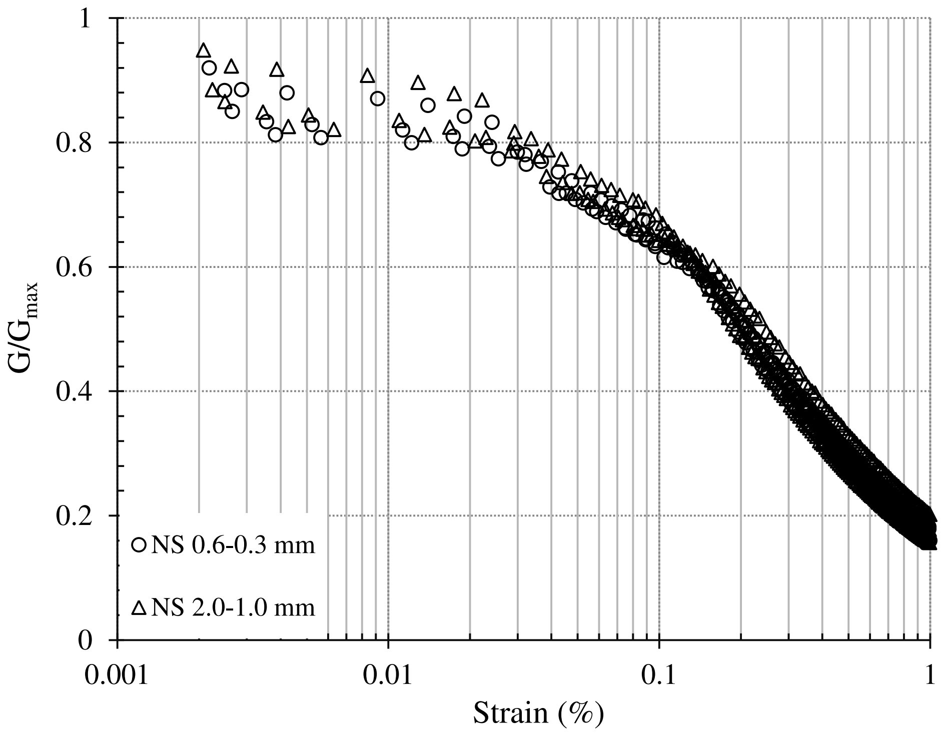

Figure 4.79 Shear modulus degradation curve for clay-NS sand mixtures at effective stress of 50 kPa.

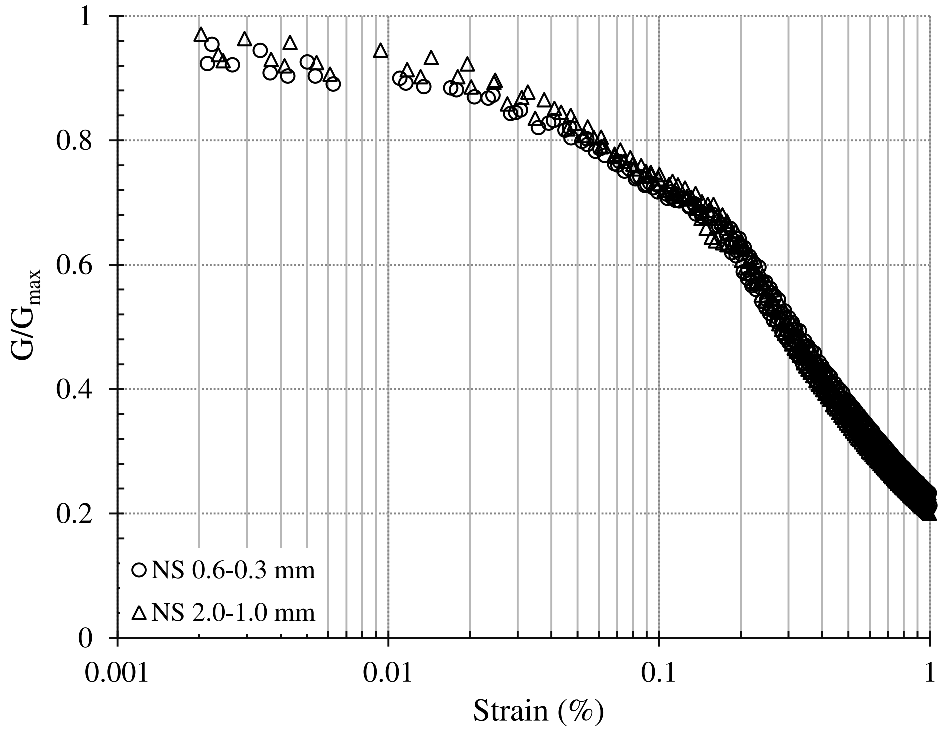

Figure 4.80 Shear modulus degradation curve for clay-NS sand mixtures at effective stress of 100 kPa.

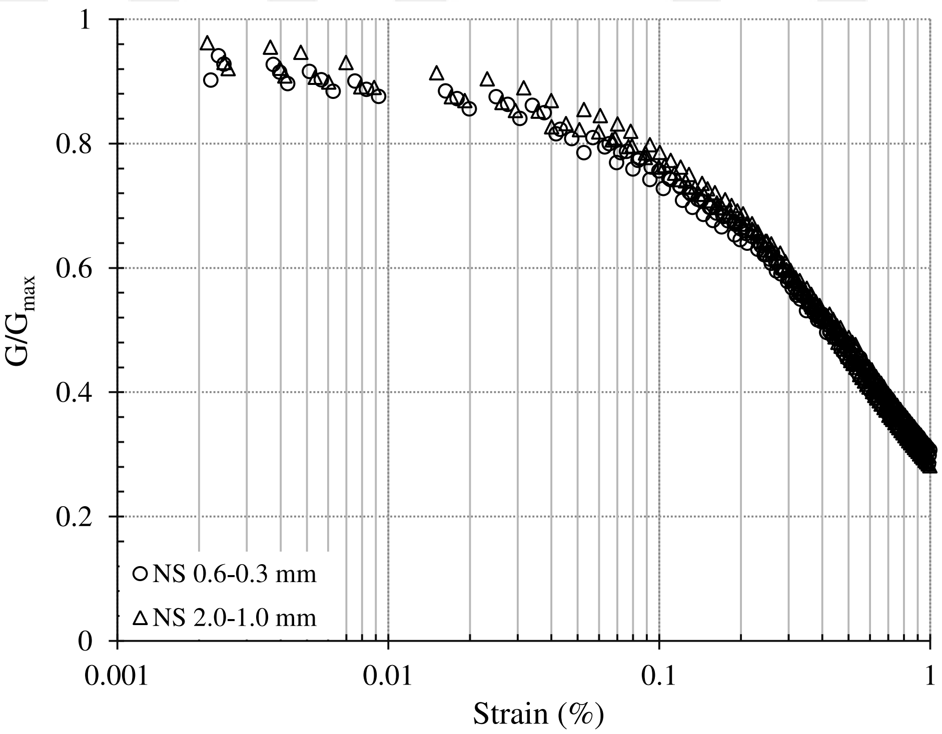

Figure 4.81 Shear modulus degradation curve for clay-NS sand mixtures at effective stress of 200 kPa.

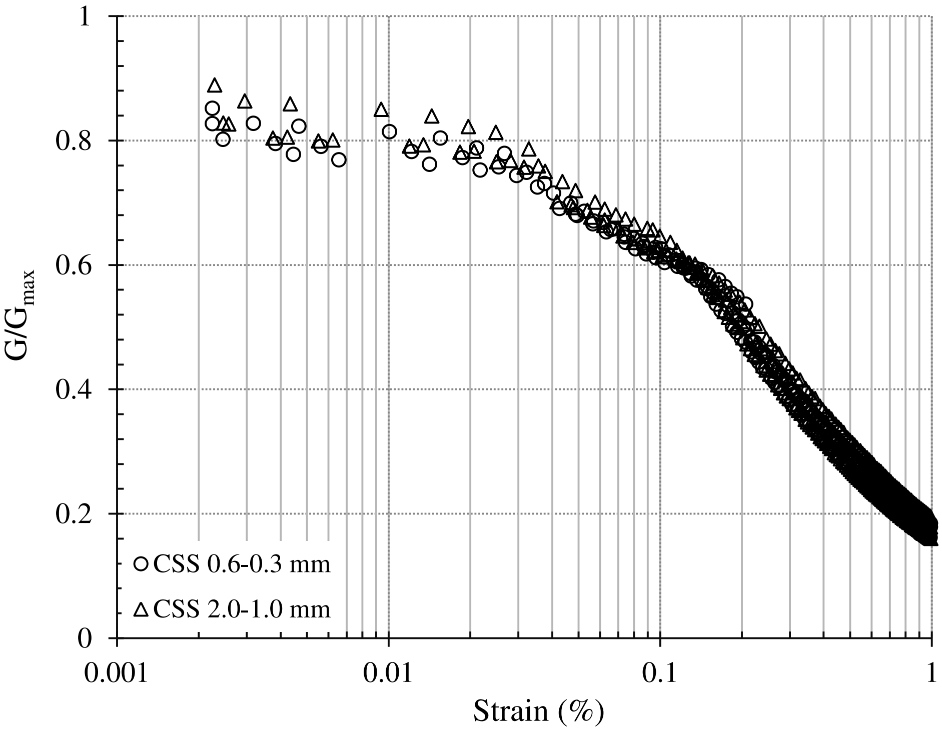

Figure 4.82 Shear modulus degradation curve for clay-CSS sand mixtures at effective stress of 50 kPa.

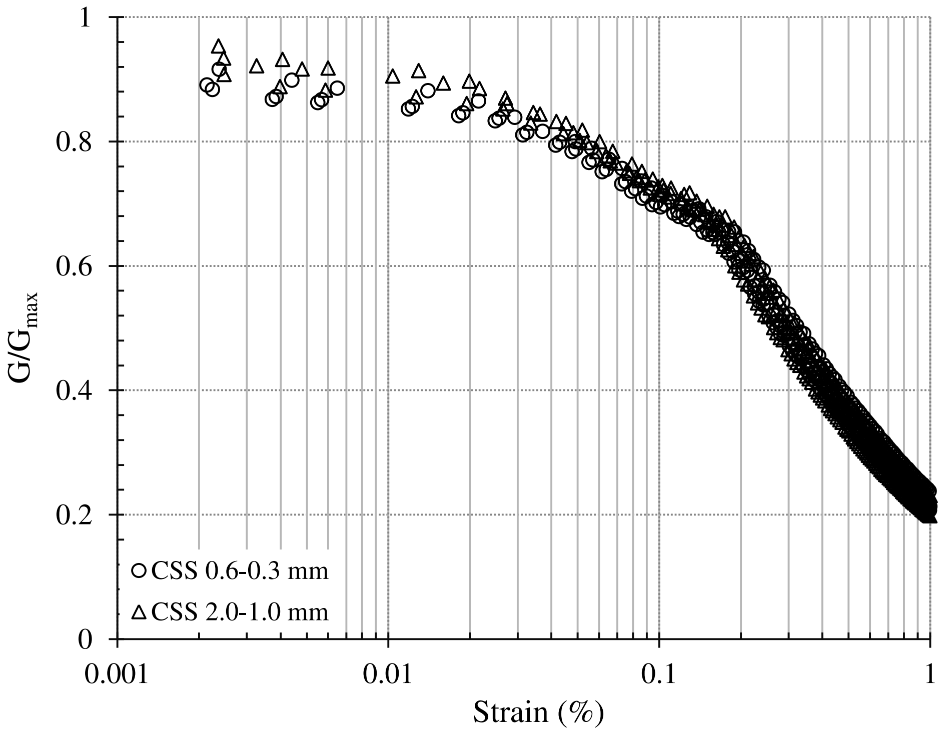

Figure 4.83 Shear modulus degradation curve for clay-CSS sand mixtures at effective stress of 100 kPa.

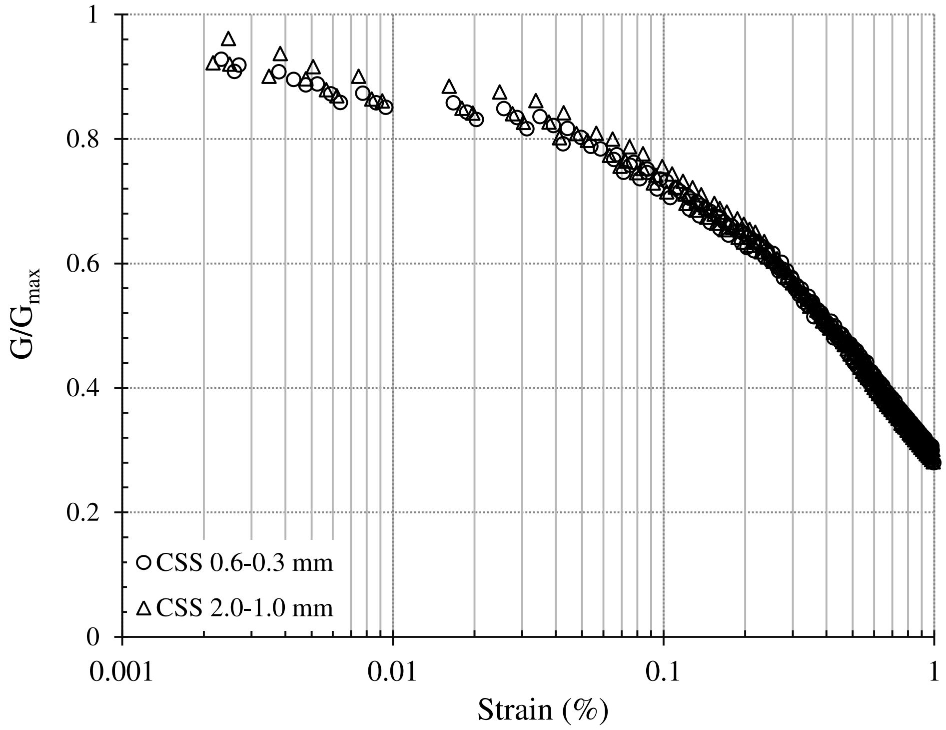

Figure 4.84 Shear modulus degradation curve for clay-CSS sand mixtures at effective stress of 200 kPa.

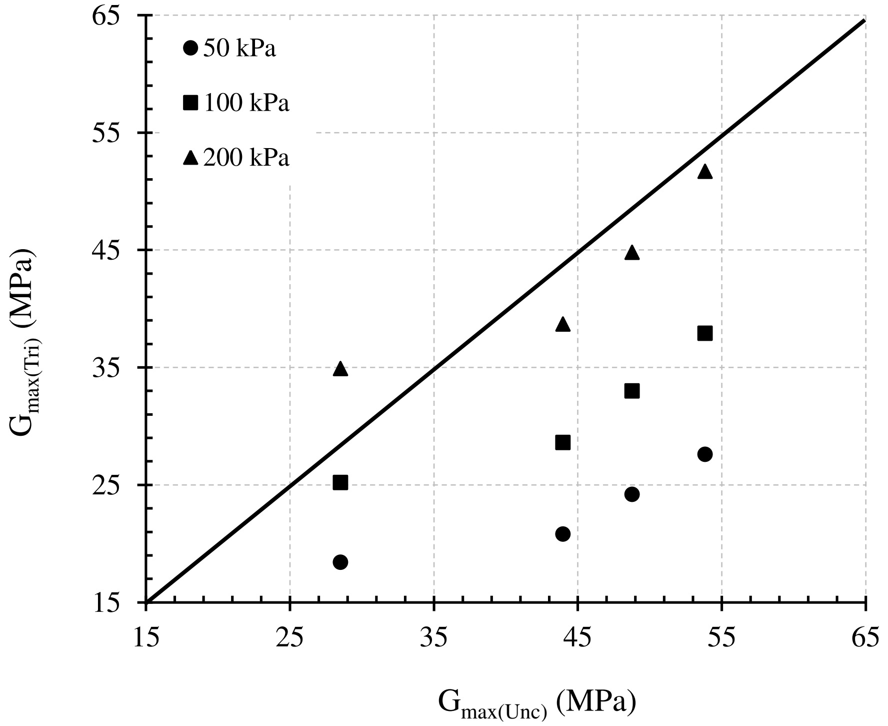

Figure 4.85 $G_{max(Tri)}$ versus $G_{max(Unc)}$ for clay-NS sand with size 0.6-0.3 mm.

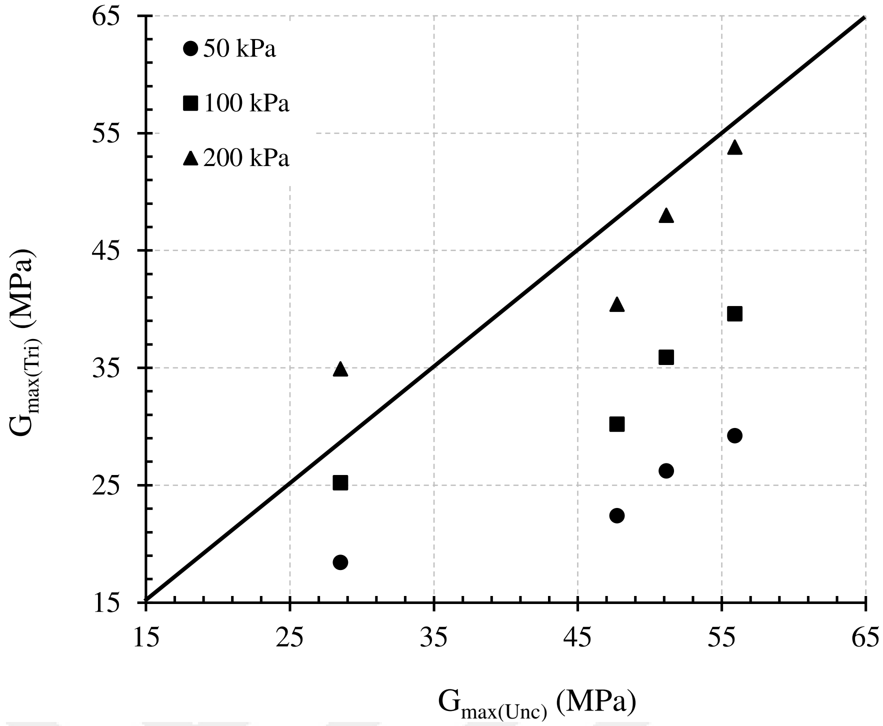

Figure 4.86 $G_{max(Tri)}$ versus $G_{max(Unc)}$ for clay-NS sand with size 2.0-1.0 mm.

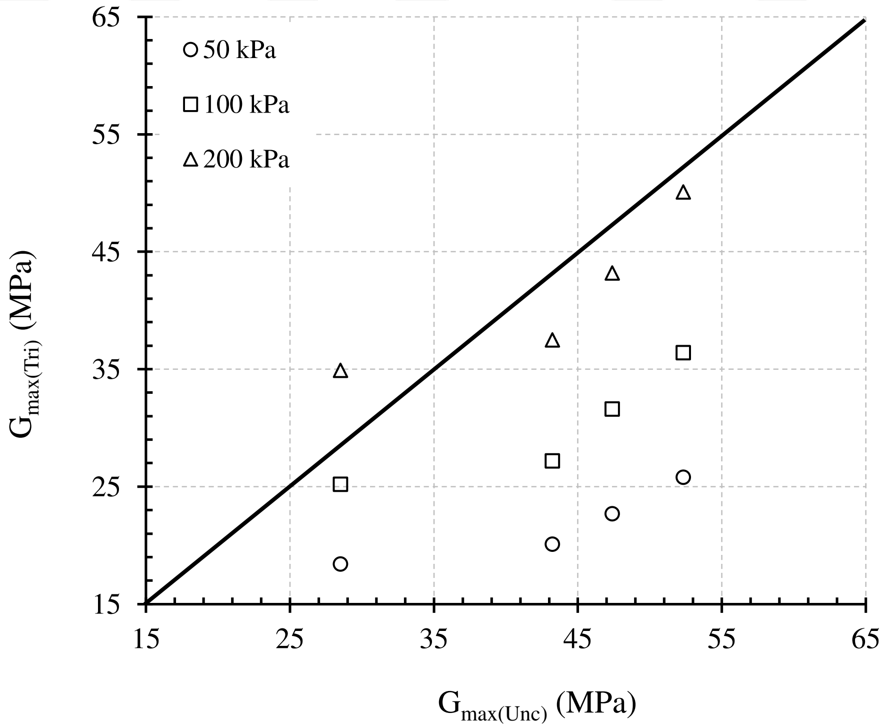

Figure 4.87 $G_{max(Tri)}$ versus $G_{max(Unc)}$ for clay-CSS sand with size 0.6-0.3 mm.

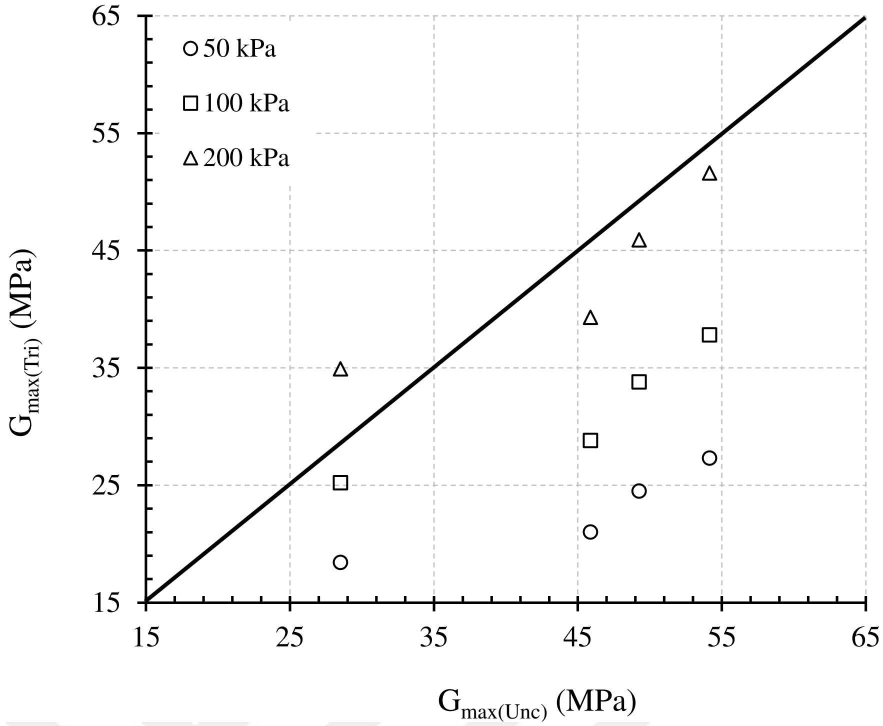

Figure 4.88 $G_{max(Tri)}$ versus $G_{max(Unc)}$ for clay-CSS sand with size 2.0-1.0 mm.

CHAPTER 5

CONCLUSIONS AND RECOMMENDATIONS

5.1 Conclusions

The research presented in this thesis focused on investigating the engineering properties, particularly, G_{max} as a dynamic properties of clayey soil mixed with different sizes and shapes of sandy soil grains using an unconfined compression machine equipped with bender elements. Also, an attempt was made to study the effect of the sand content, shape and size on the shear modulus and shear strength parameters (cohesion and angle of internal friction) using triaxial device equipped with bender elements. Hence, the conclusions drawn from the current study are displayed in two parts; (1) conclusions drawn from the unconfined compression machine equipped with bender elements tests, (2) conclusions drawn from the triaxial compression machine equipped with bender elements tests.

1- Conclusions drawn from the unconfined compression machine equipped with bender elements tests:

- For both clay and clay-sand mixtures shear wave velocity decreases with increase in input frequency of bender element test. The Vs decreases sharply after 5 kHz frequency, then decreases gradually.

- The determination of travel time of shear wave in the BE tests is affected by the input frequency. The near-field is decreased by increasing the input frequency, but high input frequency resulted in attenuation. The results obtained are more consistent when the input frequency is 5 kHz ($L/\lambda \approx 4\text{-}6$).

- In all of the cases, the addition of sand to the clayey soil causes increment in G_{max} and decreasing in q_u for rounded and angular sand and for all sizes that utilized in this study.

- The G_{max} values of the clay-sand mixtures increased from about 29 MPa for clayey soil to about 56 MPa for clay with 50% sand, while the qu values of the clayey soil decreased from 355 kPa to about 170 kPa when it was mixed with 50% sand for all sizes and shapes.

- Both the G_{max} and q_u values of clay-sand mixture with rounded grains of sand are higher than that of clay-sand mixture with angular grains of sand for all sand sizes and contents. This mean as roundness and sphericity increased (irregularity and angularity decreased) G_{max} and q_u increased for all sizes of sand.

- As grains size of sand increased, G_{max} and q_u values of clay-sand mixtures increased for rounded and angular sand.

- An empirical correlation between G_{max} and unconfined compressive strength of clay-sand mixtures has been found for rounded and angular sand of clay-sand mixtures.

2- Conclusions drawn from the triaxial compression equipped machine with bender elements tests:

- The deviatoric stress of clay-sand mixtures increased as the effective stress increased for all contents, shapes and sizes of sand that investigated in this study.

- The deviatoric stress increased as the sand content of clay-sand mixtures increased for all sizes and both types of sand (NS and CSS).

- The deviatoric stress of clay-CSS sand mixtures is lower than the deviatoric stress of clay-NS sand mixtures. The deviatoric stress decreased as the angularity and irregularity of the sand grains of clay-sand mixtures increased.

- The deviatoric stress values for the clay with larger grains of sand in the clay-sand mixtures were found to be always higher than those with smaller sand grains.

- Generally, the generation of pore water pressure of clay-sand mixtures increased as the effective stress increased.

- For all the cases studied, the pore water pressure generation decreased as the sand content of the clay-sand mixtures increased.

- The pore water pressure values of the clay-NS sand mixtures are lower than their values for the clay-CSS sand mixtures. The pore water pressure increased as the roundness and sphericity of the sand grains of the clay-sand mixtures decreased.

- The pore water pressure generation decreased with the increasing of sand size of clay-sand mixtures for clay-NS sand and clay-CSS sand mixtures.

- For all the sand sizes and both types of sand (NS and CSS) of clay-sand mixtures, as the sand content increased in the mixtures, the cohesion decreased, while the angle of internal friction increased.

- The clay-sand mixtures with CSS sand have lower values of cohesion and angle of internal friction for all sizes and contents of sand that investigated in this study.

- As the size of sand grain increased, the angle of internal friction of clay-sand mixtures increased, while cohesion the of clay-sand mixtures decreased for all sand contents and for two shapes of sand (NS and CSS).

- The G_{max} values of clay-sand mixtures increasing with the increasing of effective stress for all contents, shapes and sizes of sand that investigated in this study.

- The G_{max} values increased as the sand content increased for NS and CSS sand of clay-sand mixtures for all sand sizes and for all effective stresses that investigated in this study.

- The sand grains with rounded shape have higher G_{max} values for all sizes and contents of sand of clay-sand mixtures. G_{max} values increased as roundness and sphericity of sand grains increased.

- The sand grains with smaller sizes have lower G_{max} of clay-sand mixtures values than those with larger sizes for both types of sand (NS and CSS).

- An empirical correlation between G_{max}, voids ratio and effective stress of clay-sand mixtures has been found for rounded and angular sand of clay-sand mixtures.

5.2 Recommendations for Future Studies

From the findings of the current research to investigate the effect of shape and size of sand grains on clay-sand mixtures, some recommendations are proposed for the further studies:

1- These studies were carried out to study the effect of sand contents, shapes and sizes on engineering properties, particularly, dynamic properties on low-plasticity clay. These studies could be conducted to investigate these effects on the engineering properties of high-plasticity clay.

2- It is recommended to study the effect of sand contents, shapes and sizes on clay-sand mixtures using another devices equipped with bender elements, such as resonant column, dynamic triaxial or odometer to relate another engineering properties with G_{max}.

3- Further research is required to investigate the effect of shape and size of sand grains on the engineering properties of unsaturated soil, such as suction and soil water characteristic curve (SWCC).

4- It can be investigated the effect of gravel size on the engineering properties of sandy or clayey soil using unconfined compressive and triaxial devices equipped with bender elements.

5- This study investigated the effect of sand content up to 50%. This content could be increased to study the effect of high content of sand on the engineering properties of clay-sand mixtures.

REFERENCES

Ackerley, S.K., Standing, J.R., Hosseini, R. (2016). A system for measuring local radial strains in triaxial apparatus, *Géotechnique,* **66(6)**, 515-522.

Airey, D., Mohsin, A.K.M. (2013). Evaluation of shear wave velocity from bender elements using cross-correlation, *Geotechnical Testing Journal,* **36**, 506-514.

Alramahi, B., Alshibli, K., Fratta, D., and Trautwein, S. (2008). A suction-control apparatus for the measurement of p and s-wave velocity in soils, *Geotechnical Tesing Journal*, **31(1)**, 12-23.

Alshameri, B., Bakar, I., Madun, A., Abdeldjouad, L., Dahlan. S.H. (2016) Effect of coarse materials percentage in the shear strength, IOP Conference Series: Materials Science and Engineering. 136, 012017.

Arroyo, M., Muir Wood, D., Greening, P.D. (2003). Source near-field effects and pulse tests in soil samples, *Géotechnique,* **53(3)**, 337-345.

Arroyo, M., Muir Wood, D., Greening, P.D., Medina, L., Rio, J. (2006). Effects of sample size on bender-based axial G_0 measurements, *Géotechnique,* **56(1)**, 39-52.

Arroyo, M., Pineda, J.A., Romero, E. (2010). Shear wave measurements using bender elements in argillaceous rocks, *Geotechnical Testing Journal,* **33**, 1-11.

Arulnathan, R., Boulanger, R.W., Reimer, M.F. (1998). Analysis of bender element tests, *Geotechnical Testing Journal,* **21**, 120-131.

Asadi, M.B., Asadi, M.S., Orense, R.P., Pender, M.J. (2018). Geotechnical Earthquake Engineering and Soil Dynamics V : Slope Stability and Landslides, Laboratory Testing and In Situ Testing.

ASTM, American Society for Testing and Materials (2006). Standard Test Methods for Unconfined Compressive Strength of Cohesive Soil, D2166-2006, West Conshohocken, PA.

Belkhatir, M., Schanz, T., Arab, A., Della, N., Kadri, A. (2014). Insight into the effects of gradation on the pore pressure generation of sand–silt mixtures, *Geotechnical Testing Journal,* **37(5)**, 922-931.

Black, J., Sivakumar, V., McKinley, J.D. (2007). Performance of clay samples reinforced with vertical granular columns, *Canadian Geotechnical Journal,* **44(1)**, 89-95.

Bonal, J., Donohue, S., McNally, C. (2012). Wavelet analysis of bender element signals, *Géotechnique,* **62(3)**, 243-252.

Brignoli, E.G., Gotti, M., Stokoe, K.H. (1996). Measurement of shear waves in laboratory specimens by means of piezoelectric transducers, *Geotechnical Testing Journal,* **19(4)**, 384-397.

Brosse, A., Hosseini, R., Jardine, R.J., Coop, M.R. (2017). The shear stiffness characteristics of four Eocene-to-Jurassic UK stiff clays, *Géotechnique,* **67(3)**, 242-259.

Bui, T. (2009). Influence of some particle characteristics on the small strain response of granular materials. Doctoral dissertation, University of Southampton.

Bui, T., Clayton, C.R.I., Priest, A. (2010). The universal void ratio function for small strain shear modulus. International Conferences on Recent Advances in Geotechnical Earthquake Engineering and Soil Dynamics.

Cabalar, A.F. (2010). Applications of the oedometer, triaxial and resonant column tests to the study of micaceous sands, *Engineering Geology,* **112**, 21- 28.

Cabalar, A.F. (2015). Stress fluctuations in granular material response during cyclic direct shear tests, *Granular Matter,* **17(4)**, 439- 446.

Cabalar, A.F., Awraheem, M.H., Khalaf, M.M. (2018). Geotechnical Properties of a Low-Plasticity Clay with Biopolymer, *Journal of Materials in Civil Engineering,* **30(8)**, 04018170.

Cabalar, A.F., Dulundu, K., Tuncay, K. (2013). Strength of various sands in triaxial and cyclic direct shear tests, *Engineering Geology,* **156**, 92-102.

Cabalar, A.F., Hasan, R.A. (2013). Compressional behaviour of various size/shape sand-clay mixtures with different pore fluids, *Engineering Geology,* **164**, 36-49.

Cabalar, A.F., Mustafa, W.S. (2015). Fall cone tests on clay-sand mixtures, *Engineering Geology,* **192**, 154-165.

Cabalar, A.F., Mustafa, W.S., (2017). Behavior of sand-clay mixtures for road pavement subgrade, *International Journal of Pavement Engineering,* **18(8)**, 714-726.

Cabarkapa, Z., Cuccovillo, T. (2006). Automated triaxial apparatus for testing unsaturated soils, *Geotechnical Testing Journal,* **29(1)**, 21-29.

Cai, Y., Dong, Q., Wang, J., Gu, C., Xu, C. (2015). Measurement of small strain shear modulus of clean and natural sands in saturated condition using bender element test, *Soil Dynamics and Earthquake Engineering,* **76**, 100-110.

Callisto, L., Calabresi, G. (1998). Mechanical behaviour of a natural soft clay, *Géotechnique,* **48(4)**, 495-513.

Camacho-Tauta, J.F., Cascante, G., Viana da Fonseca, A., Santos, J.A. (2015). Time and frequency domain evaluation of bender element systems, *Géotechnique,* **65(7)**, 548-562.

Camacho-Tauta, J.F., Jimenez Alvarez, J.D., Reyes-Ortiz, O.J. (2012). A procedure to calibrate and perform the bender element test. *Dyna,* **79(176)**, 10-18.

Camacho-Tauta, J.F., Reyes-Ortiz, O.J., Jimenez Alvarez, J.D. (2013). Comparison between resonant-column and bender element tests on three types of soils. *Dyna*, **80(182)**, 163-172.

Castelli, F., Cavallaro, A., Grasso, S., Lentini, V. (2016). Seismic microzoning from synthetic ground motion earthquake scenarios parameters: the case study of the City of Catania (Italy), *Soil Dynamics and Earthquake Engineering,* **88**, 307-327.

Chan, K.H., Boonyatee, T., Mitachi, T. (2010). Effect of bender element installation in clay samples, *Géotechnique,* **60(4)**, 287-291.

Chang, N.P.N., Heymann, G. (2005). Shear wave velocity of gold tailings, *Journal of the South African Institution of Civil Engineering*, **47(2)**, 15-20.

Chapuis, R.P., (1990). Sand-bentonite liners: predicting permeability from laboratory tests, *Canadian Geotechnical Journal*, **27(1)**, 47-57.

Chattopadhya, B.C., Saha, S. (1981). Effect of grain size of cohesionless soil on its shear strength characteristics. In Geomech. 81 Proc. vol. 1, Symposium on Engineering Behaviour of Coarse Grained Soils, Boulders and Rock, 291-297.

Chen, G., Zhou, Z., Sun, T., Wu, Q., Xu, L., Khoshnevisan, S., Ling, D. (2018). Shear modulus and damping ratio of sand-gravel mixtures over a wide strain range, *Journal of Earthquake Engineering,* 1-34.

Chenari, R.J., Tizpa, P., Rad, M.R.G., Machado, S.L. Fard, M.K. (2015). The use of index parameters to predict soil geotechnical properties, *Arabian Journal of Geoscience,* **8(7)**, 4907-4919.

Cherian, A.C., Kumar, J. (2015). A study on arrival time corrections by using extender and bender elements, *International Journal of Geotechnical Engineering,* **9(4)**, 403-415.

Chien, L.K., Oh, Y.N. (2002). Influence of fines content and initial shear stress on dynamic properties of hydraulic reclaimed soil, *Canadian Geotechnical Journal,* **39(1)**, 242-253.

Cho, G.C., Dodds, J., Santamarina, J.C. (2006). Particle shape effects on packing density, stiffness and strength: Natural and crushed sands, *Journal of Geotechnical and Geoenvironmental Engineering,* **132(5)**, 591-602.

Clayton, C.R.I. (2011). Stiffness at small strain: research and practice, *Géotechnique,* **61(1)**, 5-37.

Clayton, C.R.I., Abbireddy, C.O.R., Schiebel, R. (2009). A method of estimating the form of coarse particulates, *Géotechnique,* **59(6)**, 493-501.

Consoli, N.C., Viana da Fonseca, A., Cruz, R.C., Heineck, K.S. (2009). Fundamental parameters for the stiffness and strength control of artificially cemented sand, *Journal of Geotechnical and Geoenvironmental Engineering,* **135(9)**, 1347-1353.

Cubrinovski, M., Ishihara, K. (2002). Maximum and minimum void ratio characteristics of sands, *Soils and Foundations,* **42(6)**, 65-78.

Cubrinovski, M., Rees, S. (2008). Effects of fines on undrained behaviour sands, In Geotechnical Earth Engineering and Soil Dynamics IV, 1-11.

Darendeli, M.B. (2001). Development of a new family of normalized modulus reduction and material damping curves. Ph.D. thesis, University of Texas at Austin, Austin, TX.

Dyskin A.V., Estrin Y., Kanel-Belov A.J., Pasternak E., (2001). Toughening by fragmentation—how topology helps, *Advanced Engineering Materials,* **3(1)**, 885-888.

Dyvik, R., Madshus, C. (1985). Lab measurements of G_{max} using bender elements. Advances in the art of testing soils under cyclic conditions. Proceedings of the ASCE conference, Detroit, MI, 24 October 1985. NewYork: *American Society of Civil Engineerings (ASCE)*, 186-96.

Dyvik, R., Olsen, T.S. (1991). G_{max} measured in oedometer and DSS tests using bender elements. *Publikasjon-Norges Geotekniske Institutt,* **181**, 1-4.

El Mosallamy, M., El Fattah, T.T.A., El Khouly, M. (2014). Experimental study on the determination of small strain-shear modulus of loess soil. *HBRC Journal,* **12(2)**, 181-190.

Enomoto, T., Qureshi, O.H., Sato, T., Koseki, J. (2013). Strength and deformation characteristics and small strain properties of undisturbed gravelly soils. *Soils and Foundations,* **53(6)**, 951-965.

Fabbrocino, S., Lanzano, G., Forte, G., de Magistris, F.S., Fabbrocino, G. (2015). SPT blow count vs. shear wave velocity relationship in the structurally complex formations of the Molise Region (Italy). *Engineering Geology,* **187**, 84-97.

Fakharian, K., Evgin, E., (1997). Cyclic simple-shear behavior of sand-steel interfaces under constant normal stiffness condition. *Journal of Geotechnical and Geoenvironmental Engineering*. **123(12)**, 1096-1105.

Fam, M.A., Cascante, G., Dusseault, M.B. (2002). Large and small strain properties of sands subjected to local void increase, *Journal of Geotechnical and Geoenvironmental Engineering,* **128(12)**, 1019-1025.

Fei, K. (2016). Experimental study of the mechanical behavior of clay–aggregate mixtures, *Engineering Geology,* **210**, 1-9.

Fei, K., Xu, J. (2017). Dynamic Behavior of Clay-Aggregate Mixtures, *Advances in Materials Science and Engineering,* Article ID 2479507, 10 pages, 2017.

Ferreira, Viana Da Fonseca, C., Santos, A. (2007). Comparison of simultaneous bender elements and resonant column tests on Porto residual soil. Geotechnical Symposium in Rome, **146**, 523-536.

Finno, R., Cho, W. (2010). Recent stress-history effects on compressible Chicago glacial clays, *Journal of Geotechnical and Geoenvironmental Engineering,* **137(3)**, 197-207.

Fioravante, V. (2000). Anisotropy of small strain stiffness of Ticino and Kenya sands from seismic wave propagation measured in triaxial testing, *Soils and Foundations,* **40(4)**, 129-142.

Fioravante, V., Capoferri, R. (2001). On the use of multi-directional piezoelectric transducers in triaxial testing, *Geotechnical Testing Journal,* **24(3)**, 243-255.

Flores, R.D., Di Emidio, G., Van Impe, W.F. (2009). Small-strain shear modulus and strength increase of cement-treated clay, *Geotechnical Testing Journal*, **33(1)**, 1-10.

Fraser, H. J. (1935). Experimental study of the porosity and permeability of clastic sediments, *The Journal of Geology,* **43(8)**, 910-1010.

Gajo, A., Fedel, A. Mongiovi, L. (1997). Experimental analysis of the effects of fluid-solid coupling on the velocity of elastic waves in saturated porous media, *Géotechnique,* **47**,993-1008.

Gasparre, A., Hight, D.W., Coop, M.R., Jardine, R.J. (2014). The laboratory measurement and interpretation of the small-strain stiffness of stiff clays. *Géotechnique,* **64(12)**, 942-953.

Ghayoomi, M., Suprunenko, G., Mirshekari, M. (2017). Cyclic triaxial test to measure strain-dependent shear modulus of unsaturated sand, *International Journal of Geomechanics,* **17(9)**, 04017043.

Giang, P.H.H., Van Impe, P.O., Van Impe, W.F., Menge, P., Haegeman, W. (2017). Small-strain shear modulus of calcareous sand and its dependence on particle characteristics and gradation, *Soil Dynamics and Earthquake Engineering,* **100**, 371-379.

Gordon, M.A., Clayton, C.R.I. (1997). Measurement of stiffness of soils using small strain triaxial testing and bender elements, *Geological Society, London, Engineering Geology Special Publications,* **12(1)**, 365-371.

Gryczmanski, M. (2009). State of the art in modelling of soil behaviour at small strains, *Architecture Civil Engineering Environment,* **2(1)**, 61-80.

Gu X., Yang J., Huang M. (2013). Laboratory measurements of small strain properties of dry sands by bender element, *Soils and Foundations,* **53(5)**, 735-745.

Guimaraes, M. (2002). Crushed stone fines and ion removal from clay slurries—fundamental studies. Ph.D. thesis. Georgia Institute of Technology, Atlanta.

Gupta, A.K. (2009). Effect of particle size and confining pressure on breakage and strength parameters of rockfill materials, *Electronic Journal of Geotechnical Engineering,* **14(H)**, 1-12.

Hamidi, A., Hooresfand, M. (2013). Effect of fiber reinforcement on triaxial shear behavior of cement treated sand, *Geotextiles and Geomembranes,* **36**, 1-9.

Hardin, B.O. (1961). Study of elastic wave propagation and damping in granular materials. University of Florida at Gainesville, Florida.

Hardin, B.O. (1978). The nature of stress-strain behavior for soils, In Proceedings of the ASCE Specialty Conference on Earthquake Engineering and Soil Dynamics, 3-90.

Hardin, B.O., Black, W.L. (1968). Vibration modulus of normally consolidated clay, *Journal of the Soil Mechanics and Foundations Division,* **94(2)**, 353-369.

Hardin, B.O., Black, W.L. (1969). Vibration modulus of normally consolidated clay (closure), *Journal of the Soil Mechanics and Foundations Division,* **95(6)**, 1531-1537.

Hardin, B.O., Drnevich, V.P. (1972). Shear modulus and damping in soils: measurement and parameter effects, *Journal of Soil Mechanics and Foundation Division,* **6**, 603-624.

Hardin, B.O., Kalinski, M.E. (2005). Estimating the shear modulus of gravelly soils, *Journal of Geotechnical and Geoenvironmental Engineering,* **131(7)**, 867-875.

Hardin, B.O., Richart J.F.E. (1963). Elastic wave velocities in granular soils, *Journal of Soil Mechanics and Foundations Division,* **89**, 33-65.

Herbold E.B., Nesterenko V.F., Benson D.J., Cai, J., Vecchio, K.S., Jiang, F., Addiss J.W., Walley, S.M., Proud W.G. (2008). Particle size effect on strength , failure and shock behavior in polytetrafluoroethylene-AL-W granular composite materials, *Journal of Applied Physics,* **104(10)**, 103903-1 to 9.

Holtz, W.G., Willard, M. (1956). Triaxial shear characteristics of clayey gravel soils, *Journal of Soil Mechanics and Foundation Engineering*, **82**,1-22.

Holubec, I., D'Appolonia, E. (1973). Effect of particle shape on the engineering properties of granular soils. Evaluation of relative density and its role in geotechnical projects involving cohesionless soils, ASTM, STP523, West Conshohocken, PA, 304-318.

Hoyos, L.R., Suescun-Florez, E.A., Puppala, A.J. (2015). Stiffness of intermediate unsaturated soil from simultaneous suction-controlled resonant column and bender element testing, *Engineering Geology,* **188**, 10-28.

Humphries, W.K. Wahls, E.H. (1968). Stress history effects on dynamic modulus of clay, *Journal of the Soil Mechanics and Foundation Division,* **94(2)**, 371-389.

Ibrahim, A., Orense, R., Pender, M., (2011). Determination of very small strain shear modulus of Auckland residual soils using bender elements. W: Proceedings of the 9th Pacific Conference on Earthquake Engineering. Building an Earthquake-Resilient Society, Auckland.

Ishibashi, I., Chen, Y., Chen, M. (1991). Anisotropic behavior of Ottawa sand in comparison with glass spheres. *Soils and Foundations*, **31(1)**, 145-155.

Ishihara, K., Koseki, J. (1989). Cyclic shear strength of fines-containing sands, earthquake geotechnical engineering, Proceedings of the Discussion Session on Influence of Local Conditions on Seismic Response, 12th ACSMFE Rio de Janeiro, 101-106.

Islam, M.N., Asad, M.A., Rahman, A., Siddika, A., Hossain, M.B., Ali, M. M.Y. (2011), Shear strength behaviour of granular materials: effect of grain size, Proceedings of the Conference on Engineering Research, Innovation and Education 2010 CERIE 2010, 11-13 January, Sylhet, Bangladesh, paper id cerie-389.

Islam. M.N. (2009). Effect of Intermediate Principal Stress on the Shear Behavior of Granular Materials using 3D-DEM, Master's Thesis, Department of Civil and Environmental Engineering Saitama University, Japan

Iwasaki, T., Tatsuoka, F. (1977). Effect of grain size and grading on dynamic shear moduli of sand, *Soils and Foundations,* **38(1)**, 19-35.

Jafari, M.K., Shafiee, A. (2004). Mechanical behavior of compacted composite clays, *Canadian Geotechnical Journal*, **41(6)**, 1152-1167.

Jamiolkowski, M., Leroueil, S., Lo Presti, D.C.F. (1991). Theme lecture: Design parameters from theory to practice, in 'Proceedings of the international conference on geotechnical engineering for coastal development, Geo-Coast 1991', Yokohama, Japan, 877-917.

Jia, X., Williams, R.A. (2001). A packing algorithm for particles of arbitrary shapes, *Powder Technology,* **120(3)**, 175-186.

Jovicic, V., Coop, M. R. (1998). The measurement of stiffness anisotropy in clays with bender element tests in the triaxial apparatus, *Geotechnical Testing Journal*, **21(1)**, 3-10.

Jovicic, V., Coop, M. R., Simic, M. (1996). Objective criteria for determining G_{max} from bender element tests, *Géotechnique,* **46(2)**, 357-362.

Kakou, B.G., Shimizu, H., Nishimura, S. (2001). Residual strength of colluvium and stability analysis of farmland slope, *Agricultural Engineering International: CIGR Journal,* **3**, 1-12.

Kallioglou, P., Tika, T.H., Pitilakis, K. (2008). Shear modulus and damping ratio of cohesive soils, *Journal of Earthquake Engineering*, **12(6)**, 879-913.

Kara, E., Meghachou, M. Aboubekr, N. (2013). Contribution of particles size ranges to sand friction, *Engineering Technology and Applied Science Research*, **3(4)**, 497-501.

Karabash, Z., Cabalar, A.F. (2015). Effects of sand grains shape on the behaviour of sand clay mixtures. Geotechnical Engineering for Infrastructure and Development: XVI European Conference on Soil Mechanics and Geotechnical Engineering.

Katzenbach, R., Schmitt, A. (2004). Micromechanical modeling of granular materials under triaxial and oedometric loading, *Numerical Modeling in Micromechanics via Particle Methods,* 313-322.

Kenny, T.C. (1977). Residual strength of mineral mixture, Proc. 9th International Conference of Soil Mechanics and Foundation Engineering, 155-160.

Khosravi, A., McCartney, J.S. (2012). Impact of hydraulic hysteresis on the small-strain shear modulus of low plasticity soils, *Journal of Geotechnical and Geoenvironmental Engineering,* **138(11)**, 1326-1333.

Kim, U., Hyodo, M., Koga, C., Orense, R. (2006). Effect of fines content on the monotonic shear behavior of sand-clay mixtures. *Geomechanics and Geotechnics of Particulate Media,* 133-138.

Kokusho, T., Yoshida, Y., Esashi, Y. (1982). Dynamic properties of soft clays for wide strain range, *Soils and Foundations,* **22(4)**, 1-18.

Kramer, S.L. (1996). Geotechnical Earthquake Engineering. Prentice-Hall Inc, Upper Saddle River, NJ.

Krumbein, W.C. Sloss L.L. (1963). Stratigraphy and Sedimentation. San Francisco: W. H. Freeman and Company.

Krumbein, W.C. (1941). Measurement and geological significance of shape and roundness of sedimentary particles, *Journal of Sedimentary Petrology,* **11(2)**, 64-72.

Kumar, J., Madhusudhan, B.N. (2010). Effect of relative density and confining pressure on Poisson ratio from bender and extender elements tests, *Géotechnique,* **60(7)**, 561-567.

Kumar, S.S., Krishna, A.M., Dey, A. (2016). Local Strain Measurements in Triaxial Tests Using On-Sample Transducers. In Geotechnical Characterisation and Geoenvironmental Engineering, 93-101, Springer, Singapore.

Kuwano, R., Jardine, R.J. (2004). On the applicability of cross-anisotropic elasticity to granular materials at very small strains, *Géotechnique,* **54(1)**, 75-76.

Kuwano, R., Connolly T.M., and Jardine, R.J. (1999). Anisotropic stiffness measurements in a stress-path triaxial cell, *Geotechnical Testing Journal,* **23(2)**, 141-157.

Lee, J.S., Santamarina, J.C. (2005). Bender Elements: Performance and Signal Interpretation, *Journal of Geotechnical and Geoenvironmental Engineering*, **131**, 1063-1070.

Lehane, B.M., Jardine, R.J., Bond, A.J., Frank, R., (1993). Mechanisms of shaft friction in sand from instrumented pile tests. *Journal of Geotechnical Engineering*, **119(1)**, 19-35.

Leong, E.C., Cahyadi, J., Rahardjo, H. (2009). Measuring shear and compression wave velocities of soil using bender–extender elements, *Canadian Geotechnical Journal*, **46**, 792-812.

Leong, E.C., Yeo, S.H., Rahardjo, H. (2005). Measuring shear wave velocity using bender element, *Geotechnical Testing Journal,* **28**, 488-498.

Li, Y.R., Chan, L.S., Yeung, A.T., Xiang, X.Q. (2011). Effects of test conditions on shear behavior of composite soil, Institution of Civil Engineers Proceedings Geotechnical Engineering.

Li, Y., Huang, R., Chan, L.S., Chen, J. (2013). Effects of particle shape on shear strength of clay-gravel mixture, *KSCE Journal of Civil Engineering,* **17(4)**, 712-717.

Likitlersuang, S., Teachavorasinskun, S., Surarak, C., Oh, E., Balasubramaniam, A. (2013). Small strain stiffness and stiffness degradation curve of Bangkok clays, *Soils and Foundations,* **53(4)**, 498-509.

Lim, M.S., Wijeyesekera, D.C., Zainorabidin, A., Bakar, I. (2013). The effects of particle morphology (shape and sizes) characteristics on its engineering behaviour and sustainable engineering performance of sand, *International Journal of Integrated Engineering,* **4(4)**.

Lings M.L., Greening P. D. (2001). A novel bender/extender element for soil testing, *Géotechnique,* **51(8)**, 713-717.

Liu, X.L., Loo, H., Min, H., Deng, J. H., Tham, L.G., Lee, C.F. (2006). Shear strength of slip soils containing coarse particles of Xietan landslide, In Advances in Earth Structures: Research to Practice, 142-159.

Liu, X., Yang, J., Wang, G., Chen, L. (2016). Small-strain shear modulus of volcanic granular soil: An experimental investigation, *Soil Dynamics and Earthquake Engineering,* **86**, 15-24.

Lo Presti, D.C.F., Jamiolkowski, M., Pallara, O., Cavallararo, A., Pedroni, S. (1997). Shear modulus and damping of soils, *Géotechnique,* **47(3)**, 603-617.

Lo Presti, D.C.F., Pallara, O., Lancellota, R., Armandi, M., Maniscalco, R. (1993). Monotonic and cyclic loading behavior of two sands at small strains, *Geotechnical Testing Journal,* **16(4)**, 409-424.

Luke, B., Werkema, D., Andersen, S. (2013). Laboratory investigation of seismic effects of nanoparticle dispersions in saturated granular media. In Proceedings of the 18th International Conference on Soil Mechanics and Geotechnical Engineering, Paris.

Lupini, J.F., Skinner, A.E., Vaughan, P.R. (1981). The drained residual strength of cohesive soils, *Géotechnique,* **31(2)**, 181-213.

Macari, E.J., Ko, H.Y. (1994). A Study of an anisetropically overconsolidated silt by the resonant column method, *Geotechnical Testing Journal,* **17(3)**, 315-324.

Mancuso, C., Vassallo, R., d'Onofrio, A. (2002). Small strain behavior of a silty sand in controlled-suction resonant column torsional shear tests, *Canadian Geotechnical Journal,* **39(1)**, 22-31.

Margolis, S.V., Krinsley, D.H. (1974). Processes of formation and environmental occurrence of microfeatures on detrital quartz grains, *American Journal of Science,* **274(5)**, 449-464.

Martinez, B.N. (2003). Strength Properties of Granular Materials, Master's Thesis, Department of Civil and Environmental Engineering, Louisiana State University and Agricultural and Mechanical College, USA.

McKelvey, D., Sivakumar, V., Bell, A., Graham, J. (2004). Modeling vibrated stone columns in soft clay. *Proceedings of the Institution of Civil Engineers-Geotechnical Engineering,* **157(3)**, 137-149.

Menq, F.Y. (2003). Dynamic properties of sandy and gravelly soils. Ph.D. thesis, University of Texas at Austin, Austin, TX.

Miller, E.A., Sowers, G.F. (1958). The strength characteristics of soil-aggregate mixtures & discussion, *Highway Research Board Bulletin,* **183**, 16-23.

Mitchell, J.K. (1976). Fundamental of soil behavior. John Wiley & Sons, Inc.

Miura, K., Maeda, K., Furukawa, M., Toki, S. (1998). Mechanical characteristics of sands with different primary properties, *Soils and Foundations,* **38(4)**, 159-172.

Mojezi, M., Biglari, M., Jafari, M.K., Ashayeri, I. (2018). Determination of shear modulus and damping ratio of normally consolidated unsaturated kaolin, *International Journal of Geotechnical Engineering,* 1-22.

Monkul M., Ozden G. (2007). Compressional behaviour of clayey sand and transition fines content, *Engineering Geology,* **89**,195-205.

Muszynski, M.R., Vitton, S.J. (2012). Particle shape estimates of uniform sands: visual and automated methods comparison, *Journal of Materials in Civil Engineering*, **24(2)**, 194-206.

Najjar, S.S., Sadek, S., Maakaroun, T. (2010). Effect of sand columns on the undrained load response of soft clays, *Journal of Geotechnical and Geoenvironmental Engineering,* **136(9)**, 1263-1277.

Nakata, Y., Hyodo, M., Hyde, A.F.L., Kato, Y., Murata, H. (2001). Microscopic particle crushing of sand subjected to high pressure one-dimensional compression, *Soils and Foundations*, **41(1)**, 69-82.

Ni, Q., Tan, T.S., Dasari, G.R., Hight, D.W. (2004). Contribution of fines to the compressive strength of mixed soils, *Géotechnique,* **54(9)**, 561-569.

Nishimura, S., Abdiel, M.D. (2017). Cataloguing stiffness anisotropy of natural sedimentary soils–From clays to intermediate soils, *Japanese Geotechnical Society Special Publication,* **5(2)**, 101-106.

Nishimura, S. (2014). Assessment of anisotropic elastic parameters of saturated clay measured in triaxial apparatus: Appraisal of techniques and derivation procedures, *Soils and Foundations,* **54(3)**, 364-376.

Omar, T. and Sadrekarimi, A. (2014). Specimen size effects on behavior of loose sand in triaxial compression tests, *Canadian Geotechnical Journal,* **52(6)**, 732-746.

Otsubo, M., Osullivan, C., Sim, W.W., Ibraim, E. (2015). Quantitative assessment of the influence of surface roughness on soil stiffness, *Géotechnique,* **65(8)**, 694-700.

Oztoprak, S., Bolton, M.D. (2013). Stiffness of sands through a laboratory test database, *Géotechnique,* **63(1)**, 54-70.

Pandian, N.S., Nagaraj, T.S., Raju, P.N. (1995). Permeability and compressibility behavior of bentonite-sand/soil mixes, *Geotechnical Testing Journal,* **18(1)**, 86-93.

Panuska, J., Frankovska, J. (2016). Effect of a void ratio on the small strain shear modulus G_{max} for coarse-grained soils, *Procedia Engineering,* **161**, 1235-1239.

Payan, M., Senetakis, K., Khoshghalb, A., Khalili, N. (2017). Characterization of the small-strain dynamic behaviour of silty sands; contribution of silica non-plastic fines content, *Soil Dynamics and Earthquake Engineering,* **102**, 232-240.

Pennington, D.S., Nash, D.F.T., Lings, M.L. (2001). Horizontally mounted bender elements for measuring anistropic shear moduli in triaxial clay specimens, *Geotechnical Testing Journal,* **24(2)**, 133-144.

Pitman, T.D., Robertson, P.K. Sego, D.C. (1994). Influence of fines on the collapse of loose sands, *Canadian Geotechnical Journal,* **31(5)**, 728-739.

Powers, M.C. (1953). A new roundness scale for sedimentary particles, *Journal of Sedimentary Research,* **23(2)**, 117-119.

Prakasha K.S., Chandrasekaran V.S. (2005). Behavior of marine sand-clay mixtures under static and cyclic triaxial shear, *Journal of Geotechnical and Geoenvironmental Engineering*, **131(2)**, 213-222.

Qiu, T., Huang, Y., Guadalupe-Torres, Y., Baxter, C.D., Fox, P.J. (2015). Effective soil density for small-strain shear waves in saturated granular materials, *Journal of Geotechnical and Geoenvironmental Engineering,* **141(9)**, 04015036

Rahman, M.E., Pakrashi, V., Banerjee, S., Orr, T. (2016). Suitable Waves for Bender Element Tests: Interpretations, Errors and Modelling Aspects, *Periodica Polytechnica Civil Engineering,* **60(2)**, 145.

Rahman, M.M., Lo, S.R. (2008). The prediction of equivalent granular steady state line of loose sand with fines, *Geomechanics and Geoengineering: An International Journal,* **3(3)**, 179-190.

Ratananikom, W., Likitlersuang, S., Yimsiri, S. (2013). An investigation of anisotropic elastic parameters of Bangkok Clay from vertical and horizontal cut specimens, *Geomechanics and Geoengineering,* **8(1)**, 15-27.

Robertson, P.K., Sasitharan, S., Cunning, J.C., Sego, D.C. (1995). Shear-wave velocity to evaluate in-situ state of Ottawa sand, *Journal of Geotechnical Engineering,* **121(3)**, 262–273.

Roshan, H., Masoumi, H., Regenauer-Lieb, K. (2017). Frictional behaviour of sandstone: A sample-size dependent triaxial investigation, *Journal of Structural Geology,* **94**, 154-165.

Rothenburg, L., Bathurst, R.J. (1989). Analytical study of induced anisotropy in idealized granular materials, *Géotechnique,* **39(4)**, 601-614.

Sanchez-Salinero, I., Roesset, J. M., Stokoe, I.I., Kenneth, H. (1986). Analytical studies of body wave propagation and attenuation, Report GR 86-15, University of Texas: Austin, TX, USA.

Santagata, M., Germaine, J.T., Ladd, C.C. (2005). Factors affecting the initial stiffness of cohesive soils, *Journal of Geotechnical and Geoenvironmental Engineering,* **131(4)**, 430-441.

Santamarina, J.C., Cascante, G. (1998). Effect of surface roughness on the wave propagation parameters, *Géotechnique,* **48(1)**, 129-136.

Santamarina, J.C., Cho, G.C. (2004). Soil behaviour: the role of particle shape. Proc. Skempton Conference, March, London.

Santamarina, J.C., Klein, K., Fam, M. (2001). Soils and Waves, J. Wiley and Sons, Chichester, UK.

Sas, W., Gabryś, K., Szymański, A. (2017). Experimental studies of dynamic properties of Quaternary clayey soils, *Soil Dynamics and Earthquake Engineering,* **95**, 29-39.

Sawangsuriya, A. (2012). Wave propagation methods for determining stiffness of geomaterials, In Wave Processes in Classical and New Solids. InTech.

Sawangsuriya, A., Bosscher, P.J., Edil, T.B. (2005). Alternative testing techniques for modulus of pavement bases and subgrades. Proceedings of the 13th Annual Great Lakes Geotechnical and Geoenvironmental Engineering Conference, Geotechnical Applications for Transportation Infrastructure, ASCE, Geotechnical Practice Publication, No.3, Milwaukee, WI, 108-121.

Schultheiss P.J. (1981). Simultaneous measurements of P and S wave velocities during conventional laboratory soil testing procedures, *Marine Geotechnology,* **4(4)**, 343-367.

Seed, H.B., Wong, R.T., Idriss, I.M. Tokimatsu, K. (1986). Moduli and damping factors for dynamic analyses of cohesionless soil, *Journal of Getechnical Engineering,* **112(11)**, 1016-1024.

Senetakis, K., Anastasiadis, A., Pitilakis, K. (2013). Normalized shear modulus reduction and damping ratio curves of quartz sand and rhyolitic crushed rock, *Soils and Foundations,* **53(6)**, 879-893.

Shafiee, A., Tavakoli, H.R., Jafari, M.K. (2008). Undrained behavior of compacted sand-clay mixtures under monotonic loading paths, *Journal of Applied Sciences*, **8(18)**, 3108-3118.

Shakoor, A. Cook, B.D. (1990). The effect of stone content, size and shape on the engineering properties of a compacted silty clay, *Bulletin of the Association of Engineering Geologists,* **27(2)**, 245-253.

Shibuya, S., Tanaka, H. (1996). Estimate of elastic shear modulus in Holocene soil deposits, *Soils and Foundations,* **36(4)**, 45-55.

Shimobe S., Moroto N. (1995). A new classification chart for sand liquefaction. *Earthquake Geotechnical Engineering,* 315-320.

Shin, H., Santamarina, J.C. (2012). Role of particle angularity on the mechanical behavior of granular mixtures, *Journal of Geotechnical and Geoenvironmental Engineering,* **139(2)**, 353-355.

Shirley, D.J. (1978). An improved shear wave transducer, *The Journal of the Acoustical Society of America*, **63(5)**, 1643-1645.

Shirley, D.J., Hampton, L.D. (1978). Shear-wave measurement in laboratory sediments, *The Journal of the Acoustical Society of America,* **63(2)**, 607-613.

Shivaprakash, B.G., Dinesh, S.V. (2018). Effect of plastic fines on initial shear modulus of sand-clay mixtures. *KSCE Journal of Civil Engineering,* **22(1)**, 73-82.

Simoni, A. Houlsby, G.T. (2006). The direct shear strength and dilatancy of sand-gravel mixtures, *Geotechnical and Geological Engineering,* **24(3)**, 523-549.

Sivakumar, V., McKelvey, D., Graham, J., Hughes, D. (2004). Triaxial tests on model sand columns in clay, *Canadian Geotechnical Journal,* **41(2)**, 299-312.

Skempton, A.W. (1954). The pore-pressure coefficients A and B, *Géotechnique,* **4(4)**, 143–147.

Souto, A., Hartikainen, J., Ozudogru, K. (1994). Measurement of dynamic properties of road pavement materials by the bender element and resonant column tests, *Géotechnique,* **44(3)**, 519-526.

Stavridakis, E.I. (2005). Presentation and assessment of clay influence on engineering parameters of cement-treated clayey mixtures, *Electronic Journal of Geotechnical Engineering,* **10**.

Steiakakis, E., Lazaropoulos, A., Vafidis, A., Agioutantis, Z., Kritikakis, G. (2017). Determination of shear wave velocities in sediment deposits, *International Journal of Geotechnical Engineering*, 1-11.

Stephenson, R.W. (1978). Ultrasonic testing for determining dynamic soil moduli, In Dynamic Geotechnical Testing. ASTM International.

Strassburger, E. (1982). Use of piezoelectric transducers for stiffness and density measurements of soils. MS Special Report, Geotechnical Engineering, Department of Civil Engineering, University of Texas at Austin, August, 135.

Styler, M.A., Howie, J.A. (2014). Continuous monitoring of bender elements shear wave velocities during triaxial testing, *Geotechnical Testing Journal,* **37(2)**, 218-229.

Sukolrat, J. (2007). Structure and destructuration of Bothkennar clay. PhD thesis, University of Bristol.

Surarak, C., Likitlersuang, S., Wanatowski, D. (2012). Stiffness and strength parameters for hardening soil model of soft and stiff Bangkok clays. *Soils and Foundations,* **52(4)**, 682–697.

Szilvagyi, Z., Hudacsek, P., Ray, R.P. (2016). Soil shear modulus from resonant column, torsional shear and bender element tests, *International Journal of Geomate,* **10(2)**, 1822-1827.

Tabibnejad, A., Heshmati, A., Salehzadeh, H. and Tabatabaei, S. H. (2015). Effect of gradation curve and dry density on collapse deformation behavior of a rockfill material, *KSCE Journal of Civil Engineering,* **19(3)**, 631-640.

Tan, T.S., Goh, T.C., Karunaratne, G.P., Lee, S.L. (1994). Shear strength of very soft clay-sand mixtures, *Geotechnical Testing Journal,* **17(1)**, 27

Tanaka, Y., Kudo, K., Nishi, K., and Okamoto, T. (1994). Shear modulus and damping ratio of gravelly soils measured by several methods, *Pre-Failure Deformation of Geomaterials (1S-Hokkaido),* **1**, 47-53.

Tang, A.M., Vu, M.N., Cui, Y.J. (2011). Effects of the maximum soil aggregates size and cyclic wetting-drying on the stiffness of a lime-treated clayey soil, *Géotechnique,* **61(5)**, 421-429.

Tao, M., Figueroa, J., Saada, A. (2004). Influence of nonplastic fines content on the liquefaction resistance of soils in terms of the unit energy, Cyclic Behavior of Soils and Liquefaction Phenomena. Bochum, Germany, **31**, 223-231.

Tatsuoka, F., Shibuya, S., Kuwano, R. (Eds.). (2001). Advanced laboratory stress-strain testing of geomaterials. Swets & Zeitlinger BV.

Teachavorasinskun, S., Lukkanaprasit, P. (2008). Stress induced and inherent anisotropy on elastic stiffness of soft clays, *Soils and Foundations,* **48(1)**, 127-132.

Thevanayagam, S. (1998). Effect of fines and confining stress on steady state strength of silty sands, *Journal of Geotechnical and Geoenvironmental Engineering,* **124(6)**, 479-491.

Thevanayagam, S., Mohan, S. (2000). Intergranular state variables and stress-strain behaviour of silty sands, *Géotechnique,* **50(1)**, 1-23.

Thevanayagam, S., Shenthan, T., Mohan, S., Liang, J. (2002). Undrained fragility of clean sands, silty sands, and sandy silts, *Journal of Geotechnical and Geoenvironmental Engineering,* **128(10)**, 849-859.

Thomann, T.G., Hryciw, R.D. (1990). Laboratory measurement of small strain shear modulus under K_0 conditions, *Geotechnical Testing Journal,* **13(2)**, 97-105.

Thornton, C. (2000). Numerical simulations of deviatoric shear deformation of granular media, *Géotechnique,* **50(1)**, 43-53.

Troncoso, J.H., Verdugo, R. (1985). Silt content and dynamic behavior of tailing sands. Proc. 11th International Conference on Soil Mechanics and Foundation Engineering, 3, 1311-1314.

Vallejo, L.E., Zhou, Y. (1994). The mechanical properties of simulated soil-rock mixtures. In Proceedings of the International Conference on Soil Mechanics and Foundation Engineering-International Society for Soil Mechanics and Foundation Engineering, 1, 365-365.

Vangla, P., Latha, G.M. (2015). Influence of particle size on the friction and interfacial shear strength of sands of similar morphology, *International Journal of Geosynthetics and Ground Engineering,* **1(1)**, 6.

Vardanega, P.J., Bolton, M.D. (2013). Stiffness of clays and silts: Normalizing shear modulus and shear strain, *Journal of Geotechnical and Geoenvironmental Engineering*, **139(9)**, 1575-1589.

Vardanega, P.J., Lau, B.H., Lam, S.Y., Haigh, S.K., Madabhushi, S.P.G., Bolton, M.D. (2015). Laboratory measurement of strength mobilization in kaolin: Link to stress history, *Géotechnique Letters,* **2(1)**, 9-15.

Viana da Fonseca, A.V., Carvalho, J., Ferreira, C., Santos, J.A., Almeida, F., Pereira, E., Feliciano, J., Grade, J., Oliveira, A. (2006). Characterization of a profile of residual soil from granite combining geological, geophysical and mechanical testing techniques. *Geotechnical & Geological Engineering,* **24(5)**, 1307-1348.

Viggiani, G., Atkinson, J.H. (1995). Stiffness of fine-grained soil at very small strains, *Géotechnique,* **45(2)**, 249-265.

Vucetic, M., Dobry, R. (1991). Effect of soil plasticity on cyclic response, *Journal of Geotechnical Engineering,* **117(1),** 89-107.

Wadell, H. (1932). Volume, shape, and roundness of rock particles, *Journal of Geology,* **40(5)**, 443-451.

Wang, Y.H., Lo, K.F., Yan, W.M., Dong, X.B. (2007). Measurement biases in the bender element test, *Journal of Geotechnical and Geoenvironmental Engineering,* **133(5)**, 564-574.

Wang, Y., Benahmed, N., Cui, Y.J., Tang, A.M. (2016). A novel method for determining the small-strain shear modulus of soil using the bender elements technique, *Canadian Geotechnical Journal,* **54(2)**, 280-289.

Wicaksono, R.I., Tsutsumi, Y., Sato, T., Koseki, J., Kuwano, R. (2008). Stiffness measurements by cyclic loading, triggger accelerometer, and bender element on sand & gravel, *Deformational Characteristics of Geomaterials, Atlanta, GA,* **2**, 733-39.

Wichtmann, T., Triantafyllidis, T. (2010). On the influence of the grain size distribution curve on P-wave velocity, constrained elastic modulus M_{max} and Poisson's ratio of quartz sands, *Soil Dynamics and Earthquake Engineering,* **30(8)**, 757-766.

Wichtmann, T., Triantafyllidis, T. (2009). On the influence of the grain size distribution curve of quartz sand on the small strain shear modulus G_{max}, *Journal of Geotechnical and Geoenvironmental Engineering,* **135(10)**, 1404-1418.

Wild, K.M., Barla, M., Turinett, G., Amann, F. (2017). A multi-stage Triaxial testing procedure for low permeable geomaterials applied to Opalinus Clay, *Journal of Rock Mechanics and Geotechnical Engineering,* **9(3)**, 519-530.

Wood, M.D., Kumar, G.V. (2000). Experimental observations of behaviour of heterogeneous soils, *Mechanics of Cohesive-frictional Materials,* **5(5)**, 373-398.

Wu, C., Ye, G., Han, L., Wang, J. (2014). Preliminary study on small- strain triaxial testing method for soft shanghai clays, In the Soil Behavior and Geomechanics, Shanghai, China: 379-388.

Yamada, S., Hyodo, M., Orense, R., and Dinesh, S. (2008). Initial Shear Modulus of Remolded Sand-Clay Mixtures, *Journal of Geotechnical and Geoenvironmental Engineering,* **134(7)**, 960-971.

Yamamuro, J.A., Bopp, P.A., Lade, P.V. (1996). One dimensional compression of sands at high pressures, *Journal of Geotechnical Engineering,* **122(2)**, 147-154.

Yamamuro, J.A., Wood, F.M. (2004). Effect of depositional method on the undrained behavior and microstructure of sand with silt, *Soil Dynamics and Earthquake Engineering,* **24(9-10)**, 751-760.

Yang, J., Gu, X.Q. (2013). Shear stiffness of granular material at small strains: Does it depend on grain size?, *Géotechnique,* **63(2)**, 165-179.

Yang, J., Liu, X. (2016). Shear wave velocity and stiffness of sand: the role of non-plastic fines, *Géotechnique,* **66(6)**, 500-514.

Yang, Z., Yuan, J., Liu, J., Han, B. (2017). Shear modulus degradation curves of gravelly and clayey soils based on kik-net in situ seismic observations, *Journal of Geotechnical and Geoenvironmental Engineering*, **143(9)**, 06017008.

Yimsiri, S., Ratananikom, W., Likitlersuang, S. (2009). Investigation of some anisotropic characteristics of Bangkok Clay. In the 17th International Conference on Soil Mechanics and Geotechnical Engineering, Alexandria, Egypt: 1068-1071.

Yin, J.H. (1999). Properties and behaviour of Hong Kong marine deposits with different clay contents, *Canadian Geotechnical Journal,* **36(6)**, 1085-1095.

Youn, J.U., Choo, Y.W., Kim, D.S. (2008). Measurement of small-strain shear modulus G_{max} of dry and saturated sands by bender element, resonant column, and torsional shear tests, *Canadian Geotechnical Journal*, **45**, 1426-1438.

Zhou, Y.G., Chen, Y.M, Huang, B. (2005). Experimental study of seismic cyclic loading effects on small strain shear modulus of saturated sands. *Journal of Zhejiang University-Science A*, **6(3)**, 229-236.

CURRICULUM VITAE

PERSONAL INFORMATION

Name and Surname: Mohammed Mukhlif KHALAF

Nationality: Iraqi

Birth place and date: Mosul-Iraq / 15-09-1981

Marial status: Married-2 child

Phone number: 05342443428

Email: mohmk1981@yahoo.com

EDUCATION

Degree	Graduate school	Year
Master	University of Mosul	2007
Bachelor	University of Mosul	2004
High School	Al-Sharqia High School	1999

WORK EXPERIENCE

Year	Place	Enrollment
2008-Present	University of Mosul	Assistant Lecturer

PUBLICATIONS

A. International Journals

1- Cabalar, A.F., **Khalaf, M.M.**, Karabash, Z. (2018). Shear modulus of clay-sand mixtures using bender element test. *Acta Geotechnica Slovenica,* **15(1)**, 3-15.

2- Cabalar, A.F., Awraheem, M.H., **Khalaf, M.M.** (2018). Geotechnical Properties of a Low-Plasticity Clay with Biopolymer. *Journal of Materials in Civil Engineering*, **30(8)**, 04018170.

3- Suhail Idrees Khattab, **Mukhlif Aljobouri, M.** (2012). Effect of combined stabilization by lime and cement on hydraulic properties of clayey soil selected from Mosul area. *AL Rafdain Engineering Journal*, **20(6)**, 139-153.

4- Cabalar, A.F., **Khalaf, M.M.** (2018). A Comparative study on the undrained shear strength results of fall cone and vane shear tests in the sand-clay mixtures. *Arabian Journal of Geoscinces,* (under review).

5- Cabalar, A.F., Demir, S., **Khalaf, M.M.** (2018). Response of different size/shape sand-clay mixtures using a pair of bender element mounted mould. *Journal of Testing and Evaluation,* (under review).

B. International/National Congress, Conference and Symposium

1- Karabash, Z., Cabalar, A.F., **Khalaf, M.M.** (2018). Triaxial response of the sand-waste tire rubber mixtures. 13th International Congress on Advances in Civil Engineering, ACE, 12-14 September, Izmir/ Turkey.